

# **Vertical Distribution of Tropospheric Ozone over Cairo, Egypt**

By

TIRUSHA THAMBIRAN

Submitted in fulfillment of the academic  
requirements for the degree of  
Master of Science  
School of Environmental Sciences  
University of KwaZulu-Natal

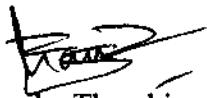
Durban  
2006

## PREFACE

---

The work presented in this thesis was carried out in the School of Environmental Sciences, University of KwaZulu-Natal (Howard College), from January 2004 to December 2005, under the supervision of Professor R.D. Diab.

This study represents original work by the author unless specifically stated to the contrary in the text, and has not been submitted in any form to another university.



Tirusha Thambiran

## ACKNOWLEDGMENTS

---

**The support and contributions of the following people are gratefully acknowledged:**

Professor Roseanne D. Diab for her exceptional supervision and support. Her commitment to this project was unfailing despite her demanding schedule. Her careful reading of this work has improved the standard of this dissertation.

Valarie Thouret, Jean-Pierre Cammas and Jerome Brioude from the CNRS for providing data and useful insight into the study.

Frank Sokolic for interpolation of the MOZAIC data and for always sharing his technical expertise.

Lisa Ramsay for assisting me with the use of SPSS.

Ashena, Nancy, Tamara and Sena for their friendship and understanding during this research process.

Nerosha, Sharlene and Yuri for all the laughs, friendship and support.

Alvin and Maria for all their assistance to our family.

My sisters, Mona and Namo, for their encouragement, and Bandit for reducing my stress levels.

My parents for all their support, guidance and sacrifices that have enabled me to reach this point in my life. I will always be grateful to the both of you.

## ABSTRACT

---

Cairo is a key location that is situated on the southern and eastern boundaries of the Mediterranean Basin, where summer tropospheric ozone levels are known to be elevated as a result of the persistence of a semi-stationary anticyclone that favours northerly flow from Europe, where anthropogenic emissions of ozone precursor gases are high. Strong levels of insolation, the absence of wet removal mechanisms, and low deposition velocities over the Mediterranean Sea further promote the summer enhancement of ozone.

Ozone profiles at Cairo, recorded by MOZAIC (Measurement of OZone and wAter Vapor aboard In-service AirCRAFT) aircraft, were examined with a view to assessing the relative influence of a range of factors on the vertical distribution of tropospheric ozone. These included long-range transport of ozone and precursor gases from Europe, North America and Asia, assessed through back trajectory analysis with the aid of the HYSPLIT (Hybrid Single Particle Integrated Trajectory) modelling programme. The influence of local pollution sources was determined using local pollution monitoring data, satellite measurements of nitrogen dioxides ( $\text{NO}_2$ ) and MOZAIC carbon monoxide (CO) data.

Results show that lower and mid-tropospheric ozone values at Cairo are enhanced in summer relative to other seasons, with high upper tropospheric values occurring in February and April. The upper tropospheric variability is attributed to stratospheric intrusions during the movement of the tropopause which is consistent with the known springtime enhancement due to stratospheric-tropospheric exchange (STE).

The lower tropospheric summer enhancement is linked to the effects of local pollution and polluted air masses originating from Europe. This summer ozone enhancement extends to a height of 8 km, which is fairly unusual for the region. The mid-tropospheric ozone enhancement appears to be a unique feature observed over Cairo, as other Mediterranean cities such as Athens, Greece usually display peaks in the upper and lower troposphere only. Therefore this enhancement is of considerable interest as it is unique to the region.



In the mid-troposphere mean ozone values in summer (JJA) range between 70-80 ppbv, with values approaching 100 ppbv on individual days. Investigations into the probable causes of this enhancement suggest that the enhanced ozone is not created in the mid-troposphere due to low levels of ozone precursor gases occurring in the mid-troposphere. Further, convective uplift of near-surface ozone is unlikely to occur as local pollution is confined to below 1000 hPa. It is therefore suggested that the enhanced ozone in the mid-troposphere is being brought into the region by the long-range of polluted air masses from distant sources.

Hierarchical classification of ozone profiles using the Statistical Package for the Social Sciences (SPSS version 11, 2001) programme allowed for the determination of least and most polluted profiles to emerge, which when related to air mass origins, highlights the significant role of long-range transport to mid-tropospheric ozone summer enhancement.

## TABLE OF CONTENTS

---

<b>PREFACE</b>	<b>i</b>
<b>ACKNOWLEDGEMENTS</b>	<b>ii</b>
<b>ABSTRACT</b>	<b>iii</b>
<b>LIST OF FIGURES</b>	<b>viii</b>
<b>LIST OF TABLES</b>	<b>xi</b>

### **CHAPTER ONE: INTRODUCTION**

1.1 Background	1
1.2 Description of Study Area	3
1.3 Statement of Purpose	6
1.4 Structure of Thesis	6

### **CHAPTER TWO: PHOTOCHEMICAL AND DYNAMICAL INFLUENCES ON THE TROPOSPHERIC OZONE BUDGET**

2.1 Introduction	7
2.2 Chemical Processes	
2.2.1 Stratospheric Ozone Chemistry	8
2.2.2 Tropospheric Chemistry	
2.2.2.1 The Role of the Hydroxyl Radical	10
2.2.2.2 Chemistry of Tropospheric Ozone Production	11
2.2.2.3 The Role of the Nitrate (NO <sub>3</sub> ) Radical in Tropospheric Ozone Chemistry	13
2.3 Factors that Influence the Tropospheric Ozone Budget	
2.3.1 Biomass Burning	15
2.3.2 Biogenic Emissions	16
2.3.3 Urban-Industrial Emissions	17
2.3.4 Lightning	18
2.4 Stratospheric-Tropospheric Exchange	
2.4.1 Tropopause Folding	20
2.4.2 Cut-Off Lows	20
2.4.3 Filamentation	21
2.4.4 Movement of the Tropopause	21
2.5 Advective Transport	22
2.6 Sources and Sinks of Tropospheric Ozone over Africa	

2.6.1 Biomass Burning	22
2.6.2 Biogenic Emissions	23
2.6.3 Urban-Industrial Emissions	24
2.6.4 Lightning	25
2.6.5 Stratosphere-Troposphere Exchange	25
2.6.6 Intercontinental Transport	26
2.7 Summary	29
 <b>CHAPTER 3: DATA AND METHODOLOGY</b>	
3.1 Introduction	30
3.2 MOZAIC Data	
3.2.1 Background	30
3.2.2 MOZAIC ozone and CO Profile Data over Cairo	34
3.3 SCIAMACHY Data	36
3.4 Vertical Velocity Data	37
3.5 Back Trajectory Modelling	
3.5.1 HYSPLIT Model	38
3.5.2 Lagrangian Analysis Tool (LAGRANTO) model	39
3.6 Classification of Vertical Ozone Profiles	39
3.7 Summary	41
 <b>CHAPTER 4: RESULTS AND ANALYSIS</b>	
4.1 Introduction	42
4.2 Total Tropospheric Ozone	42
4.3 Vertical Distribution of Tropospheric Ozone	44
4.4 Chemical and Dynamical Influences on the Summer Enhancement over Cairo	
4.4.1 Local Sources of Ozone Precursors	
4.4.1 General Overview of Local Pollution Sources in Cairo	52
4.4.4.2 Nitrogen Dioxide	53
4.4.4.3 Carbon Monoxide	57
4.4.2 Mid-Tropospheric Sources of Ozone	60
4.4.3 Vertical Exchange between the Boundary Layer	62
4.4.4 Long-Range Transport	67
4.4.5 Summary	69
4.5 Case Study (9-12 July 2003)	70

4.6 Classification of MOZAIC Data	
4.6.1 Introduction	73
4.6.2 Classification of MOZAIC Profiles	73
4.6.3 Results of Classification	75
4.6.4 Summary of Data Classification	84
4.7 Summary	86
 <b>CHAPTER FIVE: CONCLUSION</b>	
5.1 Summary	87
5.2 Recommendations	89
 <b>REFERENCES</b>	91
 <b>APPENDICES</b>	
Appendix A: Mean monthly total column ozone over Cairo (TOMS, 2005)	110
Appendix B: Tropospheric NO <sub>2</sub> over Africa for JJA (TEMIS, 2004b)	112
Appendix C: Vertical velocity (Pa/s) Maps JJA FOR 1999- 2002 (NCEP-DOE Reanalysis Data, 2004)	118
Appendix D: Back Trajectories for SPSS Groups 1-5 (NOAA-ARL, 2005b)	123

## LIST OF FIGURES

	<b>Page</b>
<b>Figure 1.1</b> Map showing the location of Cairo, Egypt in Africa and in the Mediterranean Region	3
<b>Figure 2.1</b> Diagrammatic representation of ozone in the atmosphere (Fahey, 2003)	7
<b>Figure 2.2</b> Representation of the near surface and 500 hPa circulation associated with a cut-off low (Tyson and Preston-Whyte, 2000)	21
<b>Figure 2.3</b> Air mass trajectories representing transport during 3 days in the lower troposphere (Lelieveld <i>et al.</i> , 2002)	27
<b>Figure 2.4</b> Air mass trajectories representing transport during 3 days in the middle troposphere (Lelieveld <i>et al.</i> , 2002)	27
<b>Figure 2.5</b> Air mass trajectories representing transport during 3 days in the upper troposphere (Lelieveld <i>et al.</i> , 2002)	28
<b>Figure 2.6</b> Model calculation of pollution transport from South Asia (Lawrence <i>et al.</i> , 2003)	28
<b>Figure 3.1</b> Geographical coverage and the distribution of flights per region (MOZAIC website, 2005a)	31
<b>Figure 3.2</b> Pitot tube and Rosemount housing (MOZAIC website, 2005b)	32
<b>Figure 3.3</b> MOZAIC CO Analyzer (Nedelec <i>et al.</i> , 2003)	33
<b>Figure 4.1</b> Mean Monthly TTO (DU) above Cairo for the period 1998 – 2002 based on MOZAIC aircraft data	43
<b>Figure 4.2</b> Seasonal variations in tropospheric vertical ozone structure (ozone in ppbv) over Cairo during the period 1998-2002	45
<b>Figure 4.3</b> Seasonal variation of the tropospheric vertical ozone structure (ozone in ppbv) over Athens, Greece (Kalabokas <i>et al.</i> , 2004)	46
<b>Figure 4.4</b> Seasonal plots of MOZAIC ozone data for the a) lower, b) middle and c) upper Troposphere	48
<b>Figure 4.5</b> a) Seasonal mean ozone profiles over Cairo Egypt. b) Summer mean with a single sigma envelope	50
<b>Figure 4.6</b> Annual average diurnal variations of ozone measured in Egypt	

	2000-2002 (Mohamed, 2004)	53
<b>Figure 4.7</b>	Weekly cycle of mean tropospheric NO <sub>2</sub> (1996 – 2001) normalized according to the weekly mean value (Beirle <i>et al.</i> , 2003)	54
<b>Figure 4.8</b>	Tropospheric NO <sub>2</sub> over Africa for June, July and August (JJA) 1998 from the GOME satellite (TEMIS, June 2004b)	56
<b>Figure 4.9</b>	Mean seasonal CO profiles (CO in ppbv) over Cairo for the period 2000 -2002 based on MOZAIC data	57
<b>Figure 4.10</b>	Frequency of exceedances of the 8- hour mean CO AQL value of 10mg/m <sup>3</sup> at three sites in Cairo (Mohamed., 2004)	58
<b>Figure 4.11</b>	Annual seasonal distribution of lightning activity b) seasonal distribution of lightning activity for June July and August annualized in units of fl km <sup>-2</sup> yr <sup>-1</sup> (Christian <i>et al.</i> , 2003)	61
<b>Figure 4.12</b>	a) 500 hPa vertical velocity (Pa/s) maps JJA for 1998 (NCEP-DOE Reanalysis Data, 2004)	63
<b>Figure 4.12</b>	b) 700 hPa vertical velocity (Pa/s) maps JJA for 1998(NCEP-DOE Reanalysis Data, 2004)	64
<b>Figure 4.12</b>	c) 850 hPa vertical velocity (Pa/s) maps JJA for 1998(NCEP-DOE Reanalysis Data, 2004)	65
<b>Figure 4.12</b>	c) 1000 hPa vertical velocity (Pa/s) maps JJA for 1998(NCEP-DOE Reanalysis Data, 2004)	66
<b>Figure 4.13</b>	Composite summer (JJA) back trajectories over Cairo for period 1998 – 2002	68
<b>Figure 4.14</b>	Daily carbon monoxide and ozone values for 9 -12 July 2003	70
<b>Figure 4.15</b>	Back trajectory analysis for 11 July 2003, for the lower, middle and upper troposphere based on the LAGRANTO model	71
<b>Figure 4.16</b>	Dendogram for classification of MOZAIC ozone profiles over Cairo	74
<b>Figure 4.17</b>	Mean ozone profile for Group 1 resulting from a cluster analysis over Cairo (1998-2002) with value cloud	76
<b>Figure 4. 18</b>	Composite of five day back trajectories for all days in Group 1. Trajectories originating at 2,5km are red, 5 km green, 7.5 km blue and 10 km purple	76
<b>Figure 4.19</b>	Mean ozone profile for group 2 resulting from a cluster analysis	

	over Cairo (1998-2002) with value cloud	78
<b>Figure 4.20</b>	Composite of five day back trajectories for all days in Group 2. Trajectories originating at 2,5km are red, 5 km green, 7.5 km blue and 10 km purple	78
<b>Figure 4.21</b>	Mean ozone profile for group 3 resulting from a cluster analysis over Cairo (1998-2002) with value cloud	80
<b>Figure 4.22</b>	Composite of five day back trajectories for all days in Group 3. Trajectories originating at 2,5km are red, 5 km green, 7.5 km and 10 km purple	80
<b>Figure 4.23</b>	Mean ozone profile for group 4 resulting from a cluster analysis over Cairo (1998-2002) with value cloud	82
<b>Figure 4.24</b>	Composite of five day back trajectories for all days in Group 4. Trajectories originating at 2,5km are red, 5 km green, 7.5 km blue and 10km purple	82
<b>Figure 4.25</b>	Mean ozone profile for group 5 resulting from a cluster analysis over Cairo (1998-2002) with value cloud	83
<b>Figure 4.26</b>	Composite of five day back trajectories for all days in Group 5. Trajectories originating at 2.5 km are red, 5 km green, 7.5 km blue and 10 km purple	84
<b>Figure 4.27</b>	Comparison of least polluted and most polluted profiles over Cairo	85

## LIST OF TABLES

	<b>Page</b>
<b>Table 3.1</b>	Number of MOZAIC flights per month over Cairo, for 1998-2002 34
<b>Table 4.1</b>	24 hour average NO <sub>2</sub> ( $\mu\text{g}/\text{m}^3$ ) average concentrations measured in at selected stations in Cairo during June – August 2000 (adapted from EIMP, 2000d; EIMP, 2000e and EIMP, 2000f) 53
<b>Table 4.2</b>	Seasonality of MOZAIC profiles 73
<b>Table 4.3</b>	Profiles in Group 1 of classification 75
<b>Table 4.4</b>	Profiles in Group 2 of classification 77
<b>Table 4.5</b>	Profiles in Group 3 of classification 79
<b>Table 4.6</b>	Profiles in Group 4 of classification 81
<b>Table 4.7</b>	Profiles in Group 5 of classification 83
<b>Table 4.8</b>	Summary of the seasonality of the hierarchical classification 84



## CHAPTER 1

### INTRODUCTION

---

#### 1.1 Background

In recent years the Mediterranean Basin and its surrounding regions have been the subject of many observations and model studies (Huntrieser *et al.*, 2002, Lelieveld *et al.*, 2002 Millan *et al.*, 1997, Ramanathan *et al.*, 2001, Ziomas, 1998) which indicate that in summertime the Mediterranean stands out as being one the most polluted regions in the world. Furthermore, results from these studies have led to the region being described as a 'large natural photochemical reactor' (Millan *et al.*, 1997) and a 'global pollution crossroads' (Lelieveld *et al.*, 2002).

In summer, the Mediterranean lies directly below the descending branch of the Hadley circulation (Lelieveld *et al.*, 2002), with the result that the area is prone to drought and air pollution due to cloud free, high solar radiation conditions.

In addition to this, due to the persistence of a semi-stationary anticyclone (Millan *et al.*, 1997) the area experiences a near surface northerly flow which provides a pathway for polluted air from Europe to reach the region (Lelieveld *et al.*, 2001). The accumulation of pollutants is so severe that the summertime Mediterranean is considered to have one of the highest aerosol radiative forcings in the world (Lelieveld *et al.*, 2002). It has been reported that near-surface ozone values can peak at about 200 ppbv in metropolitan areas and other Mediterranean coastal regions (Nolle *et al.*, 2002). Thus the levels of pollutants in the region often exceed air quality standards for the region (Nolle *et al.*, 2002).

The Mediterranean Intensive Oxidation Study (MINOS) campaign was an international, multi-platform field campaign that measured long-range transport of air pollution and aerosols from south-east Asia and Europe towards the Mediterranean basin (Lelieveld *et al.*, 2002). Measurements of atmospheric ozone, carbon monoxide (CO), nitrogen oxides (NO<sub>x</sub>) and hydrocarbons were made (Roelofs *et al.*, 2003). Results of the MINOS campaign have shown that the concentrations of trace gases and aerosols are generally

much higher over the Mediterranean region than for example the North Pacific Ocean in summer (Lelieveld *et al.*, 2002). The levels of pollutants in the region, are high indicative of *in situ* production due to local pollution sources. However, there is also a contribution of anthropogenic sources from parts of Europe, North America and Asia. In the lower troposphere (1-4 km), the strongest influences are western Europe (areas such as France and Germany) and in the eastern Mediterranean (areas such as Poland and Russia). Both these regions contribute 60 to 80% of the CO that is found in the lower tropospheric regions of the Mediterranean Basin (Lelieveld *et al.*, 2002; Traub *et al.*, 2003).

In the middle troposphere CO values ranged from 75 to 80 ppbv with the largest contributor being Asia (40 to 50%). The CO plume from Asia combines with emissions originating from North America and then crosses the Atlantic Ocean. However, in this part of the troposphere the variability of CO is low due to the fact that the lifetime of CO here is in order of 1 to 2 months. Western and eastern Europe generally account for 10% of the pollution (Lelieveld *et al.*, 2002).

In the upper troposphere, CO mixing ratios of up to 100 ppbv were recorded. Further there is a strong influence of an Asian pollution plume from the east (Lelieveld *et al.*, 2002). This plume is associated with Asian monsoon convection and the extended high-pressure trough in the upper troposphere. Anticyclonic flow transports the pollution northward over Africa (Lelieveld *et al.*, 2002).

The MINOS campaign ultimately served to improve our understanding of the chemical composition of tropospheric air in the Mediterranean region, providing in-depth analysis on the transport and chemistry of pollutants to the central and eastern regions. Numerous studies have investigated tropospheric ozone at European sites. However, there is lack of studies that have focused on tropospheric ozone in coastal North African cities. It is within this context that this investigation is carried out, in order to gain an understanding of the tropospheric ozone characteristics of a North African city that borders the Mediterranean Basin.

## 1.2 Description of Study Area

Egypt is located in Northern Africa and borders the Mediterranean Sea (Fig.1.1). The area is primarily a desert with the exception of the coastlines and the Nile Valley. Due to its location in the Mediterranean Region, the climate of coastal Egyptian cities is similar to places such as Greece, Italy, Spain and France.

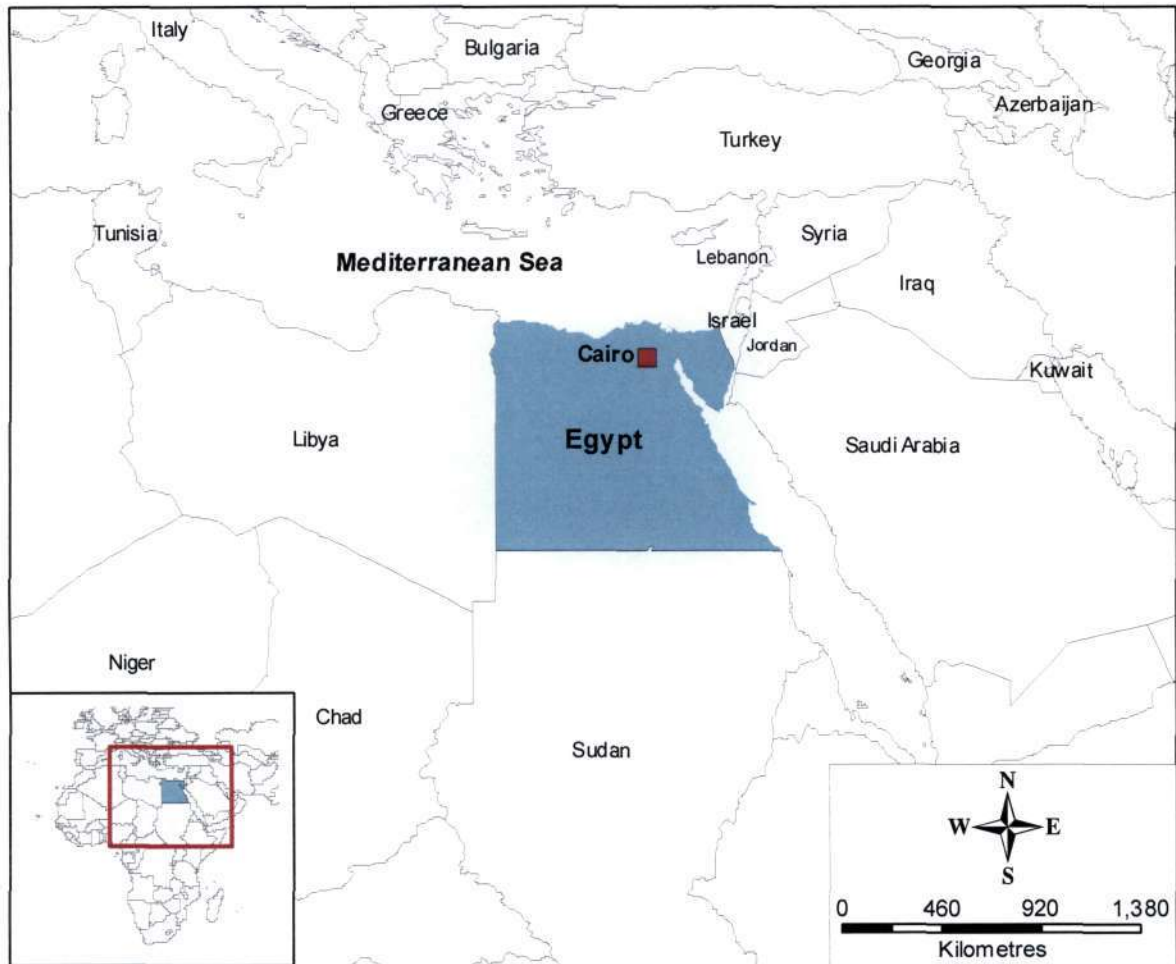


**Figure 1.1: Map showing the location of Cairo, Egypt in Africa and in the Mediterranean Region (Baijnath, 2005)**

Egypt is considered to be the second most populous African country with a population of over 68 million people (Bakarat, 2004). It is also a country that is undergoing rapid industrialization with a focus on raw metals and chemical industries. Over 50% of Egypt's industrial activities is situated in the capital city, Cairo (Barakat, 2004), which is the most populous city in Egypt consisting of one third of the population (Molina and Molina, 2004).

Industries located in Cairo include large metallurgical industries such as ore and scrap-based steel plants, ferro-alloys, copper, lead and aluminium smelters, chemical, and cement industries. Air pollution from these industries comes from both process and combustion sources (Ezz, 2003), specifically the quarrying of limestone and cement factories, fertilizer factories, ceramic brick manufacturers and power stations that burn fuel. These industries are major polluters, as 60% of the production that occurs at these plants follows inefficient wet processes (Shaw *et al.*, 2004).

A prime example of the industrialization of Cairo is the “Shubra El-Khima” industrial complex which has over 550 industrial plants of various sizes. Activities at these sites range from textile manufacturing, engineering construction, and chemical, electrical and petroleum industries (Robaa, 2003).

The other major source of pollution in Cairo is emissions from traffic. It is estimated that 1.2 million vehicles are on the streets of Cairo. The emissions that emanate from industries and vehicles consist of particulate matter, sulphur dioxide (SO<sub>2</sub>), NO<sub>x</sub> and CO. Furthermore, agriculture accounts for 17% of the Gross Domestic Product and as such the city is affected by the pollution effects of biomass burning, with about 2 million tons of rice straw being burnt annually releasing carbon dioxide (CO<sub>2</sub>) and other particulates (Waguih, 2002, Shaw *et al.*, 2004).

In Cairo, lead (Pb) levels are amongst the highest levels in the world, even though Cairo began phasing out leaded gasoline in 1996. Industrial lead smelters continue to be the larger source of this pollutant (Molina and Molina, 2004). The annual mean value for the total suspended particles for Cairo is 583 mg/m<sup>3</sup>, which is 7 times higher than the Egyptian air quality standard value (Shaltout *et al.*, 2001). In the industrial areas of greater Cairo, the suspended particulate matter is 5 to 10 times higher than international standards; SO<sub>2</sub> is 2 to 20 times higher; and NO<sub>x</sub> is two times higher (Ezz, 2003).

The emissions of CO, NO<sub>x</sub> and volatile organic compounds (VOC's) from agricultural and urban/industrial emissions are of concern as they are known to play important roles in the formation of tropospheric ozone (as discussed in Chapter 2).

In summer, Cairo is characterized by high temperatures, low relative humidity, low wind speeds, and strong vertical temperature gradients. Situated in the Mediterranean, the area is known to have strong insolation, an absence of wet removal mechanisms, and is affected by the occurrence of intercontinental transport of polluted air masses. The climate situation leads to increased photochemical processing in the atmosphere (Zakey *et al.*, 2004), which allows for enhanced production of tropospheric ozone.

Furthermore, the climate of Cairo has been changed by the effects of urbanization and industrialization, with a well documented 'urban heat island' phenomenon occurring which contributes further to enhancing pollution events (Zakey *et al.*, 2004). Air quality problems are exacerbated by adverse weather conditions, high humidity and strong temperature inversions at a few meters above the surface (Sivertsen, 1999).

Investigations into the tropospheric ozone over Cairo are limited to surface observations with data collection and analysis focusing on near-surface pollution levels. Such studies include EL-Hussainy *et al.* (2003), EL-Shahawy *et al.* (2003), Güsten *et al.* (1994); Sivertsen (1999), Zakey (2004) and Zakey and Abel-Wahab (2004). However, there is no detailed study on the vertical distribution of tropospheric ozone over Cairo.

It is thus of interest to determine if ozone enhancements experienced elsewhere in the Mediterranean region extend to Cairo. Cairo is located on the southern and eastern boundaries of the Mediterranean Basin (Fig.1.1), and is representative of a North African city. Cairo is thus strategically placed to explore this through the availability of vertical profile ozone data and a variety of meteorological parameters.

### 1.3 Statement of Purpose

The aim of this study is to characterize the vertical distribution of tropospheric ozone at Cairo and to assess the relative contributions from a range of sources. The specific objectives are as follows:

1. To describe and analyse the vertical distribution of ozone at Cairo;
2. To characterize the seasonal variability in tropospheric ozone, in particular to identify a mean background or minimum ozone profile and a maximum profile indicative of seasonal enhancement;
3. To assess the relative contribution of local and long-range pollution sources to concentrations of tropospheric ozone at Cairo.

The key questions to be addressed are as follows:

1. Does Cairo display a summer lower tropospheric ozone enhancement similar to that observed over the Mediterranean Basin?
2. To what extent is any enhancement observed due to long - range transport from Europe, North America or Asia, as opposed to local pollution sources?

### 1.4 Structure of Thesis

**Chapter 2** contains a detailed literature review of tropospheric ozone, covering the chemistry of ozone in the atmosphere as well as sources and sinks that contribute to its variability in the troposphere. **Chapter 3** discusses the data sources and the methods that have been used to analyze the data. The overall results and analysis are presented in **Chapter 4**. **Chapter 5** summarizes the findings of the research and presents conclusions and recommendations for further study.

## CHAPTER 2

### PHOTOCHEMICAL AND DYNAMICAL INFLUENCES ON THE TROPOSPHERIC OZONE BUDGET

---

#### 2.1 Introduction

Ozone ( $O_3$ ) is a form of oxygen, containing three oxygen atoms per molecule. It is a naturally occurring gas that is found primarily in two regions of the atmosphere. About 10% of atmospheric ozone is found in the troposphere which extends from the ground up to a height of about 16 km and the remaining 90% of ozone is found in the stratosphere (Anderson, 1996; Fahey, 2003). This is diagrammatically represented in Figure 2.1.

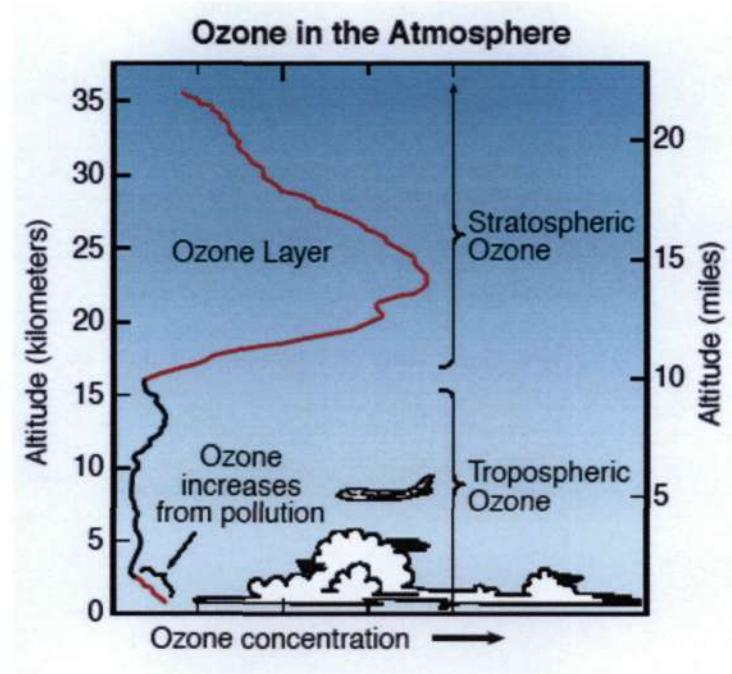


Figure 2.1. Diagrammatic representation of ozone in the atmosphere (Fahey, 2003)

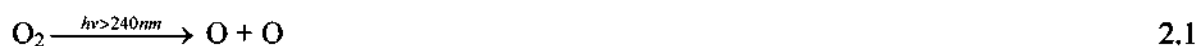
Tropospheric ozone plays an important role in the oxidation processes in the Earth's atmosphere through the formation of hydroxyl (OH) radicals, as these radicals control the lifetime of many gases (Lelieveld *et al.*, 2000). However, ozone is a pollutant, and is known to be a greenhouse gas. Furthermore, at the surface it affects humans and is considered to be phytotoxic (Kourtidis *et al.*, 2002). Epidemiological studies have shown that when exercising outdoors during photochemical pollution episodes, significant changes to lung functioning can occur and furthermore, tropospheric ozone is associated with asthma morbidity (Kalabokas *et al.*, 2000).

Tropospheric ozone is both transported from the stratosphere via stratospheric-tropospheric exchange (STE) and is produced in the troposphere by chemical reactions involving naturally occurring gases, and gases from pollution (Fahey, 2003). In addition to this there is horizontal advection from outside a region of interest (i.e. long-range and intercontinental transport). Thus a review of the photochemical and dynamical influences on the tropospheric ozone budget is relevant.

## 2.2 Chemical Processes

### 2.2.1 Stratospheric Ozone Chemistry

Ozone is produced and destroyed naturally in the stratosphere via the interaction of ultra-violet (UV) radiation with oxygen atoms and naturally occurring nitrogen compounds (Bridgman, 1997). This process of production is described as follows (Bunce, 1994):





The equations below describe the chemical reaction for the destruction of ozone in the stratosphere.



Where X represents a naturally occurring catalyst such as chlorine (Cl), nitrogen oxides (NO<sub>x</sub>), hydroxyl radical (OH) or hydrogen (H) (Bunce, 1994).

This balance between the natural creation and destruction of ozone is disrupted by the activities of humans. One of the major pollutants to impact on this process are chlorofluorocarbons (CFCs), which were used until recently in aerosol spray cans, in the manufacture of foams, and as refrigerants. CFC's have long lifetimes, and when exposed to ultraviolet radiation, are destroyed, releasing free chlorine atoms. The highly reactive chlorine atom disrupts the normal cycle of ozone formation and destruction (Bridgman, 1997).

In addition to CFC's, brominated CFC analogs (halons) that are commercially used in fire extinguishers, are also ozone depleters. The concern over halons stems from the fact that they are able to migrate freely into the stratosphere, where the chlorine-bromine bond is easily cleaved and can destroy ozone (Bunce, 1994).

NO<sub>x</sub> are also known stratospheric ozone depleters. Nitrous oxide (N<sub>2</sub>O) for example is a naturally occurring gas in the atmosphere that is biologically produced by denitrification (Bunce, 1994). However, due to increased usage of nitrogenous fertilizers, the concentrations of N<sub>2</sub>O are increasing, and are of concern as there is no known sink for it in the stratosphere, where it breaks down photochemically. This process is described as follows (Bunce, 1994):



where O<sup>\*</sup> represents an oxygen radical

Thus,  $\text{N}_2\text{O}$  decomposition leads to an increase in nitric oxide (NO), which from equations 2.3 and 2.4, is known to decompose ozone in the stratosphere. Furthermore, NO concentrations are increasing due to supersonic transport aircraft and space shuttles (Bunce, 1994). Nuclear weapons testing has also been linked to increased NO, as such explosions result in hot tropospheric air containing NO being directly injected from the troposphere into the stratosphere. Bojkov *et al.* (1990) reported that stratospheric ozone decline up until the 1970's could in part be attributed to the effects of nuclear testing.

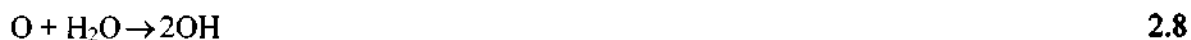
Natural events such as volcanic eruptions can have a similar effect to nuclear explosions, as gases are directly injected into the stratosphere (Bunce, 1994). An example of such an event is that of Mount. Pinatubo in 1991, after which a significant decline in total column ozone concentrations was observed (Hosseinian and Gough, 2000). However, according to Bojkov (1993), the effect of the eruption was temporary and is only partially responsible for the observed decline.

## **2.2.2 Tropospheric Chemistry**

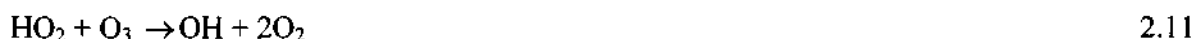
Tropospheric ozone is a secondary pollutant that has two sources. In the upper troposphere, the major source is through the transportation of ozone from the stratosphere (discussed later in section 2.4), whereas, in the middle and lower troposphere, ozone is produced by chemical reactions involving naturally occurring gases and gases from pollution (Bridgman, 1990; Fahey, 2003).

### **2.2.2.1 The Role of the Hydroxyl Radical**

The hydroxyl radical (OH) is one of the most important substances in the initial attack on the oxidizable materials in both the unpolluted and polluted troposphere (Bunce, 1994). The formation of OH in the troposphere is dependent on various factors including solar flux, latitude and the concentration of  $\text{NO}_2$  and is formed by the dissociation of ozone in the troposphere (Guicherit and Roemer, 2000) as shown below:



Studies in the 1970's have shown that ample amounts of OH are produced in the troposphere allowing for the oxidation of carbon monoxide (CO) and methane (CH<sub>4</sub>) (Jacobs, 1999). Thus in the unpolluted troposphere, OH reacts mainly with CO and CH<sub>4</sub>. As the two principle sinks of OH, these gases have an important role to play in controlling the concentrations of OH and in driving radical chemistry in the troposphere (Jacobs, 1999). In remote, unpolluted areas, where NO concentrations are low, the net reaction of the sequence is actually a sink for ozone, as the HO<sub>2</sub> reacts with the ozone rather than the NO (Bunce, 1994). This is shown below using CO, as an example.



The production of ozone thus depends on OH catalyzed chain oxidation of hydrocarbons in the presence of sufficient of NO<sub>x</sub>. Further, the concentration of H<sub>2</sub>O plays an important role in the photolytic loss of O<sub>3</sub>.

#### **2.2.2.2 Chemistry of Tropospheric Ozone Production**

The prime pollutants that are linked to the increases in tropospheric ozone are NO<sub>x</sub> gases produced due to fossil fuel combustion at high temperature and volatile organic compounds (VOC's) from natural and anthropogenic sources (Anderson, 1996). Vehicle emissions and biomass burning are hypothesised as being the main sources of trace gases released into the atmosphere. Gases such as CO and NO<sub>x</sub> are released from these processes and react in the

atmosphere to produce ozone (Jacobs, 1999). Further consideration is now given to the photochemical production of ozone.

Trace levels of NO<sub>x</sub> that result from combustion, lightning, and soil emissions are responsible for the production of ozone in the unpolluted troposphere (Jacobs, 1999). Ozone can be produced in the troposphere from the photolysis of NO<sub>2</sub> (Gruicheit and Roemer, 2000).



Tropospheric ozone and NO<sub>2</sub> exist in pseudo - equilibrium, as follows:



Thus in the absence of other gases, the relative concentrations of NO, NO<sub>2</sub> and ozone should depend on solar flux. Ozone is not produced by these reactions but merely recycled along with NO<sub>x</sub>. This is due to the absence of CO or organic compounds (Gruicheit and Roemer, 2000).

However, in urban air photochemical ozone formation is complicated due to ozone formation as a byproduct of hydrocarbon oxidation (Bunce, 1994). The reactions that occur are illustrated below (Fishman and Crutzen, 1978):



The net reaction is given below:



These equations show that under urban conditions of high NO concentrations, CO produces ozone as a byproduct, in addition to that which is produced by the pseudo - equilibrium.

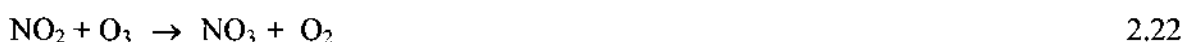
NO<sub>x</sub> emissions thus play a vital role in the photochemical production of tropospheric ozone. In the absence of organic material or CO, the HO<sub>2</sub> radicals destroy ozone or combine to form peroxides (Lelieveld and Dentener, 2000). However, in VOC or CO rich air, ozone is produced.

This means that in parts of the globe, where NO<sub>x</sub> levels are low, destruction of ozone could exceed its production, whereas in areas of high emissions, the opposite would be true (Lelieveld and Dentener, 2000).

#### **2.2.2.3 The Role of the Nitrate (NO<sub>3</sub>) Radical in Tropospheric Ozone Chemistry**

It is well known that air quality is dependent on the impact of various components on the atmosphere, including emissions, chemical transformation and the deposition of trace gases (Vrekoussis *et al.*, 2004). The ability of the troposphere to cleanse itself of these factors is important for good air quality. OH, NO<sub>3</sub>, and ozone radicals are known to be important determinants in the self cleansing efficiency of the troposphere. The role of OH has been discussed earlier and a brief examination of the role of NO<sub>3</sub> is given at this stage.

The major source of NO<sub>3</sub> is given as follows (Vrekoussis *et al.*, 2004):



The hydroxyl radical plays a major role during the day but at night this role is reduced and the lifetime of NO<sub>3</sub> during the day is much shorter due to its conversion to NO<sub>2</sub> shown below.



This means that NO<sub>3</sub> has the ability to play a dominant role in the troposphere at night (Vrekoussis *et al.*, 2004). During this time, NO<sub>3</sub> plays a role in eliminating NO<sub>x</sub> by HNO<sub>3</sub> formation and through the formation of particulate nitrate (Vrekoussis *et al.*, 2004). NO<sub>3</sub> reacts with NO<sub>2</sub> to produce nitrogen pentoxide (N<sub>2</sub>O<sub>5</sub>) as illustrated in equation 2.24. This reaction thus leads to a net loss of NO<sub>3</sub> from the atmosphere (Bunce, 1994; Vrekoussis *et al.*, 2004).



NO<sub>3</sub> has an important role to play in the troposphere as it contributes to the removal of NO<sub>x</sub>. It is estimated that 1.5 to 2 ozone molecules are lost when NO is removed in the form of N<sub>2</sub>O<sub>5</sub>, as the NO<sub>x</sub> is lost before it can contribute to photochemical ozone production (Parrish *et al.*, 1999).

### 2.3. Factors that Influence the Tropospheric Ozone Budget

Ozone is highly variable in space and time due to various dynamical and photochemical considerations (Newchurch *et al.*, 2003). Ozone, NO<sub>x</sub>, and VOC chemistry determines radical and oxidant processes in the troposphere (Bey *et al.*, 2001). However, various emissions play an important role in this chemistry. These include emissions from biomass burning, lightning, biogenic sources and anthropogenic sources. These factors influence the amount of NO<sub>x</sub> and volatile organic compounds that are available for photochemical production or destruction of ozone. In addition to this, ozone variability is influenced by transport of ozone rich air through stratosphere-troposphere exchange and horizontal advection of ozone and its precursor gases.

### 2.3.1 Biomass Burning

Biomass burning is a process that involves the combustion of living and dead matter for reasons that range from use for domestic energy to industrial fuel and the disposal of agricultural waste material.

Ideally when biomass burning occurs the following reaction should occur to allow for the complete combustion of the materials with CO<sub>2</sub> and H<sub>2</sub>O as the products (Levine, 1994).



From this equation it is evident that CO<sub>2</sub> is being returned to the atmosphere and as such it gives the impression that the CO<sub>2</sub> that is used up in the breakdown of CH<sub>2</sub>O, is being replaced (Andreae, 1991). This implies that biomass burning is not affecting the atmospheric CO<sub>2</sub> levels but merely restoring a balance. However, the problem with this notion is that biomass is burned at a faster rate than the rate at which, it is replaced. Thus CO<sub>2</sub> remains in the atmosphere until it is removed by some other process (Andreae, 1991). Furthermore, Levine (1994) points out that the above equation represents an ideal situation and that in all conditions, complete combustion during biomass burning is not achieved. As a result of incomplete combustion byproducts such as CO, CH<sub>4</sub>, particulate carbon, nitrogen and sulphur species also occur (Levine, 1994). CO and CH<sub>4</sub> are known to be greenhouse gases.

Furthermore, the changes in the biological activity in soils due to biomass burning and other perturbations may impact the atmospheric CO<sub>2</sub> budget, at least on a local scale. Following a fire, CO<sub>2</sub> is released through soil respiration and decomposition of non-living organic matter produced in the fire. CO<sub>2</sub> is reincorporated into biomass during the post-burn recovery period, thus offsetting its release by soil respiration. During the period in which soil respiration exceeds photosynthetic uptake, however, there is a net emission of CO<sub>2</sub> (Scholes and Andreae, 2000).

The pollutants that result from biomass burning are not restricted to the source regions. During a biomass burning event the fires rise buoyantly and entrain ambient air. In tropical regions the level to which the plume rises is limited by trade wind inversions. These plumes carry large amounts of hydrocarbons and NO<sub>x</sub> released from the biomass burning and have large amounts of ozone that range from 50 to 100 ppbv, at altitudes from 1 to 5 km. These concentrations of ozone can often be larger than that produced by industrial activities (Andreae, 1991).

In addition to the influence on ozone levels, biomass burning also plays a significant role in the radiative forcing of the climate, emitting black carbon which absorbs solar radiation and organic carbon which scatters it (UNEP, 2001).

### **2.3.2 Biogenic Emissions**

VOC's are major precursors to the production of tropospheric ozone. Biogenic sources play a major role in the emission of these VOC's (Bell and Ellis, 2004). One such source of VOCs is from the ammonium and nitrate that is present in the soil. These nutrients are used for nitrifying and denitrifying microorganisms to produce biogenic emissions of N<sub>2</sub>O and NO. This occurs in wetlands, swamps and rice paddies (Levine, 1994).

Typically the most abundant biogenic VOC species is isoprene (2-methyl 1, 3-butadiene) (Potter *et al.*, 2001), which is the most reactive VOC and thus plays an important role in the boundary layer ozone formation. Monoterpenes ( $\alpha$ -pinene, limonene and  $\beta$ -pinene) are also considered as an important VOC though it has a secondary effect on the formation of ozone (Varinou *et al.*, 1999).

Biogenic emissions from dry soils of forests and savannas are known to increase after rain events (Levine *et al.*, 1996). The rain activates the water-stressed nitrifying bacteria, which leads to the consumption of nitrogen that has accumulated, and as a result large pulses of NO are released (Jeagle *et al.*, 2004). Furthermore, biomass burning also impacts on the level of



biogenic emissions. In wetlands, increased biogenic emissions occur post-burn (Levine, 1994), as discussed in section 2.3.1.

The amount of emissions that occur depend on the type of vegetation, light, stress, humidity and the stage of leaf development (Bell and Ellis, 2004). Further, often in some areas, the vegetative sources of VOC's surpass anthropogenic sources (Bell and Ellis, 2004). Unlike biomass burning emissions that are limited to the dry season, these emissions are continuous throughout the year (Scholes and Andreae, 2000). Biogenic emissions are of concern as they are not easy to control and it is very difficult to obtain accurate measurements.

### **2.3.3 Urban-Industrial Emissions**

Anthropogenic activities in urban and industrial areas contribute to hydrocarbon emissions through processes such as fossil fuel burning power plants, chemical plants, petroleum refineries, solid waste disposal, slash burning and transportation (Mohamed *et al.*, 2002). Of particular interest are VOC's that are the result of incomplete combustion of these processes. Urban air polyaromatic hydrocarbons (PAHs) are among the most important VOC's and contribute to the production of tropospheric ozone (Fenger, 1999, Mohamed *et al.*, 2002).

Wang and Jacob (1998) have shown that anthropogenic emissions since pre-industrial times have resulted in an increase of 120% of tropospheric ozone production and a doubling of the total tropospheric ozone source (including transport from the stratosphere). In the period of 1901 – 1940 in Athens, Greece ozone values were around 20 ppbv, compared to present day values which are in some instances 10 fold greater (Vingarzan, 2004). It is assumed that this increase can be attributed in part to anthropogenic emissions of NO<sub>x</sub> and hydrocarbons from fossil fuel combustion and biomass burning.

Motor vehicles are known to be emitters of benzene, toluene, ethylbenzene and xylene (BTEX) and as such are a major contributor to tropospheric ozone formation. The magnitude of these emissions depends on the volume of traffic and the composition of the emissions is dependent on the vehicle design (Mohamed *et al.*, 2002).

### 2.3.4 Lightning

There are two main sources of  $\text{NO}_x$  into the atmosphere, namely natural, and anthropogenic sources. Anthropogenic sources have been discussed as being biomass burning, vehicle emissions and industrial processes. One of the natural sources of  $\text{NO}_x$  is lightning. NO is produced by lightning when the air around the discharge cools from 30 000 K to about 2000 K.  $\text{NO}_2$  is then created due to the oxidation of NO by  $\text{O}_3$  (Lee *et al.*, 1997). The production of  $\text{NO}_x$  by lightning is dependent on various factors that include pressure, the distribution of lightning, the energy that is given off by each lightning flash and the rate at which  $\text{NO}_x$  is produced per joule of energy (Bond *et al.*, 2002).  $\text{NO}_x$  that is produced by lightning can be transported by convection to the upper levels of the troposphere, where it has a longer lifetime (Labrador *et al.*, 2004)

To assess the importance of lightning as a natural  $\text{NO}_x$  source and its role in tropospheric ozone formation, Bond *et al.* (2002) compared lightning production of  $\text{NO}_x$  to that of  $\text{NO}_x$  emissions from the other major sources such as biomass burning, industrial sources and emissions from soils. It was found that lightning ranked as the third largest contributor to  $\text{NO}_x$  levels and that it has a significant contribution throughout the year, one that is comparable to the other three sources.

Furthermore, according to Bond *et al.* (2002), there is a geographical aspect to the production of  $\text{NO}_x$  by lightning, as investigations into the relative strength of lightning production shows that the levels of  $\text{NO}_x$  vary spatially. Most of  $\text{NO}_x$  production by lightning occurs over islands and the continents. Also, lightning is the most important source of  $\text{NO}_x$  over the oceans, with the only other significant source being ships.

The production of the amount of  $\text{NO}_x$  that is supplied by lightning is surrounded by uncertainty, as there still exists aspects of the lightning itself that are not well understood. There is also uncertainty around the factors that are linked to the production of  $\text{NO}_x$ , such as how many NO molecules are produced per lightning flash (Bond *et al.*, 2002; Labrador *et al.*, 2004).

## **2.4 Stratospheric - Tropospheric Exchange**

Stratospheric-tropospheric exchange (STE) refers to the exchange of material across the tropopause. This flux of ozone from the stratosphere to the troposphere is highly episodic, occurring mostly in conjunction with baroclinic instability and the amplification of large-scale troughs in the upper tropospheric flow (Vaughan, 1988). The main source of ozone is in the middle stratosphere from where it is transported into the lower stratosphere, which is involved in the exchange of air with the tropopause (Gruicheit and Roemer, 2000).

As established earlier in the chapter stratospheric ozone is formed by the photolysis of oxygen mostly in the tropical stratosphere. The Brewer Dobson circulation then plays an important role in the transport of this tropical stratospheric ozone poleward in order to create the ozone layer. The circulation is induced by waves that originate in the troposphere by air flow over mountains which is brought about by synoptic wave conditions and deep convection (Lelieveld and Dentener, 2000).

They propagate into the stratosphere where they dissipate, which exerts a drag force onto the stratospheric westerlies (Lelieveld *et al.*, 2000). By thermal wind balance the wave forcing induces poleward motion and downward mass flux toward the mid latitude and high latitude troposphere. The stratospheric mass balance is maintained by upward motion across the tropical tropopause (Lelieveld and Dentener, 2000). The stratospheric ozone contribution to tropospheric ozone is dependent on latitude, tropospheric altitude and the time of day and year.

An understanding of the relationship between the stratosphere and the troposphere is of importance as the exchange of anthropogenic sources from the troposphere can lead to ozone depletion in the stratosphere. Stratospheric intrusions into the troposphere allows for ozone input into the troposphere. In recent years there has been extensive work done on the mechanisms that control STE, which include tropopause folding, cut-off lows and filamentation.

### **2.4.1 Tropopause Folding**

Tropopause folding is a mechanism for moving ozone-rich air from the stratosphere to the troposphere. Reed (1955) initially documented this phenomenon and the interaction between the stratosphere and the troposphere was subsequently studied in detail by Danielson (1968). He found that stratospheric air from high latitudes is transported southward and downward into the troposphere (in the Northern Hemisphere) as the tropopause folds, and reported on numerous case studies in the United States. Hoskins and Bretherton (1972) showed that the formations of these folds are within the framework of the semigeostrophic theory, such that the tropopause is defined by a threshold value of potential vorticity as opposed to a thermal definition (Elbern *et al.*, 1997). The flux of air into the tropopause is caused by upper tropospheric frontogenesis that is a result of flow field deformation and the rise of horizontal temperature gradients at the tropopause height levels (Elbern *et al.*, 1997).

Tropopause folding occurs at the upper tropospheric frontal zones in conjunction with upper tropospheric jet streams (Sorenson and Nielsen, 2001). Conditions suitable for the formation of tropospheric folds are found in the confluence zone of a jet stream, preferably with cold air advection along stream axis (Sorenson and Nielsen, 2001). At mid-latitudes, stratospheric intrusions into the troposphere induced by tropopause folds are believed to be an important term in the ozone budget (Gouget, 2003).

### **2.4.2 Cut-off Lows**

Cut-off lows are baroclinic systems that are unstable, and which slope to the west with increasing height. In addition to this, cut-off lows, especially when they are deepening, are associated with strong convergence and vertical motion (Tyson and Preston-Whyte, 2000). The characteristics that are associated with these features are diagrammatically represented below in Figure 2.2. This figure is a representation of the near surface and 500hPa circulation associated with a cut-off low, that provides the conditions that are conducive to the movement of air from the stratosphere to the troposphere.

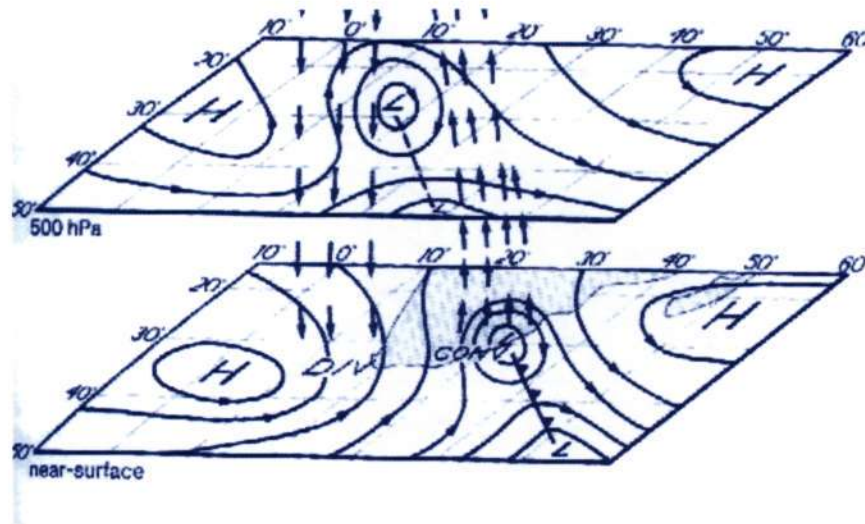


**Figure 2.2 Representation of the near surface and 500 hPa circulation associated with a cut-off low (Tyson and Preston-Whyte, 2000)**

Price and Vaughan (1992), provide a detailed description of the three main types of cut-off lows. Further, cut-off lows are well-known mechanisms in the middle and polar latitudes (Baray *et al.*, 2003). However, cut-off lows are generally considered to play a minor role in STE, compared to that of tropopause folding.

### **2.4.3 Filamentation**

Filamentation occurs when Rossby wave breaking occurs. As the wave breaking process occurs, an irreversible deformation of isentropic potential vorticity (PV) contours takes place (Baray *et al.*, 2003). These filaments are of stratospheric origin and allow for the mixing of air masses between the stratosphere and upper troposphere.

### **2.4.4 Movement of the Tropopause**

The tropopause varies as a function of altitude and season and on a daily basis, which has important implications for the amount of ozone present in the troposphere. During spring there is an upward movement of the tropopause which results in ozone rich air from the stratosphere

flowing into the troposphere. In autumn, this is reversed with a downward movement of the tropopause and the flow of ozone from the troposphere into the stratosphere (Appenzeller *et al.*, 1996; Staley, 1962).

## **2.5 Advective Transport**

In addition to photochemical processes and dynamical factors that affect tropospheric ozone concentration (Sections 2.2 and 2.4 above), there is horizontal advective transport that can affect the tropospheric ozone budget.

The horizontal transport of atmospheric trace substances occurs over differing temporal and spatial scales. Intercontinental transport (ICT) can occur on timescales that are in the order of 3–30 days. Various chemical species such as ozone, its precursor gases and aerosol pollutants can be affected by ICT (Stohl *et al.*, 2002). Pollution problems that arise in a particular location can often be linked to long-range atmospheric transport processes (Wild and Akimoto, 2001). Techniques such as remote sensing and atmospheric transport modeling are useful tools in studies which try to establish long distance connections between sources and receptors.

## **2.6 Sources and Sinks of Tropospheric Ozone over Africa**

The general overview of sources and sinks of tropospheric ozone is now further considered with particular relevance to the African continent. Africa has a rich mixture of sources of tropospheric ozone precursor gases giving rise to tropospheric ozone concentrations that are equivalent to many highly industrialized countries.

### **2.6.1 Biomass Burning**

In Africa biomass burning activities are linked to land clearing for agriculture, domestic energy usage and fires in natural vegetation. These events occur during the dry period July to October (Southern Hemisphere) and December to March (Northern Hemisphere). During the

dry seasons there is increased photodissociation due to reduced cloudiness which enhances the rate of ozone production (de Laat, 2002).

Numerous studies have focused on the impact of biomass burning in Africa. These include the Southern Africa Fire-Atmosphere Research Initiative (SAFARI-92, SAFARI-2000), the Transport and Atmospheric Chemistry near the Equator-Atlantic (TRACE-A), and the Experiment for Regional Sources and Sinks of Oxidants in central Africa (EXPRESSO) (de Laat, 2002). These studies have indicated that observations of pollution plumes from Africa are linked to biomass burning and in particular to the vegetation fires on the continent (Helas *et al.*, 1995). Furthermore, it is estimated that Africa contributes 40% to global biomass burning activities, a large amount of which originates from the burning of savanna. Biomass burning is thus an important source of  $\text{NO}_x$  and CO in Africa (de Laat, 2002).

According to the modeling study by Marufu *et al.* (2000), pyrogenic emissions account for 16% of the total tropospheric ozone over Africa. In the planetary boundary layer over Africa, the contribution due to biomass burning is ~24 % (Marufu *et al.*, 2000). A percentage of the ozone that results from biomass burning is also transported off the continent.

### 2.6.2 Biogenic Sources

The largest sources of emissions of isoprene are from forested regions, in particular tropical ecosystems (Potter *et al.*, 2001). Two-thirds of tropical savannas are located in Africa, 60% of which lie south of the equator. Biogenic emissions over Africa are variable with rates in tropical forests and Sudan woodlands ranging from  $1.9 - 4.9 \text{ mg Cm}^{-2}\text{h}^{-1}$ , Central African savannas ranging between  $2.4 - 4.9 \text{ mg Cm}^{-2}\text{h}^{-1}$  and South African savannas ranging between  $0.6 - 9.0 \text{ mg Cm}^{-2}\text{h}^{-1}$  (Otter *et al.*, 2002). Jeagle *et al.* (2004) estimate that the largest influence of soil  $\text{NO}_x$  on tropospheric ozone is over and downwind of west Africa during June to August, with significant biogenic  $\text{NO}_x$  emissions present in North Africa, particularly in June (Jeagle *et al.*, 2003).

Marufu *et al.* (2000) estimate that biogenic emissions account for 12 % of the total tropospheric ozone over Africa.

### **2.6.3 Urban-Industrial Emissions**

Africa's contribution to pollutants released from industrial and vehicles is not as significant as that from the Europe and North America. Fossil fuel CO<sub>2</sub> emissions are considered to be low in terms of per capita as well as in absolute terms. Five African countries are considered to be mainly responsible for Africa's fossil fuels emissions, with South Africa being the greatest emitter contributing 39 % to the total. Algeria, Egypt, Libya and Nigeria together account for 42 % of the emissions (UNEP, 2000).

The number of motor vehicles in most countries in North Africa has nearly doubled in the past 10 to 15 years and importantly many vehicles are of the older types (UNEP, 2000). Older vehicles emit 20 times more hydrocarbons and CO and four times more NO<sub>x</sub> than new vehicles. Particulate emissions are also relatively higher from poorly maintained diesel-maintained vehicles (UNEP, 2000).

Local pollution monitoring has revealed that the most abundant VOC's measured in Cairo, are isopentane and *n* pentane, which are associated with motor vehicle emissions. In addition to this, high levels of propane, isobutene, toluene and benzene are also fairly abundant (Molina and Molina, 2004).

Marufu *et al.* (2000) assessed that industrial emissions account for 19% of the total tropospheric ozone over Africa. In the tropical and extra tropical regions of the Southern Hemisphere fossil fuel emissions contribute 10-20% to tropospheric ozone (Lelieveld and Dentener, 2000).



#### **2.6.4 Lightning**

There is little agreement on the amount of NO<sub>x</sub> that lightning produces each year, however, estimates range between 0.8 to 12Tg N yr<sup>-1</sup>. Lightning NO<sub>x</sub> production is dependent on seasons. In the Southern Hemisphere summer, South America, Australia, and Southern Africa have most of the NO<sub>x</sub> that is produced by lightning, whereas for the Northern Hemisphere summer, Northern America, central Africa, and Asia have most of this production.

In Africa it is estimated that lightning produces over 40% of NO<sub>x</sub> per year, whereas the contribution to the tropics on an annual basis is about 23%. For the Southern Hemisphere, the southern half of Africa experiences the most NO<sub>x</sub> production by lightning whereas in the Northern Hemisphere summer, central Africa has the most (Bond *et al.*, 2002). During the Northern Hemisphere summer, the value of NO<sub>x</sub> production by lightning (as opposed to other sources) ranges from 10 to 90% over North America and northern Africa. According to Marufu *et al.* (2000), lightning accounts for 27 % of the total tropospheric ozone over Africa.

#### **2.6.5 Stratosphere-Troposphere Exchange**

Estimates of the flux of ozone that is transferred from the stratosphere to the troposphere are between 360 – 820 Tg/y (Gruicheit and Roemer, 2000). It is suggested that the flux of ozone is greater in the Northern Hemisphere than in the Southern Hemisphere (Beekman *et al.*, 1997).

According to Marufu *et al.* (2000), STE account for 26% of the total tropospheric ozone over Africa.

In the Mediterranean region ozone can be transported from the stratosphere to the tropopause by tropopause folds that originate at about 40°N over the Atlantic Ocean and Europe, moving eastward and downward (Lelieveld *et al.*, 2002,). Model results suggest that about 20 to 40% of the ozone in the Mediterranean region originates from the stratosphere (Lelieveld *et al.*, 2002).

### 2.6.6 Intercontinental Transport

In addition to natural and local pollution sources, Africa is affected by the distant transfer of polluted air masses. Studies by Thompson *et al.* (2002) and Diab *et al.* (2003) have linked high ozone events in central and southern African cities, in part, to imported polluted air masses. Of particular interest in this study is the northern region of Africa, which borders the Mediterranean Sea.

The Mediterranean Intensive Oxidation Study (MINOS) campaign measured the long-range transport of air-pollution and aerosols from south-east Asia and Europe towards the Mediterranean Basin. It was found that in the lower troposphere (0 – 4 km) an east-west pressure gradient develops between the Azorean high and the Asian monsoon low pressure system which results in a northerly flow from Europe to the Mediterranean Basin (Lelieveld *et al.*, 2002). Lelieveld *et al.* (2002) have shown that 60 – 80% of CO in the boundary layer over the Mediterranean in summer is due to European sources that lead to regular exceedances of the 8-hour ozone standard. The region can be significantly affected by the transport of air pollutants released in the southern part of Europe with air masses reaching the mid-tropospheric layers of the Inter-tropical Convergence Zone (ITCZ) region over Africa within a time period of a few days (4-6), which results in a massive upward transport of various ‘aged’ pollutants (Kallos *et al.*, 1998).

The area is characterized by the absence of wet removal mechanisms and is thus dominated by dry removal mechanisms which are slower at removing pollutants. As a result, the emissions from Europe and the rest of the Mediterranean region have sufficient time to travel to North Africa and it is proposed that this time is sufficient for gas to particle conversion and deposition to occur. For example, emissions of SO<sub>2</sub> require ~100 hours to convert to sulphates, which is the time it would take for the pollution plume to move from the Mediterranean and reach the ITCZ (Kallos *et al.*, 1998).

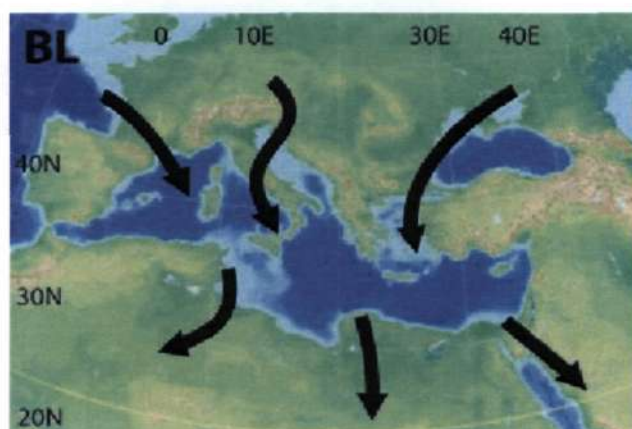


**Figure 2.3** Air mass trajectories representing transport during 3 days in the lower troposphere (Lelieveld *et al.*, 2002).

The middle troposphere (4 – 8km) is characterized by air masses that originate from the west as shown below (Fig.2.4) (Lelieveld *et al.*, 2002). This is representative of flow from the North Atlantic and North America. The trace gas concentrations of these westerlies were found to be less than that of Europe and the contribution to surface ozone in Europe was 2 - 4 ppbv (Lelieveld *et al.*, 2002).

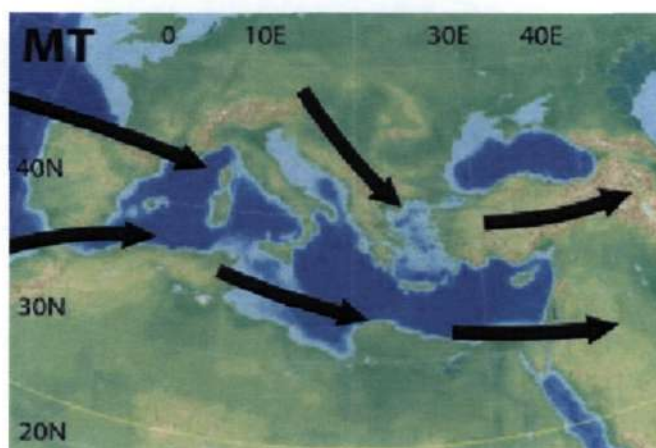


**Figure 2.4** Air mass trajectories representing transport during 3 days in the middle troposphere (Lelieveld *et al.*, 2002)

The upper troposphere is characterized by a south-easterly flow (Fig.2.5), originating over south-east Asia and in particular India and from the west (Lawrence *et al.*, 2003 ; Roelofs *et al.*, 2003; Traub *et al.*, 2003).

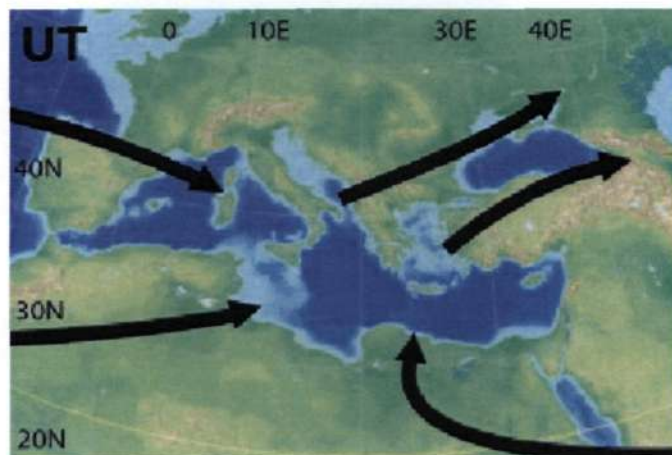


**Figure 2.5** Air mass trajectories representing transport during 3 days in the upper troposphere (Lelieveld *et al.*, 2002).

During the summer monsoon period, deep convection lofts pollutants from southern Asia into the upper troposphere. The pollution originates in an easterly tropical jet stream and turns north over the eastern Mediterranean (Fig.2.6). From there it can even penetrate the lower stratosphere, thus carrying Asian pollution into the lower part of the ozone layer (Lelieveld *et al.*, 2004).

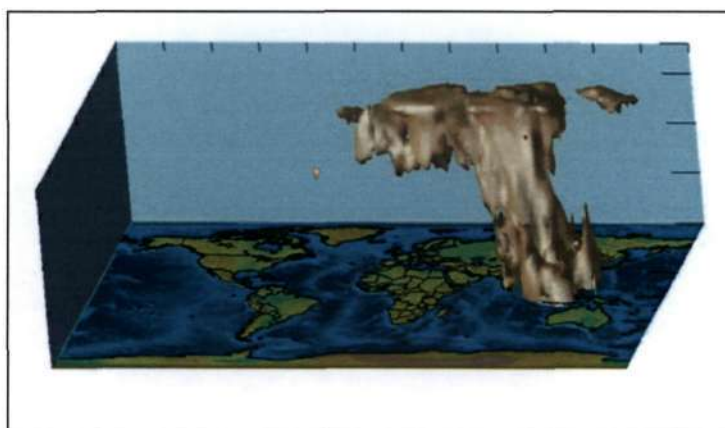


**Figure 2.6** Model calculation of pollution transport from South Asia (Lawrence *et al.*, 2003).

Previous studies such as those carried out during the Indian Ocean Experiment (INDOEX) showed that this Asian plume contains high concentrations of ozone precursors and aerosols from the populated south Asian region. High altitude easterlies carry Asian pollution across northern Africa and the Mediterranean (Scheeren *et al.*, 2003)

## **2.7 Summary**

From the above discussions we can conclude that ozone is predominantly found in the stratosphere, from where it is transported to the troposphere through various processes such as tropopause folding, cut off lows, and filamentation. However, due to natural and anthropogenic sources, ozone is also photochemically produced in the troposphere. Increased vehicle emissions and biomass burning contribute to high levels of pollutants in the troposphere, resulting in greater ground level ozone production. In addition to this, there is a contribution from long-range transport of ozone and its precursor gases.

## CHAPTER 3

### DATA AND METHODOLOGY

---

#### 3.1 Introduction

This section provides an overview of the data used in this study and the methods that were used to analyse the data. Ozone is measured in numerous ways, which include satellites, by instruments carried on aircrafts and ground-based measurements such as ozonesondes. Such observations can focus on stratospheric, tropospheric or even total column ozone. For this study data originates from the MOZAIC (Measurement of **O**Zone and wAter vapor aboard **I**n-service airCRAFT) programme and the focus of the data is on tropospheric ozone.

Ozone and carbon monoxide (CO) profile data above Cairo (30°10'N, 31°37'E) that were recorded as part of the MOZAIC programme were used in this study. The ozone profiles have been recorded since 1994 and CO profiles since 2002.

#### 3.2 MOZAIC Data

##### 3.2.1 Background

The MOZAIC programme was developed and funded by the European Commission. The programme was launched in January 1993 and the first phase involved the development and installation of instruments. This was followed by the second phase of the programme which started in October 1996 (Marengo *et al.*, 1998). The third phase of the programme involved the installation of new instruments for CO, total odd-nitrogen (NO<sub>y</sub>) and a new data acquisition system. The main objective of the programme was to enhance our understanding of the physical and chemical atmosphere. The MOZAIC data set provides regular samples of the upper troposphere and lower troposphere (UTLS) region (Thouret *et al.*, 1998). In addition to MOZAIC there are other programmes that utilize aircraft for obtaining measurements of gases in the UTLS region. These include CARIBIC (Civil Aircraft for Regular Investigation of the



Atmosphere Based on an Instrument Container) ([www.caribic-atmospheric.com](http://www.caribic-atmospheric.com)) and the JAL Foundation ([www.jal-foundation.or.jp/](http://www.jal-foundation.or.jp/)).

The MOZAIC programme uses commercial Airbus A340's to measure atmospheric concentrations of important gases. The instruments are carried free of charge on Lufthansa, Air France, Austrian Airlines and Sabena, and have been designed for long term operation in rough commercial aircraft conditions. Figure 3.1 presents the geographical distribution of the MOZAIC flights and include areas such as Africa, Asia and South America, which are traditionally poorly scientifically studied regions. Nedelec *et al.* (2003) reported that at present there is database of over 20 000 flights, representative of about 160 000 hours of flying time.

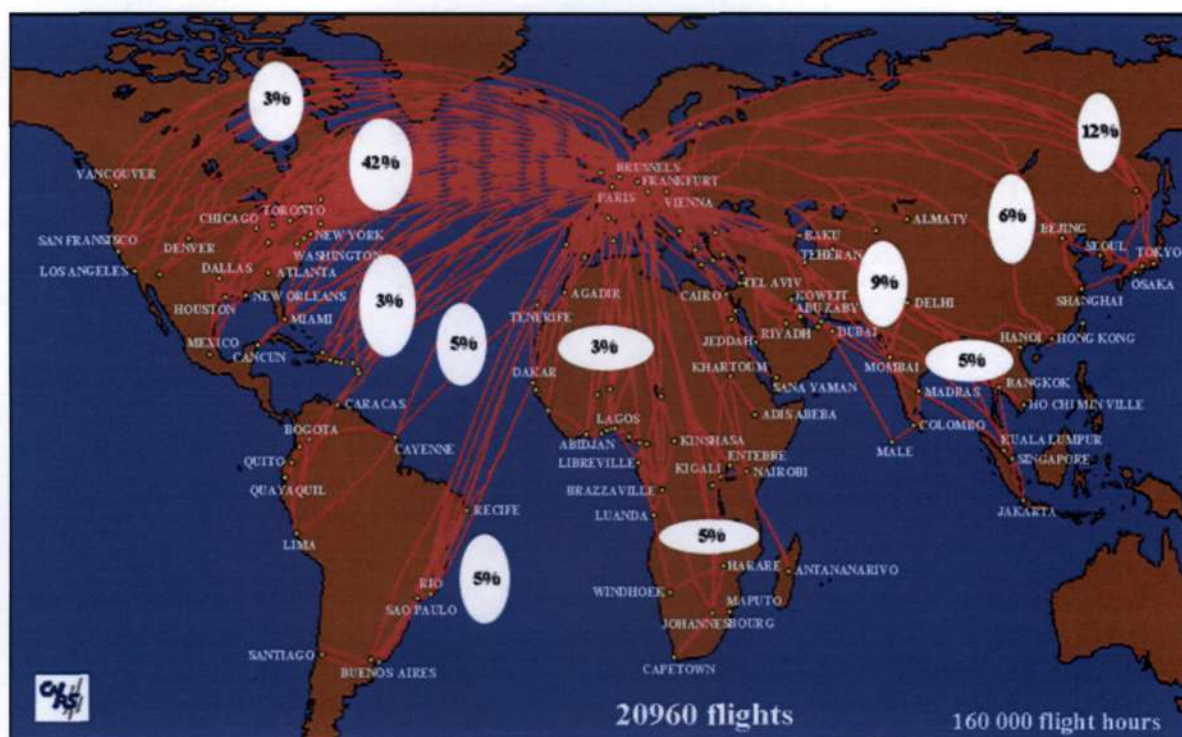


**Figure 3.1 Geographic coverage and the distribution of flights per region of MOZAIC (MOZAIC website, 2005a)**

The programme allows for the sampling of the atmosphere both in the tropopause region and during the aircraft landing and descent. The external sampling of air takes place after take off and before landing to ensure that the input line is not contaminated by local pollution sources whilst on the ground (Marenco *et al.*, 1998). The cruise altitudes that the aircraft ascend to or

descend from are prescribed by air traffic regulations. These are 9.6 km, 10.4 km, 11.3 km, 12.1 km and 13 km (Thouret *et al.*, 1998).

Measurements are taken automatically by equipment installed below the cockpit of the plane and on the fuselage, several meters away from the nose of the plane. The pitot tubes and Rosemount housing (shown in Figure 3.2) are placed such that the inlets are sufficiently outside the aircraft's boundary layer (Marenco *et al.*, 1998). The measurements are recorded every 4 seconds and begin after take off and continue up until landing. In addition to collecting data on chemical species, other parameters such as time, wind velocity, altitude, latitude, and longitude are also recorded (Marenco *et al.*, 1998). High capacity removable disks are used to store the data obtained (Marenco *et al.*, 1998).

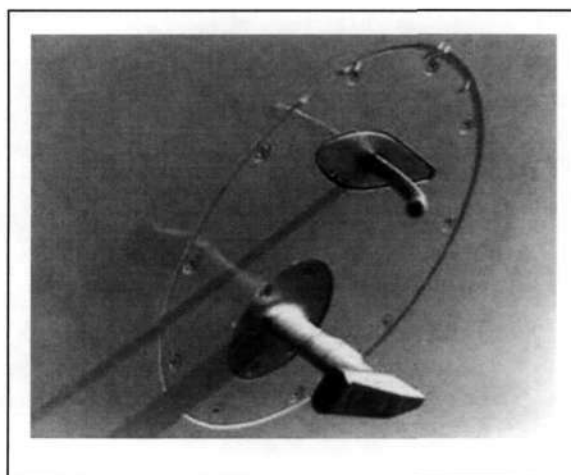


**Figure 3.2 Pitot tube and Rosemount housing (MOZAIC website, 2005b)**

As mentioned earlier, this study made use of ozone and CO measurements from the MOZAIC programme. Consideration is now given to the instruments used to obtain these measurements. Firstly, for ozone, a dual beam UV absorption instrument is used, specifically the Thermo-Electron, Model 49-103. A pump is used to pull the air through the analyser and this occurs at an external pressure of 150 - 250 hPa when at cruise altitude. Under these conditions, the ozone measurements that are taken have a detection limit of 2 ppbv, with an overall precision of  $\pm [2 \text{ ppbv} + 2\%]$  (Bojkov and Hilsenrath, 2005).



CO measurements are taken by a CO analyser that uses the Infra Red (IR) gas filter correlation method. According to Nedelec *et al.* (2003), this analyser represents an improved version of a commercial model from Thermo Environmental Instruments. Furthermore, as with the ozone analyser, the instrument was chosen due to the fact that the programme requires continuously operated systems that can function for long periods without maintenance. This system also ensures that other gases do not interfere with the detector signal which ensures that the analyser responds specifically to CO. A schematic representation of the analyser is given below (Fig. 3.3).

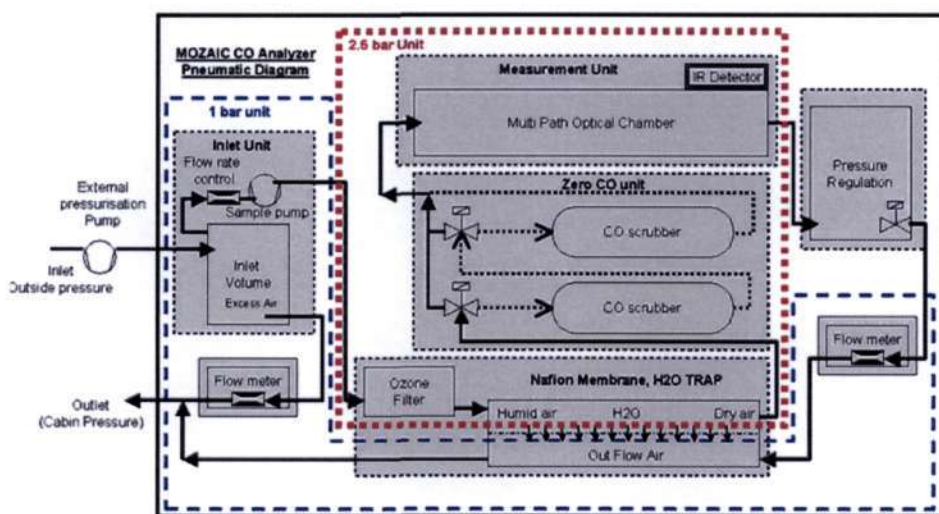


**Figure 3.3 MOZAIC CO analyzer (Nedelec *et al.*, 2003)**

Thus far, the CO analyser has proven to be reliable under difficult operational conditions. The analyser has a  $5 \text{ ppbv} \pm 5\%$ , instrument performance with good agreement with other measurement techniques. However, it should be noted that there are plans to make improvements to this instrument, which includes an improvement of the sensitivity/response time, as well as plans for a weight reduction by integrating the ozone and CO instruments with a single acquisition computer (Nedelec *et al.*, 2003).

There are limitations associated with the use of aircraft to measure ozone levels. Firstly, the MOZAIC programme depends on commercial aircraft to carry their instruments. These commercial flights are controlled by airline companies who determine the number of flights and the distribution throughout the year (Cammass, 1998). Biases in the data may also occur as

the MOZAIC flights occur within certain time periods within a day (Law *et al.*, 2000). However, there are also numerous benefits to the MOZAIC programme, as scientific research using aircraft is expensive and the instruments are carried on the airlines free of charge. Satellite observations are limited with regard to precision, vertical resolution and the species that are observable (Singh and Jacob, 2000). Aircraft measurements on the other hand, allow for a more detailed study of the atmosphere that is not available from satellites. Furthermore, MOZAIC data have been compared by Law *et al.* (2000) to results obtained from Chemical Transport Models (CTMs), and it was found that the model results compared well with MOZAIC data for regions that have been extensively studied (such as Europe).

### 3.2.2 MOZAIC Ozone and CO Profile Data above Cairo

MOZAIC ozone profiles at Cairo recorded during aircraft ascent and descent were used in the statistical analysis of the vertical distribution of ozone in the troposphere. Ozone profiles that had data missing over a vertical distance of 1000 m were excluded from the study. The profiles that were used in this study were chosen if the vertical distance between missing data was less than 1000 m. The missing data were interpolated at 150 metre intervals from 75 metres upwards.

A total of 115 profiles over the period of 1998-2002 were analyzed. The profiles are distributed throughout the seasons with the majority of the profiles occurring in autumn. The distribution of profiles by month and year is shown in Table 3.1.

**Table 3.1 Number of MOZAIC flights per month over Cairo, for 1998-2002**

	Jan	Feb	Mar	Apr	May	Jun	Jul	Aug	Sep	Oct	Nov	Dec	Total
<b>1998</b>								2					
<b>1999</b>				2	2	1		7		2		3	
<b>2000</b>		12		5		1	10	5	2	13			
<b>2001</b>								5	3	4	1	7	
<b>2002</b>	3		8				3		3	2	7	2	
<b>Total</b>	3	12	8	7	2	2	13	19	8	21	8	12	115

Monthly mean ozone values (in ppbv) were calculated over the study period at each of the available heights. These means were used to generate a contour mean monthly plot of vertical ozone distribution using the Surfer programme.

Seasonal mean ozone profiles were obtained by grouping the data according to seasons, such that averaging of June, July, August (JJA) ozone profiles represent a summer mean, September, October, November (SON) ozone profiles represent an autumn mean, December, January, February (DJF) ozone profiles represent a winter mean and March, April and May (MAM) ozone profiles represent a spring mean. The means of these groups were then represented graphically.

The determination of Total Tropospheric Ozone (TTO) is useful for comparing tropospheric ozone in different seasons and at different locations. Temporal and spatial variations in total tropospheric ozone (TTO) are due to photochemical and dynamical influences.

Estimates of TTO are determined by the definition of the tropopause height (Browell *et al.*, 1996; Diab *et al.*, 1996). There are two common methods that are used in studies to define the height of the tropopause. The first is based on a thermal tropopause where the tropopause is defined as the lower boundary of a 2 km thick layer, in which the air temperature lapse rate is less than 2 K/km, and the second is a dynamical tropopause, which is characterized by a sharp gradient in potential vorticity (Thouret *et al.*, 2005).

For this study TTO was obtained by integrating values between the surface and 11.3 km. As mentioned earlier there are 5 prescribed cruise altitudes of MOZAIC flights. In the MOZAIC ozone profile data available for analysis, these altitudes varied within the prescribed limits. Therefore an altitude of 11.3 km was chosen as it was an altitude achieved by all ozone profiles in the data set. The integration of ozone between the surface and 11.3 km resulted in a TTO value, measured in Dobson Units (DU), where 1 DU is equivalent to 100<sup>th</sup> of a millimeter, when reduced to standard temperature and pressure (Bodeker, 1994). The following equation was used to calculate TTO.

$$O_{DU} = \left( \frac{O_{ppbv} \times 10^{-9} \times P \times \Delta H \times 273.15 \times 1000}{1013.25 \times T_K} \right) \times 100$$

where,

$O_{DU}$  = ozone in Dobson Units

$O_{ppbv}$  = ozone in ppbv

$P$  = pressure in hPa

$\Delta H$  = difference in height between two successive layers/2(gpm)

$T_K$  = temperature in Kelvin

CO data from the MOZAIC programme were available for the period 2000 to 2002. The data were averaged and the missing data interpolated in the same way as the ozone data described above.

Case studies of a series of high ozone events (where an event is characterized as having ozone values over 100 ppbv), were selected from available summer data for 2003. The period chosen extended from 9 -12 July 2003. Graphs were created using both daily CO and ozone concentrations so as to make comparisons for each of the days.

### 3.3 SCIAMACHY Data

The importance of nitrogen oxides ( $NO_x$ ) as a key species in the formation of tropospheric ozone has been highlighted in the previous chapter. Column densities of  $NO_x$  can be detected from space using satellite platforms that employ differential optical absorption spectroscopy (DOAS) (Beirle *et al.*, 2004). The Global Ozone Monitoring Experiment (GOME) has provided 8 years of  $NO_2$  column densities. Recently though, the SCanning Imaging Absorption SpectroMeter for Atmospheric CHartography (SCIAMACHY) has taken over from GOME and provides total  $NO_2$  columns with a horizontal resolution of  $60 \times 30 \text{ km}^2$ , compared to GOME's resolution of  $320 \times 40 \text{ km}^2$ . The improved resolution means that structures such as large cities can be identified (Beirle *et al.*, 2004).

The DOAS retrieval technique is used for obtaining  $NO_2$ , which provides for a good signal to noise ratio. Further, with GOME results there have been clear correlations with enhanced  $NO_2$

and areas known to be industrialized and there have also been observations of signatures of NO<sub>2</sub> produced by lightning (TEMIS, 2004a).

However, there are problems with the derivation of quantitative tropospheric NO<sub>2</sub> amounts due to factors such as clouds, the stratospheric column of NO<sub>2</sub>, the trace gas profile, and aerosols (TEMIS, 2004a). SCIAMACHY compensates for some of the errors in retrieval due to the fact that it uses a smaller ground pixel size than its predecessor GOME. Thus, the variability of the measurements is better and there will be more cloud free pixels improving the overall quality of the retrieval (TEMIS, 2004a).

These maps were accessed on the Tropospheric Emission Monitoring Internet Service website (<http://www.temis.nl/>). Tropospheric NO<sub>2</sub> columns are available at this site for individual days and monthly means at a region or global scale. For this study, NO<sub>2</sub> maps were obtained as monthly means for Africa for June, July and August for the period of 1998 -2002. These maps thus represent monthly averages of tropospheric NO<sub>2</sub> for each of the summer months and can be used determine trends in the level of NO<sub>2</sub>.

### **3.4 Vertical Velocity Data**

Vertical velocity refers to the upward or downward motion of air on a synoptic scale and is a measure of the speed at which the air is rising or sinking. The vertical movement of air is associated with cloud formation, precipitation and the type of precipitation (rising air motion) or the reduction of clouds and dry and sunny weather (falling air motion) (Haby, 2005). Deep convection can remove pollutants from the lower atmosphere and inject them rapidly into the middle and upper troposphere and, occasionally, into the stratosphere.

There are two main ways of depicting vertical velocity values. This is usually in meters per second ( $ms^{-1}$ ), where a negative value represents downward motion and a positive value represents upward motion. Vertical velocity may also be represented as pascals per second ( $Pas^{-1}$ ), where a positive value is representative of the downward motion of air (Haby, 2005).

The maps of vertical velocity used in this study were obtained from the National Center for Environmental Prediction/Department of Energy (NCEP-DOE) reanalysis monthly pressure

files found at the following website: [http://nomad1.ncep.noaa.gov/cgi-bin/pdisp\\_mp\\_r2.sh](http://nomad1.ncep.noaa.gov/cgi-bin/pdisp_mp_r2.sh). Maps were generated for four different pressure levels, namely 500, 700, 850 and 1000 hPa for the months of June, July and August for each year of the study period 1998 – 2002. Vertical velocity maps available at this site can be obtained on a continental basis or for specified latitudes and longitudes. In order to obtain a clear picture of North Africa the range of 25-35° N and 25-35° E was chosen.

### **3.5 Back Trajectory Modelling**

Back trajectories are useful tools for determining the flow fields at different levels. In air quality studies trajectories are useful for determining the source–receptor relationships in air pollution field campaigns (Fast and Berkowitz, 1993).

#### **3.5.1 HYSPLIT (Hybrid Single Particle Integrated Trajectory) Model**

The HYSPLIT model is a product of the National Oceanic and Atmospheric Administration (NOAA), and had been modified by the Australian Bureau of Meteorology (Draxler and Hess, 1998). The upgrade has allowed for improved advection algorithms, updated stability and dispersion equations and the option to include modules for chemical transformations. Without the additional dispersion modules, HYSPLIT computes the advection of a single pollutant particle, or simply its trajectory (NOAA-ARL, 2005a).

This model is available interactively on the HYSPLIT website and allows for the meteorological data to be downloaded to a Windows computer. The trajectories were obtained from the following site: <http://www.arl.noaa.gov/ready/open/traj.html>

For this study, 5-day back trajectories were obtained at three heights, namely 2.5, 5 and 7.5 km for each of the summer months, that is June, July August, over the study period. These trajectories were used to create a composite plot in ARCMAP.

### **3.5.2 Lagrangian Analysis Tool (LAGRANTO) Model**

LAGRANTO is a three-dimensional trajectory model that is dependent on the wind fields of the European Centre for Medium-Range Weather Forecasts (ECMWF). This model allows for the calculation of kinematic Lagrangian trajectories (Spichtinger *et al.*, 2004). LAGRANTO was used to obtain back trajectories for the period of high ozone events that were investigated in order to determine the source regions during the study period. Back trajectory results of LAGRANTO were obtained from the Centre National de la Recherche Scientifique (CNRS), courtesy of J.P.Cammas.

### **3.6 Classification of Vertical Ozone Profiles**

Studying the vertical distribution of ozone is critical to understanding the photochemical and dynamic processes that are operational in the atmosphere and their role in the tropospheric ozone budget (Diab *et al.*, 2003). Generally, mean profiles are averaged by season or year, and presented together with a measure of variability. However the use of annual and seasonal mean profiles for such purposes is seen as being insufficient (Diab *et al.*, 2003).

An explanation that justifies this is that there is variability in the vertical structure of ozone on a day to day basis (Diab *et al.*, 2003). Diab *et al.* (2003) state that it is not only the altitudinal level and amounts of the highest and lowest values that change but that there also appear to be irregularities in the vertical structure of the profile, with single or multiple peaks occurring. Thus the profiles can take on a variety of structures that range from one that is uniform to a profile that exhibits marked vertical layering. Ultimately each ozone profile serves to represent a 'unique response' to the processes that are operating (Diab *et al.*, 2003).

Due to such evidence on the limitations of annual and seasonal mean profiles, scientists have been encouraged to search for new solutions. The study by Raghunandan (2002) proposed a new approach by using the mean profiles from hierarchically classified groups. For this study Raghunandan (2002) used the TWINSpan (Two-Way Indicator Species Analysis) programme to carry out cluster analysis.

With classification, the aim is to find patterns and order in the profiles. Studying the structure of the profiles should provide insight into the unique regional tropospheric ozone conditions that are operating at the time (Ramsay, 2003). These conditions would be determined by the time of year, processes operating (both dynamical and photochemical) and the dominant source (Ramsay, 2003).

The work by Ramsay (2003) was a continuation of the approach used by Raghunandan (2002) to analyse ozone data. However, in this study Ramsay (2003) successfully made use of the Statistical Package for the Social Sciences (SPSS version 11, 2001) to generate mean vertical ozone profiles for distinct clusters. Further, the use of SPSS was found by Ramsay (2003) to be more suitable for ozone data as opposed to TWINSpan which was used in studies by Raghunandan *et al.* (2003). This is due to the fact that TWINSpan was designed for dealing with ecological data and therefore data sets that are not 100% dense and data that are not normally distributed.

Ramsay (2003), states that the main aim of cluster analysis is to summarize large data sets with the result that similar entities are assigned to clusters according to a mathematical algorithm. Agglomerative methods proceed by a series of successive fusions of  $n$  entities into groups and are most commonly used. The output obtained from the classification process can be non-hierarchical arrangements, where entities are assigned to clusters based on their similarities or hierarchical arrangements which groups similar entities in a hierarchical manner (Ramsay, 2003).

For a cluster analysis, the Euclidean distance matrix is considered to be the most appropriate clustering method. The distance shows the gap that exists between any pair of units. Another important factor is the measure of similarity. In SPSS there are various options that are available, including methods such as group linkages, nearest neighbour etc. These methods are agglomerative, thus initially the  $n$  units being clustered form  $n$  clusters with one member per cluster and these are then combined sequentially according to their similarity with members of other clusters (Ramsay, 2003).

For this study, SPSS (version 11, 2001) was used for data classification. The MOZAIC ozone profiles which have ozone in ppbv and height in meters were submitted to cluster analysis.



Hierarchical cluster analysis was undertaken, with the square Euclidean distance approach being used. The agglomerations were stopped when the rescaled distance from the first total group was greater than 15 rescaled units. Results of the dendrogram were used to place profiles into their respective groups. SPSS was used to obtain a mean profile for each group. Composites of 5-day back trajectories were obtained for each group using the HYSPLIT model.

### **3.7 Summary**

The results of the methods described in this section will serve to highlight important information about tropospheric ozone over Cairo, Egypt. Firstly, a description and analysis of the vertical distribution of ozone at Cairo will be possible. This will allow for an assessment as to whether Cairo shares a summer lower tropospheric ozone enhancement similar to that observed over the Mediterranean Basin. Furthermore, an understanding of the factors that contribute to the enhancement will be obtained. Back trajectory modeling using HYSPLIT and LAGRANTO will enable the identification of source regions of enhanced ozone. Data classification of ozone profiles using SPSS will allow the identification of the minimum ozone profile and characterize the enhancement.

## CHAPTER 4

### RESULTS AND ANALYSIS

---

#### 4.1 Introduction

In recent years the Mediterranean Basin and its surrounding regions has been the subject of many observations and model studies which have highlighted characteristics of the Mediterranean region which are suitable for the formation of high summer tropospheric ozone levels. Previous investigations in the region have primarily focused on Europe and the eastern Mediterranean. Cairo is situated at the southern and eastern boundaries of the Mediterranean and is ideally located to investigate the tropospheric ozone budget, as representative of a North African coastal city.

This chapter provides a quantitative understanding of tropospheric ozone values over Cairo, Egypt. Specifically, a statistical summary of vertical profile data at Cairo is provided, as well as back trajectory modelling from enhanced layers to determine source regions of air masses. In addition to this, results of data classification are presented to provide insights into the vertical structure of ozone over Cairo. The results of the classification allow for more distinct patterns to emerge that are not evident from conventional seasonal means.

#### 4.2 Total Tropospheric Ozone

Figure 4.1 presents the mean monthly Total Tropospheric Ozone (TTO) above Cairo, for the study period, revealing that there is no distinct seasonal cycle. A maximum value of 42 DU occurs in April, which is also the time of the peak in total column ozone (Appendix A). Stratospheric-tropospheric exchange (STE) is most effective during spring and late winter (Danielson, 1968) during which time in the mid-latitudes, the lower stratosphere is subject to isentropic mixing (Guicherit and Roemeer, 2000). During spring it is also known that the altitude of the tropopause increases which allows for stratospheric air to flow into the tropopause (Appenzeller *et al.*, 1996). The relatively high TTO values (>35 DU) in

June and August most likely correspond to increased photochemical activity in summer months.

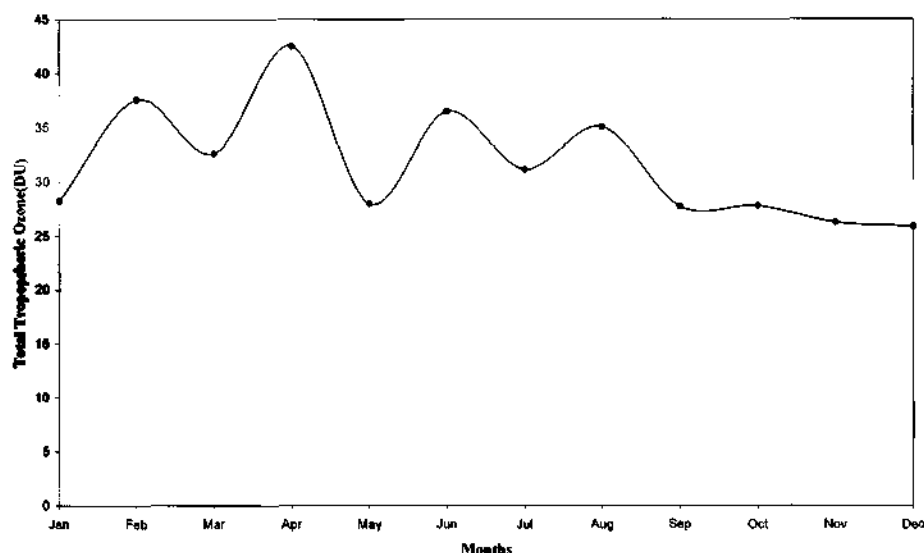


**Figure 4.1 Mean monthly TTO (DU) above Cairo for the period 1998 – 2002 based on MOZAIC aircraft data**

There has been no previous analysis of TTO over North Africa, though it is possible to compare results of this study to those obtained for European cities and similar latitudes which share similar dynamical influences. Kourtidis *et al.* (2002) integrated tropospheric ozone column data for the Greek city of Thessaloniki (40°38'N; 22°55'E) based on ozonesonde ascents. Results showed that for individual days in May and June TTO values ranged between 38 – 65 DU. From December to February, TTO was 20 – 30 DU and in early spring (March) 20 – 55 DU, with no data available for the rest of the months. A similar seasonal trend to the results of this study is evident. Highest values occur in late spring and summer and lowest values occur in winter.

Zbinden *et al.* (2005) studied Tropospheric Ozone Columns (TOC) calculated from the ground to the dynamical tropopause, for four mid-latitude locations namely, Frankfurt, Paris, New York and Japan, using MOZAIC data. The seasonal cycles of the two European cities reveal a similar broad maximum from April to August of about 35 DU, with a minimum value below 25 DU in December.

Further confirmation of the seasonal trend is available from satellite data. Fishman *et al.* (2003) determined tropospheric ozone calculated as the difference between total ozone amounts from the Total Ozone Mapping Spectrometer (TOMS) and stratospheric ozone

values determined by the Solar Backscattered Ultraviolet (SBUV) instrument. This was undertaken for the period of 1979 to 2000 for latitudes between 50°N and 60°S. Spring to summer ozone values over North Africa were found to range between 35 – 45 DU, whereas in autumn and winter values ranged between 30 and 35 DU.

The maximum of tropospheric ozone in spring is a common feature in many locations in the Northern Hemisphere (Chan *et al.*, 1998). The onset of the increasing values in spring is linked to stratospheric-tropospheric exchange though it is also suggested that the increase in solar radiation in spring results in more intense photochemistry on accumulated nitrogen oxides (NO<sub>x</sub>) and volatile organic compounds (VOC's) that have built up during winter, resulting in the greater ozone production (Li *et al.*, 1987; Vingarzan, 2004; Zbinden *et al.*, 2005). Furthermore, a shift or continuation in the tropospheric ozone maximum from spring to summer months is a signal that the contribution of the photochemical production of tropospheric ozone, due to the emissions of the anthropogenically produced ozone precursors, is the determining factor in the tropospheric ozone budget (Kalabokos *et al.*, 2000).

#### **4.3 Vertical Distribution of Tropospheric Ozone**

The vertical distribution of ozone in the troposphere has important implications for the oxidizing capacity of the troposphere as well as an influence on the radiative forcing of the atmosphere (Creilson *et al.*, 2003). A statistical summary of the vertical profile data is presented so as to determine the seasonal background and maximum ozone concentrations over Cairo. The determination of these seasonal means allows for the detection of various chemical and dynamical influences.

MOZAIC ozone profile data for the study period were used to generate a contour plot showing the seasonal variation of the tropospheric vertical ozone structure over Cairo (Fig 4.2). Near surface values generally do not exceed 40 ppbv, with the exception of the summer months (June, July and August) when values range between 40 and 60 ppbv. This trend is indicative of the seasonal solar radiation cycle as high amounts of ozone can be photochemically produced in the presence of strong solar radiation and sufficient ozone precursor gases, which enhance the rate of ozone formation. The role of sunlight as a major requirement for the production of tropospheric ozone was discussed in Chapter 2 and the

well known accompanying summer maximum in tropospheric ozone noted by many authors, for example Chameides *et al.* (1992) and Newchurch *et al.* (2003).

In the lower troposphere (1- 4 km), June and August ozone values are enhanced relative to other months. This is not unexpected as Cairo, located in the Mediterranean region, shares similar conditions for ozone formation to locations in southern Europe as discussed in Chapter 2. The summer ozone enhancement extends to higher levels in the troposphere (up to 8km) and peak values of 70 – 80 ppbv are found. The decreasing trend in ozone above 8km, suggests that this mid-tropospheric summer ozone enhancement is not linked to stratospheric input and requires further investigation.

In the upper troposphere, high ozone values of over 150 ppbv are observed in February and April, indicative of stratospheric injection. STE is known to be a maximum in spring as noted earlier.

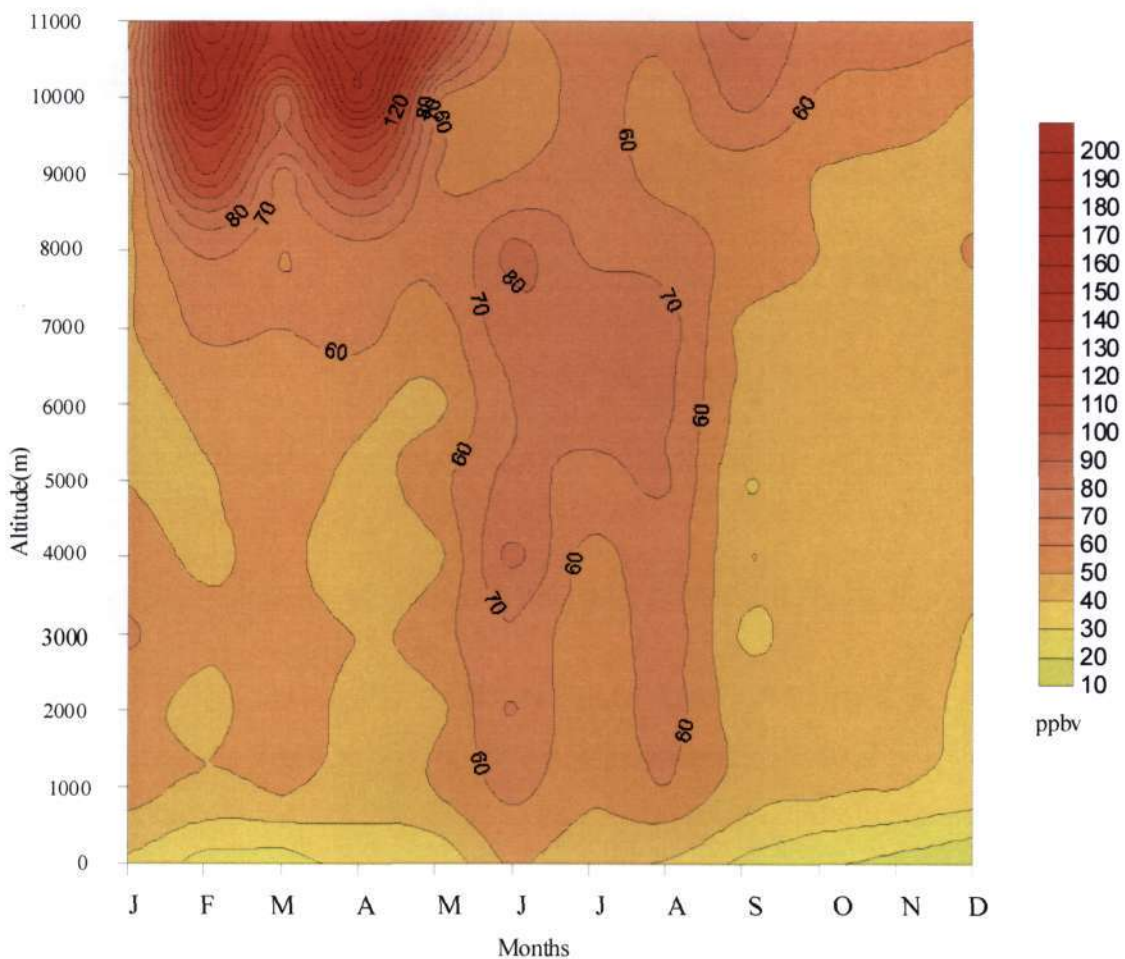


**Figure 4.2 Seasonal variations in tropospheric vertical ozone structure (ozone in ppbv) over Cairo during the period 1998-2002**

The seasonal variation in the vertical distribution of ozone at Athens is presented for comparison. Athens is located at 37° 58'N and 23° 43'E, approximately 7° north of Cairo. It too experiences a Mediterranean climate, with mild, wet winters and hot, dry summers. Furthermore, Athens is known to be a heavily polluted city due to it containing 40% of all Greece's industry and 50% of all the automobiles in Greece (Gusten *et al.*, 1998). In Figure 4.3 the seasonal variation of the tropospheric vertical ozone structure over Athens is presented. Lower tropospheric maximum values are found in summer (May to August) and range from 70 - 80 ppbv, whilst minimum values occur from October to January (Kalabokas *et al.*, 2004). Upper tropospheric values show a peak in spring, which coincides with the stratospheric peak as well as a peak in mid-summer. Thus, as opposed to Cairo, this plot displays two upper tropospheric maxima one in spring and the other in mid-summer. The distinct mid-tropospheric ozone enhancement observed over Cairo is not present over Athens.

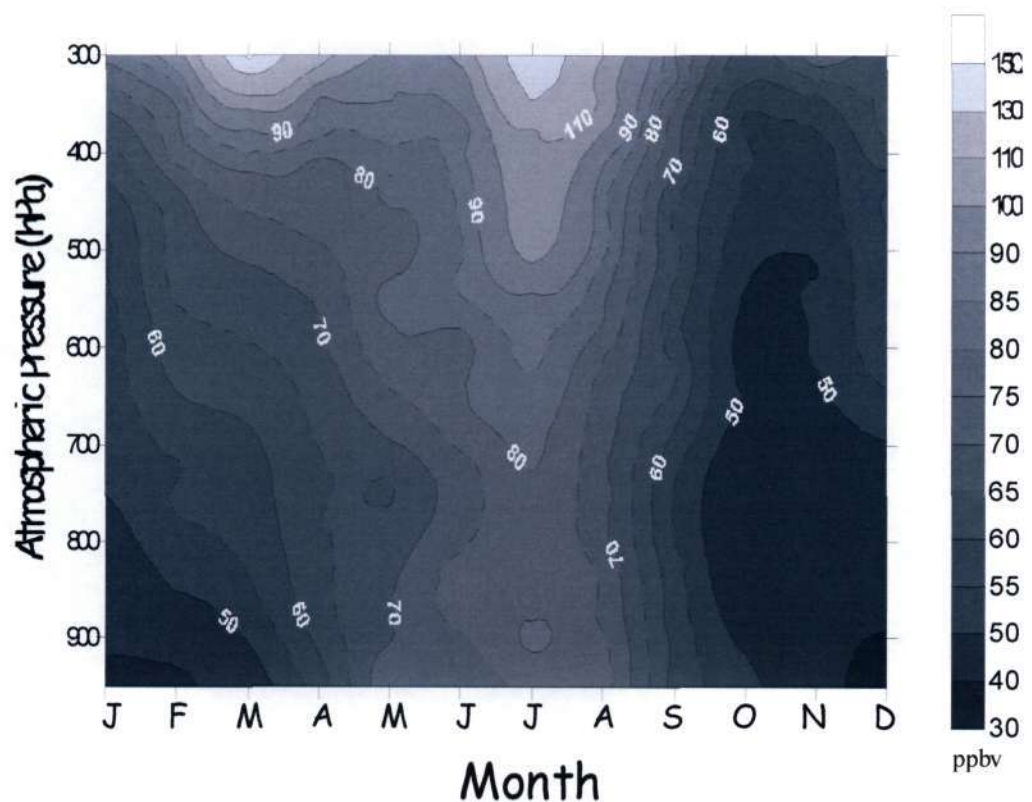


**Figure 4.3** Seasonal variation of the tropospheric vertical ozone structure (ozone in ppbv) over Athens, Greece (Kalabokas *et al.*, 2004).

Figure 4.4 shows the mean monthly tropospheric ozone concentrations at selected altitudes for the lower, middle and upper troposphere. The seasonal cycle of near-surface ozone peaks in the summer months of June, July and August. This enhancement extends from the surface to 3 km, where the most notable enhancement occurs in June. July mean ozone values are relatively lower than those of June and August (Fig.4.4a). The lowest near-surface mean ozone values are observed in December with values less than 20 ppbv. For the rest of the year near-surface values are generally between 20 and 40 ppbv.

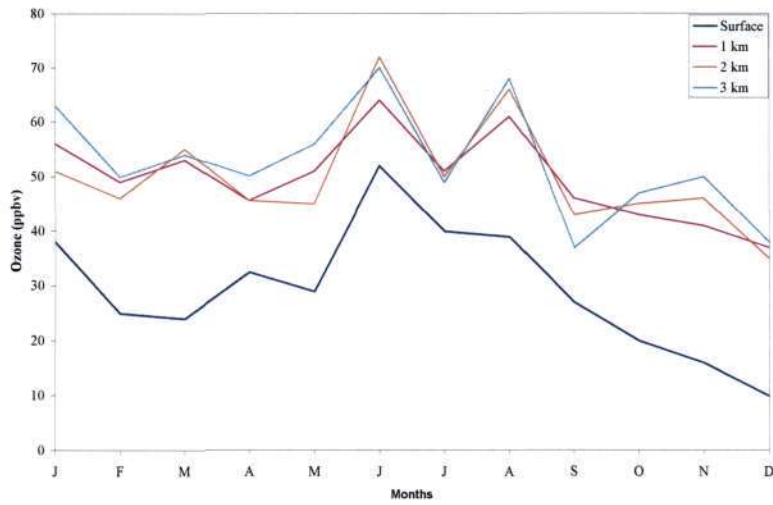
In the middle troposphere (Fig.4.4b), mean ozone values are below 55 ppbv up to a height of 6 km from January to May. For this period at an altitude of 7 km, the mean ozone values are slightly higher, ranging between 50 – 65 ppbv. In June, mean ozone values approach 80 ppbv and it is noted that values are particularly high at the 4 km level. In August mean ozone values range between 50 - 80 ppbv. However, for the month of July at 4 to 5 km the ozone values are relatively lower (generally below 60 ppbv), than the other summer months. At the 6 and 7 km levels, ozone values are consistently high throughout summer, including the month of July.

In the upper troposphere ( $\geq 9$  km, Fig.4.4.c), the first half of the year displays high mean ozone values with notable peaks in February and April. Ozone values exceed 150 ppbv, at both the 10 and 11 km levels. Studies such as Austin and Follows, (1991) which was conducted in the Northern Hemisphere, have also shown high spring values in the upper troposphere which is related to the intrusion of ozone rich stratospheric air. Law *et al.* (2000) also highlighted well defined seasonal variations in the upper troposphere for the Northern Hemisphere, with a peak in spring based on monthly mean ozone concentrations using MOZAIC aircraft data. Law *et al.* (2000) showed that the maximum values were related to the position of the flight level relative to the tropopause, thus allowing for the possibility of stratospheric air to be injected in the troposphere.

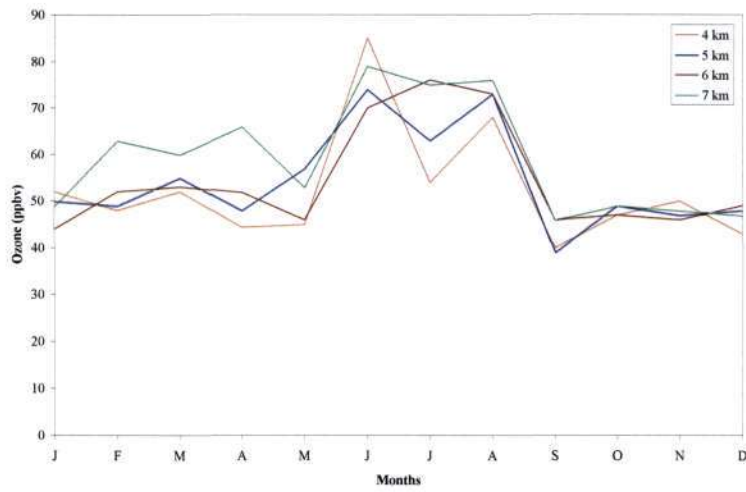
From June onwards there is a dramatic drop in ozone values in the upper troposphere. Concentrations are fairly consistent ranging between 50 and 75 ppbv, indicating that stratospheric-tropospheric injection of ozone rich air is unlikely to occur. The seasonal variation in ozone at the 8 km level is interesting in that it is distinct from the variations above 9 km, suggesting that 9 km is the lower limit of effects of STE.



(a)



(b)



(c)

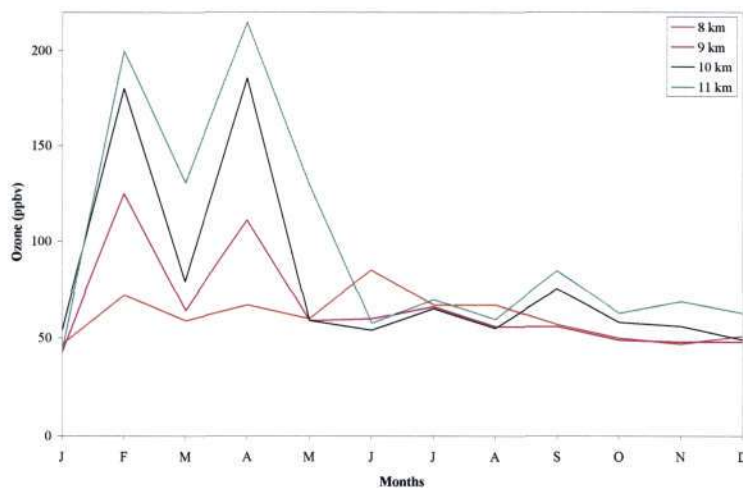


**Figure 4.4** Seasonal plots of MOZAIC ozone data for the a) lower, b) middle and c) upper troposphere



It has been well established (Bojkov, 1986; Kalabokos *et al.*, 2000; Varotsos *et al.*, 2004) through measurements throughout the troposphere that ozone displays seasonal and inter-annual variations. Figure 4.5 a) shows tropospheric mean ozone profiles over Cairo for winter (DJF), summer (JJA), autumn (SON) and spring (MAM) based on MOZAIC data.

In the boundary layer a steep gradient is observed across all the seasons. This is characterized by a rapid increase in ozone from the surface to 1 km. This is indicative of local pollution, which has also been reported in recent studies, such as Zakey *et al.* (2004). It should be noted that the steepest gradient in the boundary layer occurs in summer. In spring and winter, ozone values are about 20 ppbv lower than in summer, indicative of substantial photochemical production of ozone in the summer months.

Data from the Egyptian Environmental Affairs Agency-Environmental Information and Monitoring Programme (EEAA-EIMP) in Cairo, have revealed that highest surface ozone values are found from midday to the afternoon with the summer months having the highest recorded values at an average of 71ppbv ( $\sim 140\mu\text{g}/\text{m}^3$ ) (EEAA-EIMP, 2000a). The night-time values have revealed a minimum of less than 20 ppbv ( $40\mu\text{g}/\text{m}^3$ ). In summer, surface ozone concentrations are 39 – 56 ppbv ( $78 - 108\mu\text{g}/\text{m}^3$ ) in Europe (Ribas and Penuelas, 2004). A further study by Kourtidis *et al.* (2002) has shown that summer surface ozone values at Sidi barani, a coastal Egyptian city located at  $31^{\circ}37\text{ N}$  and  $25^{\circ}25\text{ E}$ , vary between 39 – 64 ppbv. All studies support the summer surface maximum and correspond well with the mean summertime surface ozone value of about 42 ppbv at Cairo, obtained in this study.

The mean spring, autumn and winter profiles show fairly uniform concentrations from 2 – 8 km (Fig 4.5a), in the order of 40-50ppbv. By comparison, the mean summer (JJA) profile shows values that are consistently greater than 60 ppbv and peak values of 70 - 80 ppbv in the mid-troposphere. Thus, there is an enhancement of 40 – 60% in summer, which will be investigated further in the following sections.

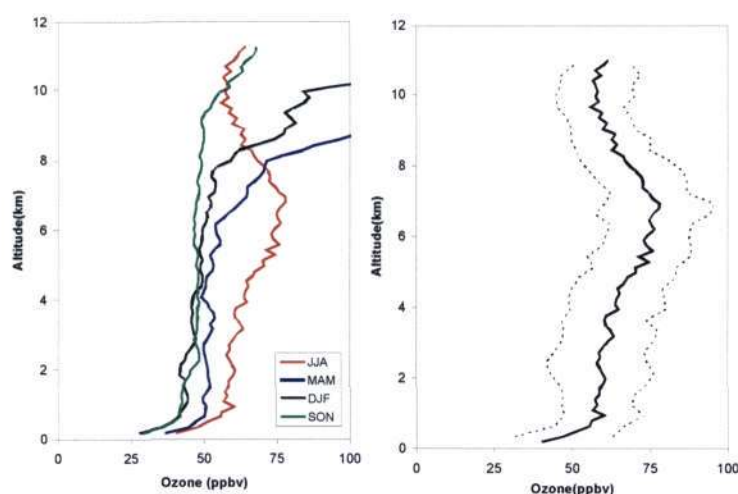


**Figure 4.5 a) Seasonal mean ozone profiles over Cairo Egypt. b) Summer mean with a single sigma envelope**

Figure 4.5 (b) presents the mean ozone profile for summer (JJA) with a single sigma envelope. This graph gives an indication of the variation of each value about the mean, where the dotted lines indicate fluctuations within one standard deviation from the mean. The most significant variability occurs in the middle troposphere.

#### 4.4 Chemical and Dynamical Influences on the Summer Enhancement over Cairo

The seasonal cycle of ozone is determined by numerous processes that act on various temporal and spatial scales that range from the impact of local phenomena to those of a more regional or global scale (Monks, 2000). In order for there to be a comprehensive understanding of the contributing factors to the seasonal ozone enhancements, in particular in the mid-troposphere, there is a need to investigate the influence of photochemistry and horizontal and vertical transport at each of these scales.

With regard to the mid-tropospheric ozone enhancement, there is a need to establish if the ozone enhancements in the middle troposphere could potentially be created in the middle troposphere. Studies by Wang *et al.* (1998) have shown that the middle troposphere is a major source region for ozone in the troposphere, despite it not being a region of net ozone production. This has been further supported by studies by Thompson *et al.* (1996), who

have shown ozone production in the middle troposphere to be more efficient than that of the lower troposphere. Furthermore, lightning is known to influence ozone production, particularly over the tropical regions as it directly releases  $\text{NO}_x$  into the middle and upper troposphere (Strand and Hov, 1996). The lifetime of  $\text{NO}_x$  in the boundary layer is about one day which does not allow for transport over long distances. Therefore the only source of  $\text{NO}_x$  in the mid-troposphere is likely to be lightning (Wenig *et al.*, 2003). Alternatively, it is important to consider whether conditions exist for locally created near-surface pollution to be uplifted to the middle troposphere.

A third alternative explanation for the mid-tropospheric ozone enhancement could be the influence of intercontinental air masses. Pollution from industrial regions of the Northern Hemisphere is known to influence air quality on intercontinental scales (Jacobs *et al.*, 1999). In the Mediterranean Intensive Oxidant Study (MINOS) campaign the role of long-range transport of polluted air masses in the summer enhancements was conclusively noted (Lelieveld *et al.*, 2002).

Finally, the intrusion of ozone from the lower stratosphere to the upper and middle troposphere has been the subject of numerous studies (Baray *et al.*, 1998; Bithel *et al.*, 2000; Gouget *et al.*, 2000; Mahlman, 1997; Waugh *et al.*, 2000). In this study, the occurrence of the mid-tropospheric ozone peak is isolated and occurs when upper troposphere ozone values are relatively lower (Fig. 4.2). Furthermore, STE is only likely to occur in the first half of the year in spring (Fig.4.4.c). Therefore, the possibility of a stratospheric origin of ozone enriched air is not explored as a contributing factor in this study.

The following sections attempt to explore the relative influences of these processes.

#### **4.4.1 Local Sources of Ozone Precursors**

##### **4.4.4.1 General Overview of Local Pollution Sources in Cairo**

Surface ozone concentrations are dependent on complex combinations of meteorological influences and chemical processes. Figure 4.5 shows high boundary layer concentrations of ozone throughout the year with a summer enhancement. There are numerous sources that create pollution within Cairo and the concentrations of air pollutants are a sum of the interaction from these sources. The sources of air pollution at ground level consist of emissions from various industries and motor vehicles. These emissions are close to the surface and can be trapped under stable atmospheric conditions.

According to EL-Shahawy and Hanna (2003), the contributing factors that have previously led to high surface pollution events have been the frequent prevalence of an upper air high pressure ridge over the Nile Delta and the occurrence of thermal temperature inversions. Surface temperature values for Cairo reach a maximum of over 40° C during the day in summer and reach a minimum of about 11° C at night (EEAA-EIMP, 2000b). With such a marked diurnal temperature range, the development of surface radiation inversions at night is likely to be common. Indeed, it has been noted in pollution studies over the city that very stable atmospheric conditions inhibit dispersion of pollutants (Sivertsen, 1999).

Data from local pollution monitoring initiatives have revealed the diurnal characteristics of ozone, with a minimum ozone value occurring during the early morning and the maximum ozone value in the early afternoon (Fig. 4.6). Daytime maxima of 90 to 100  $\mu\text{g}/\text{m}^3$  (46 – 51 ppbv) are observed. The night time minimum in ozone can be quite pronounced due to the rapid reaction with NO (El-Hussainy *et al.*, 1999). This is linked to traffic and industrial activities that create NO<sub>x</sub> (Mohamed, 2004).

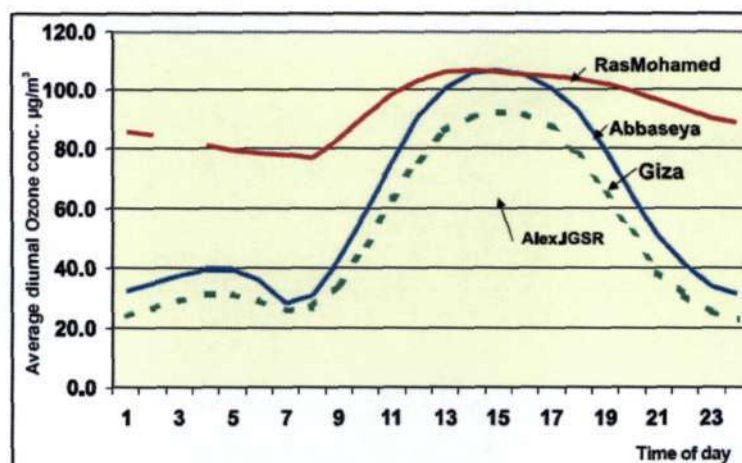


**Figure 4.6 Annual average diurnal variations of ozone measured in Egypt 2000 -2002 (Mohamed, 2004)**

#### 4.4.4.2 Nitrogen Dioxide

Local sources of  $\text{NO}_x$  in Cairo are generally known to originate from a number of sources that include vehicular and industrial emissions, and emissions from burned agricultural and domestic waste (Ezz, 2003). The ambient air quality limit values in Egypt for  $\text{NO}_2$  are  $400 \mu\text{g}/\text{m}^3$  and  $150 \mu\text{g}/\text{m}^3$  for hourly and daily averages respectively (EEAA, 1994). According to the results of the Cairo Air Improvement Project (CAIP), the levels of  $\text{NO}_2$  generally fall within the limits prescribed for  $\text{NO}_2$ . However, this did not apply to industrial areas or those areas with high levels of traffic congestion, where values of  $\text{NO}_x$  often exceeded Egyptian and the United Kingdom ( $150 \mu\text{g}/\text{m}^3$ ) standards, as depicted in Table 4.1. The high  $\text{NO}_2$  values provide evidence of substantial local pollution.

**Table 4.1 24 Hour Average  $\text{NO}_2$  ( $\mu\text{g}/\text{m}^3$ ) average concentrations measured in at selected stations in Cairo during June – August 2000 (adapted from EEAA-EIMP, 2000d; EEAA-EIMP, 2000e and EEAA-EIMP, 2000f)**

Station Name	June	July	August
Giza	36	51	36
Nasr City	133	152	114
Fum Elkhlig	106	123	82
Qulaly	121	164	125
Gomhomeya	168	156	104
Tabbin	41	50	42
<b>Average <math>\text{NO}_2</math></b>	<b>101</b>	<b>123</b>	<b>89</b>



With the exception of EEAA-EIMP data presented above, surface NO<sub>2</sub> data for Cairo are not readily available for analysis, though densities of NO<sub>2</sub> are detectable from satellite platforms. Beirle *et al.* (2003) provided a statistical analysis of weekly cycles of tropospheric NO<sub>2</sub> based on vertical column densities (VCD's) derived from Global Ozone Monitoring Experiment (GOME) satellite data (Fig. 4.7). VCD's of NO<sub>2</sub> are shown as average daily values that have been normalized according to the median weekly value. Values of NO<sub>2</sub> peak mid-week and the lowest values are recorded on Friday, which is a religious day in Cairo. This weekly cycle provides key evidence to support the existence of local pollution, in particular vehicular and industrial emissions.

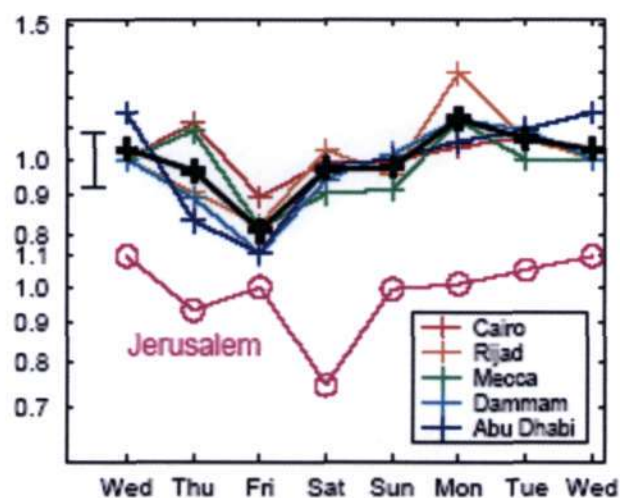


**Figure 4.7 Weekly cycle of mean tropospheric NO<sub>2</sub> (1996 – 2001) normalized according to weekly mean value (Beirle *et al.*, 2003)**

Further evidence of local pollution is provided by the shape of the diurnal variation curve in ozone (see Fig. 4.6). Areas that have sufficient amounts of NO<sub>x</sub> display diurnal cycles with maximum values in the late afternoon and lowest values in the early mornings, with the higher values being a result of photochemical production. The minimum values are due to various factors such as deposition, the conversion of NO<sub>2</sub> to O<sub>2</sub> and the reduction of mixing at night that reduces the exchange of pollutants between the lower and middle troposphere. NO<sub>x</sub> surface data thus provides supporting evidence for local pollution being a contributing factor in the ozone concentrations in the lower troposphere. The lifetime of

NO<sub>x</sub> in the lower troposphere is too short to allow for transport into the middle troposphere.

Another known source of near-surface NO<sub>x</sub> is from biomass burning. Summer periods of biomass burning over the eastern Mediterranean are known to result in a significant buildup of NO<sub>2</sub> in the region (Dermitzaki *et al.*, 2004). In Cairo, over 1 million acres of rice is grown each year which results in over two million tons of waste that is burnt. However, this burning process intensifies from mid-winter to spring (Waguhi, 2002). Therefore, the impact of biomass burning is not a common feature in summer months and the related pollutants are unlikely to contribute to the summer ozone enhancement.

Figure 4.8 presents images of mean column NO<sub>2</sub> densities over Africa for the summer months of 1998 from the GOME satellite. These images provide an overall representation of NO<sub>x</sub> concentrations in the region as opposed to only surface sources.

From these images Cairo stands out as having high tropospheric NO<sub>2</sub> levels for summer with mean NO<sub>2</sub> concentrations that range from  $2 \times 10^{15}$  molec/cm<sup>2</sup> to  $6 \times 10^{15}$  molec/cm<sup>2</sup>. NO<sub>2</sub> satellite images for 1999- 2001 from GOME and images from the SCanning Imaging Absorption SpectroMeter for Atmospheric CHartography (SCIAMACHY) satellite for 2003 are presented in Appendix B. These images show a similar trend to that observed in Figure 4.10. These maps provide evidence that NO<sub>2</sub> concentrations are high over Cairo, which in part, can be linked to the local pollution sources. However, other factors such as lightning can contribute to NO<sub>2</sub> levels, which is discussed in section 4.4.3. Ultimately the preceding information on NO<sub>x</sub> levels indicates that one of the prime conditions for the production of ozone is being met in the region.

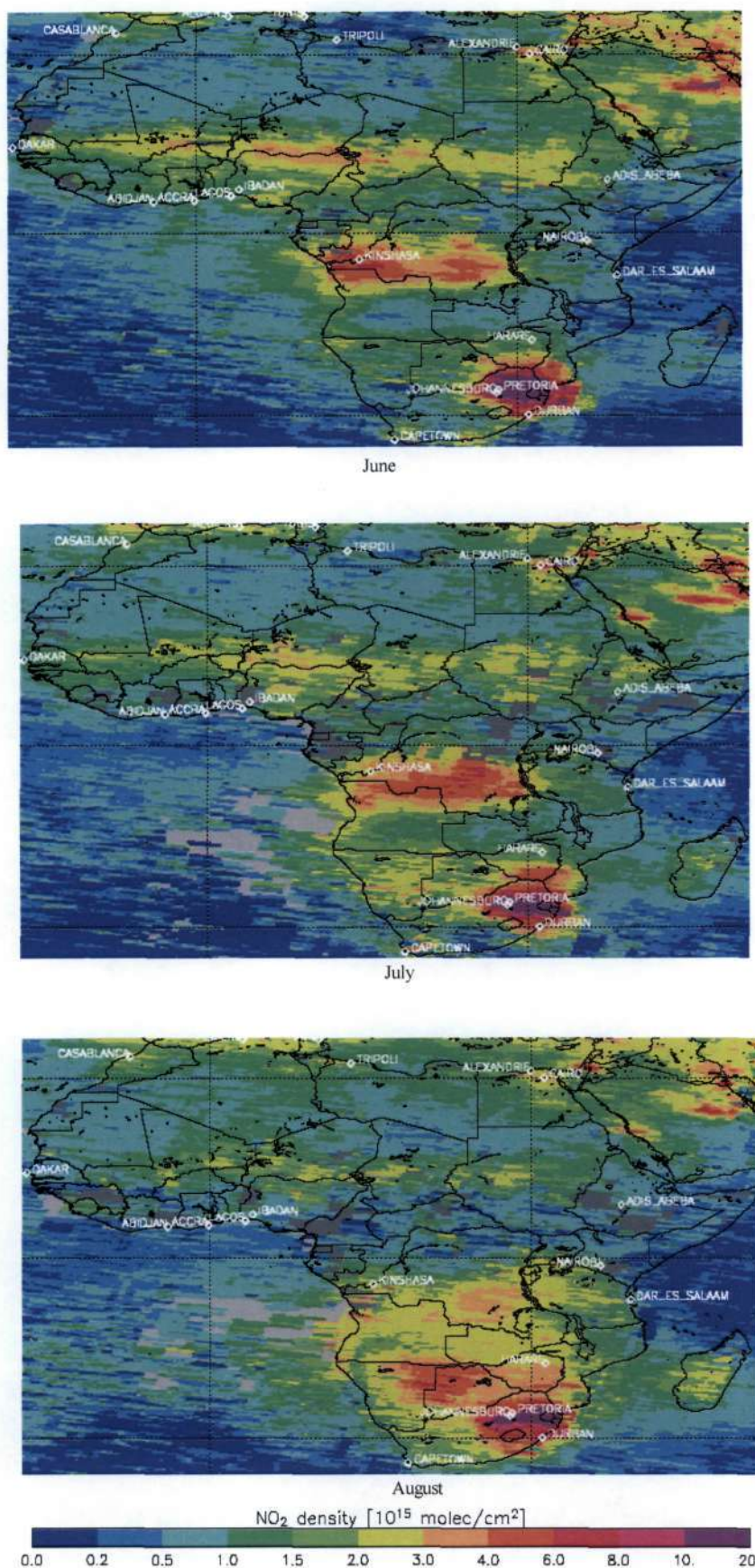


**Figure 4.8 Tropospheric NO<sub>2</sub> over Africa for June, July and August (JJA) 1998 from the GOME satellite (TEMIS, 2004b)**



#### 4.4.4.3 Carbon Monoxide

Carbon monoxide (CO) is emitted from the incomplete combustion of fossil fuels, biomass burning and the oxidation of methane and non methane hydrocarbons. It is involved in the budget of tropospheric ozone through oxidation by the hydroxyl radical (OH) in the presence of  $\text{NO}_x$ , to be a net source of tropospheric ozone (Crutzen, 1973). CO is one of the main ozone precursors and is emitted directly by human activities, thus it makes a good tracer species for anthropogenic emissions and helps us to differentiate peaks of ozone concentrations. Figure 4.9 presents mean CO profile over Cairo, based on MOZAIC data analysed as part of this study.

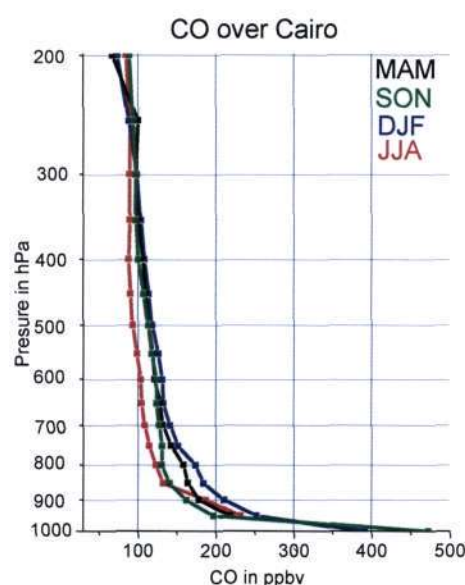


**Figure 4.9 Mean seasonal CO profiles (CO in ppbv) over Cairo for the period 2000 -2002 based on MOZAIC data**

CO values of the order of 200-500 ppbv are recorded near the surface, indicative of high local pollution levels. Sources of CO in Cairo include power stations and numerous smelters, cement industries and over one million gasoline powered motor vehicles operating in the city. In addition to this, other activities that contribute to CO levels include open air burning of agricultural and domestic waste (Ezz, 2003, Waguih, 2002). With the exception of biomass burning which occurs mainly in winter, the other sources contribute to CO throughout the year.

This high concentration of surface pollution is to be anticipated as information from the Egyptian Environmental Agency (EEA) has reported exceedances of national air quality standards and have consequently implemented many strategies to combat high CO levels (Ezz, 2003). According to EEAA-EIMP data (EEAA-EIMP, 2000d; EEAA-EIMP, 2000f), measurements of CO taken at Cairo and other Egyptian cities show that CO levels are greatest in Cairo, with frequent exceedances of the Egyptian 8-hr limit ambient air quality value, which is  $10\text{mg/m}^3$  (EEAA, 1994), as shown in Figure 4.10, which presents the frequency of exceedances of this limit at 3 sites in Cairo.

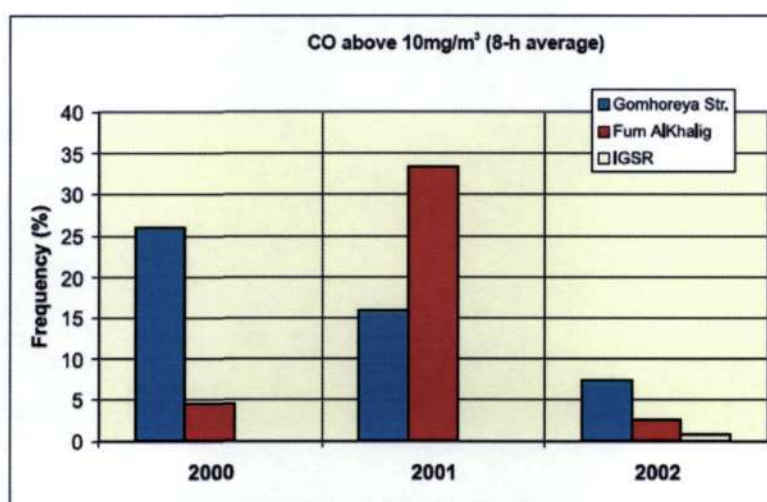


**Figure 4.10** Frequency of exceedances of the 8-hour mean CO AQL value of  $10\text{mg/m}^3$  at three sites in Cairo (Mohamed, 2004)

Furthermore, values of CO show strong diurnal variations when the measurements are in streets or close to roads. The lowest values are generally recorded at night-time between the hours of 02:00 and 06:00, whereas the values are nearly doubled by morning (Sivertsen, 2000).

High near-surface CO values occur in winter (DJF) (Fig.4.9). The occurrence of elevated CO concentrations in winter is linked to low concentrations of the principal sink of CO, which is the OH radical (Bey *et al.*, 2001).

In the vertical CO profile (Fig 4.9) throughout the remainder of the troposphere, mean CO concentrations vary little across seasons (100-150 ppbv) and are consistent with values that are generally found in the mid-latitudes.

Low CO values in the upper troposphere eliminates the possibility of enhanced pollutants in the upper troposphere contributing to the spring ozone enhancement that was evident from TTO values in Section 4.1. The low values in the middle troposphere also imply that the observed summertime ozone enhancement is not linked to enhanced values of CO. Furthermore, it means that the enhancement is in fact greater than expected background ozone values. CO is known to act as a principal sink for the OH radical and is thus used up as shown in equations 4.1 and 4.2, reducing its lifetime in the troposphere. CO reacts with OH to form hydroperoxy radicals as shown below (Wang *et al.*, 1998).



The above reaction represents the most significant OH- radical sink in the troposphere.

However, it is important to note that CO emissions occur at the surface and that the concentrations of CO decrease away from its sources. Therefore it is expected that the highest mixing ratios of CO will be found close to the surface and lower mixing ratios higher up. As opposed to this, ozone is produced by its reaction with NO, therefore ozone is not only produced near to the source regions of its precursors but it is also produced when its precursors are transported (de Laat, 2002). This process of ozone production is described as the “mix-then-cook” mechanism, where ozone values can be expected to be higher in the free troposphere than at the surface. Chatfield and Delany (1990) have clearly demonstrated this phenomenon whereby ozone does not show immediate changes during mixing, but with the injection of NO<sub>x</sub> and the passing of a few days, tropospheric ozone production continues in the middle and upper troposphere. This is generally linked to the vertical redistribution of ozone precursors by convection and subsequent transport. In the middle troposphere the lifetime of ozone will be dependant on the moisture levels as it will be removed by the reaction with OH. Moisture is known to decrease with altitude therefore the lifetime of ozone can be longer.

From this discussion it is clear that a negative correlation exists between the middle tropospheric ozone enhancement and the CO concentrations. This indicates that the observed ozone has not been created over Egypt or its vicinity.

#### 4.4.2 Mid-Tropospheric Sources of Ozone

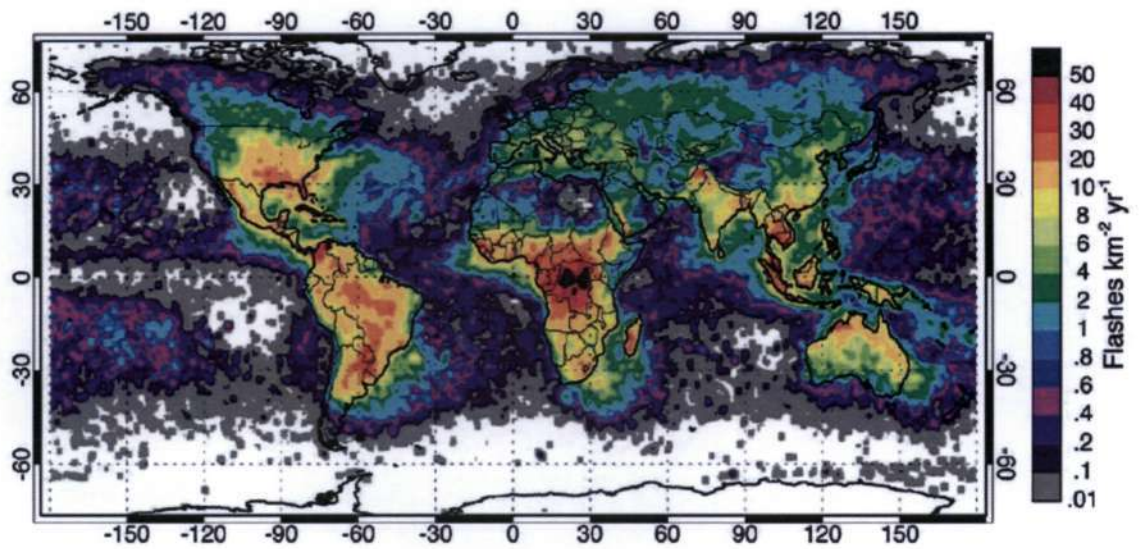
Lightning is the main source of  $\text{NO}_x$  directly into the middle troposphere and can cause an increase in  $\text{NO}_x$  by about 90% which may increase the amount of ozone by 30 % (Cutlip, 2003). Thus it has been shown that lightning plays a key role in the production of ozone.  $\text{NO}_x$  has been documented in numerous studies (Bunce, 1998) as being the limiting factor in photochemical ozone production. If the contribution of lightning  $\text{NO}_x$  to the mid-troposphere is low then the amount of ozone that is actually produced in the mid-tropospheric region will be low (Pickering *et al.*, 1992)

$\text{NO}_x$  production by lightning is seasonally dependent and ozone created by lightning  $\text{NO}_x$  is known to be at its maximum in the middle troposphere and is associated with convection in synoptic systems (Roelofs *et al.*, 2003). During the MINOS campaign it was shown that lightning contributed 6 -10 ppbv to the ozone that was observed in the middle troposphere. Lightning  $\text{NO}_x$  emissions vary with solar heating. In the case of North Africa the highest production of  $\text{NO}_x$  by lightning occurs in the summer months of June, July and August and is evident from Figure 4.11. However, in comparison to other regions such as Equatorial Africa, particularly the Democratic Republic of Congo and the south eastern parts of the United States, the number of lightning flashes annually and in summer does not result in North Africa being regarded as a hot spot region of lightning activity.

Based on these observations relative to other regions of the world, it is concluded that it is unlikely that lightning is a major contributor to the mid-tropospheric summer peak in ozone. Production of ozone in the mid-troposphere therefore does not account for the ozone enhancements observed.



(a)



(b)

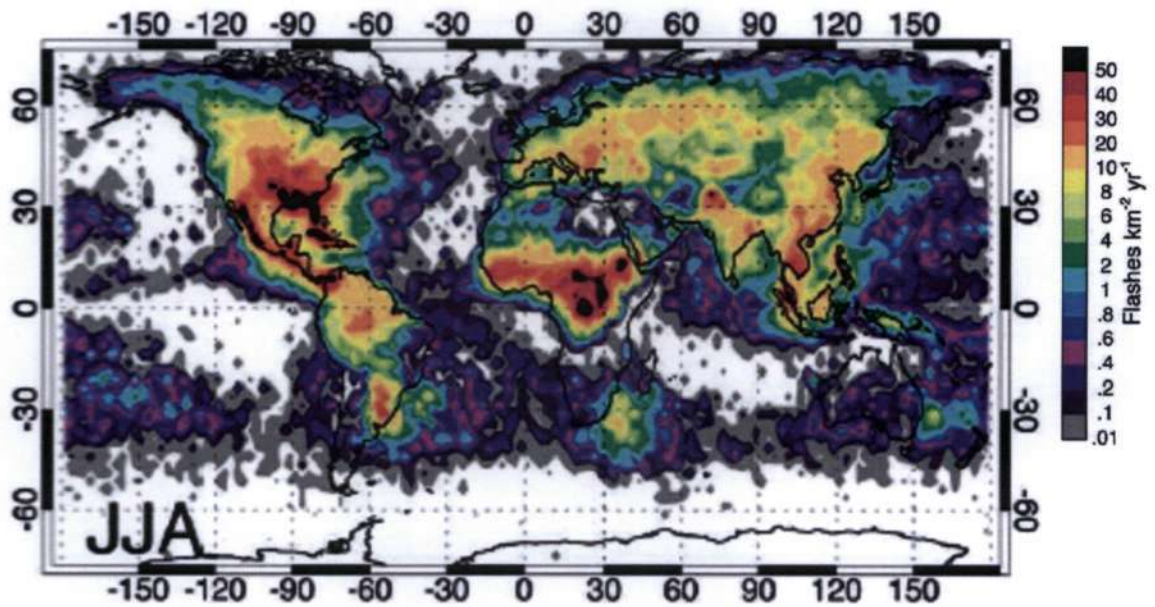


Figure 4. 11 a) Annual seasonal distribution of lightning activity b) seasonal distribution of lightning activity for June July and August annualized in units of  $\text{fl km}^{-2} \text{yr}^{-1}$  (Christian *et al.*, 2003)

#### 4.4.3 Vertical Exchange between the Boundary Layer and the Free Troposphere

Since the 1960s/1970s, there has been a continuing debate about the role of vertical transport versus local photochemical formation with regard to the annual tropospheric ozone budget. Vertical exchange of chemical constituents between the boundary layer into the free troposphere is thought to be a major mechanism for connecting continental scale source regions of primary pollutants (Lindskog *et al.*, 2005). A summer mid-tropospheric peak in ozone has been detected over Cairo and it is necessary to determine if the pollution sources from the surface could be a contributing factor. Thus, there is a need to establish the extent and nature of vertical mixing in the area. Furthermore, it would be useful to ascertain if there are stable layers that could inhibit mixing.

Vertical velocity maps for over Cairo are presented in Figure 4.12 and in Appendix C. At the 500 hPa to 850 hPa pressure levels, the region is dominated by sinking motion of air indicated by positive values of vertical velocity. At the 1000 hPa level, negative values indicate that air is being lifted. Numerous studies (Pickering *et al.*, 1991, Pickering *et al.*, 1993, Kley *et al.*, 1993 and Thompson *et al.*, 1997) have linked variability of ozone and convection. Convection is known to lead to the upward transport and diffusion of chemical species that influences the production of tropospheric ozone (Baray *et al.*, 1999). Thus ozone and its precursor gases can be moved from the boundary layer into the middle and upper troposphere.

However, in this study the air is unable to penetrate above 1000 hPa, which means that the near-surface pollution is confined to the lower troposphere.

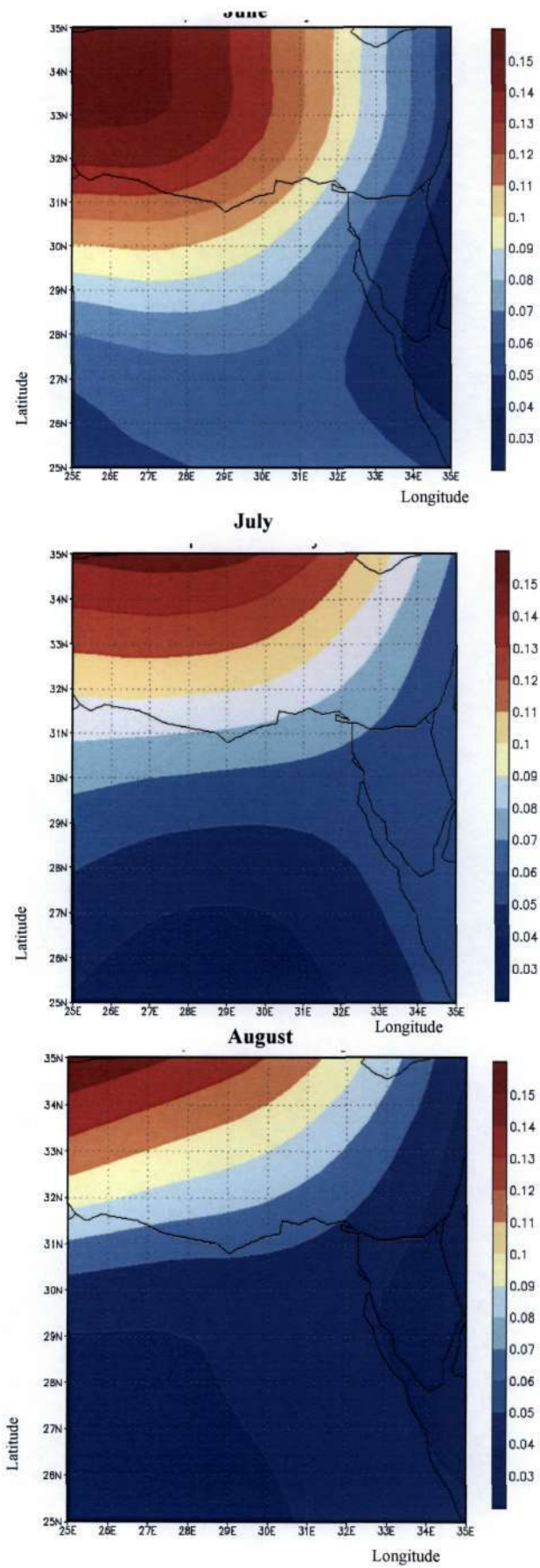
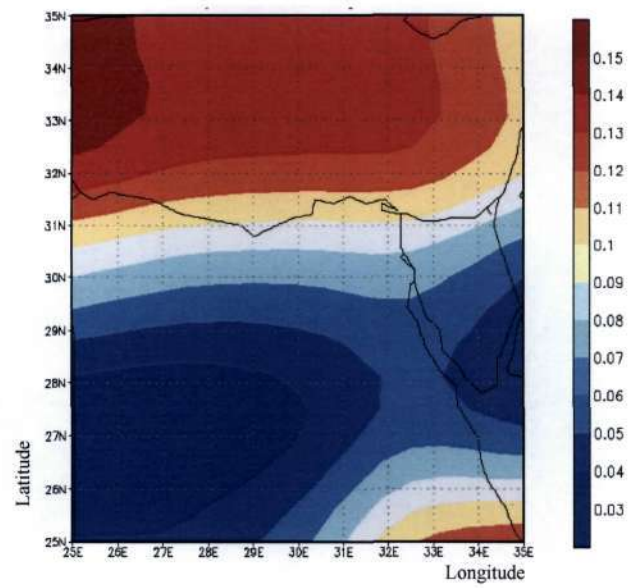
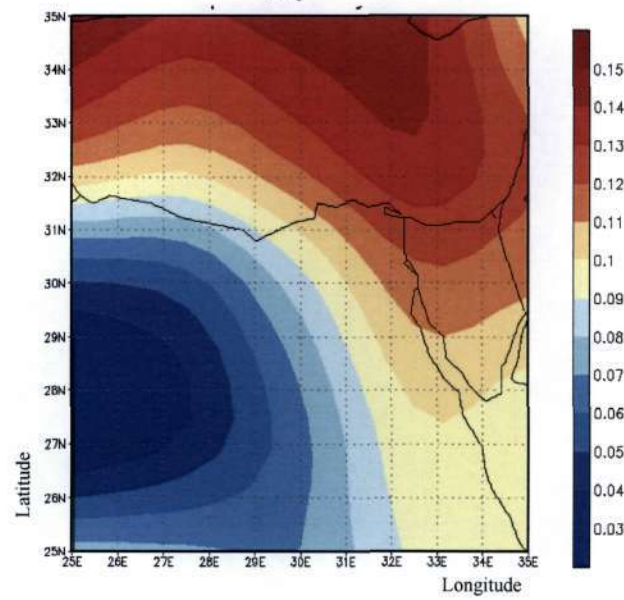


Figure 4.12a) 500 hPa vertical velocity (Pa/s) Maps JJA for 1998 (NCEP-DOE reanalysis data, 2004)





**July**



**August**

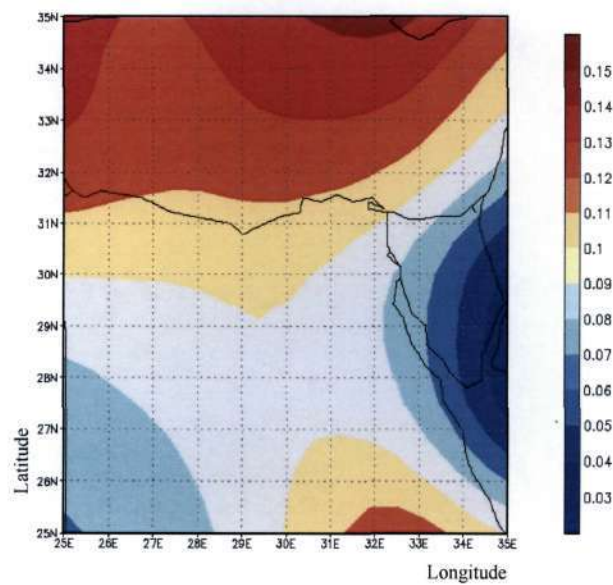


Figure 4.12b) 700 hPa vertical velocity (Pa/s) Maps JJA for 1998 (NCEP-DOE reanalysis data, 2004)



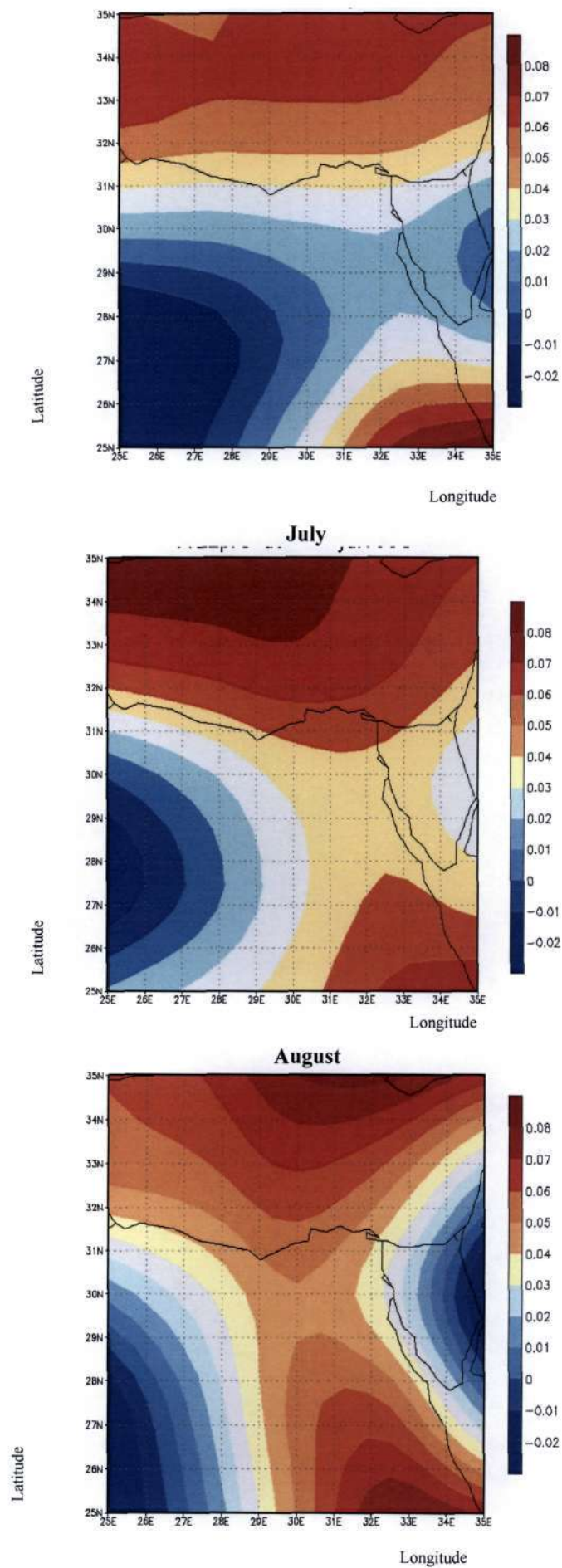
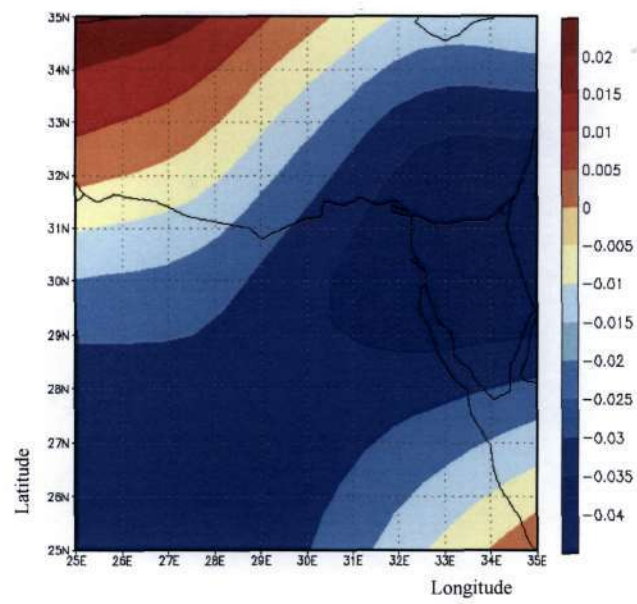
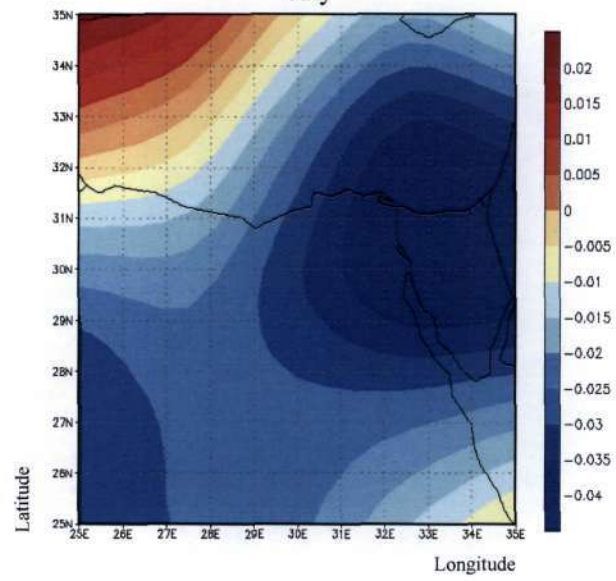


Figure 4.12 c) 850 hPa vertical velocity (Pa/s) Maps JJA for 1998 (NCEP-DOE Reanalysis Data, 2004)



July



August

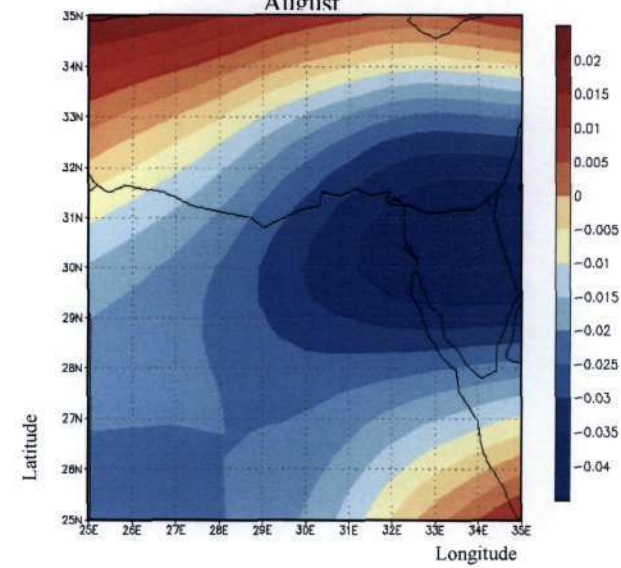


Figure 4.12d) 1000 hPa vertical velocity (Pa/s) Maps JJA for 1998 (NCEP-DOE Reanalysis Data, 2004)

#### 4.4.4 Long-Range Transport

Ozone and its precursors are known to travel thousands of kilometers from their source regions as a result of long-range transport. Numerous studies (Chatfield *et al.*, 2002; Derwent *et al.*, 1998; Lelieveld *et al.*, 2002; Millan *et al.*, 1997; Parrish *et al.*, 1992; Stohl *et al.*, 2002a; Traub *et al.*, 2003; Trickl *et al.*, 2003; Thouret *et al.*, 1998, Wild *et al.*, 1996 and Wild *et al.*, 2001), have provided evidence of long-range transport and its contribution to local pollution effects. Meteorological processes directly determine whether ozone precursor species are contained locally or are transported downwind with the resulting ozone. It is important to be able to differentiate between photochemical processes of ozone formation and the role of distant transfer.

A useful way to track ozone transport is by using back trajectory analysis. In meteorology, trajectories are defined as the paths of infinitesimally small particles of air which at a particular point can be used to trace where particles will move to (forward trajectories) or where the particles originate from (backward trajectories) (Stohl *et al.*, 2002b). Trajectory analysis is a useful way for interpreting trace gas measurements in relation to large-scale air mass transport (Stohl *et al.*, 2002b).

The MINOS campaign provides the most thorough trajectory analysis of transport in the Mediterranean region. The results show northerly flow dominating in the lower troposphere. The middle troposphere is dominated by westerly flow and in the upper troposphere easterly flow dominates (Lelieveld *et al.*, 2002). Ultimately, back trajectory analysis has been sufficiently proven as a vital tool in determining sources of enhancement and will be useful in this study to determine whether the ozone we are observing originates from local pollution sources or if it has been transported from distant sources.

Figure 4.13 presents the results of back trajectory analysis at three selected altitudes (2.5, 5 and 7.5 km) above Cairo for the summer period (JJA) for the period 1998 – 2002. The origins of the trajectory analysis confirm the findings of the MINOS campaign summarized by Lelieveld *et al.* (2002), which were presented in Chapter 2.

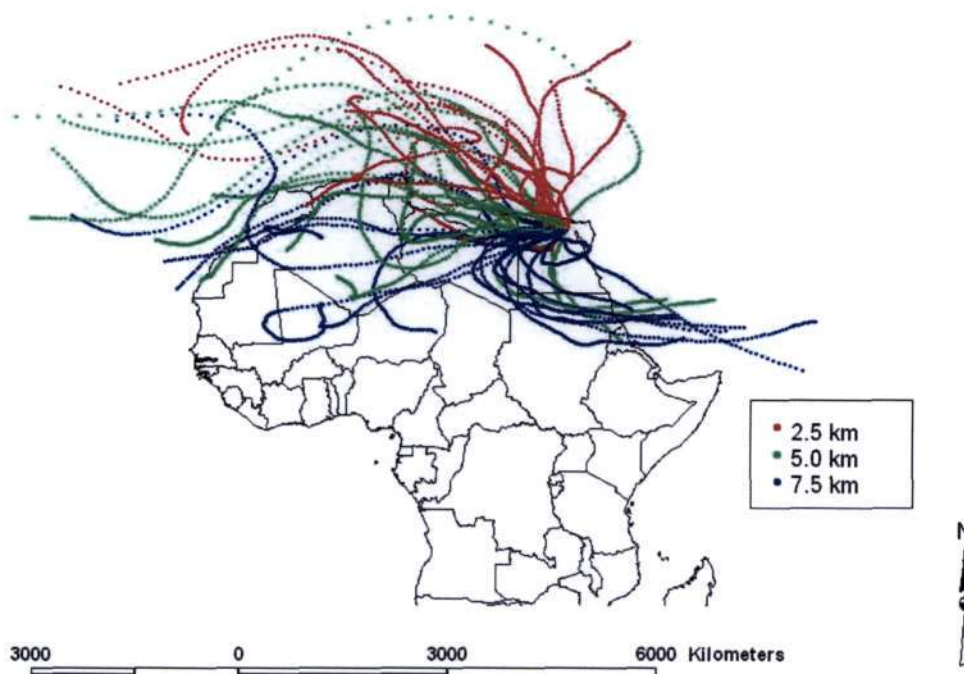


**Figure 4.13 Composite summer (JJA) back trajectories over Cairo for period 1998 - 2002**

In the lower troposphere (represented by 2.5 km back trajectories), the dominant flow is from the north. This is induced by an east–west pressure difference that is generated between the Azorean high and Asian monsoon low pressure regime that is linked to the Indian summer monsoon (Millan *et al.*, 1997). The difference in pressure results in northerly flow over the Aegean Sea (Zerefos *et al.*, 2002). This northerly flow provides a pathway for polluted air from Europe to reach the North African region.

The mid-tropospheric layer (represented by 5 km back trajectories) is characterized by weak westerly flow from the North Atlantic and North America. The air masses that originate from North America flow from west to east and transport pollutants off the continent into the North Atlantic. The processes that result in this movement of air are firstly cyclonic pressure systems and the associated warm conveyor belt processes that result in tropospheric ozone being lifted into the free troposphere. The second mechanism is through convection into the free troposphere and the third mechanism is the direct movement of lower tropospheric air by westerlies across the North Atlantic and into the Mediterranean Region (Creilson *et al.*, 2003).

Back trajectories ending in the free troposphere over Cairo commonly originate in the polar jet stream between 300-200 hPa over North America and the North Atlantic, travel



eastward to about 0 - 15°E where they turn southward and subside because of the strong dynamical barrier of the subtropical jet stream over North Africa.

Upper tropospheric transport (represented by 7.5 km back trajectories) is shown to be predominantly from the west, but also from the east. The easterly flow is associated with the seasonal movement of the ITCZ. This plume is associated with Asian monsoon convection and the extended high-pressure trough in the upper troposphere. Anticyclonic flow transports the pollution over Africa and subsequently northward. Furthermore, studies have shown that this plume has a signature of biomass burning and represents a large reservoir of pollutants near the tropopause (Scheeren *et al.*, 2003).

Back trajectory analysis highlights the influence of Europe on the lower troposphere, North America/North Atlantic on the middle troposphere and south-east Asia on the upper troposphere.

#### **4.4.5 Summary**

Enhanced near-surface tropospheric ozone values have been linked to local pollution sources and to polluted air masses originating from Europe. In the mid-troposphere there is a negative correlation between CO and ozone, which indicates that the ozone is not being created in the mid-troposphere but rather being transported into the middle troposphere. This is further supported by the fact that NO<sub>x</sub> emissions into the mid-troposphere from lightning are likely to be low, which will result in minimal production of ozone in the mid-troposphere. The mid-tropospheric ozone enhancement does not seem to be linked to the convective uplift from the near-surface layer pollution as vertical velocity maps indicate that air masses would not be able to penetrate above 1000 hPa. It is therefore concluded that the enhanced ozone in summer in the mid-troposphere is being transported into the region from a distant source, which according to back trajectory analysis, suggests a westerly origin from the North Atlantic.

#### 4.5 Case Study (9-12 July 2003)

An investigation of a case study of an extended period of high ozone levels (approaching 100 ppbv) was undertaken. The period of 9 -12 July 2003 was selected and the vertical ozone and CO concentrations for the period are presented in Figure 4.14. Ozone values during the period of this case study provide evidence of marked layering throughout the troposphere. This is considered to be typical of a stable atmosphere that is found under anticyclonic conditions (Diab *et al.*, 1996).

In addition to this there is an inverse relationship between CO and ozone. There is a sharp decline in CO from surface values of ~110 ppbv to 40 ppbv between 900-800 hPa. Thus, the effects of local pollution are limited to below 800 hPa which gives rise to a sharp discontinuity at this level. This case study highlights the contributions of locally created pollutants to the high CO values that are observed in the boundary layer in summer. The role of distant transfer in the occurrence of this period of high ozone will be considered next.

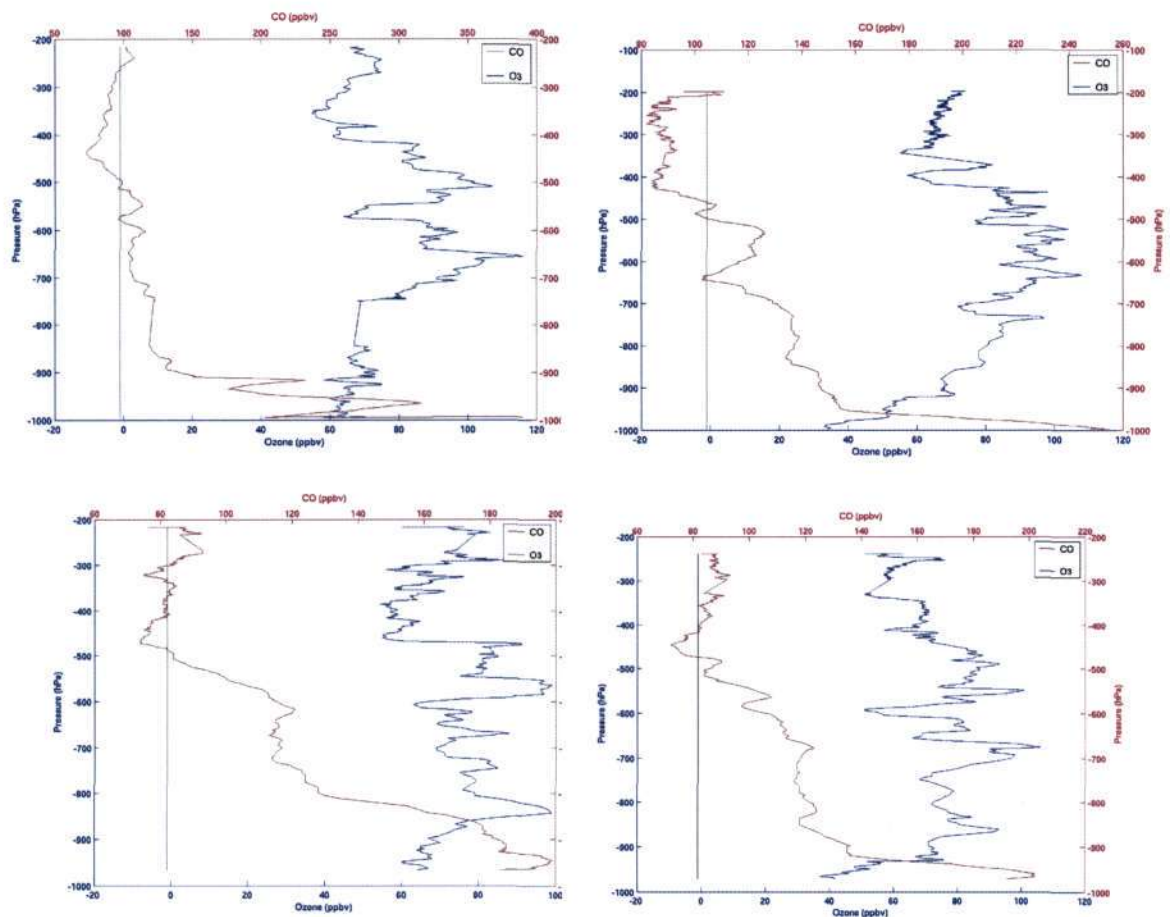
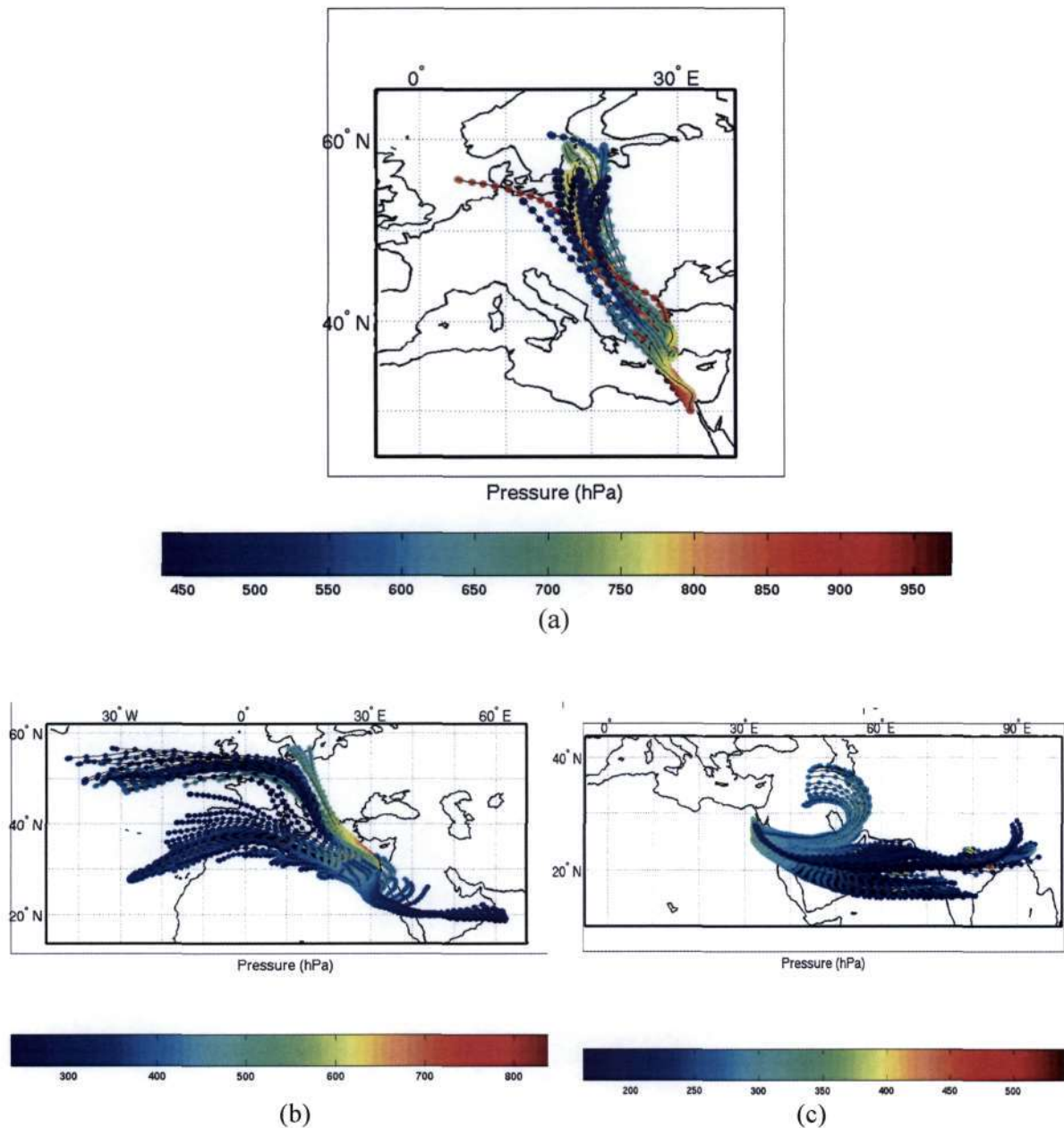


Figure 4. 14 Daily carbon monoxide and ozone values for 9 -12 July 2003

Back trajectories for 11 July 2003 for the lower, middle, and upper troposphere are presented in Figure 4.15. In the lower troposphere, the air masses originate from Europe and show enhanced ozone values through a deep tropospheric layer. In the middle troposphere, westerly flow dominates and in the upper troposphere there is easterly flow. These trajectories are thus consistent with the seasonal results that were found to dominate over the Mediterranean during the MINOS campaign and over Cairo during the study period.



**Figure 4.15** Back trajectory analysis for 11 July 2003, for the a) lower b) middle and c) upper troposphere based on the LAGRANTO model

The case study of high ozone events in summer confirms the findings of the previous section (section 4.4), with high near-surface ozone concentrations and a mid-tropospheric ozone enhancement. Ozone and CO values are anti-correlated, suggesting that the ozone is not created in the region. Local pollution sources are confined to the boundary layer, supporting the idea that the mid-tropospheric ozone occurs due to long-range transport of polluted air masses into the region.

Furthermore, in the previous section, analysis of air mass origins using back trajectory analysis, identified regions that could play an important role in the mid-tropospheric production of ozone. This case study confirms that on occasions of enhanced ozone concentrations, polluted air masses from Europe affect the lower troposphere and air masses originating over North Atlantic influence the middle troposphere. The air masses from the North Atlantic travel over western Europe and north west Africa before reaching Cairo, indicating that these regions could further pollute the air. Further studies should be conducted to investigate this possibility and gain definitive evidence of the origins of this air, which could differ from the general circulation patterns that influence the rest of the Mediterranean region.



## 4.6 Classification of MOZAIC Data

### 4.6.1 Introduction

According to Diab *et al.* (2003) hierarchical cluster analysis of a large number of ozone profiles that are collected throughout a year, over a period of time, can be used to create regionally representative mean profiles. As discussed earlier, due to the level of variability that is exhibited in tropospheric ozone, the widely used approach of seasonal mean profiles becomes inadequate as seasonal means are limited by seasonal boundaries. Results of the application of cluster analysis to the MOZAIC data for Cairo for the period 1998-2002 are presented in this section.

### 4.6.2 Classification of MOZAIC Profiles

MOZAIC ozone profile data consisted of 115 profiles for the period of 1998- 2002. Table 4.2 provides a summary of the seasonal profiles that were available for classification. This shows the distribution of the profiles in the different seasons for the study period, with autumn having the majority of the profiles.

**Table 4.2 Seasonality of MOZAIC profiles**

Spring	Summer	Autumn	Winter	Total
17	34	37	27	115

Figure 4.16 presents the dendrogram for the classification of the MOZAIC profiles, showing the ‘hierarchy of agglomeration’. A rescaled distance of 15 rescaled units was used as the point at which the SPSS agglomerations were halted. This was based on the method used by Ramsay (2003), where it is stated that the distance is progressively lessened until the resultant groupings cannot be distinguished from one another. It should be noted that this distance would vary from study to study. In this study the rescaled distance of 15 units was chosen as it was at this point that each of the 5 groups became clearly distinguishable from the next.

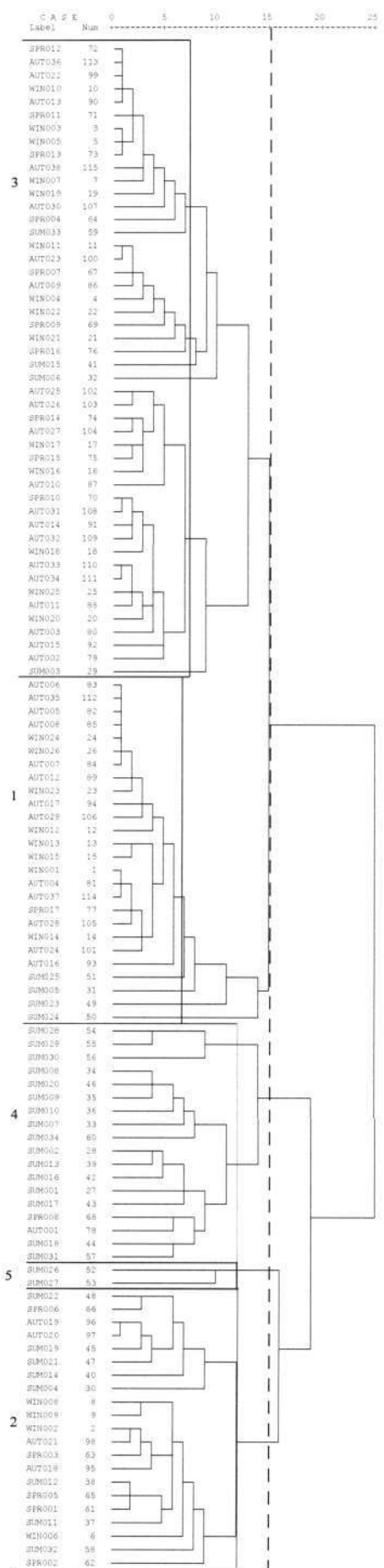


Figure 4.16 Dendrogram for classification of MOZAIC ozone profiles over Cairo

#### 4.6.3 Results of Classification

The characteristics of the 5 groups obtained from the SPSS analysis are presented below.

##### *Group 1*

This group contains 23% of the ozone profiles. Table 4.3 shows the MOZAIC ozone profiles for this group. From this table it is evident that the majority of the profiles occur in autumn (50 %) and winter (31%).

**Table 4.3 Profiles in Group 1 of classification**

Season	Spring	Summer	Autumn	Winter
Date	5-May-99	14-Jul-00	8-Oct-01	23-Dec-99
		25-Jul-02	23-Nov-02	24-Dec-99
		26-Jul-02	7-Oct-00	22-Dec-99
		27-Jul-02	9-Oct-00	2-Dec-01
			10-Oct-00	8-Dec-01
			25-Oct-00	5-Dec-01
			13-Sep-01	6-Feb-00
			5-Nov-01	4-Dec-01
			6-Oct-00	
			24-Oct-99	
			14-Oct-02	
			17-Sep-02	
			12-Sep-01	
Total	1	4	13	8

The mean profile for this group is shown in Figure 4.17, which is characterized by mean values that are below 40 ppbv at the surface and in the lower troposphere. Middle troposphere values are fairly uniform with mean values between 40 and 60 ppbv, whereas in the upper troposphere, ozone values exceed 80 ppbv. For certain individual days in the group upper troposphere values above 100 ppbv occur. These exceedances occur predominantly in winter.

The HYSPLIT model was used to generate 5 day back trajectories initiated at 2.5, 5, 7.5 and 10 km for each day in the group. The results of the individual profiles are presented in Appendix D. Figure 4.18 shows a composite of all the days in the group. Near-surface (2.5km) flow is continental from the north-west as well as from the North Atlantic and middle tropospheric (5 km) flow from over the North Atlantic. Upper tropospheric (7.5 and 10km) flow is from the North Atlantic and the east.

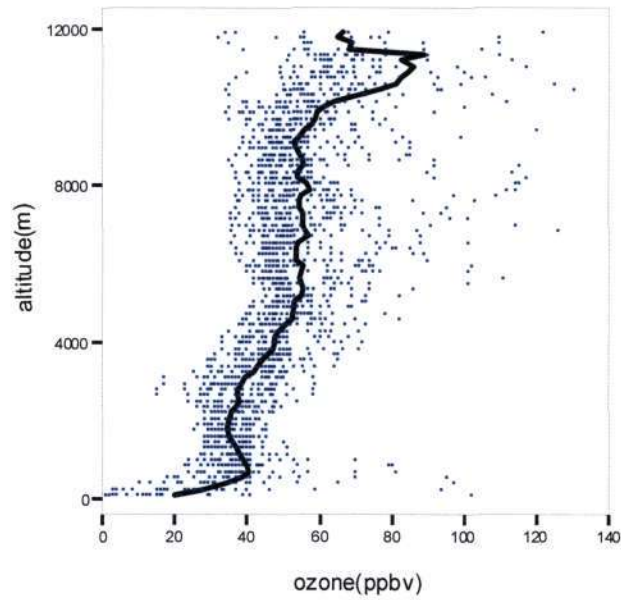


**Figure 4.17 Mean ozone profile for Group 1 resulting from a cluster analysis over Cairo (1998-2002) with value cloud**

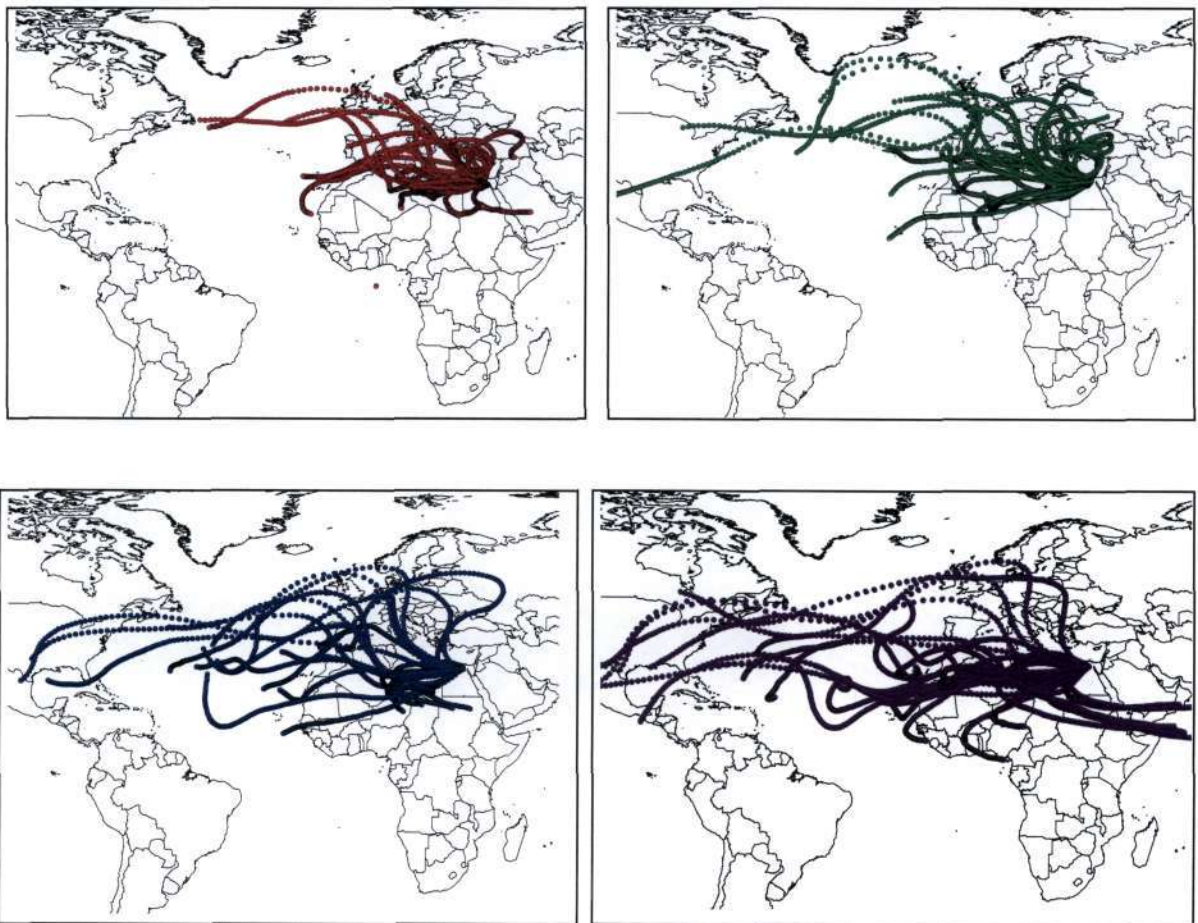


**Figure 4. 18 Composite of five-day back trajectories for all days in Group 1. Trajectories originating at 2.5 km are red, 5 km green, 7.5 km blue and 10 km purple.**

## Group 2

Group 2 contains 18% of the total ozone profiles. Table 4.4 shows the profiles for this group. Summer dominates this group, with 38% of the profiles falling into this group. Figure 4.19 depicts the mean profile for this group. Lower tropospheric mean values range from 20 to ~ 60 ppbv, indicative of local pollution sources. Middle tropospheric values display a steady increase with a mean ozone value of 50 ppbv. The greatest enhancement is in the upper troposphere peak (8-12 km).

The HYSPLIT model was used to generate 5 day back trajectories initiated at 2.5, 5, 7.5 and 10 km for each day in the group. The results of the individual profiles are presented in Appendix D. Figure 4.20 shows a composite map of all days in the group. Air mass origins in lower troposphere originate from Europe and the North Atlantic. Middle and upper tropospheric origins are from the North Atlantic and also from the east.

Individual profiles for this group do show individual days when the ozone values can exceed 150 ppbv, indicating the influence of stratospheric intrusions. Back trajectory analysis for 19 April 2000 shows air originating from above 13 km to reach 10 km. The subsidence of air indicates that stratospheric air is occurring in the troposphere thus resulting in high ozone events in the upper troposphere.

**Table 4.4 Profiles in Group 2 of classification**

Season	Spring	Summer	Autumn	Winter
Date	17-Mar-02	23-Aug-01	18-Sep-01	26-Feb-00
	20-Apr-00	22-Aug-01	22-Oct-01	27-Feb-00
	21-Apr-00	11-Aug-01	14-Sep-01	7-Feb-00
	19-Apr-00	27-Aug-00		12-Feb-00
	22-Apr-00	4-Jul-00		13-Feb-00
		31-Jul-00		
		30-Jul-00		
		14-Aug-99		
Total	5	8	3	5



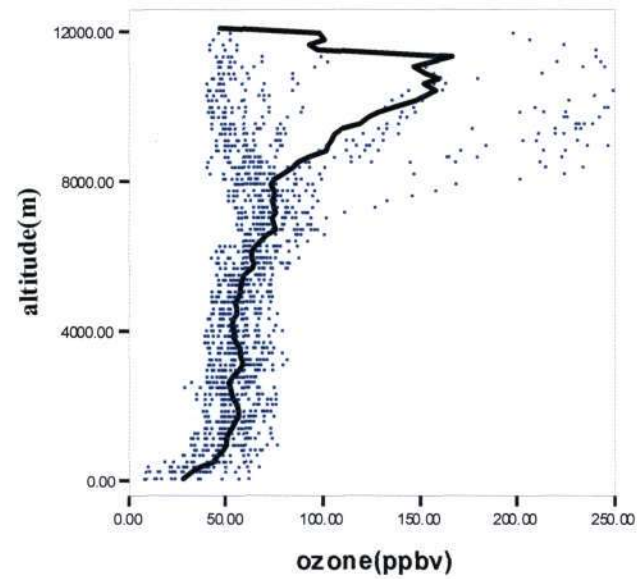


**Figure 4.19 Mean ozone profile for group 2 resulting from a cluster analysis over Cairo (1998-2002) with value cloud**

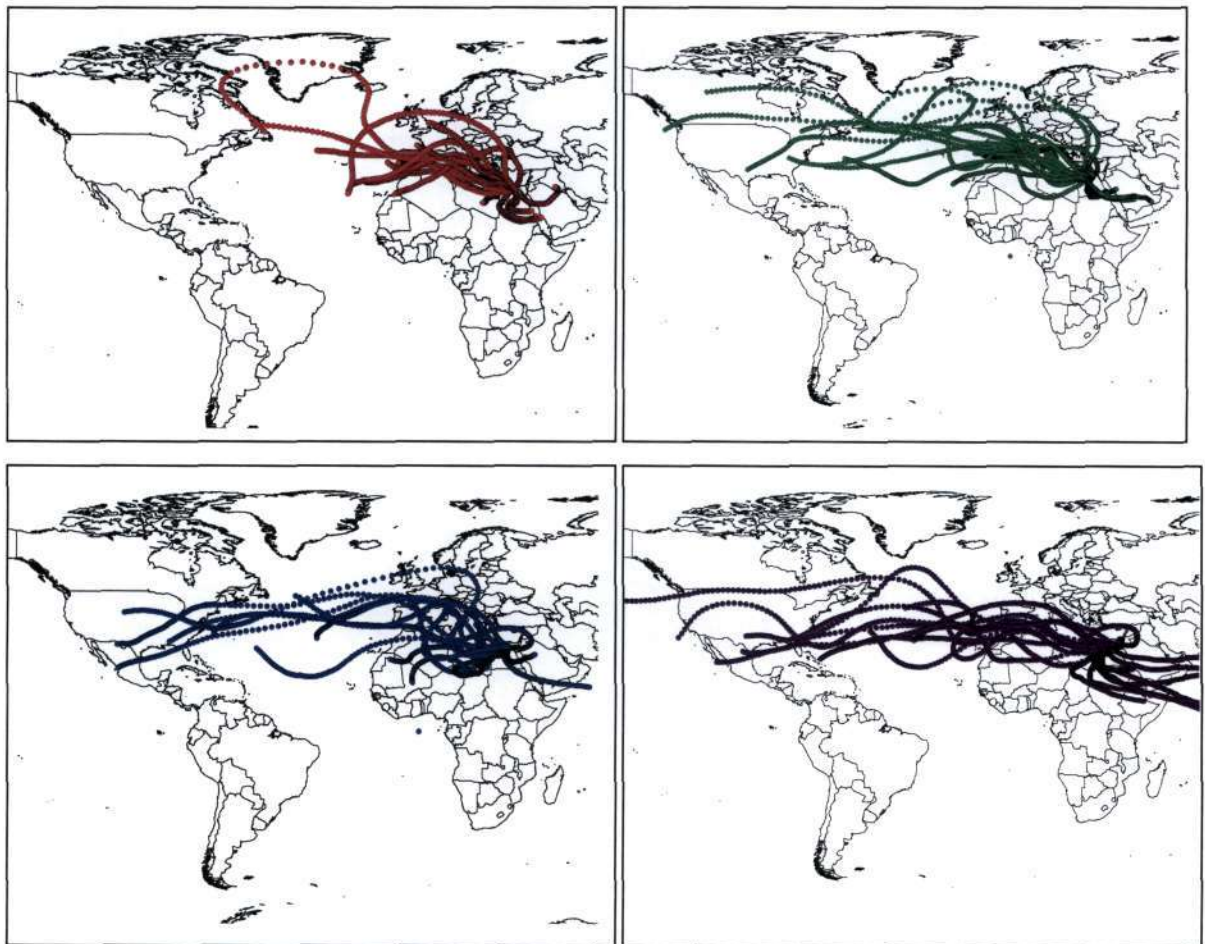


**Figure 4.20 Composite of five-day back trajectories for all days in Group 2. Trajectories originating at 2.5 km are red, 5 km green, 7.5 km blue and 10 km in purple**

### Group 3

Group 3 contains 42% of all ozone profiles. Table 4.5 presents the profiles for Group 3. Autumn dominates this group with 42 % of the profiles, though the rest of the profiles are spread across the other seasons. Figure 4.21 presents the mean profile for group 3. In this figure, there is a shallow gradient in the lower troposphere. Ozone values are generally about 50 ppbv representing a uniform distribution between 2 and 8 km. This uniformity indicates that the air is well mixed and analysis of individual profiles reveals this as well. This group is probably most representative of the background ozone conditions over Cairo as it displays the lowest ozone values between the surface and 8 km. There is a rapid increase in ozone in the upper troposphere (above 10 km) as was evident in Groups 1 and 2.

Back trajectory analysis was carried out for each of the days in this group and the results are presented in Appendix D. Figure 4.22 displays the composite plot of back trajectories originating at 2.5, 5, 7.5 and 10 km. Lower, middle and upper tropospheric flow all seem to originate from the west and in particular the North Atlantic and North America.

**Table 4.5 Profiles in Group 3 of classification**

Season	Spring	Summer	Autumn	Winter
Date	2-Mar-02	18-Aug-99	24-Nov-02	19-Feb-00
	21-Mar-02	28-Aug-00	26-Oct-01	20-Feb-00
	22-Mar-02	15-Jul-00	26-Oct-00	11-Feb-00
	21-Apr-00	3-Jul-00	25-Oct-99	25-Feb-00
	17-Mar-02		6-Nov-02	24-Jan-02
	18-Mar-02		27-Oct-01	28-Feb-00
	19-May-99		11-Oct-00	14-Feb-00
	18-Apr-99		29-Sep-02	25-Jan-02
	19-Apr-99		30-Sep-02	23-Jan-02
	20-Mar-02		13-Oct-02	9-Dec-01
			18-Oct-00	11-Dec-01
			12-Nov-02	10-Dec-01
			27-Oct-00	23-Dec-02
			13-Nov-02	24-Dec-02
			14-Nov-02	
			15-Nov-02	
			19-Oct-00	
			5-Oct-00	
			28-Oct-00	
			4-Oct-00	
Total	10	4	20	14

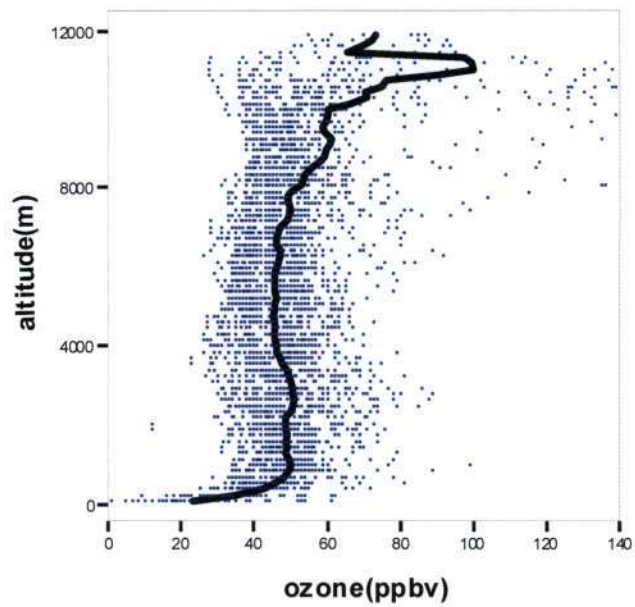


**Figure 4.21 Mean ozone profile for group 3 resulting from a cluster analysis over Cairo (1998-2002) with value cloud**

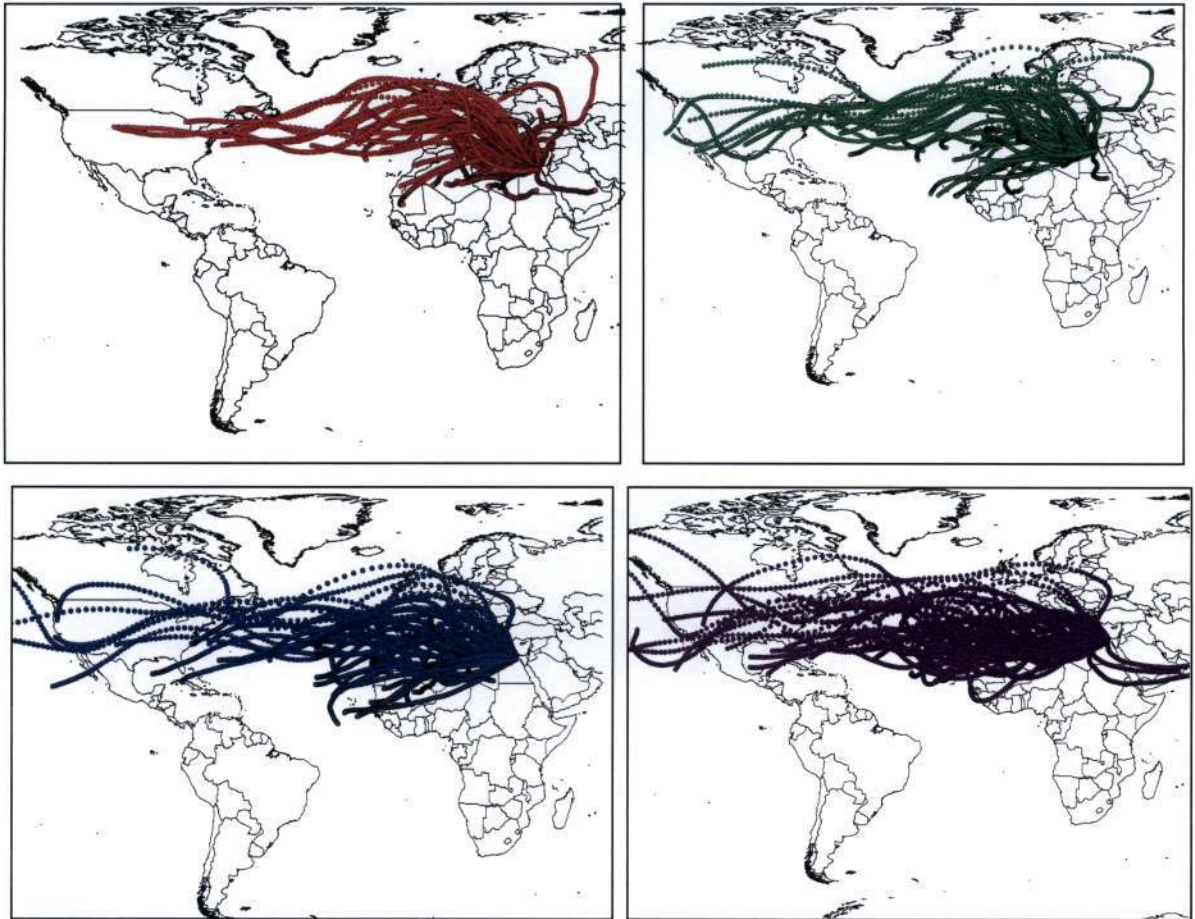


**Figure 4.22 Composite of five-day back trajectories for all days in Group 3. Trajectories originating at 2.5 km are red, 5 km green, 7.5 km blue and 10 km purple**



### Group 4

Group 4 contains 16% of the total ozone profiles. Table 4.6 presents the profiles in Group 4. Summer dominates this group with 89% of the profiles. This mean group profile (Fig 4.23) presents characteristics of being the most polluted of all the groups. Firstly, the surface ozone values are greater than 40 ppbv, which are indicative of near-surface pollution. For groups 1 to 3 the near surface ozone values were all below 20 ppbv.

In the middle troposphere values there is a mean of 70 ppbv, with values that range between 50 – 90 ppbv. In comparison with the first three profiles discussed this is the first to display a mid-tropospheric peak. Reasons for this enhancement are either due to vertical transport or long-range transport. This profile can be compared to the mean summer profile presented in Figure 4.5. Both the means are similar though in Figure 4.23 we are able to distinguish a more definitive mid-tropospheric peak. Further back trajectory analysis confirms the influence of polluted air from Europe (Fig 4.24). In the upper tropospheric (7.5 and 10 km) air masses originate from the east. Individual back trajectories for the group are presented in Appendix D.

**Table 4.6 Profiles in Group 4 of classification**

Season	Spring	Summer	Autumn	Winter
Date	16-Mar-02	4-Aug-99	1-Sep-00	
		5-Aug-99		
		8-Aug-99		
		17-Jul-00		
		22-Aug-01		
		14-Jul-00		
		18-Jul-00		
		16-Jul-00		
		29-Aug-99		
		21-Jun-00		
		23-Aug-00		
		31-Aug-00		
		19-Jun-99		
		11-Aug-01		
		12-Aug-01		
		6-Aug-99		
Total	1	16	1	

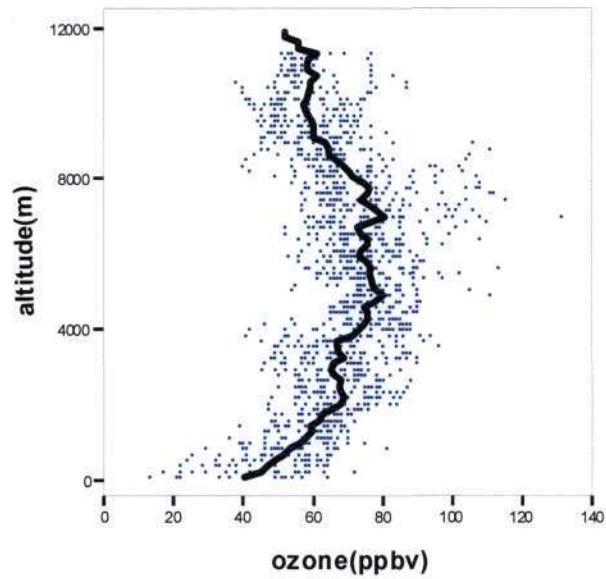


**Figure 4.23 Mean ozone profile for group 4 resulting from a cluster analysis over Cairo (1998-2002) with value cloud**

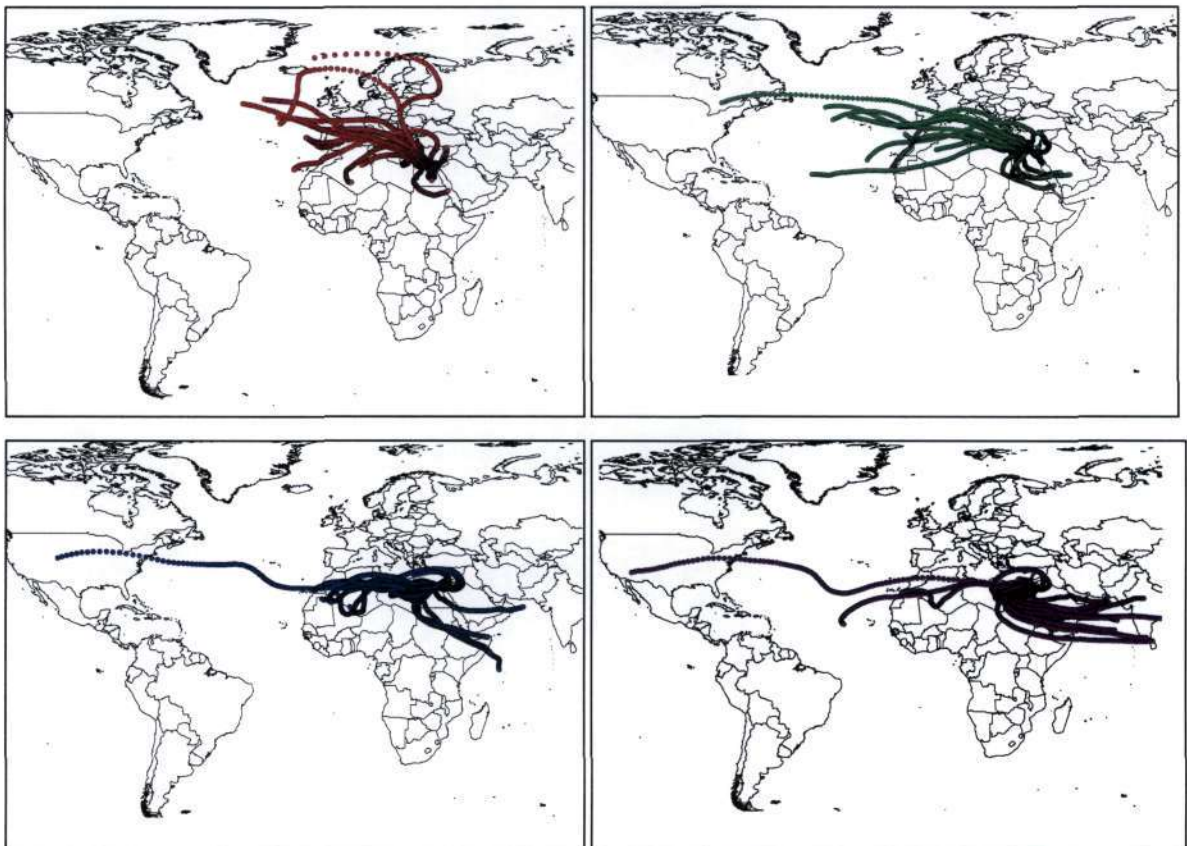


**Figure 4.24 Composite of five-day back trajectories for all days in Group 4. Trajectories originating at 2.5km are red, 5 km green, 7.5 km blue and 10 km purple**

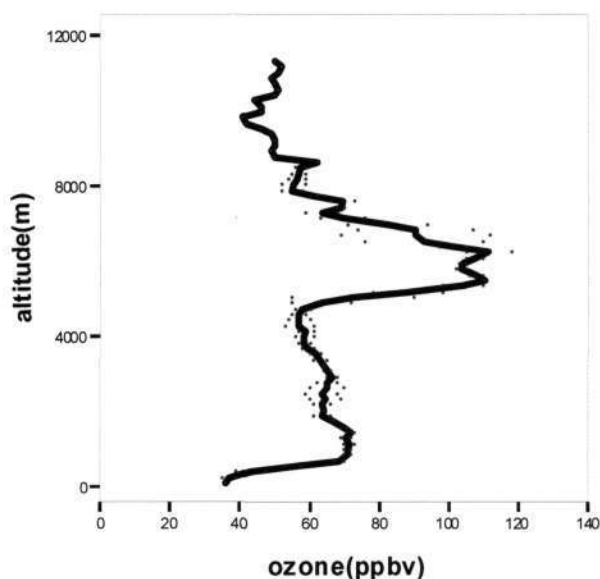
### Group 5

Table 4.7 presents profiles occurring in Group 5, of which there are only 2. This group accounts for less than 2% of the total of ozone profiles. Both profiles occur in summer and show mid-tropospheric enhancement of ozone. This profile (Fig 4.25) represents an extreme version of the mid-tropospheric enhancement that is observed in Group 4, with values approaching 120 ppbv.

Back trajectories for this group are presented in Appendix D and Figure 4.26 presents a composite of these trajectories. Air masses are generally of continental origin with the exception of 10 km trajectories which originate over southern India.

**Table 4.7 Profiles in Group 5 of classification**

Season	Spring	Summer	Autumn	Winter
Date		9-Aug-98		
		10-Aug-98		
Total		2		



**Figure 4.25 Mean ozone profile for group 5 resulting from a cluster analysis over Cairo (1998-2002) with value cloud**

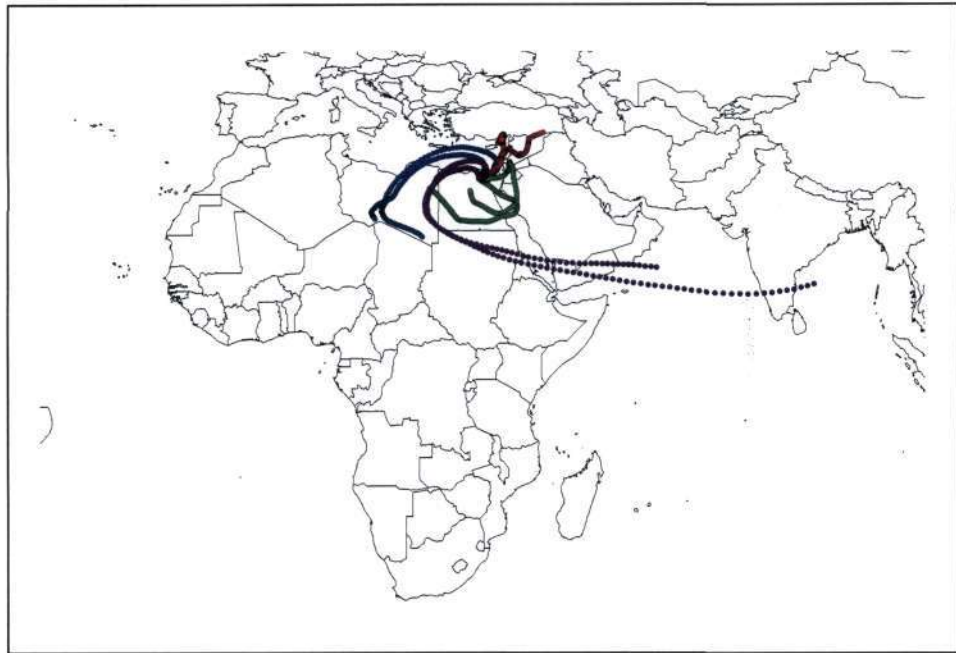


**Figure 4.26 Composite of five-day back trajectories for all days in Group 5. Trajectories originating at 2.5 km are red, 5 km green, 7.5 km blue and 10 km purple**

#### 4.6.4 Summary of Data Classification

In traditional seasonal means the microstructure of individual profiles is eliminated. Data classification allows for similar individual profiles to be grouped together, thus providing mean profiles which maintain these interesting microstructures. MOZAIC ozone data classification using SPSS has allowed for the profiles to be classified into 5 groups. Table 4.8 presents a summary of the seasonality of the classification.

**Table 4.8 Summary of the seasonality of the hierarchical classification**

<b>Group</b>	<b>1</b>	<b>2</b>	<b>3</b>	<b>4</b>	<b>5</b>	<b>Total</b>
Spring	1	5	10	1		17
Summer	4	8	4	16	2	34
Autumn	13	3	20	1		37
Winter	8	5	14			27
<b>Total</b>	<b>26</b>	<b>21</b>	<b>48</b>	<b>18</b>	<b>2</b>	<b>115</b>

Seasons are shared in groups which indicate that the mean profiles obtained from the classification procedure are different from the mean seasonal profiles that are shown in Figure 4.5. From these groups, of particular interest are the profiles that are least polluted or background conditions (Fig 4.21) and the most enhanced or polluted conditions



(Fig.4.23), which are shown together in Figure 4.27. This figure clearly highlights the mid-tropospheric enhancement.

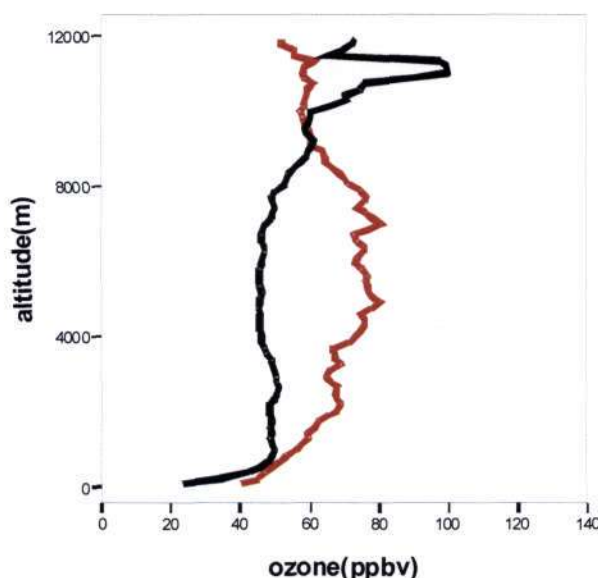


**Figure 4.27 Comparison of least polluted and most polluted mean profiles over Cairo**

Further back trajectory analysis has highlighted the role of source regions. In Group 3, air masses in the lower troposphere generally have their origins over the North Atlantic or north west Africa, with middle and upper troposphere origins from North America and the North Atlantic. In this group the middle troposphere ozone values show a mean of ~50 ppbv. In Group 4, air mass origins into the middle troposphere are from the North Atlantic and upper troposphere air mass origins are from the east. Furthermore, the enhanced profile is influenced by polluted air masses originating from Europe in the lower troposphere. The differences in the source regions for each group, provides crucial evidence to support that long-range transport plays a significant role in the mid-tropospheric ozone enhancement.

Therefore, it can be concluded that the shape of the profile is not only determined by season but also by the source regions of pollutants. In addition to the atmospheric conditions and photochemical processes that influence the seasonal cycle the source regions also play a role (Ramsay, 2003). The classification of data in this way has allowed for a clearer understanding of the enhancement that is observed, revealing that long-range transport contributes to the ozone enhancement over Cairo, with summer enhancements coinciding with the transport of polluted air masses from Europe and the North Atlantic.

Whereas, background conditions are associated with continental flow from the west and air from over North America and the North Atlantic.

#### **4.7 Summary**

Ozone profiles over Cairo have revealed evidence of stratospheric-tropospheric exchange in late winter and spring in the upper troposphere, which contributes to a maximum in TTO over that period. Furthermore, the influence of stratospheric intrusions is evident in late winter and spring with there being evidence of subsidence of air from higher altitudes.

Boundary layer pollution is enhanced in summer relative to other seasons, with there being strong evidence of local pollution sources, with CO values ranging between 200 and 500 ppbv and high levels of surface NO<sub>2</sub> observed. The lower troposphere is also influenced by polluted air masses from Europe. Enhancements in the order of 40 - 60 % are observed in the middle troposphere in summer, which is unusual for the Mediterranean Region. Conditions in the mid-troposphere are unsuitable for the production of ozone, with low levels of CO and NO<sub>x</sub> occurring in the mid-troposphere, indicating that ozone is transported into the region. Furthermore, boundary layer pollution is confined to below 1000 hPa, indicating that the near-surface ozone is not contributing to the mid-tropospheric ozone enhancement. Therefore it can be concluded that ozone is being transferred into the region by the long-range transport of polluted air masses. A case study of high ozone events in summer reaffirms that ozone is not created in the mid-troposphere and that local pollution sources are confined to the boundary layer.

Data classification using SPSS allowed for the determination of least polluted and most polluted conditions, which showed that there is a strong seasonal influence to the ozone concentrations observed in each group, with summer profiles occurring in the most polluted group. A comparison of sources regions for background and enhanced conditions confirms that long-range transport of polluted air masses into the mid-troposphere plays an important role in the observed summer mid-troposphere ozone enhancement.

## CHAPTER 5

### CONCLUSION

---

#### 5.1 Summary

This study involved the analysis of MOZAIC (Measurement of OZone and wAter Vapor aboard In-service airCraft) ozone profile data to characterize the vertical distribution of tropospheric ozone over Cairo and to assess the relative contributions from a range of sources that included surface pollution and the effects of long-range transport from Europe, Asia and the North Atlantic.

Seasonal mean total tropospheric ozone (TTO) values in Dobson Units were calculated for the study period (1998 - 2002) and revealed a peak in April, which coincided with the maximum in total column ozone. Stratospheric-tropospheric exchange (STE) is most effective during spring and late winter as the altitude of the tropopause increases which allows for stratospheric air to flow into the tropopause. High TTO values were also noted for June and August corresponding to increased photochemical activity in summer months.

Mean seasonal ozone profiles (in ppbv) revealed a near-surface and lower tropospheric ozone enhancement in summer. The influence of local pollution sources was determined by use of satellite images and available surface pollution data. High levels of surface NO<sub>2</sub> were observed provided supporting evidence of local pollution. Further, ozone concentrations show a good correlation to high carbon monoxide (CO) values, thus the enhancement was attributed to local pollution sources. Back trajectory analysis confirmed the influence of polluted air masses into the lower troposphere originating from Europe during summer, which was previously highlighted as being a contributing factor to pollution in the Mediterranean region. These air masses could therefore contribute further to the lower tropospheric ozone concentrations. This summer ozone enhancement extended to a height of 8 km, which is fairly unusual for the region, as Mediterranean cities such as Athens, Greece usually display peaks in the upper and lower troposphere only.

The mid-tropospheric summer ozone peak, is thus of considerable interest as it appears to be unique to the Mediterranean region. In the mid-troposphere, mean ozone values in summer (JJA) range between 70-80 ppbv, with values approaching 100 ppbv on individual days. Mean values are generally below 50 ppbv for the remainder of the year, giving a summer enhancement of 40-60%. A case study of a period of high ozone events conclusively revealed that ozone and CO are anti-correlated in the mid-troposphere. Since the observed summertime ozone enhancement is greater than expected background ozone values it was concluded that it was and is not linked to enhanced CO.

Numerous possibilities were investigated to determine the possible cause of the mid-tropospheric enhancement. These included the possibility of convective uplift of polluted air masses of near-surface pollution, the production of ozone in the mid-troposphere due to the injection of NO<sub>2</sub> by lightning, and the influence of distant sources by long-range transport.

It was found that in the middle troposphere, CO and ozone are anti-correlated and that NO<sub>2</sub> emissions from lightning are low. This indicates that the concentrations of ozone precursor gases in the mid-troposphere are low and are unlikely to make a significant contribution to the ozone concentrations observed. This leads to the conclusion that the high ozone concentrations in the mid-troposphere occur as a result of ozone being transported into the region. Furthermore, the mid-tropospheric ozone enhancement was not linked to the convective uplift of pollution from the near-surface layer as vertical velocity maps indicated that air masses would not be able to penetrate above 1000 hPa. It was therefore concluded that in summer, ozone is being transported into the mid-troposphere from a distant source, which according back trajectory analysis, suggests a westerly origin. The pollutants are thus transferred from the west to the middle troposphere over Cairo, where the high ozone values are experienced. A case study of high ozone events in summer substantiates the overall findings of the study, indicating that ozone is not created in the middle troposphere but that it is brought into the region by the long-range transport of polluted air masses from the west.

Upper tropospheric ozone values were found to be high in February and April. Evidence of subsidence was obtained from back trajectory analysis, which confirmed the influence of stratospheric air masses.



Hierarchical cluster analysis using the Statistical Package for the Social Sciences (SPSS version 11, 2001) allowed for the determination of 5 groups. It was found that seasons were shared in the groups indicating a difference to the conventional mean seasonal profiles.

Further, the classification process has allowed for the determination of least (background) polluted and most (enhanced) polluted profiles. The background mean ozone profile contains individual ozone profiles that are spread across the seasons, whereas the enhanced mean profile is dominated by summer ozone profiles. In the least polluted profile the middle troposphere ozone values show a mean of ~50 ppbv. The enhanced mean ozone profile shows a mean of 70 ppbv. A comparison of sources regions for these profiles suggests that long-range transport of polluted air masses into the mid-troposphere plays an important role in the observed summer mid-troposphere ozone enhancement.

This study has ultimately served to highlight a new and interesting occurrence of mid-tropospheric enhancements ozone over Cairo, which is unusual for cities in the Mediterranean region. This enhancement has been linked to the transport of polluted air masses from the west. Further studies will need to be undertaken to gain a further insights into the chemical and dynamical factors that influence ozone in the mid-tropospheric region. The following sections provide recommendations for further study into this mid-tropospheric ozone enhancement.

## **5.2 Recommendations**

It is understood that any investigations into the concentrations of tropospheric ozone have natural and anthropogenic sources. It is important to differentiate photochemical processes of ozone formation and the role of distant transfer. The long-range transport of polluted air masses has been highlighted as a reason for summer mid-tropospheric ozone enhancement. It is therefore suggested that in order for the role of long-range transport to be fully understood that trace gas analysis on the originating air masses should be undertaken in order to gain definitive evidence of the contributions of source regions.

Furthermore, there are limitations to using MOZAIC ozone profile data. Firstly, the altitudes of the MOZAIC flights are predefined by air traffic regulations and the number and seasonal distribution of the flights are determined by airlines. This creates biases in the data and as a result may not allow for the true climatology of the region to emerge. It is suggested that future studies expand the study period using most recent MOZAIC ozone profiles. Further, the limitations of MOZAIC data may be overcome by obtaining ground-based measurements of atmospheric ozone such as ozonesonde data.

In addition to this, it is suggested that further case studies of high ozone events in summer be carried out, in order to confirm the findings of this study. The case study of high ozone events carried out in this study suggests that in summer, days of enhanced ozone display marked layering throughout the troposphere, typical of a stable atmosphere that is found under anticyclonic conditions. It is therefore suggested that future studies should further investigate the possibility of stable layers in the region and if there are occasions when air masses could rise above these layers. These investigations should also focus on the circulation patterns over North Africa.

## REFERENCES

---

- Anderson, N.D. (1996). *OZONE: A sourcebook for teaching about O<sub>3</sub> in the Troposphere and Stratosphere*. Changes in the Environment Series. Kendall/Hunt Publishing Company, Iowa. 149pp.
- Andreae, M.O.(1991). Biomass burning: Its history, use and distribution and its impacts on environmental quality and global climate, In Levine, J.S. (ed), *Global Biomass Burning*, The MIT Press, Cambridge, London, England, 3 – 21.
- Appenzeller, C., Davies, H. C., and Norton, W. A. (1996). Fragmentation of stratospheric intrusions. *Journal of Geophysical Research*, 101, 1435–1456.
- Austin, J.F. and Follows, M.J. (1991). The ozone recorded at Payrene: An assessment of the cross tropopause flux. *Atmospheric Environment*, 25(9) 1873-1880.
- Baijnath, S. (2005). Map showing the location of Cairo, Egypt in Africa and in the Mediterranean Region. Produced at the School of Environmental Sciences, University of KwaZulu-Natal, Howard College, Durban.
- Barakat, A.O. (2004). Assessment of persistent toxic substances in the environment of Egypt. *Environmental International*, 30, 309-322.
- Baray, J.L., Ancellet, G., Taupin, F.G., Bessafi, M., Baldy, S. and Keckhut, P. (1998). Subtropical tropopause break as a possible stratospheric source of ozone in the tropical troposphere. *Journal of Atmospheric and Solar-Terrestrial Physics*, 60, (I) 27-36.
- Baray, J.L., Gerald, A., Ramdriabelo, T. and Baldy, S. (1999). Tropical Marlene and stratospheric-tropospheric exchange. *Journal of Geophysical Research*, 104(D11), 13953-13970.
- Beckmann M., Ancellet G., Blonsky S., De Muer D., Ebel A., Elbern H., Hendricks J., Kowol J., Mancier C., Sladkovic R., Smit H.G.J., Speth P., Trickl T. and Van Haver, P.

(1997). Regional and global tropopause fold occurrence and related ozone flux across the tropopause, *Journal of Atmospheric Chemistry*, 28, 29–44.

Beirle, S., Platt, U., Wagner, T. and Wenig, M. (2004). Weekly cycle of NO<sub>2</sub> by GOME measurements: a signature of anthropogenic sources. *Atmospheric Chemistry and Physics*, 3, 2225-2232.

Bell, M. and Ellis, H. (2004). Sensitivity analysis of tropospheric ozone to modified biogenic emissions for the Mid-Atlantic region. *Atmospheric Environment*, 38(13), 1879-1889.

Bey, I., Jacob, D.J., Yantosca, R.M., Logan, J.A., Field, B.D., Fiore, A.M., Li, Q., Liu, H.Y., Mickley, L.J. and Schultz, M.G. (2001). Global modeling of tropospheric chemistry with assimilated meteorology: Model description and evaluation. *Journal of Geophysical Research*, 106, 23073-23096.

Bithel, M., Vaughan, G. and Gray, L.G. (2000). Persistence of stratospheric ozone layers in the troposphere. *Atmospheric Environment*. 34, 2563 – 2570.

Bodeker, G.E. (1994). *Planetary Waves and the Global Ozone Distribution*. Published PhD research. Department of Physics, University of Natal. 317pp.

Bojkov, R.D. (1986). Surface ozone during the second half of the nineteenth century, *Journal of Climate and Applied Meteorology*, 25, 343 – 352.

Bojkov, R.D., Bishop, L., Hill, W.J., Reinsel, G.C. and Tiao, G.C. (1990). Statistical trend analysis of revised Dobson total ozone data over the Northern Hemisphere. *Journal of Geophysical Research*, 95, 9785-9807.

Bojkov, R.D., Zerefos, C.S., Balis, D.S., Ziomas, I.C. and Bais, A.F. (1993). Record low total ozone during northern winters of 1992 and 1993. *Geophysical Research Letters*, 20 (13), 1351 – 1354.

Bojkov, R. and Hilsenrath, E. (2005). MOZAIC: Measurement of OZone and wAter vapour by Airbus In-Service airCraft. [http://avdc.gsfc.nasa.gov/Links/Data/ABSC/MOZAIC\\_Data.html](http://avdc.gsfc.nasa.gov/Links/Data/ABSC/MOZAIC_Data.html) accessed June, 2004.

Bond, D.W., Steiger, S., Zhang, R., Tie, Z. and Orville, R.E. (2002). The importance of NO<sub>x</sub> production by lightning in the tropics. *Atmospheric Environment*, 36 (9), 1509 – 1519.

Bridgman, H. (1997). Air pollution. In *Applied Climatology: Principles and Practices*. Thompson, R.D. and Perry, A. (eds) 288-302. Routledge. London and New York.

Browell E.V., Hair, J.W., Butler, C.F., Grant, W.B., DeYoung, R.J., Fenn, M.A., Brackett, V.G., Clayton, M.B., Brasseur, L.A., Harper, D., Ridley, B.A., Klonecki, A. A., Hess, P.G., Emmons, L. K., Tie, X., Atlas, E.L., Cantrell, C.A., Wimmers, A.J., Blake, D.R., Coffey, M.T., Hannigan, J.W., Dibb, J.E., Talbot, R.W., Flocke, F.A., Weinheimer, J., Fried, A., Wert, B., Snow, J.A. and Lefer, B.L. (2003). Ozone, aerosol, potential vorticity, and trace gas trends observed at high-latitudes over North America from February to May 2000. *Journal of Geophysical Research*, 108(D4), 24 043-24 068.

Bunce, N.J. (1994). *Environmental Chemistry*. Wuerz Publishing Ltd. Winnipeg, Canada. 376pp.

Cammas, J.P., Jacoby-Koaly, S., Suhre, K., Rosset, R. and Marenco, A. (1998). The Atlantic subtropical potential vorticity barrier as seen by MOZAIC flights. *Journal of Geophysical Research*, 103, D 19, 25681-25693.

Chamedies, W. and Waller, J.G.G. (1973). A photochemical theory of tropospheric ozone. *Journal of Geophysical Research* 98, 14 783 – 14 790.

Chan, L.Y., Lui, H.Y., Lam, K.S., Wang, T., Oltmans, S.J. and Harris, J.M. (1998). Analysis of the seasonal behaviour of tropospheric ozone at Hong Kong. *Atmospheric Environment*, 32(2), 159-168.

Chatfield, R.B. and Delany, A.C. (1990). Convection links biomass burning to increased tropical ozone: However, model will tend to overpredict O<sub>3</sub>. *Journal of Geophysical Research*, 95 (D11), 18473 – 18488.

Chatfield, R.B., Guo, Z., Sachse, G.W., Blake, D.R. and Blake, N.J. (2002). The subtropical global plume in the Pacific Exploratory Mission-Tropics A (PEM-Tropics A), PEM-Tropics B, and the Global Atmospheric Sampling Program (GASP): How tropical emissions affect the remote Pacific. *Journal of Geophysical Research* 107(D16) doi: 10.1029/2001JD000497.

Creilson, J.K., Fishman, J. and Wozniak A.E. (2003). Intercontinental transport of tropospheric ozone: A study of its seasonal variability across the North Atlantic utilizing tropospheric ozone residuals and its relationship to the North Atlantic Oscillation. *Atmospheric Chemistry and Physics*, 3, 4431– 4460.

Crutzen PJ. (1973). A discussion of the chemistry of some minor constituents in the stratosphere and troposphere. *Pure and Applied Geophysics*, 106 –108, 1385–99.

Cutlip, K. (2003). *Lightning Alters Atmospheric Chemistry*. WeatherWise. EBSCO Publishing. 10-11.

Danielsen, E.F. (1968). Stratospheric-tropospheric exchange based on radioactivity, ozone and potential vorticity. *Journal of the Atmospheric Sciences*, 25, 502 – 518.

de Laat, A.T.J. (2002). On the origin of tropospheric ozone over the Indian Ocean during the winter monsoon: African biomass burning. *Atmospheric Chemistry and Physics*, 2, 943–981.

Dermitzaki, E.V., Kanadindou, M., Ladstaetter-Weissenmayer, A. and Burrows, J.P. (2004). Biomass burning impact on ozone budget over the Eastern Mediterranean region during summer 2000. Proceedings of the XX Quadrennial Ozone Symposium. Kos, Greece, 1-8 June 2004. Edited by Zerefos, C., 325-326.

Derwent, R.G., Stevenson, D.S., Collins W. J. and Johnson. C. E. (2004). Intercontinental transport and the origins of the ozone observed at surface sites in Europe. *Atmospheric Environment*, 38(13), 1891-1901.

Diab, R. D., Thompson, A.M., Zunkel, M., Coetzee, G.J.R., Combrink, J., Bodeker, G.E., Fishman, J., Sokolic, F., McNamara, D.P., Archer, C.B. and Nganga, D. (1996). Vertical ozone distribution over southern Africa and adjacent oceans during SAFARI-92. *Journal of Geophysical Research*, 101(D19), 23823-23834.

Diab, R.D., Raghunandan, A., Thompson, A. M. and Thouret, V. (2003). Classifications of tropospheric ozone profiles over Johannesburg based on mosaic aircraft data. *Atmospheric Chemistry and Physics* 3, 705-732.

Diab, R.D., Thompson, A.M., Mari, K., Ramsay, L. and Coetzee G.J.R. (2004). Tropospheric ozone climatology over Irene, South Africa, from 1990 to 1994 and 1998 to 2002. *Journal of Geophysical Research*, 109, D20301, doi: 10.1029/2004JD004793.

Draxler, R.R. and Hess, G.D. (1998). An overview of the HYSPLIT 4 modelling system for trajectories, dispersion and deposition. *Australian Meteorology Magazine*, 47, 295-308.

Dutsch, H.G. (1974). The ozone distribution in the atmosphere. *Canadian Journal of Chemistry*, 52, 1491-1504.

EEAA (Egyptian Environmental Affairs Agency). (1994). "Maximum limits for outdoor air pollutants" as given by Annex 5 of the Law number 4 for 1994. Law for the Environment, Egypt.

EEAA-EIMP (Egyptian Environmental Affairs Agency: Environmental Information and Monitoring Programme). (2000a). Surface layer ozone concentrations. Newsletter, 8 (5). <http://www.eeaa.gov.eg/eimp/news9.html>, accessed June, 2004.

EEAA-EIMP (Egyptian Environmental Affairs Agency: Environmental Information and Monitoring Programme). (2000b). Air Quality in Egypt: Annual Report.,



<http://www.eeaa.gov.eg/eimp/reports/annu2000.pdf>, accessed June, 2004.

EEAA-EIMP (Environmental Information and Monitoring Programme). (2000c). Ozone levels in Egypt. Newsletter, 9 (6). <http://www.eeaa.gov.eg/eimp/news9.html>, accessed June, 2004.

EEAA-EIMP (Egyptian Environmental Affairs Agency: Environmental Information and Monitoring Programme). (2000d). Air Quality in Egypt. Monthly report for June, 2000, <http://www.eeaa.gov.eg/eimp/reports/MR-june2000.pdf>, accessed June, 2004.

EEA-EIMP (Egyptian Environmental Affairs Agency: Environmental Information and Monitoring Programme). (2000e). Air Quality in Egypt. Monthly report for July, 2000, <http://www.eeaa.gov.eg/eimp/reports/MR-july2000.pdf>, accessed June, 2004.

EEA-EIMP (Egyptian Environmental Affairs Agency: Environmental Information and Monitoring Programme). (2000f). Air Quality in Egypt. Monthly report for August, 2000, <http://www.eeaa.gov.eg/eimp/reports/MR-august2000.pdf>, accessed June, 2004.

Elbern, H., Kowol, J., Stidkovic, R. and Ebel, A. (1997). Deep stratospheric intrusions: A statistical assessment with model guided analyses. *Atmospheric Environment*, 31(19), 3207-3226.

EL-Hussainy, F.M., Sharobiem, W.M. and Ahmed, M.D. (2003). Surface ozone observations over Egypt. *Quarterly Journal of the Hungarian Meteorological Service*, 107(2), 133-152.

EL-Shahawy, M.A. and Hanna, A.F. (2003). Meteorological conditions leading to air-pollution episodes in greater Cairo City (Egypt). *Geophysical Research Abstracts*, 5(00103).<http://www.cosis.net/abstracts/EAE03/00103/EAE03-J-00103.pdf>.

Ezz, A.E. (2003). Growth of the Environment Market of Egypt: Profitable Compliance, the Carrot not the Stick. [http://www.eeaa.gov.eg/English/main/env2003\\_documents.asp](http://www.eeaa.gov.eg/English/main/env2003_documents.asp), accessed February, 2004.

Fahey, D.W. (2003). *Twenty Questions and Answers About the Ozone Layer: Scientific Assessment of Ozone Depletion: 2002*, World Meteorological Organization, Geneva, 42pp.

Fast, J.D. and Berkowitz, C.M. (1993). Evaluation of back trajectories associated with ozone transport during the 1993 North Atlantic regional experiment. [http://www.pnl.gov/atmos\\_sciences/res\\_hi8.html](http://www.pnl.gov/atmos_sciences/res_hi8.html), accessed May, 2005.

Fenger, J. (1999). Urban air quality. *Atmospheric Environment*, 33, 4877-4900.

Fishman, J. and Crutzen, P.J. (1978). The origin of ozone in the troposphere. *Nature*, 274, 855-858.

Fishman, J., Fakhruzzaman, K., Cros, B., and Nganga, D. (1991). Identification of widespread pollution in the Southern Hemisphere deduced from satellite analyses. *Science* 252, 1963-1966.

Fishman, J., Wozniak, A.E. and Creilson, J.K. (2003). Global distribution of tropospheric ozone from satellite measurements using the empirically corrected tropospheric ozone residual technique: Identification of the regional aspects of air pollution. *Atmospheric Chemistry and Physics*, 3, 893 – 907.

Guicherit, R. and Roemer, M. (2000). Tropospheric ozone trends. *Chemosphere-Global Change Science*, 2, 167-183.

Gusten, H., Heinrich, G., Cvitas, T., Klasinc, L., Ruscic, B., Lalas, D.P. and Petrakis, M. (1988). Photochemical formation and transport of ozone in Athens, Greece. *Atmospheric Environment*, 22 (9), 1855 - 1861.

Gusten, H., Heinrich, G., Weppner, J., Abdel-Aal, M. M., Abdel-Hay, F. A., Ramadan, A.B., Tawfik, F.S., Ahmed, D.M. Hassan, G.K.Y. and Cvita, T. (1994). Ozone formation in the greater Cairo area. *The Science of the Total Environment*, 155(3), 285-295.

Gouget, H. (2003). Case study of a tropopause fold and of subsequent mixing in the subtropics of the Southern Hemisphere. *Atmospheric Environment*, 34, 2653-2658.

Haby, J. (2005). Interpretation of Upward Vertical Velocity on synoptic models. <http://www.theweatherprediction.com/habyhints/195/>, accessed March, 2005.

Helas, G., Lobert, J., Scharffe, D., Schäfer, L., Goldammer, J., Baudet, J., Ajavon, A.L., Ahoua, B., Lacaux, J.-P., Delmas, R. and Andreae, M.O. (1995). Airborne measurements of savanna fire emissions and the regional distribution of pyrogenic pollutants over western Africa, *Journal of Atmospheric Chemistry*, 22, 217-239.

Hosseinian, R. and Gough, W. (2000). Stratospheric ozone trends and mechanisms over Toronto, Ontario, Canada. *The Great Lakes Geographer*, 7, 55-65.

Huntrieser, H., Heland, J., Forster, C., Lawrence, M., Mannstein, H., Junkermann, W., Arnold, F., Aufmhoff, H., Wilhelm, S., Elbern, H., Cooper, O., Stohl, A. and Schlager, H. (2002). Convective transport of trace gases into the middle and upper troposphere over Europe. Proceedings EUROTRAC-2 Symposium, P.M. Midgley and M. Reuther (Eds.), Margraf Verlag, Weikersheim. <http://www.pa.op.dlr.de/contrace/poster-eurotrac2002.pdf>, accessed May, 2005.

Jacobs, D.J. (1999). *Introduction to Atmospheric Chemistry*. Princeton University Press, Princeton, N.J. 261 pp.

Jaegle, L., Martin, R. V., Chance, K., Steinberger, L., Kurosu, T. P., Jacob, D. J., Modi, A. I., Yoboue, V., Sigha-Nkamdjou, L. and Galy-Lacaux, V. (2004). Satellite mapping of rain-induced nitric oxide emissions from soils. *Journal of Geophysical Research*, 109, D21310, doi: 10.1029/2004JD004787.

Jaegle, L., Steinberger, L., Martin, R.V., Chance, K.V., Kurosu, T.P., Palmer, P. and Chin, M. (2003). Space-based observations of the seasonal variations in biomass burning emissions of NO<sub>x</sub> and VOCs over Africa during 2000. *American Geophysical Union, Fall meeting*, 2003AGUFM.A22C1076J.

Kalabokas, P.D., Viras, L.G., Bartzis, J.G. and Repapis, C.C. (2000). Mediterranean rural ozone characteristics around the urban area of Athens. *Atmospheric Environment*, 34, 5199-5208.

Kalabokas, P.D., Chronopoulos, G., Varatsos, C. and Zerefos, C. (2004). Vertical tropospheric ozone characteristics over Athens, Greece. Proceedings of the XX Quadrennial Ozone Symposium. Kos, Greece, 1-8 June 2004. Edited by Zerefos, C., 191-192.

Kallos, G., Kotroni, V., Lagouvardos, K. and Papadopoulos, A. (1998). On the transport of air pollutants from Europe to North Africa, *Geophysical Research Letters*, 25(5), 619–622.

Kley, D., de Laat, A.T.J., Lal, S., Lawrence, M.G., Lobert, J.M., Mayol-Bracero, O.L., Mitra, A.P., Novakov, T., Oltmans, S.J., Prather, K.A., Reiner, T., Rodhe, H., Scheeren, H. A., Sikka, D. and Williams. J. (2001). The Indian Ocean Experiment: Widespread Air Pollution from South and Southeast Asia. *Science*. 291, 1031 -1036.

Kourtidis, K., Zerefos, C., Rapsomanikis, S., Simeonov, V., Balis, D., Perros, P.E., Thompson, A.M., Witte, J., Calpini, B., Sharobiem, W.M., Pappayannis, A., Mihalopolous, N., and Drakou, R. (2002). Regional levels of ozone in the troposphere over Eastern Mediterranean. *Journal of Geophysical Research*, 107(D18), 8140, doi: 10.1029/2000JD000140.

Labrador, L. J., von Kuhlmann, R. and Lawrence, M. G. (2004). The effects of lightning-produced NO<sub>x</sub> and its vertical distribution on atmospheric chemistry: sensitivity simulations with MATCH-MPIC. *Atmospheric Chemistry and Physics*, 4, 6239–6281.

Law, K. S., Plantévin, P. H., Shallcross, D. E., Rogers, H. L., Pyle J. A., Grouhel, C., Thouret, V. and Marenco, A. (1998). Evaluation of modeled O<sub>3</sub> using Measurement of Ozone by Airbus In-Service Aircraft (MOZAIC) data. *Journal of Geophysical Research*, 103 (D19), 25721 – 25737.

Lawrence, M.G., Rasch, P.J., von Kuhlmann, R., Williams, J., Fischer, H., de Reus, M., Lelieveld, J., Cruzten, P.J., Schultz, M., Stier, P., Huntrieser, H., Heland, J., Stohl, A., Forster, C., Elbern, H., Jacobs, H. and Dickerson, R.R. (2003). Global chemical weather forecasts for field campaign planning: predictions and observation of large scale features during MINOS, CONTRACE, and INDOEX. *Atmospheric Chemistry and Physics*, 3, 267-289.

Lee, D.S., Kohler, I., Grobler, F., Rohrer, F., Sausen, R., Gallardo –Klenner, L., Olivier, J.G.J., Dentener, F.J. and Bouwman, A.F. (1997). Estimations of global NO<sub>x</sub> emissions and their uncertainties. *Atmospheric Environment*, 31, 1735 – 1749.

Lelieveld, J. and Dentener, F. J. (2000). What controls tropospheric ozone? *Journal of Geophysical Research*, 105 (D3), 3531 – 3551.

Lelieveld, J., Berresheim, H., Borrmann, S., Crutzen, P.J., Dentener, F.J., Fischer, H., Flatau, P.J., Heland, J., Holzinger, R., Korrman, R., Lawrence, M.G., Levin, Z., Markowicz, K.M., Mihalopoulos, N., Minikin, A., Ramanathan, V., de Reus, M., Roelofs, G.J., Scheeren, H.A., Sciare, J., Schlager, H., Schultz, M., Siegmund, P., Steil, B., Stephanou, E.G., Stier, P., Traub, M., Warneke, C., Williams, J. and Ziereis, H. (2002). Global air pollution crossroads over the Mediterranean. *Science*, 298, 794-799.

Levine, J.S., Winstead, E.L., Parsons, D.A.B., Scholes, M.C., Scholes, R. J., Cofer, W.R., Cahoon, D. R. and Sebacher, D.I. (1996). Biogenic soil emissions of nitric oxide (NO) and nitrous oxide (N<sub>2</sub>O) from savannas in South Africa: The impact of wetting and burning, *Journal of Geophysical Research*, 101, 23,689– 23,697.

Levine, J. S. (1994). Biomass burning and the production of greenhouse gases. In Zapp, R.G. (editor). *Climate Biosphere Interaction: Biogenic Emissions and Environmental Effects of Climate Change*. John Wiley, New York, New York, USA, 139-160.

Lindskog, A., Beekmann, M., Monks, P., Roemer, M., Schuepbach, E. and Solberg, S. (2005). Tropospheric Ozone Research – TOR-2.

<http://eurotrac.ivl.se/TOR2/final%20report%20tor%202/01Overview.pdf>, accessed October, 2005.

Liu, S., Trainer, M., Fehsenfeld, F., Parrish, D., Williams, E., Fahey, D., Hubler, G., Murphy, P. (1987). Ozone production in the rural troposphere and the implication for regional and global ozone distributions. *Journal of Geophysical Research* 92, 4191–4207.

Mahlman, J. D. (1997). Dynamics of transport processes in the upper troposphere. *Science*, 276, 1079 – 1083.

Marengo, A., Thouret, V., Nedelec, P., Smit, H.G.J., Helten, M., Kley, D., Karcher, F., Simon, P., Law, K., Pyle, J., Poschmann, G., von Wrede, R., Hume, C. and Cook, T. (1998). Measurement of ozone and water vapor by AIRBUS in-service aircraft: The MOZAIC airborne program, an overview *Journal of Geophysical Research*, 103, 25631-25642.

Marufu, L., Dentener, F., Lelieveld, J., Andreae, M.O. and Helas, G. (2000). Photochemistry of the African troposphere: Influence of biomass burning emissions. *Journal of Geophysical Research*, 105(D11), 14513-14530.

Millan, M.M., Salvador, R., Mantilla, E. and Kallos, G. (1997). Photooxidant dynamics in the Mediterranean basin during summer: Results from European research projects. *Journal of Geophysical Research*, 102 (D7), 8811 – 8823.

Mohamed, G.R. (2004). Air pollution management in Northern African Cities. Proceedings of the Regional Workshop on Better Air Quality in the Cities of Africa. Johannesburg, South Africa, 21-23 April 2004. Edited by Feresu, S., Simukanga, S., Haq, G, Hicks, K. and Schwela, D., 53-63.

Mohamed, M.F., Kang D. and Aneja V.P. (2002). Volatile organic compounds in some urban locations in United States. *Chemosphere*, 47, 863–882.

Molina M.J. and Molina, L.T. (2004). Megacities and atmospheric pollution. *Journal of Air and Waste Management Association*, 54, 644–680.

Monks, P.S. (2000). A review of the observations and origins of the spring ozone maximum. *Atmospheric Environment*, 34, 3535-3561.

MOZAIC (Measurement of Ozone and Water vapour by Airbus In-service Aircraft) website. (2005a). <http://www.aero.obs-mip.fr/mozaic/coverage.html>, accessed November, 2005.

MOZAIC (Measurement of Ozone and Water vapour by Airbus In-service Aircraft) website. (2005b). <http://www.aero.obs-mip.fr/mozaic/>, accessed November, 2005.

NCEP-DOE (National Center for Environmental Prediction-Department of Energy Reanalysis Data). (2004). Reanalysis monthly pressure files. [http://nomad1.ncep.noaa.gov/cgi-bin/pdisp\\_mp\\_r2.sh](http://nomad1.ncep.noaa.gov/cgi-bin/pdisp_mp_r2.sh), accessed October, 2004.

Nedelec, P., Cammas J.-P., Thouret, V., Athier, G., Cousin, J.-M., Legrand, C. Abonnel, C., Lecoœur, F., Cayez, G. and Marizy, C. (2003). An improved infrared carbon monoxide analyser for routine measurements aboard commercial Airbus aircraft: technical validation and first scientific results of the MOZAIC III programme. *Atmospheric Chemistry and Physics*. 3, 1551-1564.

Newchurch, M.J., Ayoub, M.A., Oltmans, S., Johnson, B. and Schmidlin F.J. (2003). Vertical distribution of ozone at four sites in the United States. *Journal of Geophysical Research*, 108(D1), 4031, doi: 10.1029/2002JD002059.

NOAA-ARL (National Oceanic and Atmospheric Administration-Air Resources Laboratory). (2005a). HYSPLIT Description. [http://www.arl.noaa.gov/ready/hysp\\_info.html](http://www.arl.noaa.gov/ready/hysp_info.html), accessed May, 2005.

NOAA-ARL (National Oceanic and Atmospheric Administration-Air Resources Laboratory). (2005b). HYSPLIT active trajectories using reanalysis data. <http://www.arl.noaa.gov/hysplitarc-bin/traj1file.pl?metdata=reanalysis>, accessed September, 2005.

Nolle, M., Ellul, R., Heinrich, G. and Gusten, H. (2002). A long-term study of background ozone concentrations in the central Mediterranean - diurnal and seasonal variations on the island of Gozo. *Atmospheric Environment*, 36 (8), 1391-1402.



Otter, L.B., Guenther, A. and Greenberg J. (2002). Seasonal and spatial variations in biogenic hydrocarbon emissions from southern African savannas and woodlands. *Atmospheric Environment*, 36, 4265–4275.

Parrish, D.D., Ryerson, T. B., Holloway, J. S., Trainer, M. and Fehsenfeld, F.C. (1999). New Directions: Does pollution increase or decrease tropospheric ozone in Winter–Spring? *Atmospheric Environment*, 33(30), 5147-5149

Parrish, D.D., Hahn, C.J., Williams, E.J., Norton, R.B., Fehsenfeld, F.C., Singh, H.B., Shetter, J.D., Gandrud, B.W., Ridley, B.A. (1992). Indications of photochemical histories of Pacific air masses from measurements of atmospheric trace species at Point Arena, California. *Journal of Geophysical Research*, 97 (15), 883–901.

Pickering, K.E., Thompson, A.M., Scala, J.R., Tao, W-K., Simpson, J. and Garstang. M. (1991). Photochemical ozone production in tropical squall line convection during NASA/GTE/ ABLE 2A. *Journal of Geophysical Research*, 96, 3099-3114.

Pickering, K. E., Thompson, A. M., Scala, J. R., Tao, W. K., and Simpson, J. (1992). Ozone production potential following convective redistribution of biomass burning emissions, *Journal of Atmospheric Chemistry*, 14, 297–313.

Pickering, K., Thompson, A. M., Tao, W. K., and Kucsera, T. (1993). Upper tropospheric ozone production following mesoscale convection during STEP/EMEX, *Journal of Geophysical Research*, 98 (D5), 8737–8749.

Potter, C.S., Alexander, S.E., Coughlan J.C and Klooster, S.A. (2001). Modeling biogenic emissions of isoprene: exploration of model drivers, climate control algorithms, and use of global satellite observations. *Atmospheric Environment*, 35, 6151-6165.

Price, J.D. and Vaughan, G. (1992). Statistical studies of cut-off low systems. *Annales Geophysicae*, 10, 96-102.

Ragunandan, A. (2002). Nature and Characteristics of Tropospheric Ozone over Johannesburg. Unpublished M.A. Thesis, School of Life and Environmental Sciences, University of Natal, Durban. 145pp.

Ramanathan, V., Crutzen, P.J., Lelieveld, J., Mitra, A.P., Althausen, D., Anderson, J., Andreae, M.O., Cantrell, W., Cass, G.R., Chung, C.E., Clarke, A.D., Coakley, J.A., Collins, W.D., Conant, W.C., Dulac, F., Heintzenberg, J., Heymsfield, A.J., Holben, B., Howell, S., Hudson, J., Jayaraman, A., Kiehl, J.T., Krishnamurti, T.N., Lubin, D., MacFarquhar, G., Novakov, T., Ogren, J.A., Podgorny, I.A., Prather, K., Priestley, K., Prospero, J.M., Quinn, P.K., Rajeev, K., Rasch, P., Rupert, S., Sadourny, R., Satheesh, S.K., Shaw, G.E., Sheridan, P. and Valero, F.P.J. (2001). The Indian Ocean Experiment: An integrated analysis of the climate forcing and effects of the great Indo-Asian haze. *Journal of Geophysical Research*, 106(D22), 28371–28398.

Ramsay, L.F. (2003). In Search of Representative Vertical Ozone Profiles for Johannesburg: A Statistical Perspective. Unpublished BSc Honours Thesis, Life and Environmental Sciences, University of Natal, Durban. 159pp.

Reed, R. (1955). A study of a characteristic type of upper-level frontogenesis. *Journal of Meteorology*, 12, 226- 237.

Ribas, A. and Penuelas, J. (2004). Temporal patterns of surface ozone levels in different habitats of the North Western Mediterranean Basin. *Atmospheric Environment*, 38, 985-992.

Richter, A., NuB, H., Burrows, J.P. and Granier, C. (2004). Long term measurements of NO<sub>2</sub> and other tropospheric species from space. Proceedings of the XX Quadrennial Ozone Symposium. Kos, Greece, 1-8 June 2004. Edited by Zerefos, C., 213-214.

Robaa, S.M. (2003). Urban-suburban/rural differences over Greater Cairo, Egypt. *Atmosfera*, 157 -171.

Roelofs, G.J., Scheeren, H. A., Heland, J., Ziereis, H. and Lelieveld, J. (2003). A model study of ozone in the eastern Mediterranean free troposphere during MINOS (August 2001). *Atmospheric Chemistry and Physics*, 4, 65- 80.

Scheeren, H.A., Lelieveld, J., Roelofs, G.J., Williams, J., Fischer, H., de Reus, M., de Gouw, J.A., Warneke, C., Holzinger, R., Schlager, H., Klüpfel, T., Bolder, M., van der Veen, C. and Lawrence, M. (2003). The impact of monsoon outflow from India and South-East Asia in the upper troposphere over the eastern Mediterranean, *Atmospheric Chemistry and Physics*, 3, 1589-1608.

Scholes, M and Andreae, M.O. (2000). Biogenic and pyrogenic emissions from Africa and their impact on the global atmosphere. *AMBIO: A Journal of the Human Environment*, 29, 23-29.

Shaltout, M.A.M., Hassan, A.H. and Fathy, A.M. (2001). Total suspended particles and solar radiation over Cairo and Aswan. *Renewable Energy* 23, 605–619.

Shaw, E., Naderzad, A. and Boies, B. (2004). Lifting the Black Cloud. <http://www.columbia.edu/~bbb58/cairo.htm>, accessed August, 2004

Staley, D.O. (1962). On the mechanism of mass and radioactivity transport from the stratosphere to the troposphere. *Journal of Atmospheric Sciences*, 19, 450 - 467.

Stohl, A., Eckhardt, O.R., Forster, C., James, C. and Spichtinger, C. (2002a). On the pathways and timescales of intercontinental air pollution transport. *Journal of Geophysical Research*, 107(D23) 4684, doi: 10.1029/2001JD001396.

Stohl, A., Eckhardt, S., Forster, C., James, P., Spichtinger, N. and Seibert, P. (2002b). A replacement for simple back trajectory calculations in the interpretation of atmospheric trace substance measurements. *Atmospheric Environment*, 36, 4635-4648.

Singh, H.B and Jacob, D.J. (2000). Future Directions: Satellite observations of tropospheric chemistry. *Atmospheric Environment*, 34, 4399 – 4401.

Sivertsen, B. (1999). Air pollution levels measured in Egypt exceed air quality limits. <http://www.nilu.no/niluweb/filer/newsletter-aq2.pdf>, accessed August, 2004.

Sivertsen, B. (2000). Understanding air quality measurements.

<http://www.nilu.no/data/inc/leverfil.cfm?id=1895&type=6>, accessed August, 2004.

Sorensen, J. H. and Nielsen, N.W. (2001). Intrusion of stratospheric ozone to the free troposphere through tropopause folds -A Case Study *Physics and Chemistry of the Earth (B)*, 26(10), 801-806.

Strand, V. and Hov, V. (1996). The impact of man-made and natural NO<sub>x</sub> emissions on upper tropospheric ozone: A two-dimensional model study. *Atmospheric Environment*, 30, (8), 1291-1303.

TEMIS (Tropospheric Emission Monitoring Internet Service). (2004a). Nitrogen dioxide and Formaldehyde. <http://www.temis.nl/products/no2.html#obs>, accessed June 2004.

TEMIS (Tropospheric Emission Monitoring Internet Service). (2004b). Tropospheric NO<sub>2</sub> from satellites. <http://www.temis.nl/airpollution/no2col/no2regiogome.php>, accessed June 2004.

Thompson, A. M., Diab, R. D., Bodecker, G. E., Zunckel, M., Coetzee, G. J. R., Archer, C. B., McNamara, D. P., Pickering, K. E., Combrink, J. B., Fishman, J. and Nganga, D. (1996). Ozone over southern Africa during SAFARI-92/TRACE A, *Journal of Geophysical Research*, 101, 23793-23808.

Thompson, A.M., Wiite, J.C., Freiman, M.T., Phahlane, N.A. and Coetzee, G.J.R. (2002). Lusaka, Zambia, during SAFARI-2000: Convergence of local and imported ozone pollution. *Geophysical Research Letters*, 29(20), doi: 10.129/2002GL015399.

Thouret, V., Marenco, A., Nédelec, P and Grouhel, C. (1998). Ozone climatologies at 9 – 12 km altitude as seen by the MOZAIC airborne program between September 1994 and August 1996. *Journal of Geophysical Research*, 103 (D19), 25653 – 25679.

Thouret, V., Cammas, J.P., Sauvage, B., Athier, G., Zbinden, R., Nedelec P., Simon, P. and Karcher, F. (2005). Tropopause referenced ozone climatology and inter-annual variability (1994–2003) from the MOZAIC programme. *Atmospheric Chemistry and Physics*, 5, 5441–5488.

Thunis P. and Cuvelier. C. (2000). Impact of biogenic emissions on ozone formation in the Mediterranean area – a BEMA modelling study. *Atmospheric Environment*, 34, (3), 467-481.

TOMS (Total Ozone Mapping Spectrometer). (2005). Earth Probe TOMS Data & Images. [http://toms.gsfc.nasa.gov/eptoms/ep\\_v8.html](http://toms.gsfc.nasa.gov/eptoms/ep_v8.html), accessed September, 2005

Traub, M., Fischer, H., de Reus, M., Kormann, R., Heland, J., Ziereis, H., Schlager, H., Holzinger, R., Williams, J., Warneke, C., de Gouw, J. and Lelieveld, J. (2003). Chemical characteristics assigned to trajectory clusters during the MINOS campaign. *Atmospheric Chemistry and Physics*, 3, 459-468.

Treffeisen, R., Grunow, K., Moller, D. and Hainsch, A. (2002). Quantification of source region influences on the ozone burden. *Atmospheric Environment*, 36, 3565 – 3582.

Trickl, T., Cooper, O., Eisele, H., James, P., Mücke, R. and Stohl, A. (2003). Intercontinental transport and its influence on the ozone concentrations over central Europe: Three case studies. *Journal of Geophysical Research*, 108(D12) 8530, doi: 10.1029/2002JD002735.

Tyson, P. D. and Preston-Whyte, R. A. (2000). *The Weather and Climate of Southern Africa*. Oxford University Press, Cape Town. 396pp.

UNEP (United Nations Environment Programme). (2000). Global environment outlook. GEO: 2000. <http://www.unep.org/geo2000/english/0058.htm>, accessed March 2004.

UNEP (United Nations Environment Programme). (2001). Climate Change 2001: Working Group I: The Scientific Basis. Intergovernmental panel on climate change. [http://www.grida.no/climate/ipcc\\_tar/wg1/235.htm](http://www.grida.no/climate/ipcc_tar/wg1/235.htm), accessed March 2004.

Varinou, M. Kallos, G., Tsiligridis, G. and Sistla, G. (1999). The role of anthropogenic and biogenic emissions on tropospheric ozone formation over Greece. *Physics and Chemistry of the Earth (C)*, 24, (5), 507-513.

Varotsos, C. and Efsthathiou, M. (2004). Observed Variability of Tropospheric Ozone at Athens- Greece. Proceedings of the XX Quadrennial Ozone Symposium. Kos, Greece, 1-8 June 2004. Edited by Zerefos, C., 865-866.

Vaughan, G. (1988). Stratosphere-troposphere exchange of ozone. In *Tropospheric Ozone* Isaksen, I.S.A. (Ed), D. Reidel Publishing, 125 – 135.

Vingarzan, R. (2004). A review of surface ozone background levels and trends. *Atmospheric Environment* 38, 3431–3442.

Vrekoussis, M., Kanakidou, M., Mihalopoulos, N., Crutzen, P.J., Lelieveld, J., Perner, D., Berresheim, H. and Baboukas, E. (2004). Role of the NO<sub>3</sub> radicals in oxidation processes in the eastern Mediterranean troposphere during the MINOS. *Atmospheric Chemistry and Physics*. 4, 169-182.

Waguih, A. (2002). Agriculture officials take on the cloud.

[http://www.amcham.org.eg/Publications/BusinessMonthly/December%2002/Reports\(AgricultureofficialstakeontheCloud\).asp](http://www.amcham.org.eg/Publications/BusinessMonthly/December%2002/Reports(AgricultureofficialstakeontheCloud).asp), accessed, February, 2004.

Wang, Y., Jacob, D.J. and Logan, J.A. (1998). Global simulation of tropospheric O<sub>3</sub>-NO<sub>x</sub>-hydrocarbon chemistry. Origin of tropospheric ozone and effects of nonmethane hydrocarbons. *Journal of Geophysical Research*, 103 (10), 757–768.

Waugh, D.W. and Polvani, L.M. (2000). Climatology of Intrusions into the Tropical Upper Troposphere. *Geophysical Research Letters*, 27(23), 3857-3860.

Wenig, M., Spichtinger, N., Stohl, A., Held, G., Beirle, S., Wagner, T., Jahne, B. and Platt, U. (2003). Intercontinental transport of nitrogen oxide pollution plumes. *Atmos. Chem. Phys.*, 3, 387–393.

Wild, O. and Akimoto, H. (2001). Inter continental transport and chemical transformation of ozone and its precursors from east Asia. *Present and Future of Modeling of Global Environmental Change*. (eds) Matsuno, T. and Kida, H. TERRAPUB, 375-382.

Wild, O., Law, K.S., McKenna, K.S., Bandy, B.J., Penkett, S.A. and Pyle, J. (1996). Photochemical trajectory modeling studies of the North Atlantic region during August 1993, *Journal of Geophysical Research*, 101, 29269-29288.

Zakey A.S. (2004). Ozone variability over Tropics and its specific features over Egypt. *Proceedings of the XX Quadrennial Ozone Symposium*. Kos, Greece, 1-8 June 2004. Edited by Zerefos, C., 266.

Zakey, A.S. and Abdel-Wahab, M.M. (2004). Ozone Chemistry over Cairo, Egypt. *Proceedings of the XX Quadrennial Ozone Symposium*. Kos, Greece, 1-8 June 2004. Edited by Zerefos, C., 226.

Zakey, A.S., Abdel-Wahab M.M. and Makar, P.A. (2004). Atmospheric turbidity over Egypt. *Atmospheric Environment* 38(11), 1579-1591.

Zbinden, R.M., Cammas, J.-P., Thouret, V., Nedelec, P., Karcher, F. and Simon, P. (2005). Mid-latitude tropospheric ozone columns from the MOZAIC program: climatology and interannual variability mid-latitude tropospheric ozone columns from the MOZAIC program: climatology and inter-annual variability. *Atmospheric Chemistry and Physics*, 5, 5489–5540.

Zerefos, C.S., Kourtidis, K.A., Melas, D., Balis, D., Zanis, P., Katsaros, L., Mantis, H.T., Repapis, C., Isaksen, I., Sundet, J., Herman, J., Bhartia, P.K. and Calpini, B. (2002). Photochemical Activity and Solar Ultraviolet Radiation (PAUR). Modulation Factors: An overview of this project. *Journal of Geophysical Research*, 107 (D18). DOI 10.1029/2000JD000134.

Ziomas, I.C. (1998). The Mediterranean Campaign of Photochemical Tracers-Transport and Chemical Evolution (MEDCAPHOT-TRACE): An outline. *Atmospheric Environment*, 32(12), 2045-2053.



**APPENDIX A**  
**Mean monthly total column ozone over Cairo**  
**(TOMS, 2005)**

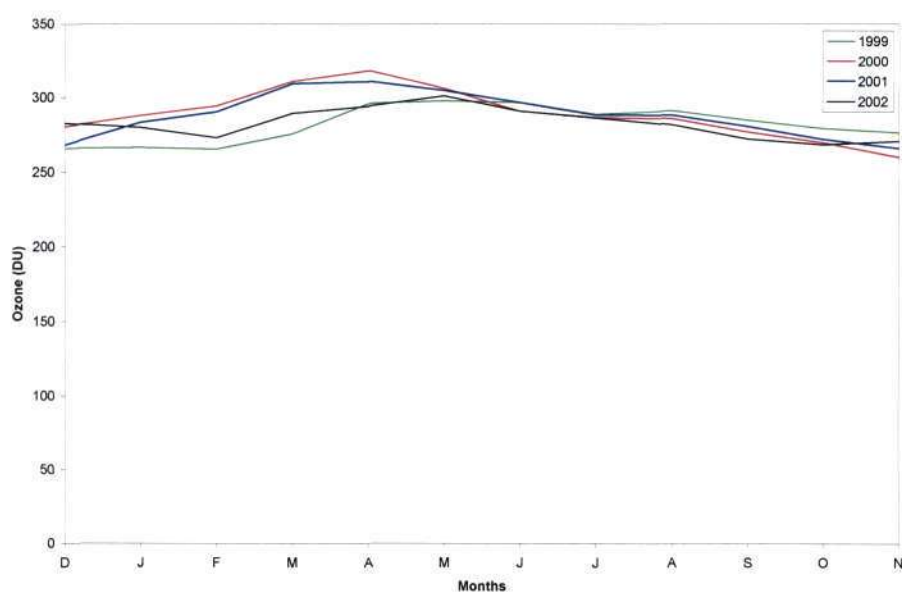
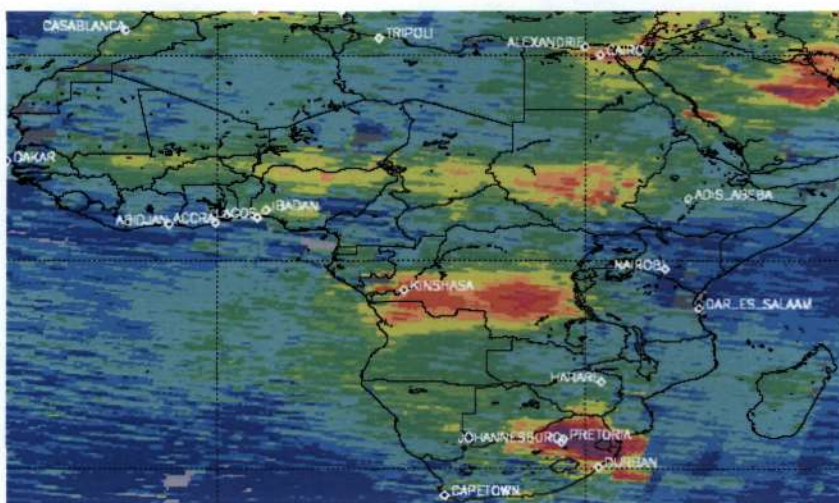
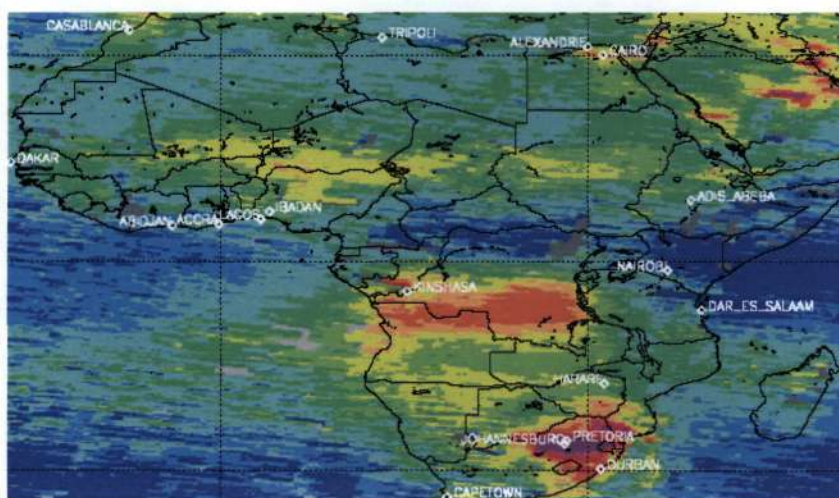


**Figure A1: Mean Monthly Total Column Ozone over Cairo for the period 1999 -2002 based on TOMS satellite data**

**APPENDIX B**  
**Tropospheric NO<sub>2</sub> over Africa for JJA**  
**(TEMIS, 2004b)**



June



July

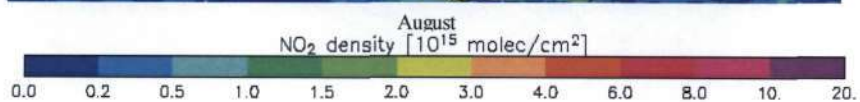
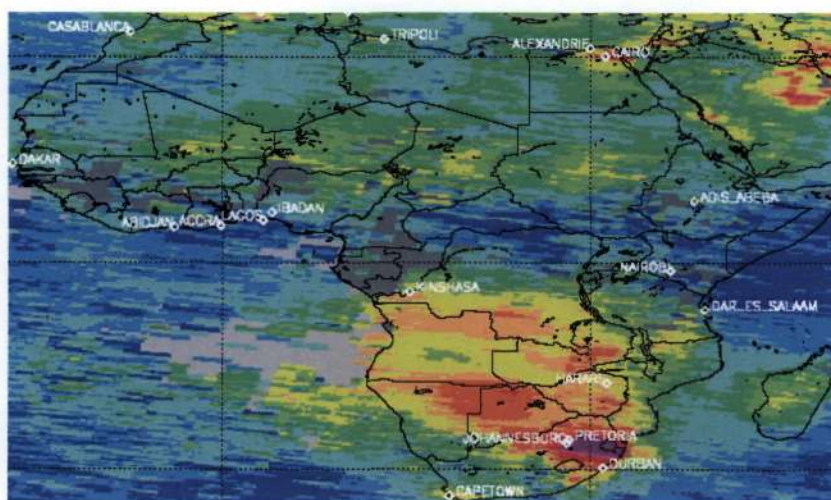
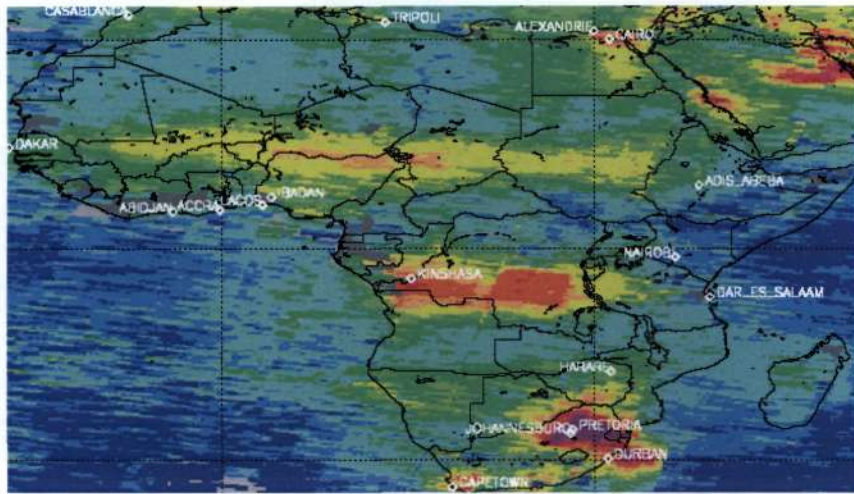
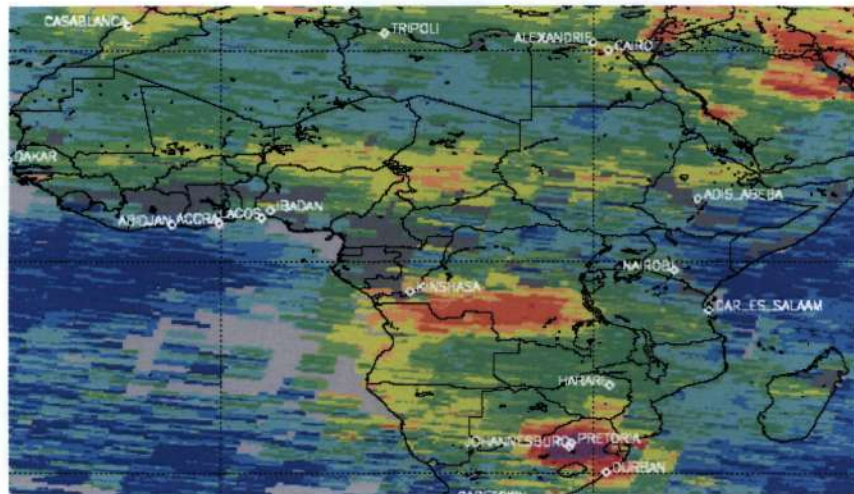


**Figure B1: Tropospheric NO<sub>2</sub> over Africa for June, July and August (JJA) 1999 from GOME**

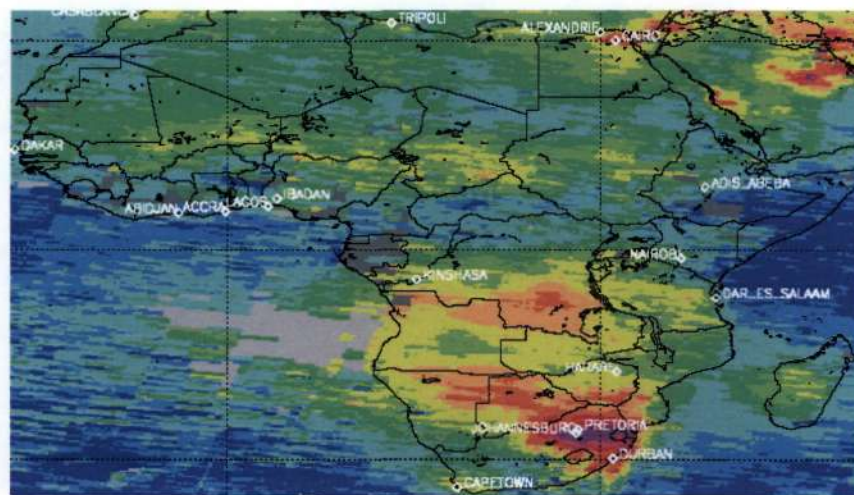




June



July



August

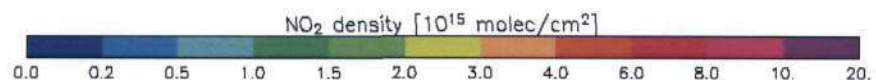
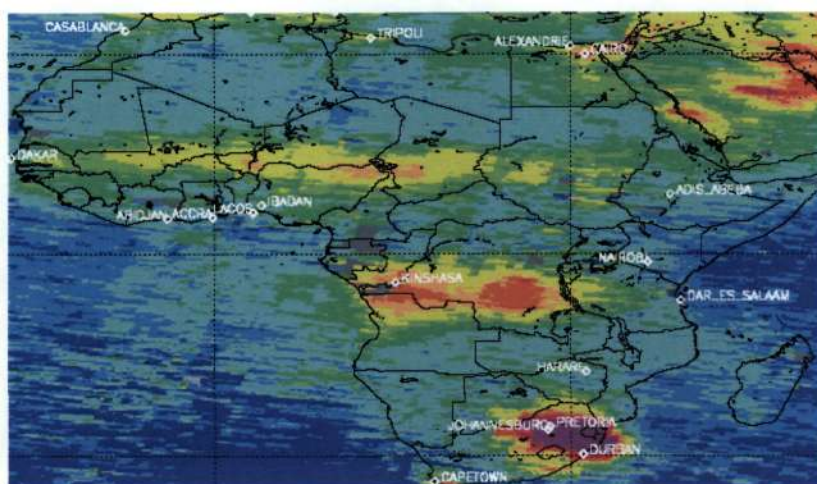
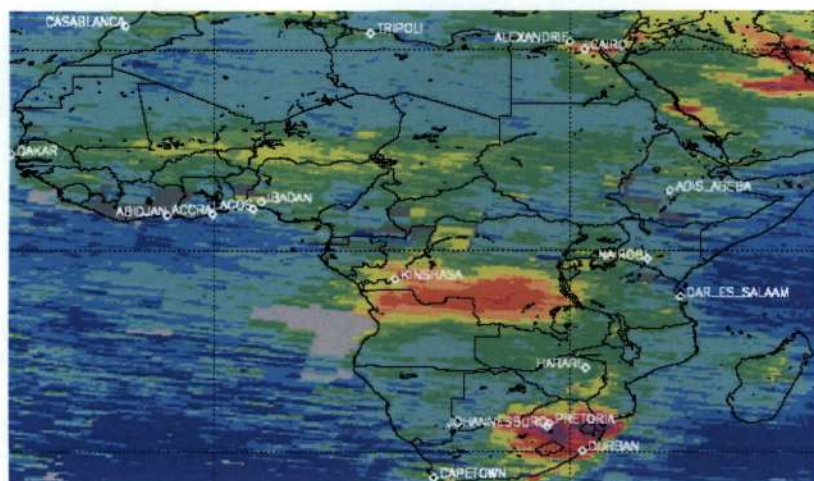


**Figure B2: Tropospheric NO<sub>2</sub> over Africa for June, July and August (JJA) 2000 from GOME**

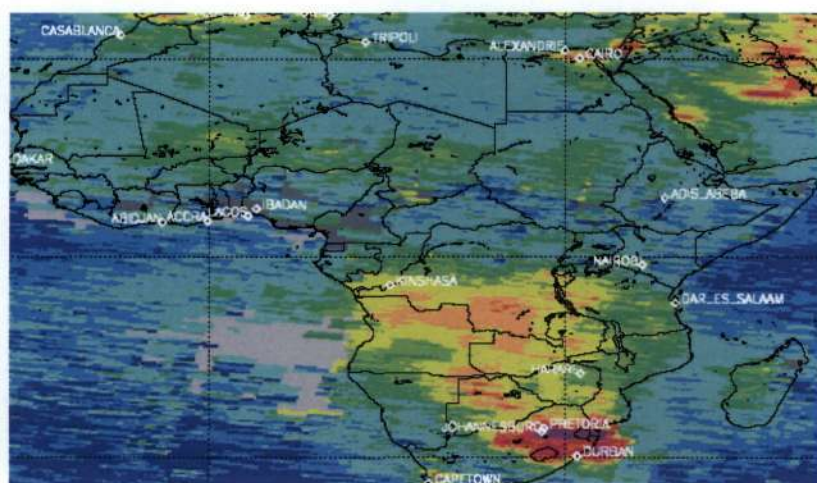




June



July



August

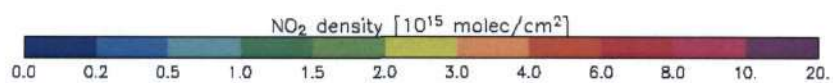
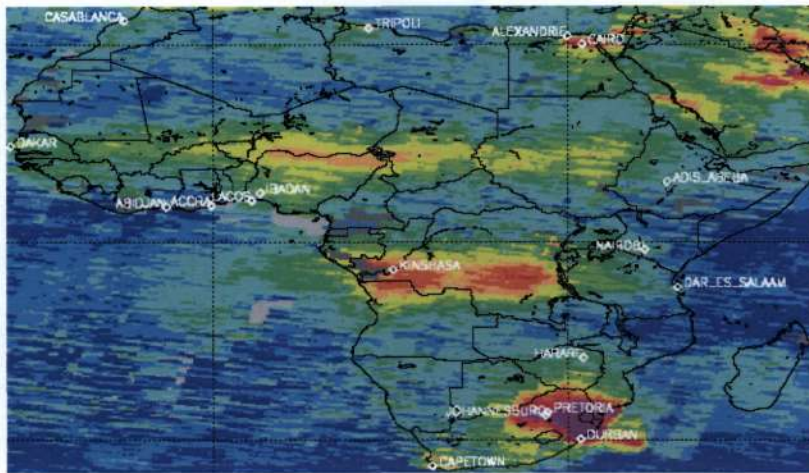
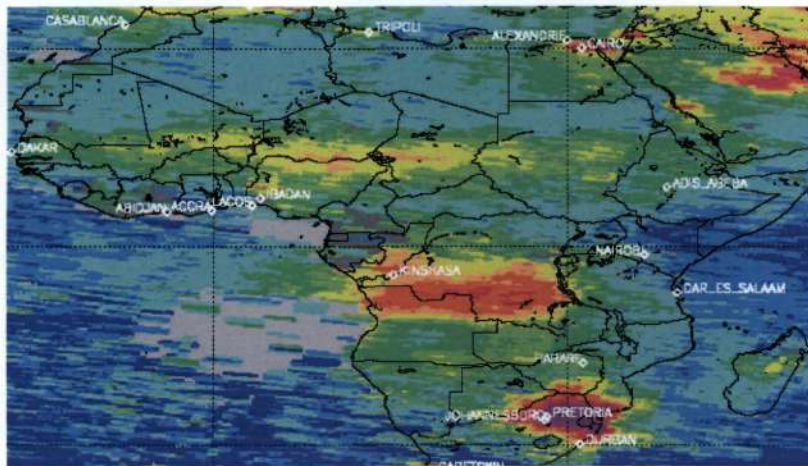


**Figure B3: Tropospheric NO<sub>2</sub> over Africa for June, July and August (JJA) 2001 from GOME**

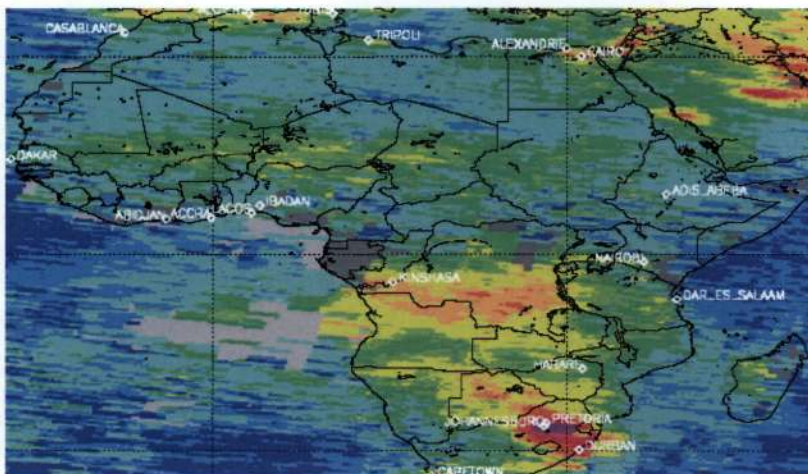




June



July



August

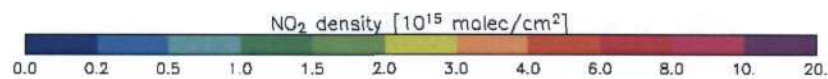
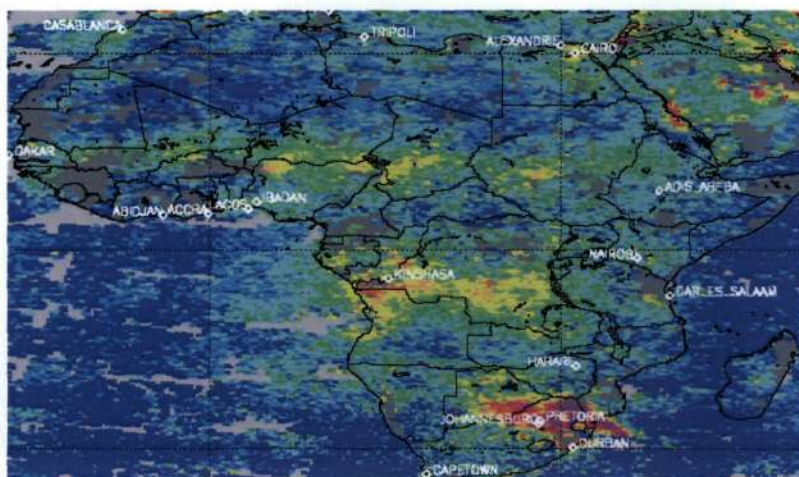
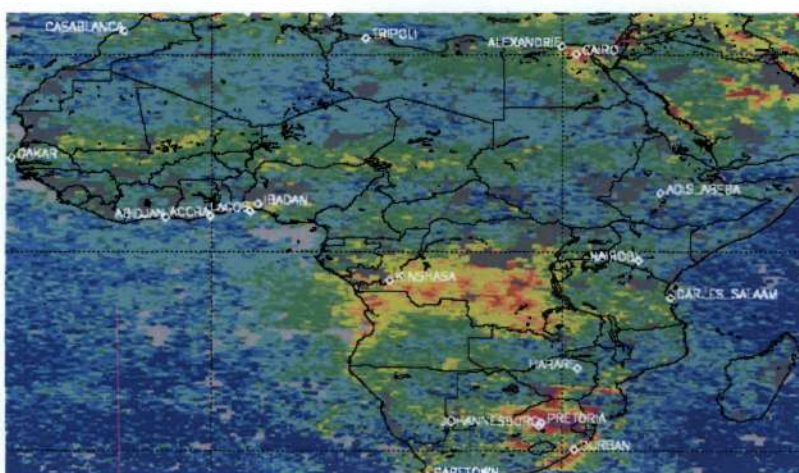


**Figure B4: Tropospheric NO<sub>2</sub> over Africa for June, July and August (JJA) 2002 from GOME**

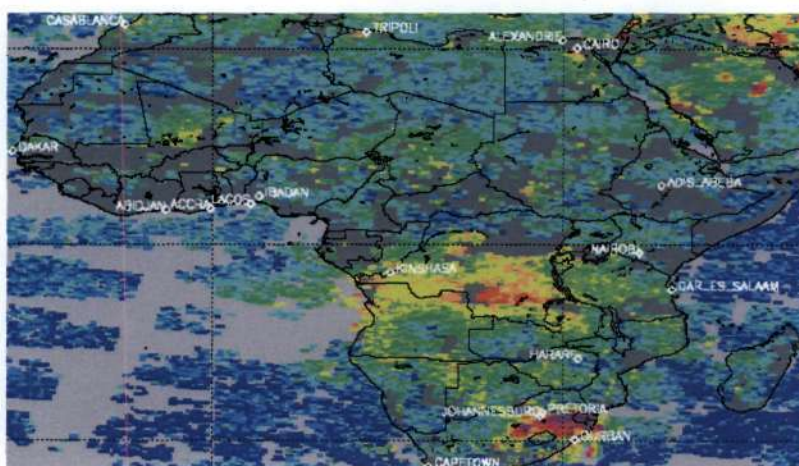




June



July



August

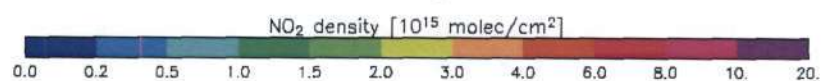


**Figure B5: Tropospheric NO<sub>2</sub> over Africa for June, July and August (JJA) 2003 from SCIAMACHY**

## **APPENDIX C**

### **Vertical velocity (Pa/s) Maps JJA FOR 1999- 2002 (NCEP-DOE Reanalysis Data, 2004)**

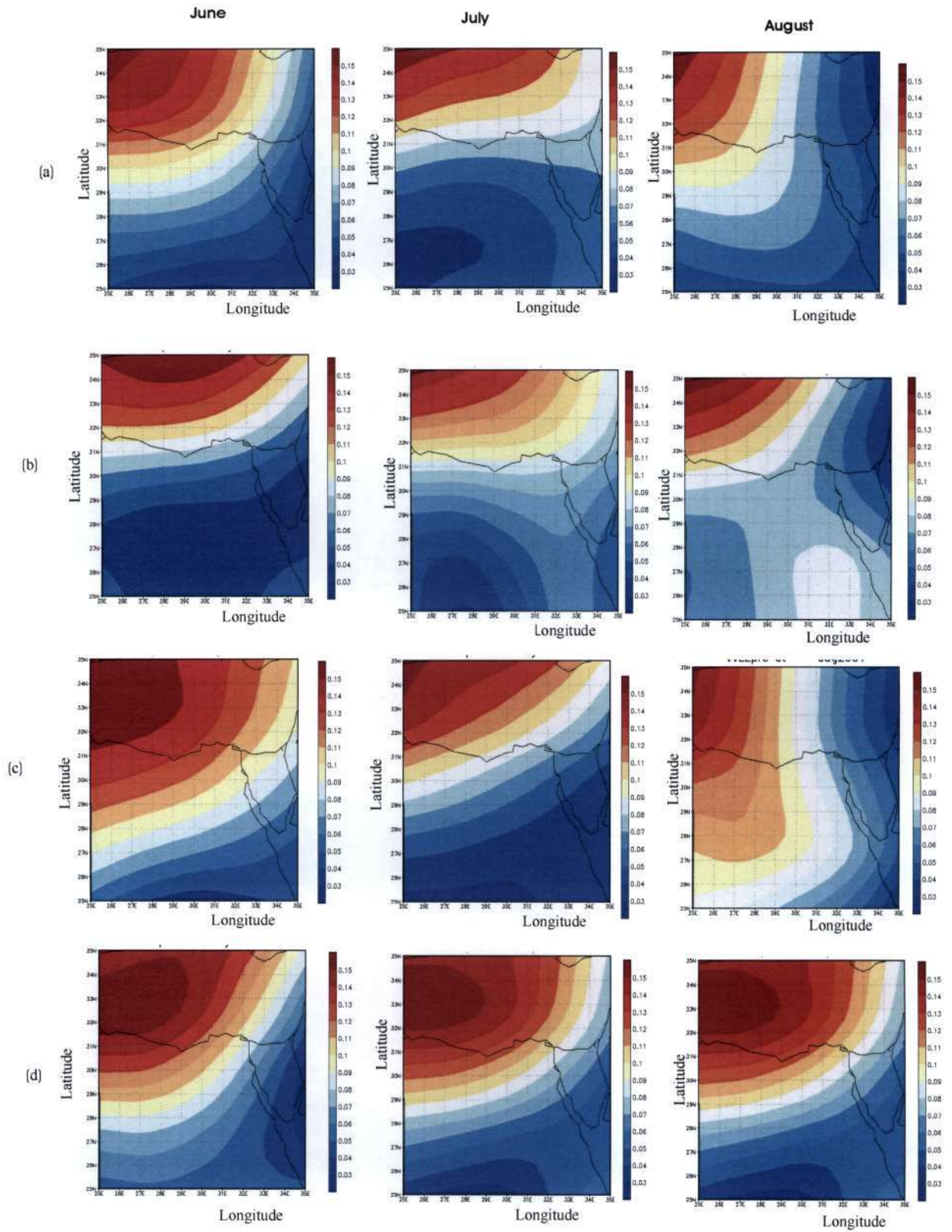


**Figure C1: 500 hPa vertical velocity (Pa/s) Maps JJA for (a) 1999 (b) 2000 (c) 2001 and (d) 2002.**



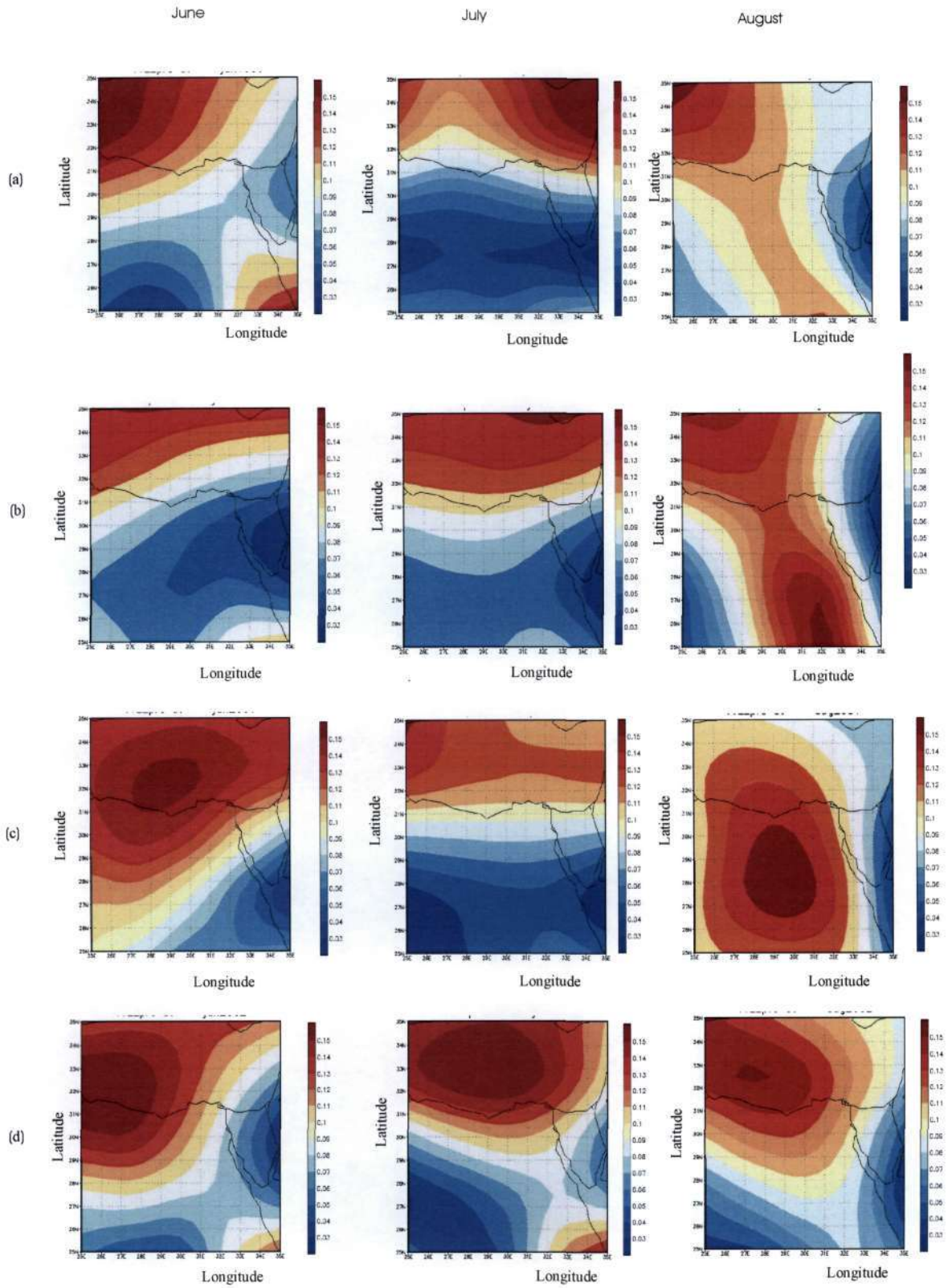


**Figure C2: 700 hPa vertical velocity (Pa/s) Maps JJA for (a) 1999 (b) 2000 (c) 2001 and (d) 2002**

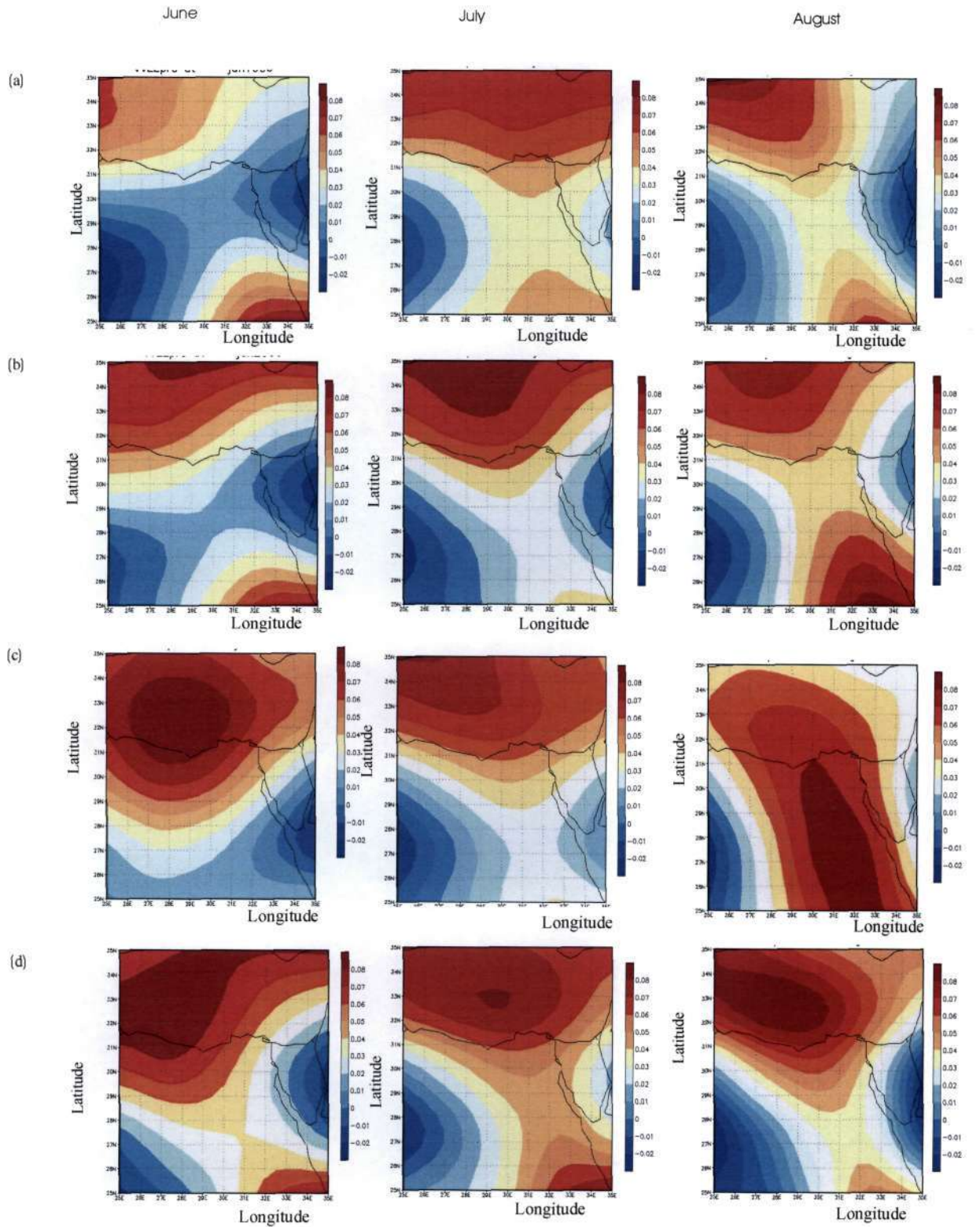


**Figure C3: 850 hPa vertical velocity (Pa/s) Maps JJA for (a) 1999 (b) 2000 (c) 2001 and (d) 2002**



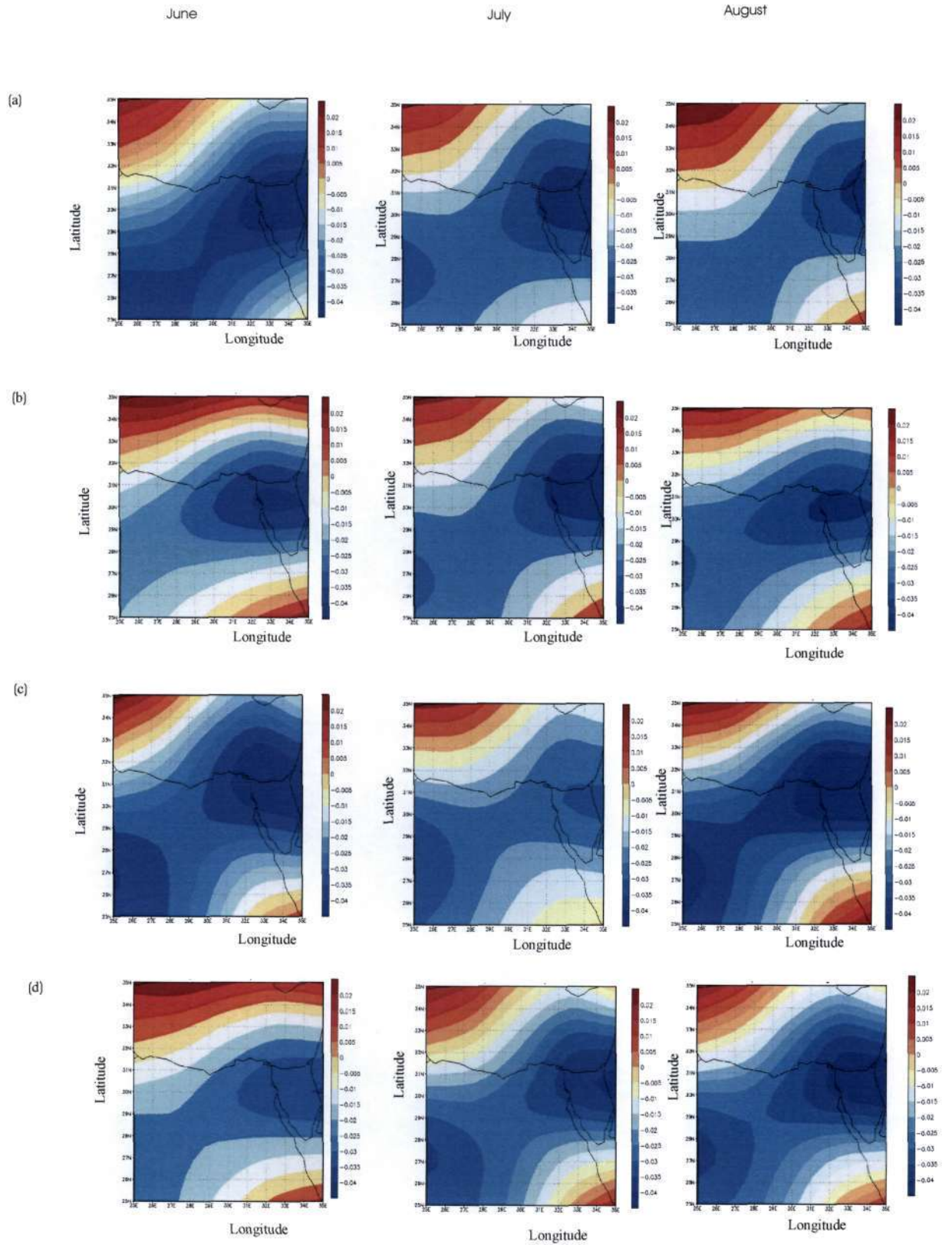


**Figure C4: 1000 hPa vertical velocity (Pa/s) Maps JJA for (a) 1999 (b) 2000 (c) 2001 and (d) 2002**

## **APPENDIX D**

### **Back Trajectories for SPSS Groups 1-5 (NOAA-ARL, 2005b)**



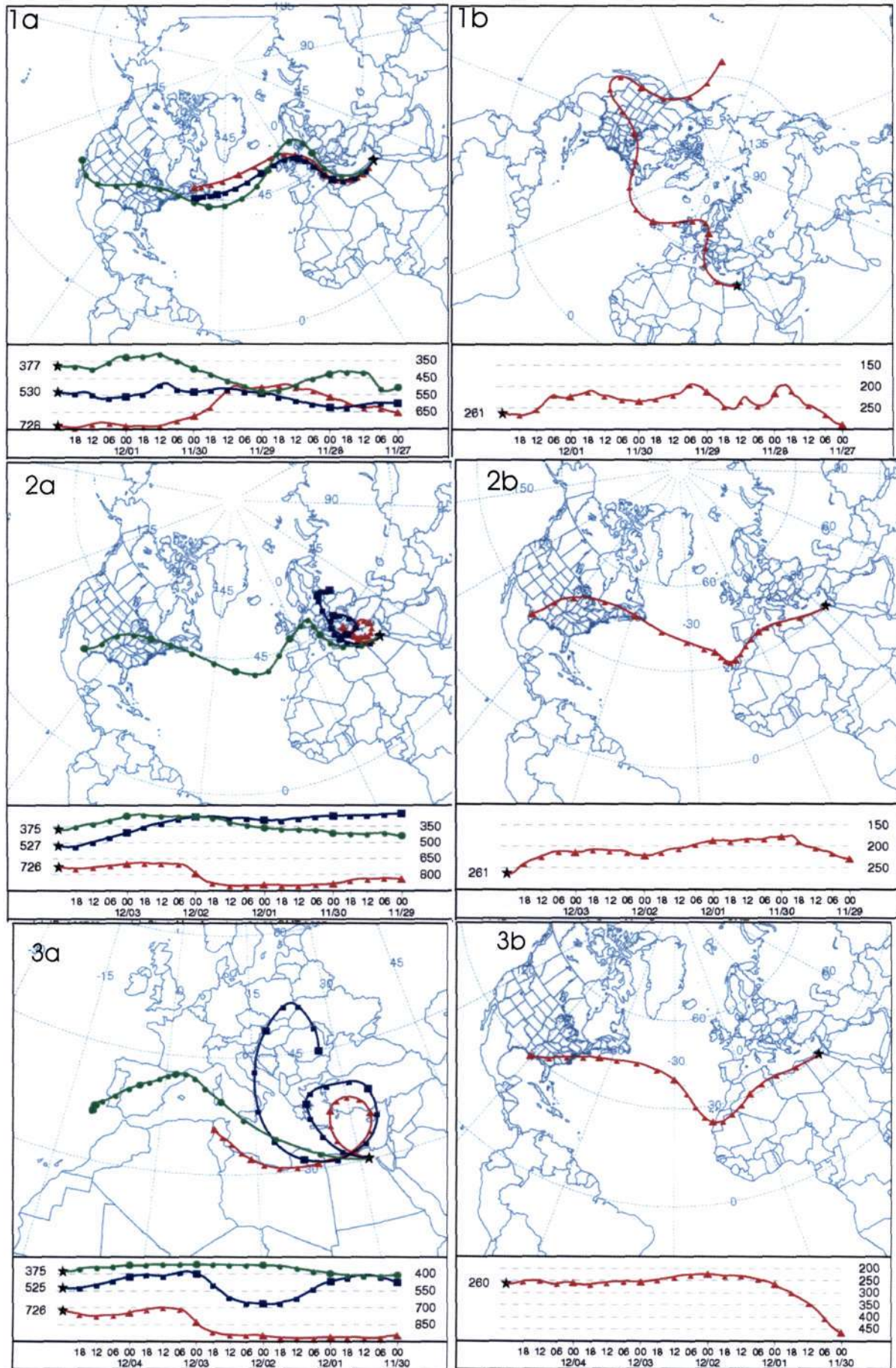
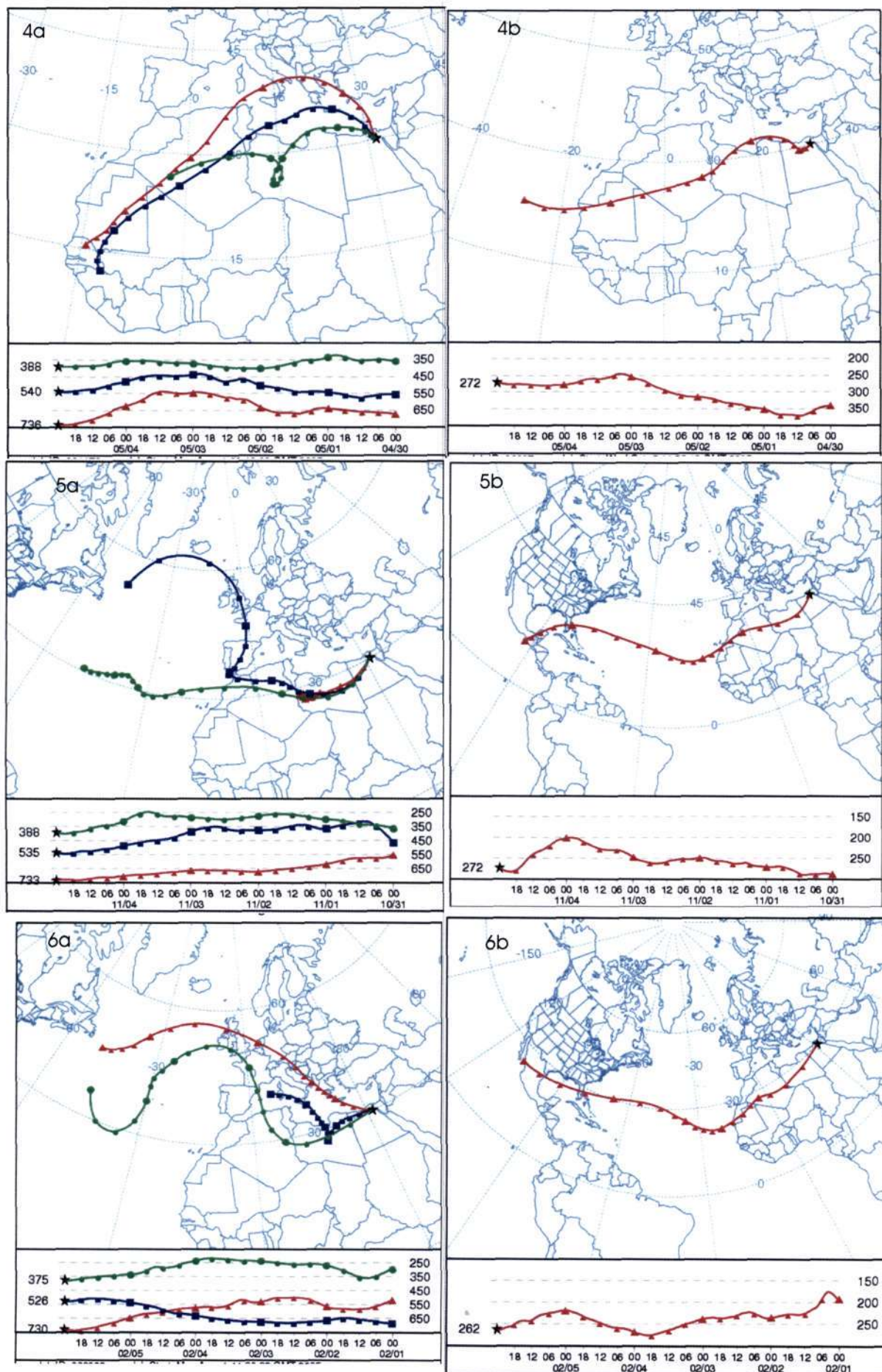
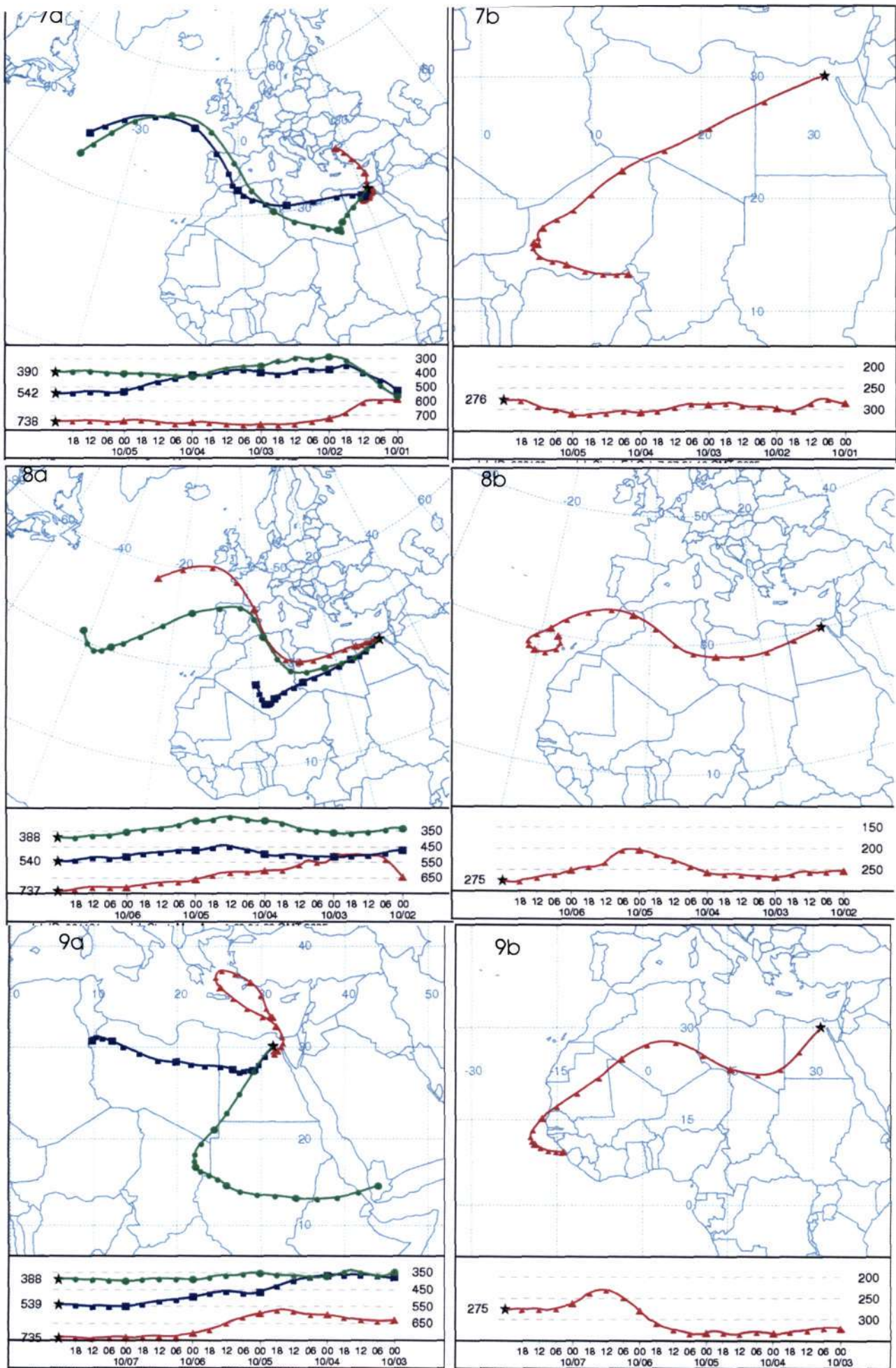


Figure D1: 5-day back trajectory HYSPLIT model results for Group 1. (1) 2 December 2001 (2) 4 December 2001 and (3) 5 December 2001  
 a) Horizontal and vertical plots of back trajectories originating at 2.5, 5 and 7.5 km  
 b) Horizontal and vertical plots of back trajectories originating at 10 km











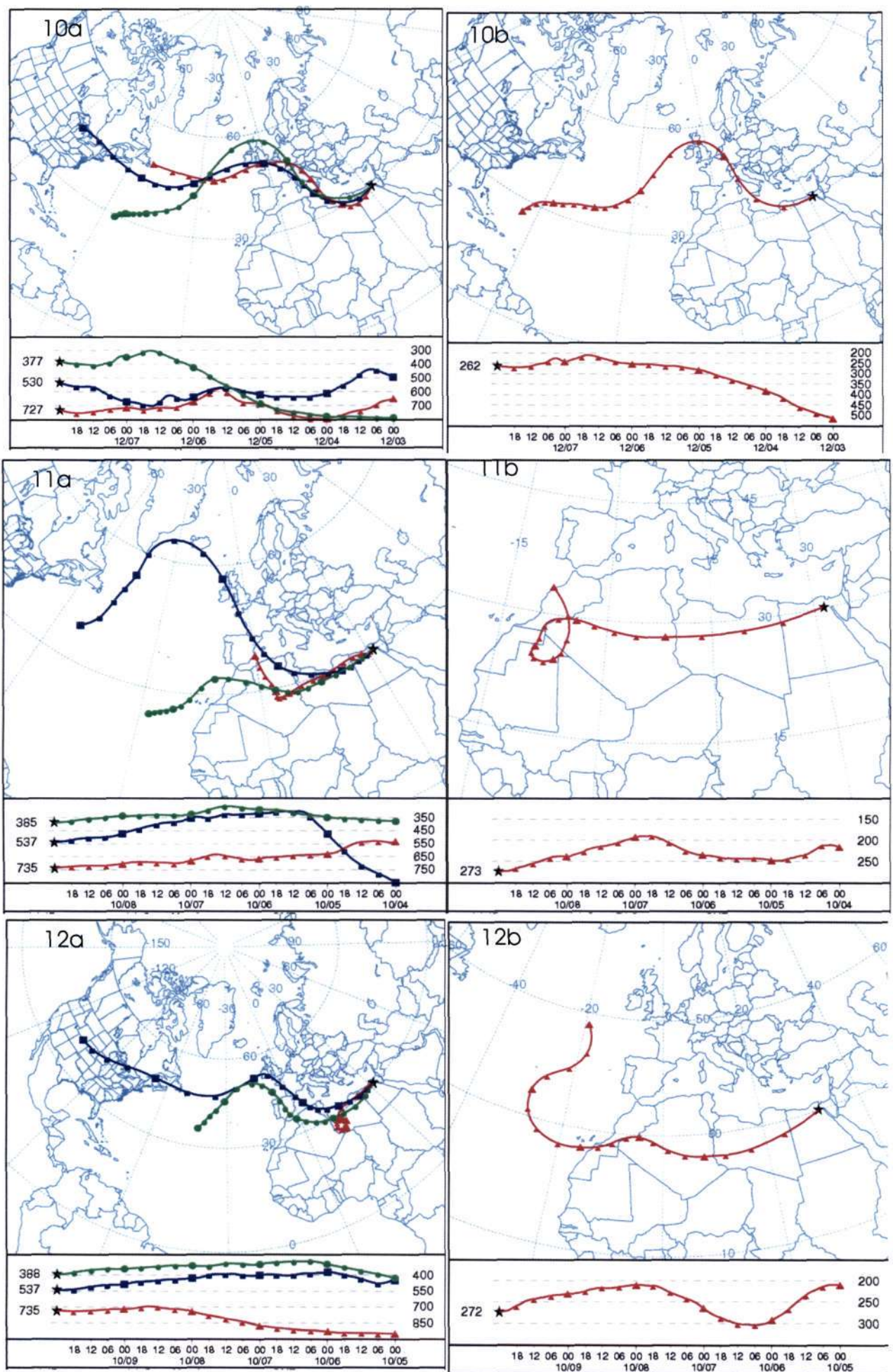


Figure D1: continued (10) 8 December 2001 (11) 9 October 2000 and (12) 10 October 2000  
 a) Horizontal and vertical plots of back trajectories originating at 2.5, 5 and 7.5 km  
 b) Horizontal and vertical plots of back trajectories originating at 10 km



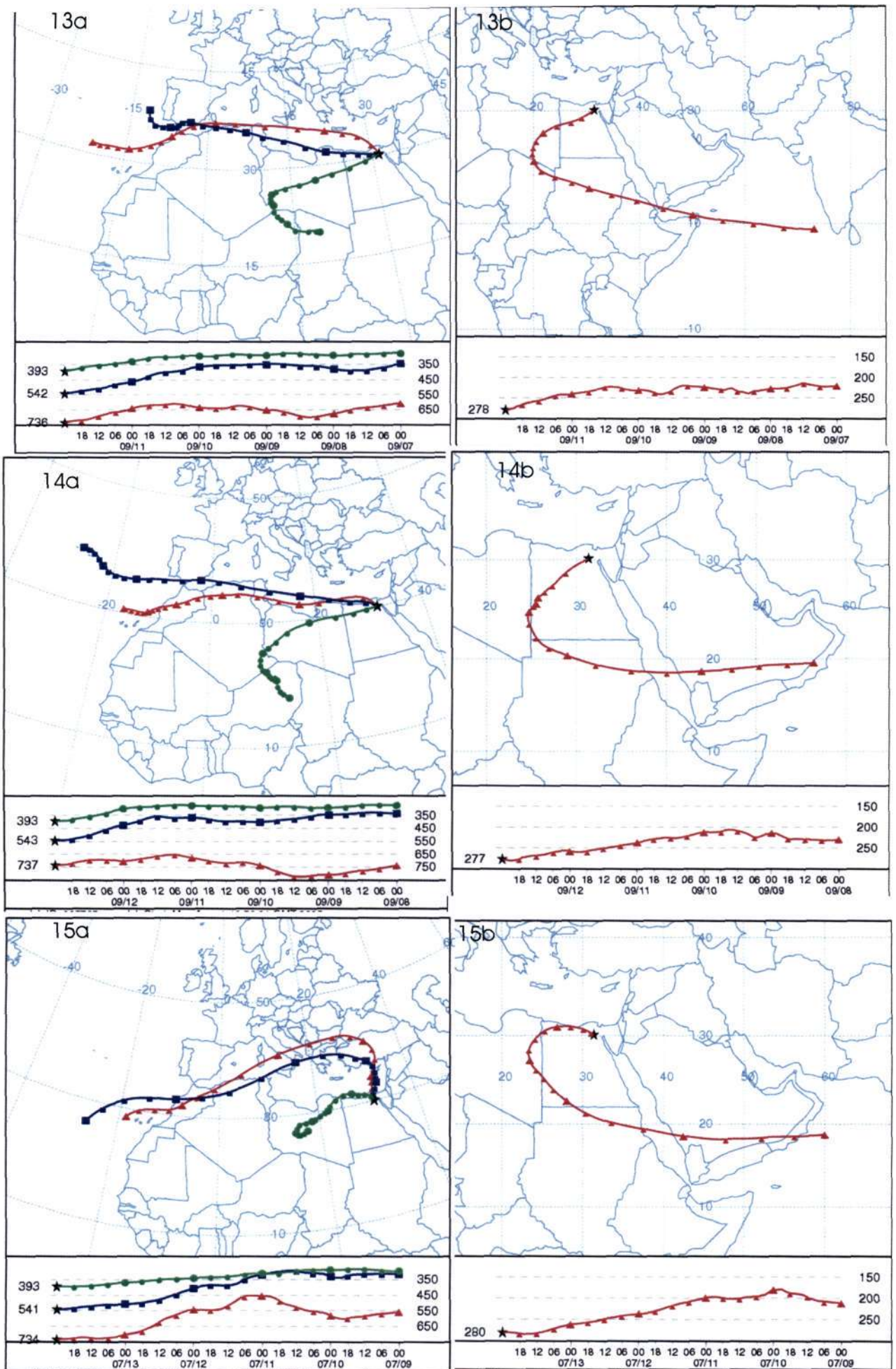
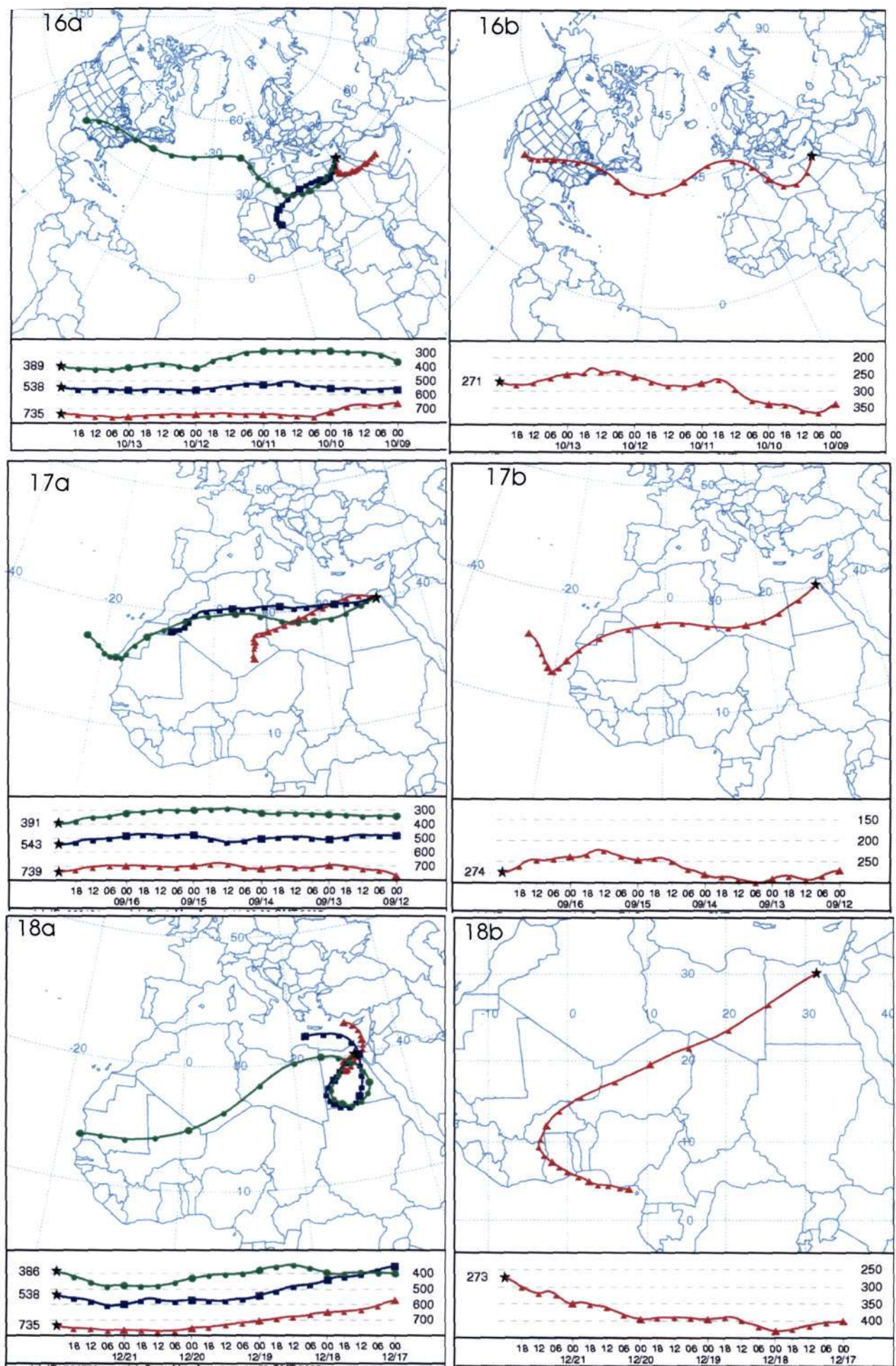


Figure D1: continued (13) 12 September 2000 (14) 13 September 2001 and (15) 14 July 2000  
a) Horizontal and vertical plots of back trajectories originating at 2.5, 5 and 7.5 km  
b) Horizontal and vertical plots of back trajectories originating at 10 km







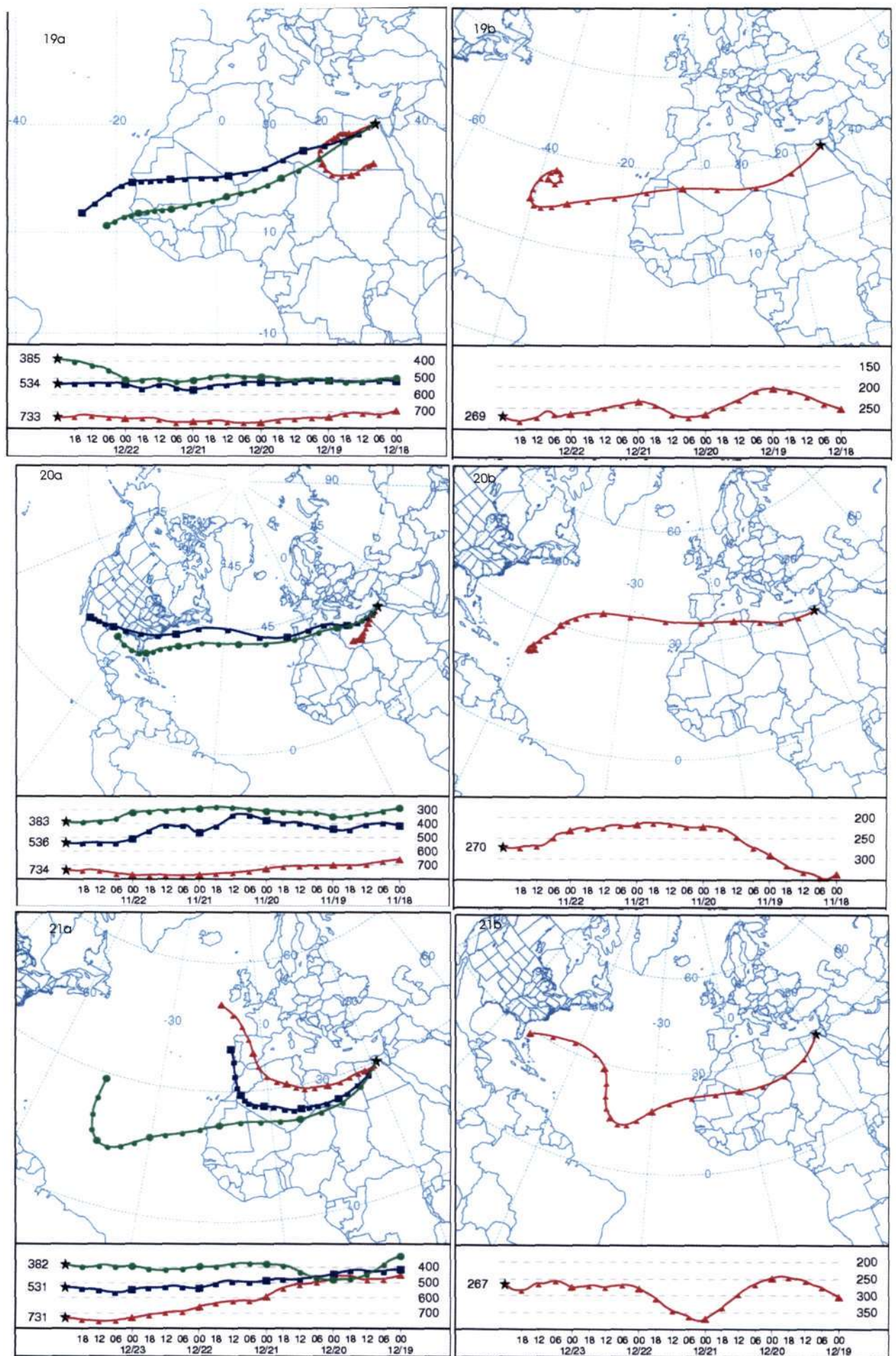


Figure D1: continued (19) 23 December 1999 (20) 23 November 2002 and (21) 24 December 1999

- a) Horizontal and vertical plots of back trajectories originating at 2.5, 5 and 7.5 km
- b) Horizontal and vertical plots of back trajectories originating at 10 km



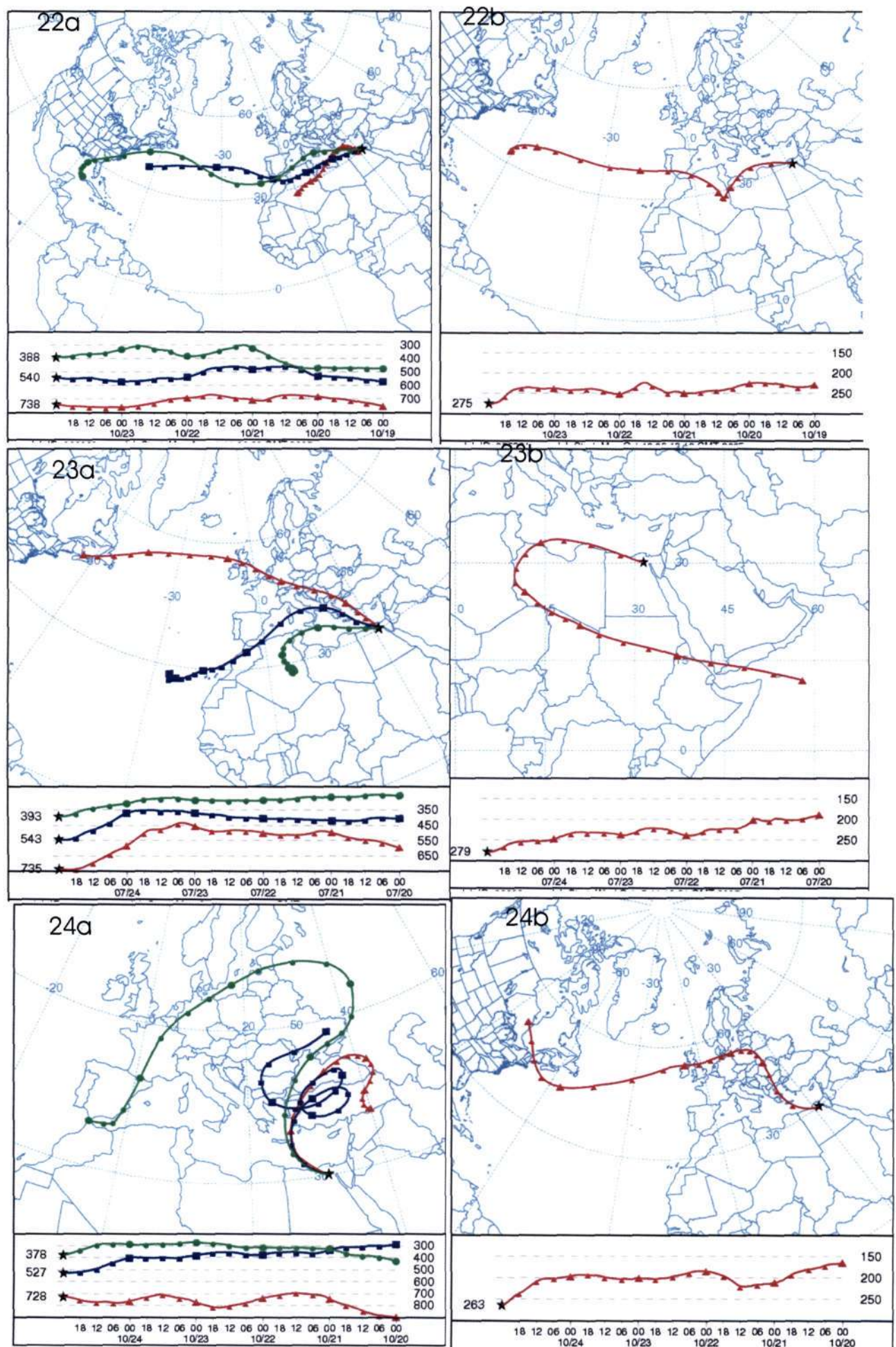


Figure D1: continued (22) 24 October 1999 (23) 25 July 2002 and (24) 25 October 2000  
a) Horizontal and vertical plots of back trajectories originating at 2.5, 5 and 7.5 km  
b) Horizontal and vertical plots of back trajectories originating at 10 km



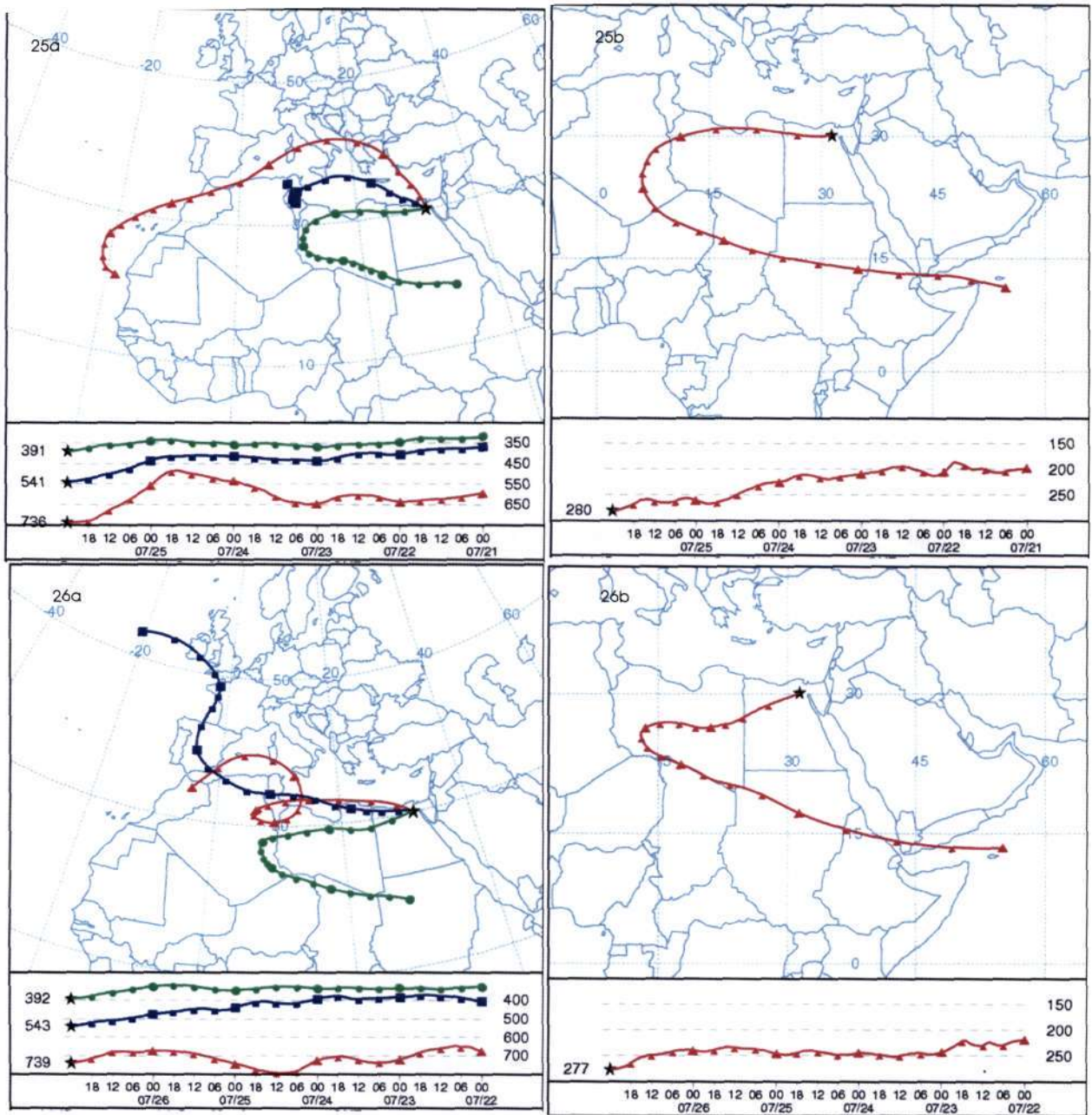


Figure D1: continued (25) 26 July 2002 and (26) 27 July 2002

- Horizontal and vertical plots of back trajectories originating at 2.5, 5 and 7.5 km
- Horizontal and vertical plots of back trajectories originating at 10 km



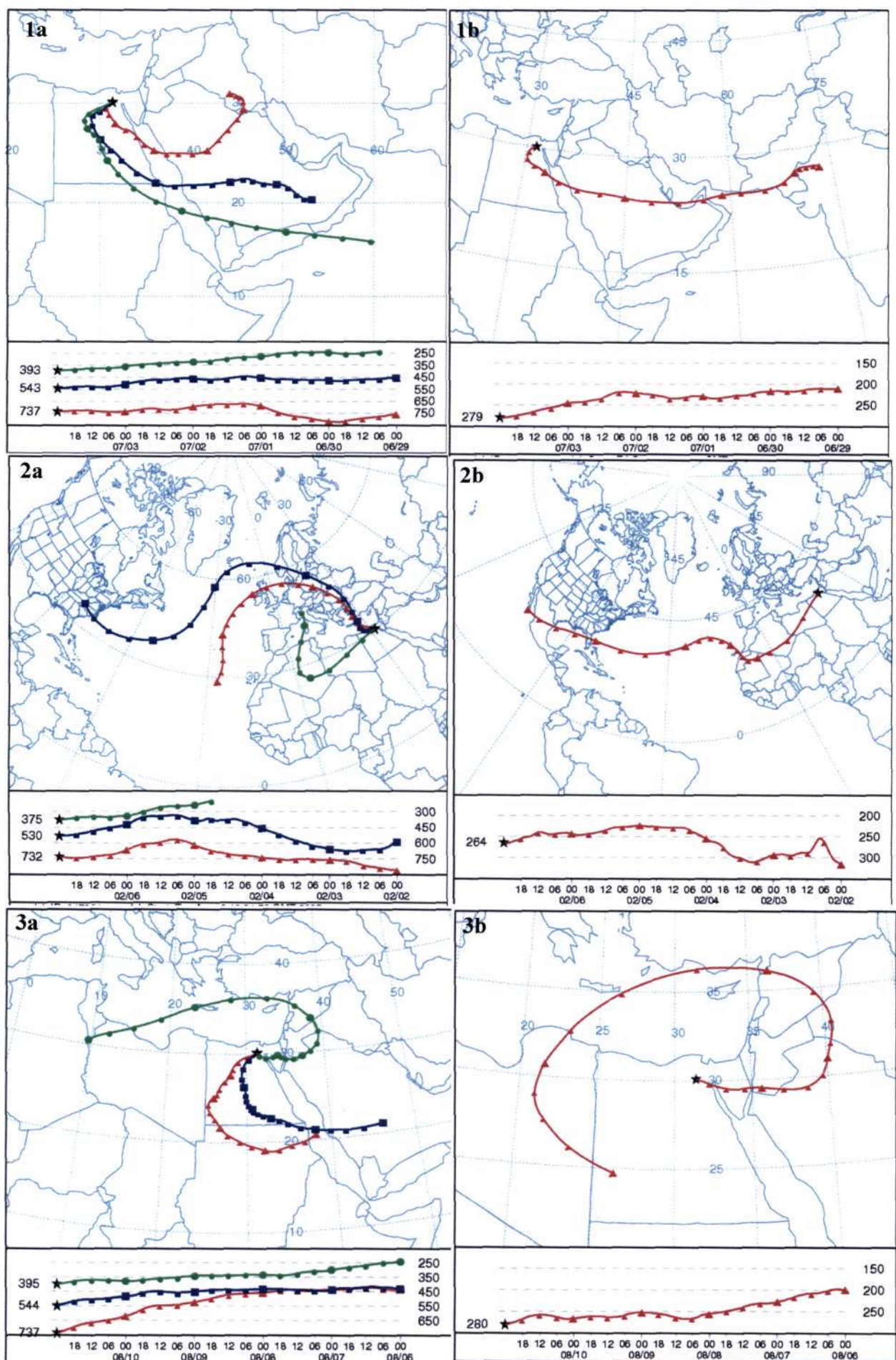


Figure D2: 5-day back trajectory HYSPLIT model results for Group 2. (1) 4 July 2000  
 (2) 7 February 2000 and (3) 11 August 2001  
 a) Horizontal and vertical plots of back trajectories originating at 2.5, 5 and 7.5 km  
 b) Horizontal and vertical plots of back trajectories originating at 10 km



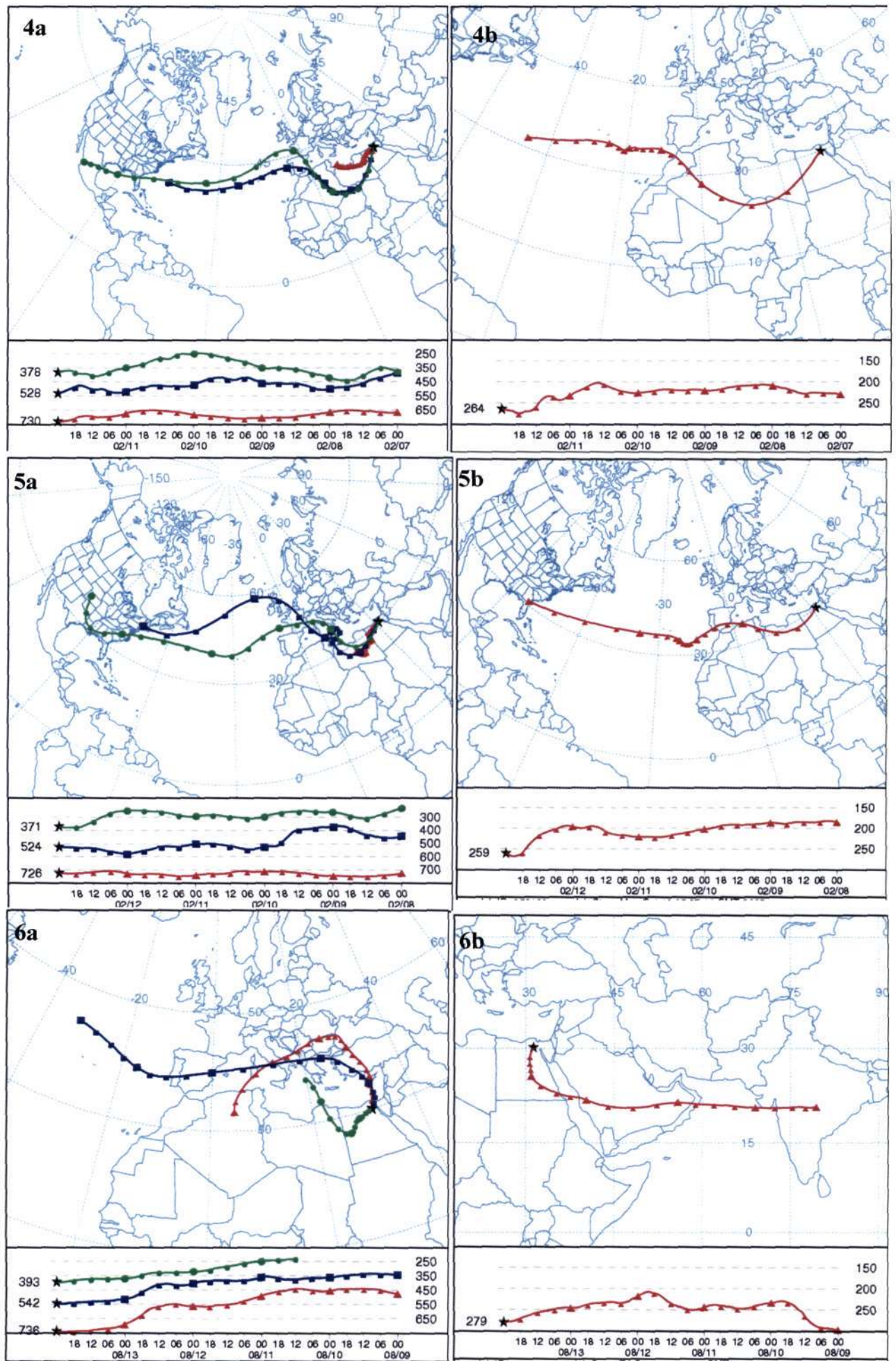


Figure D2: continued (4) 12 February 2000 (5) 13 February 2000 and (6) 14 August 1999  
a) Horizontal and vertical plots of back trajectories originating at 2.5, 5 and 7.5 km  
b) Horizontal and vertical plots of back trajectories originating at 10 km



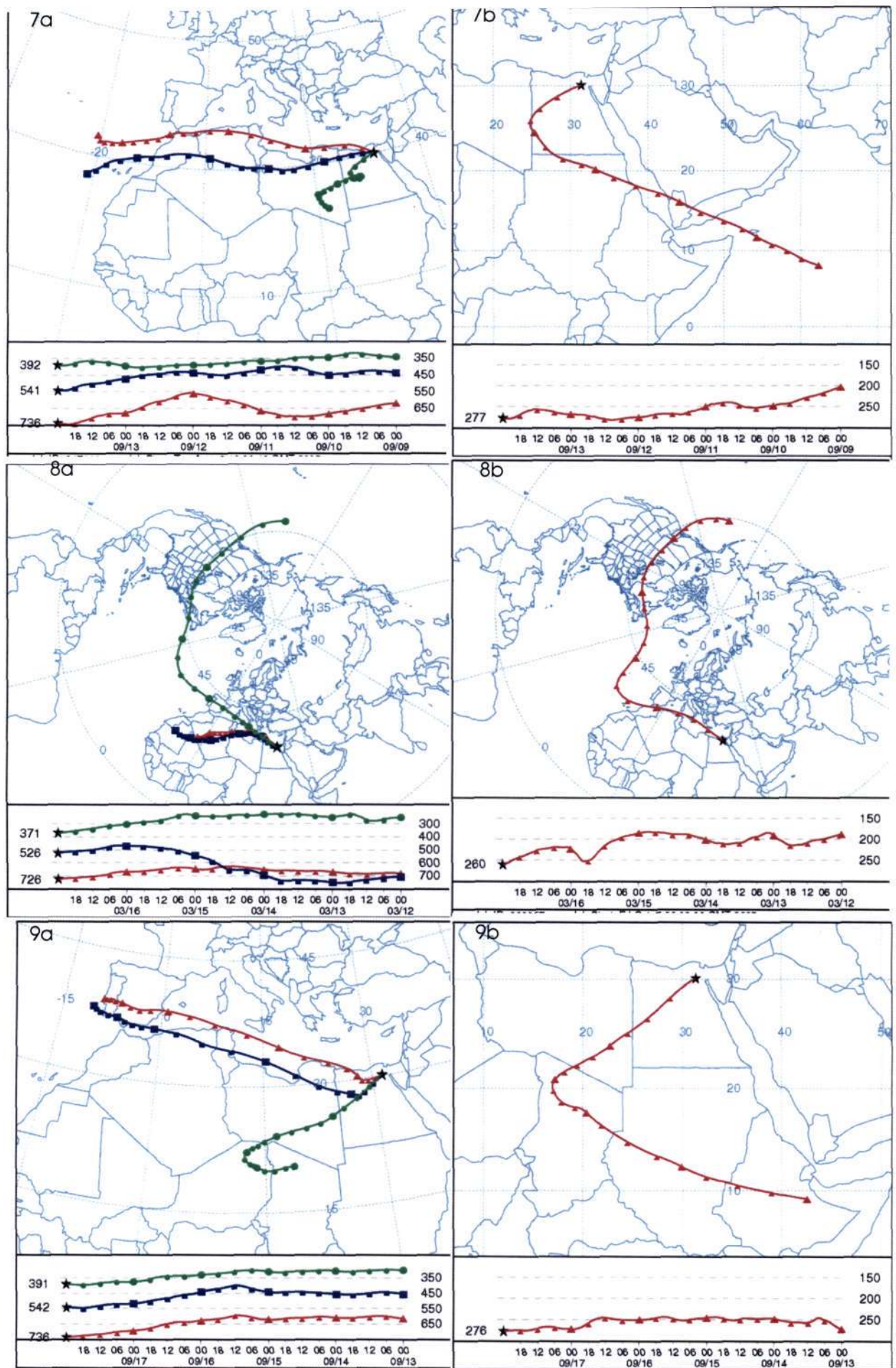


Figure D2: continued (7) 14 September 2001 (8) 17 March 2002 and (9) 18 September 2001  
a) Horizontal and vertical plots of back trajectories originating at 2.5, 5 and 7.5 km  
b) Horizontal and vertical plots of back trajectories originating at 10 km



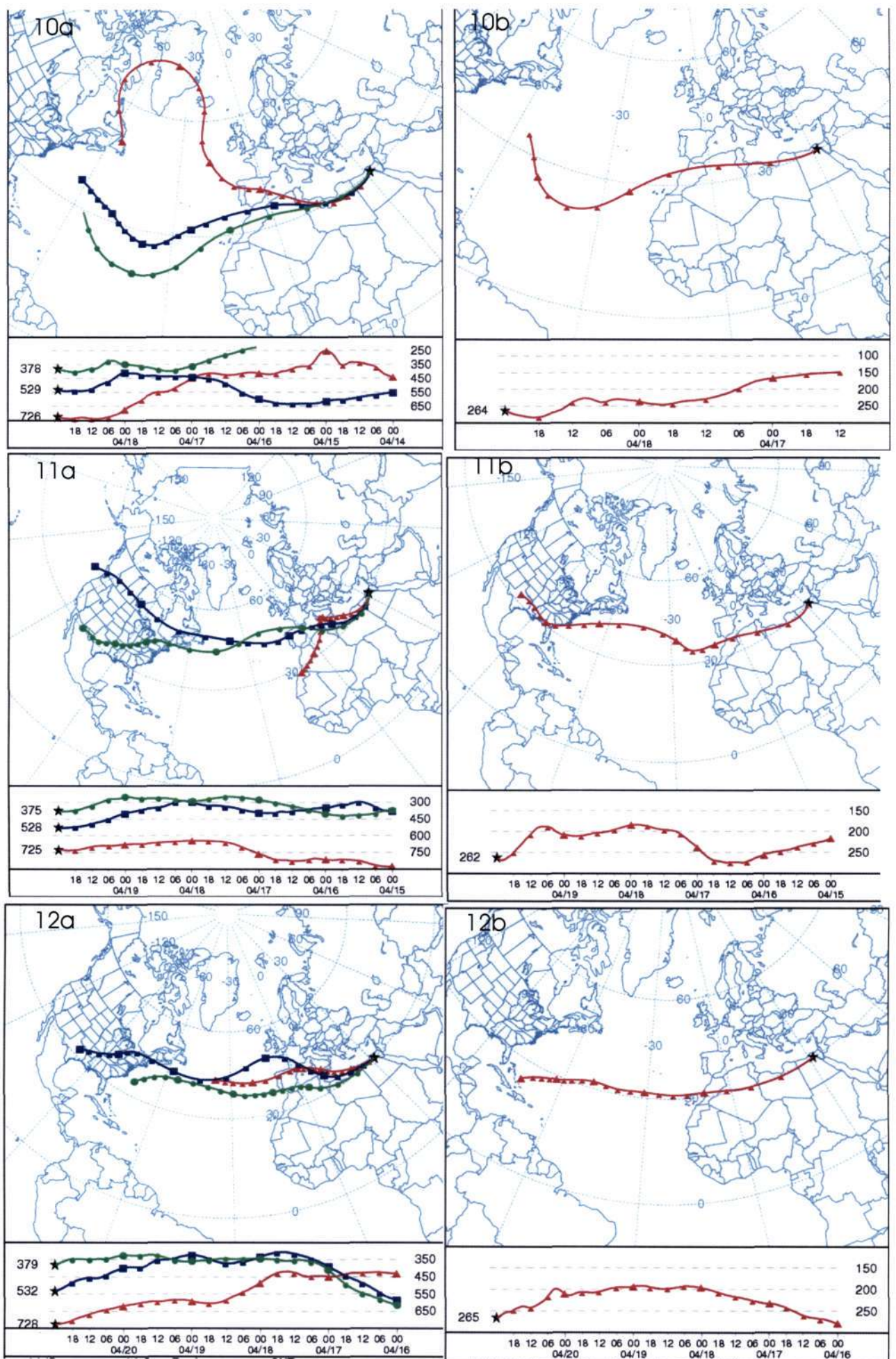


Figure D2: continued (10) 19 April 2000 (11) 20 April 2000 and (12) 21 April 2000  
a) Horizontal and vertical plots of back trajectories originating at 2.5, 5 and 7.5 km  
b) Horizontal and vertical plots of back trajectories originating at 10 km



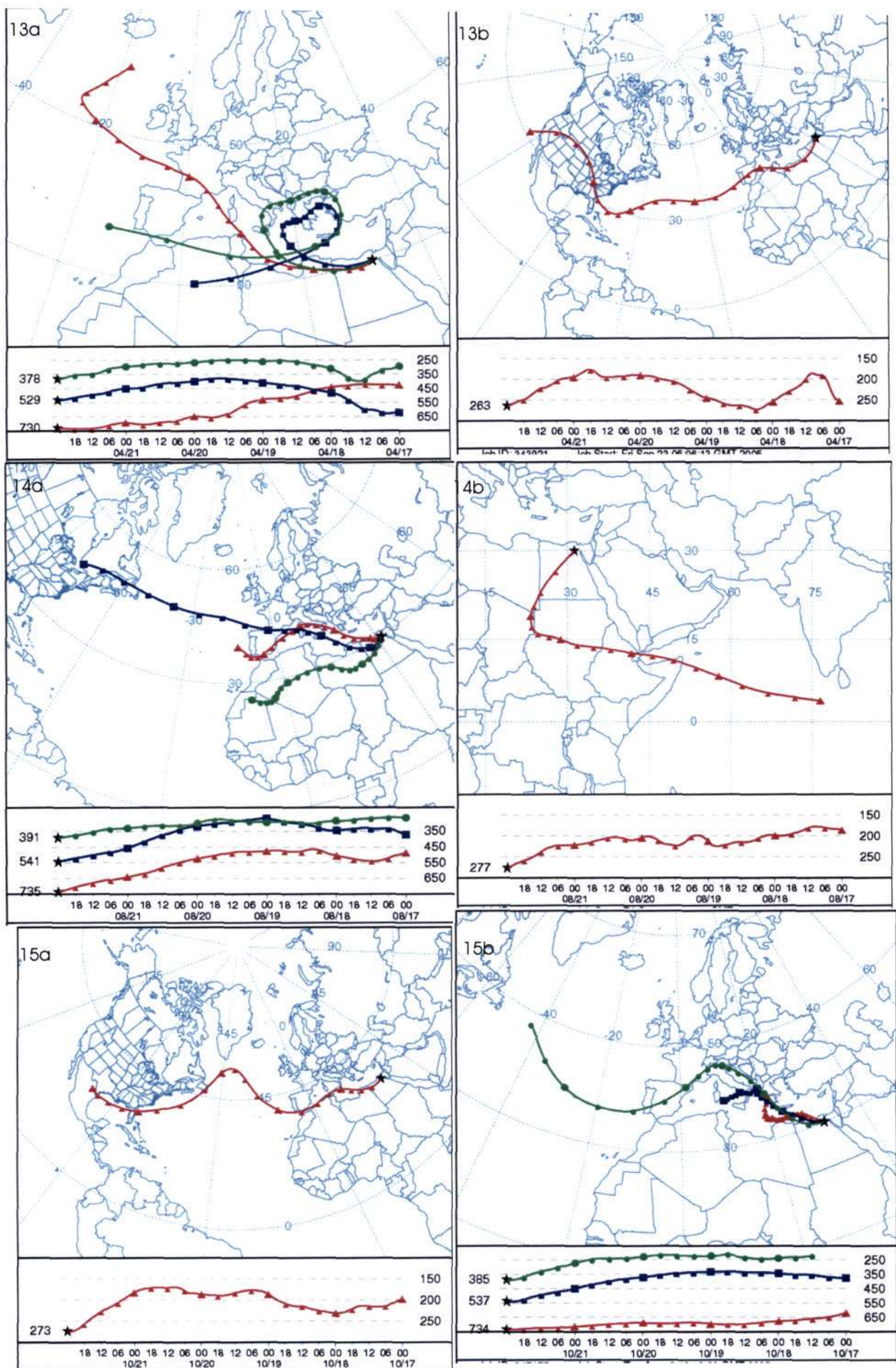


Figure D2: continued (13) 22 April 2000 (14) 22 August 2001 and (15) 22 October 2001  
a) Horizontal and vertical plots of back trajectories originating at 2.5, 5 and 7.5 km  
b) Horizontal and vertical plots of back trajectories originating at 10 km



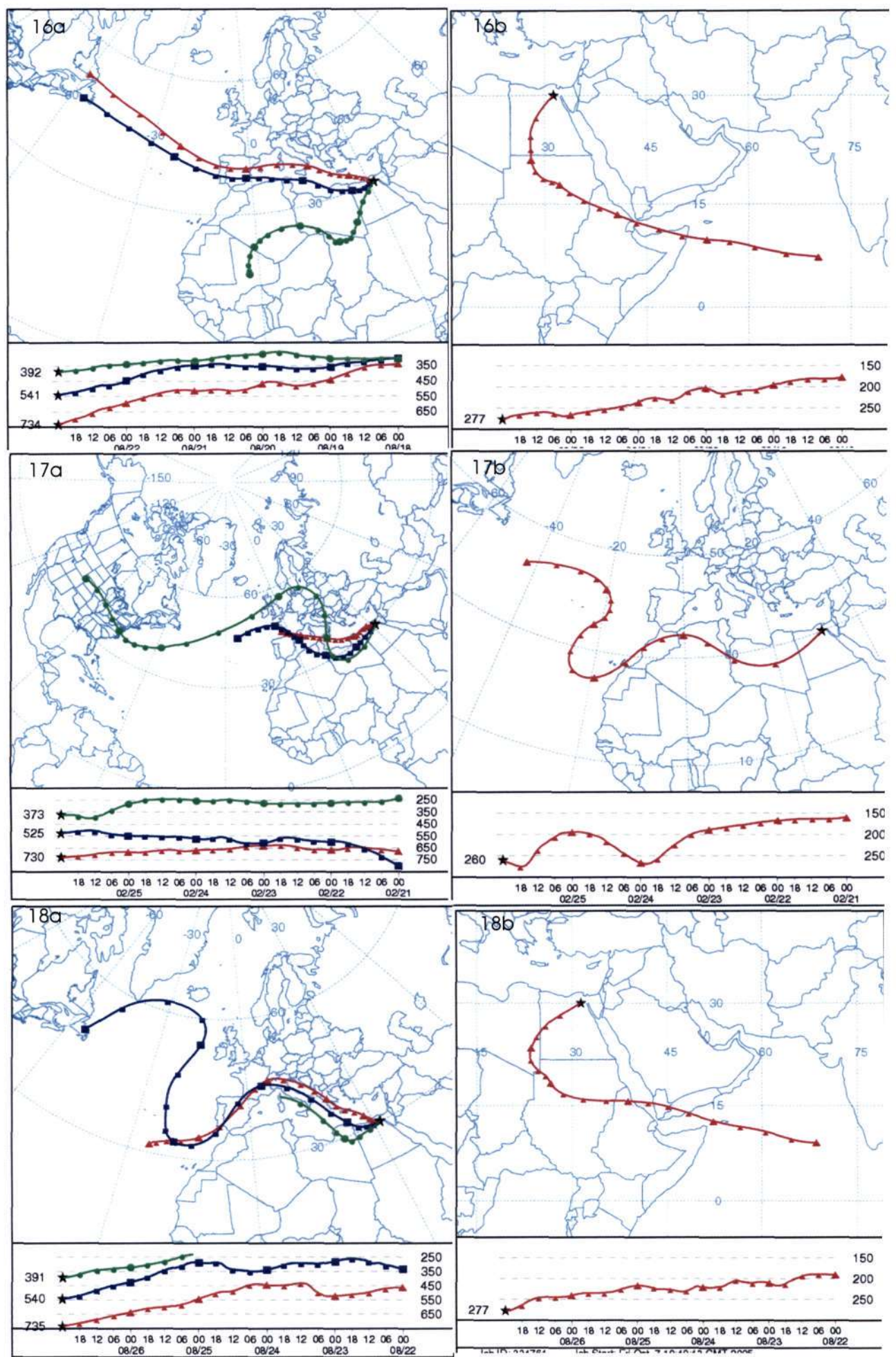


Figure D2: continued (16) 23 August 2001 (17) 26 February 2000 and (18) 27 August 2000  
a) Horizontal and vertical plots of back trajectories originating at 2.5, 5 and 7.5 km  
b) Horizontal and vertical plots of back trajectories originating at 10 km







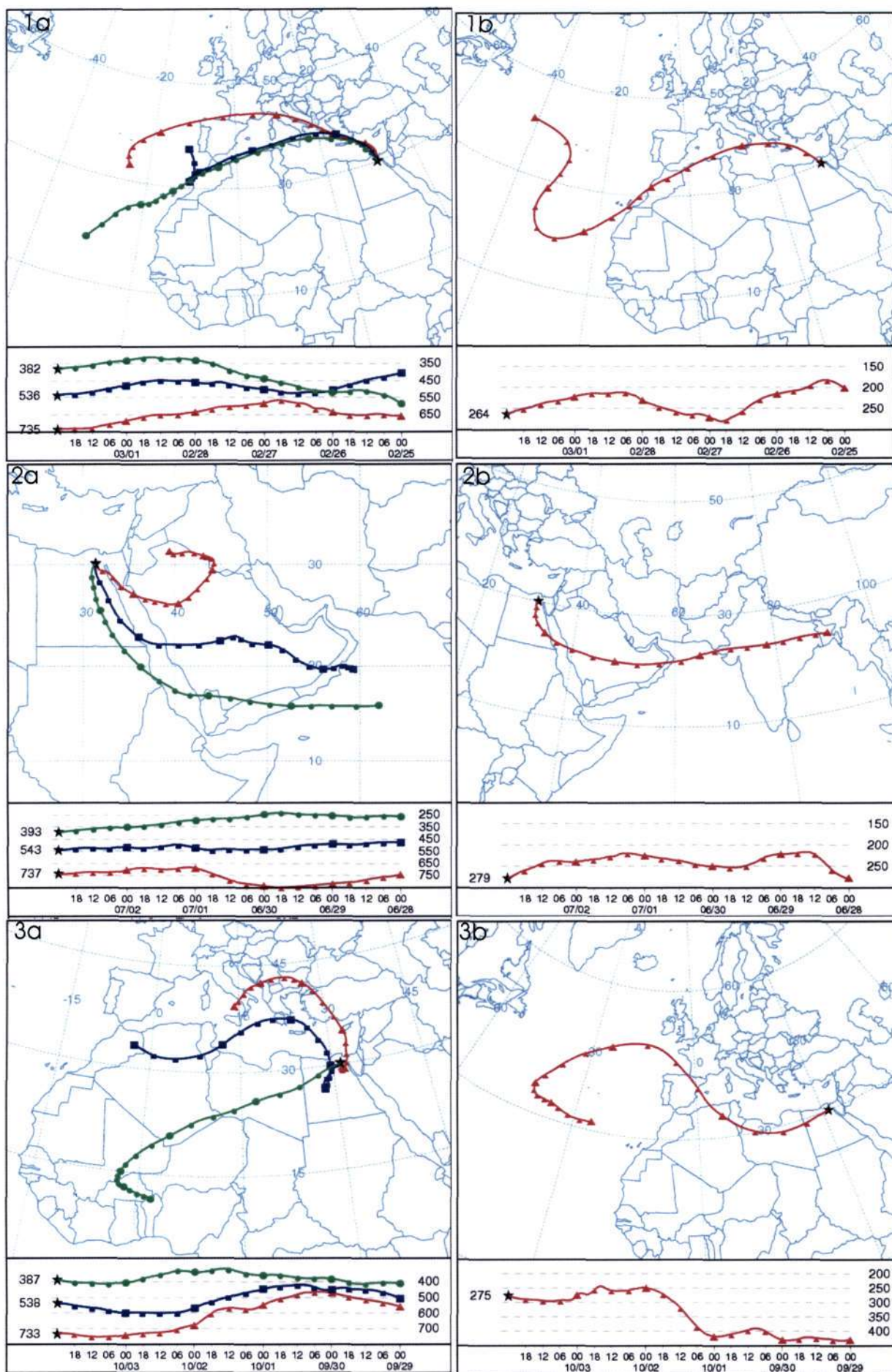


Figure D3: 5-day back trajectory HYSPLIT model results for Group 3. (1) 2 March 2002  
 (2) 3 July 2000 and (3) 4 October 2000  
 a) Horizontal and vertical plots of back trajectories originating at 2.5, 5 and 7.5 km  
 b) Horizontal and vertical plots of back trajectories originating at 10 km







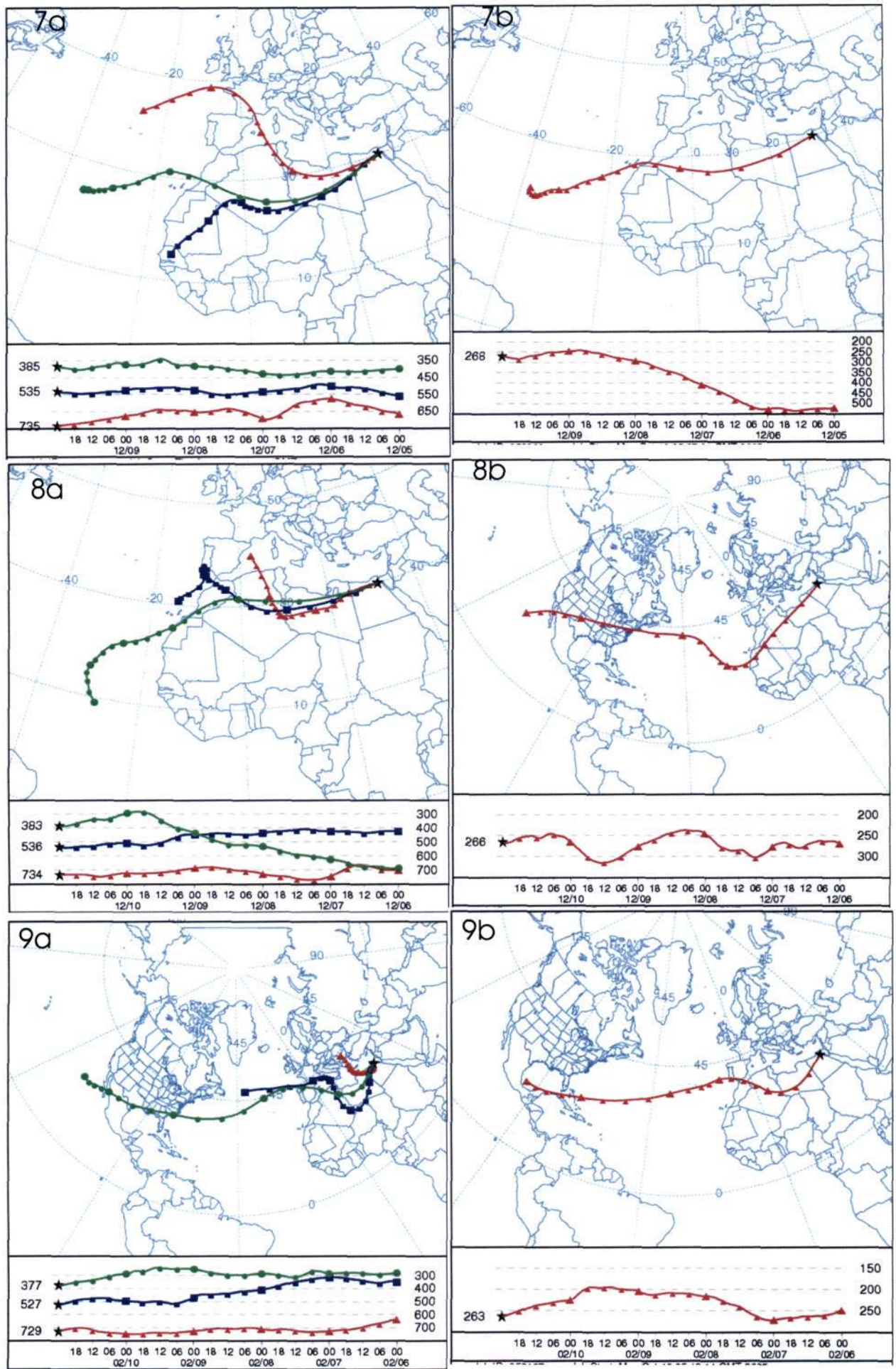


Figure D3: continued (7) 10 December 2001 (8) 11 December 2001 and (9) 11 February 2000  
a) Horizontal and vertical plots of back trajectories originating at 2.5, 5 and 7.5 km  
b) Horizontal and vertical plots of back trajectories originating at 10 km



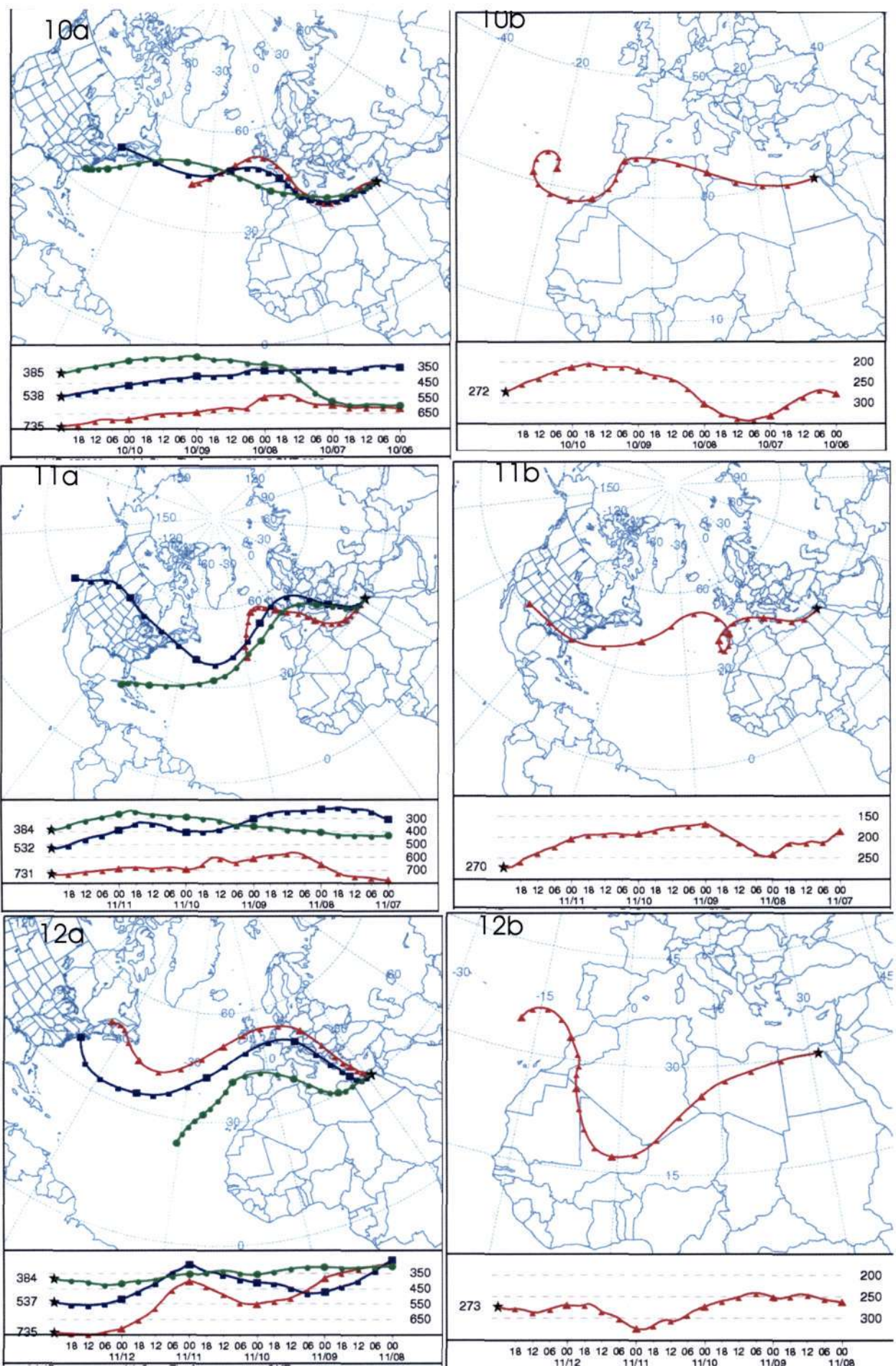


Figure D3: continued (10) 11 October 2000 (11) 12 November 2002 and (12) 13 November 2002.

- a) Horizontal and vertical plots of back trajectories originating at 2.5, 5 and 7.5 km
- b) Horizontal and vertical plots of back trajectories originating at 10 km



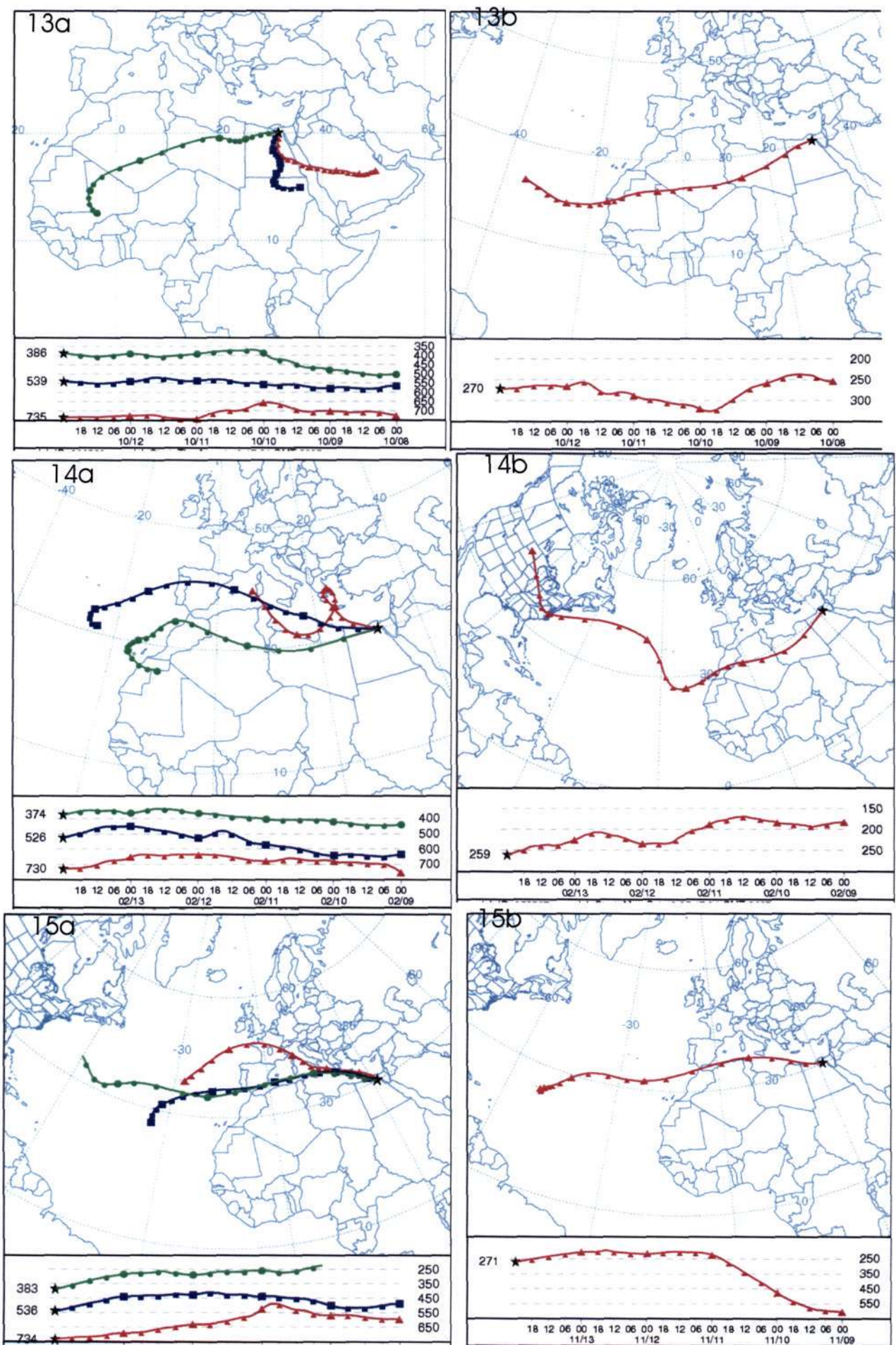


Figure D3: continued (13) 13 October 2002 (14) 14 February 2000 and (15) 14 November 2002

- a) Horizontal and vertical plots of back trajectories originating at 2.5, 5 and 7.5 km
- b) Horizontal and vertical plots of back trajectories originating at 10 km



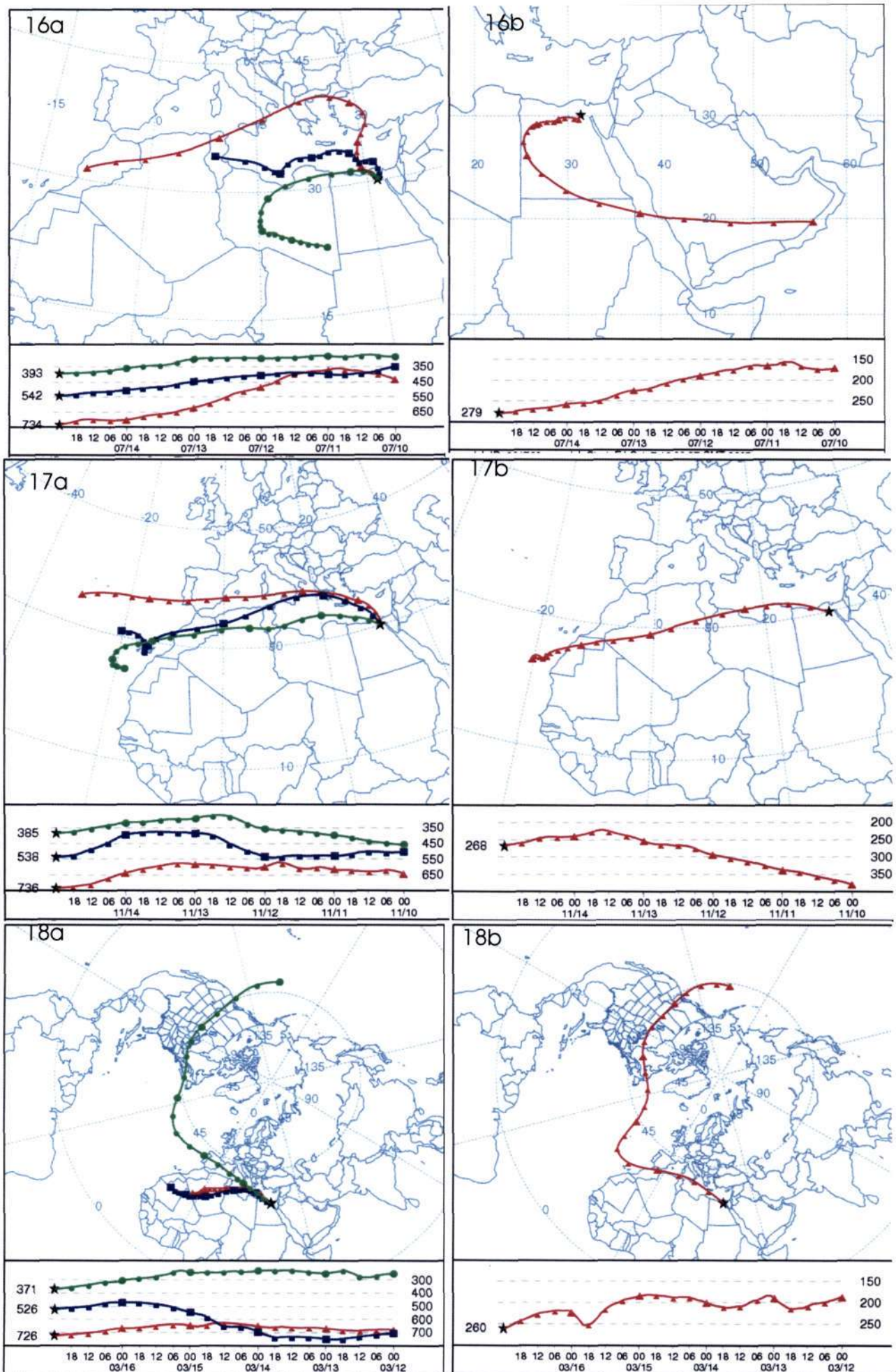


Figure D3: continued (16) 15 July 2000 (17) 15 November 2002 and (18) 17 March 2002  
a) Horizontal and vertical plots of back trajectories originating at 2.5, 5 and 7.5 km  
b) Horizontal and vertical plots of back trajectories originating at 10 km







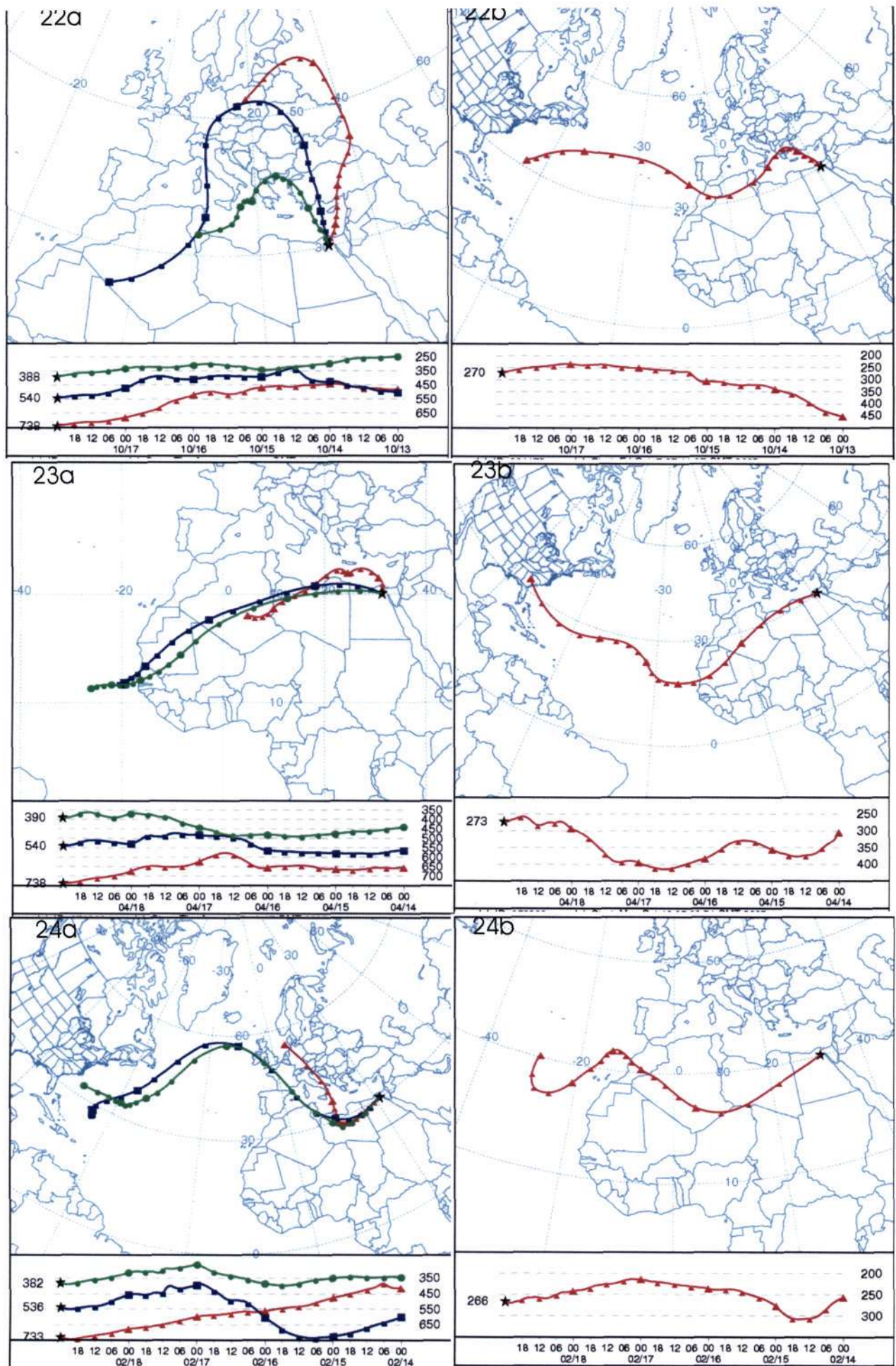


Figure D3: continued (22) 18 October 2000 (23) 19 April 1999 and (24) 19 February 2000  
a) Horizontal and vertical plots of back trajectories originating at 2.5, 5 and 7.5 km  
b) Horizontal and vertical plots of back trajectories originating at 10 km



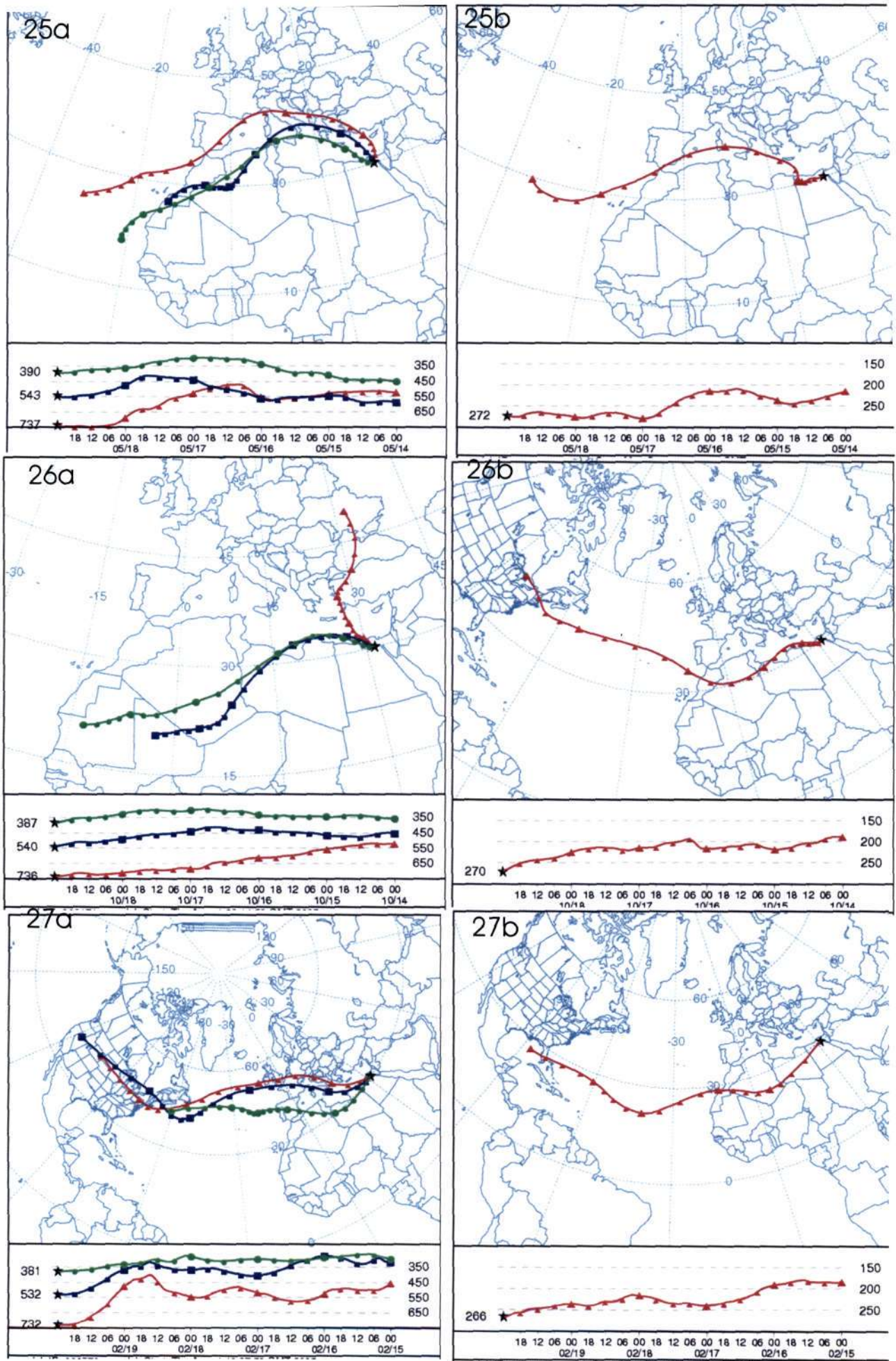


Figure D3: continued (25) 19 May 1999 (26) 19 October 2000 and (27) 20 February 2000  
a) Horizontal and vertical plots of back trajectories originating at 2.5, 5 and 7.5 km  
b) Horizontal and vertical plots of back trajectories originating at 10 km



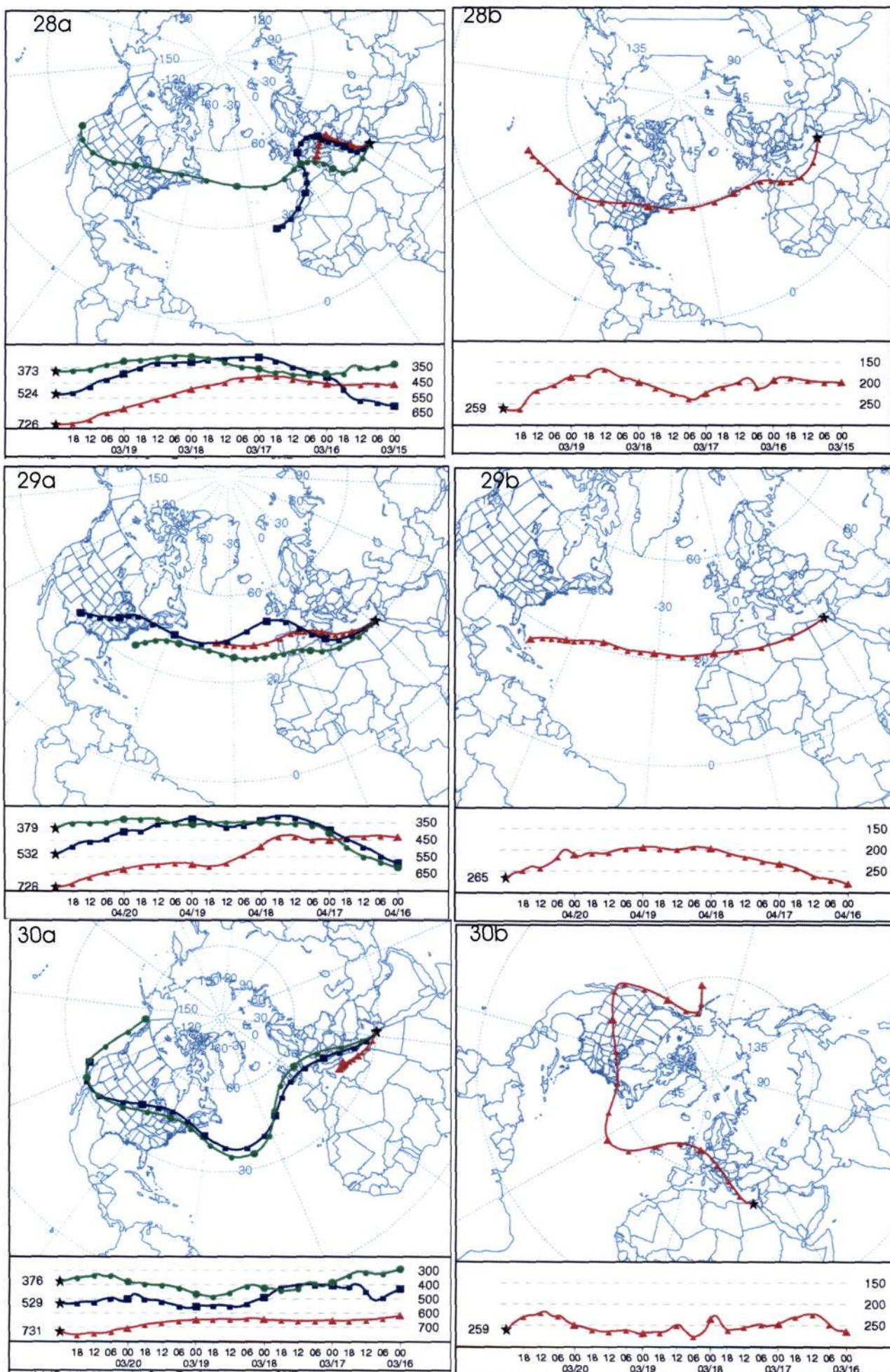


Figure D3: continued (28) 20 March 2002 (29) 21 April 2000 and (30) 21 March 2002  
a) Horizontal and vertical plots of back trajectories originating at 2.5, 5 and 7.5 km  
b) Horizontal and vertical plots of back trajectories originating at 10 km



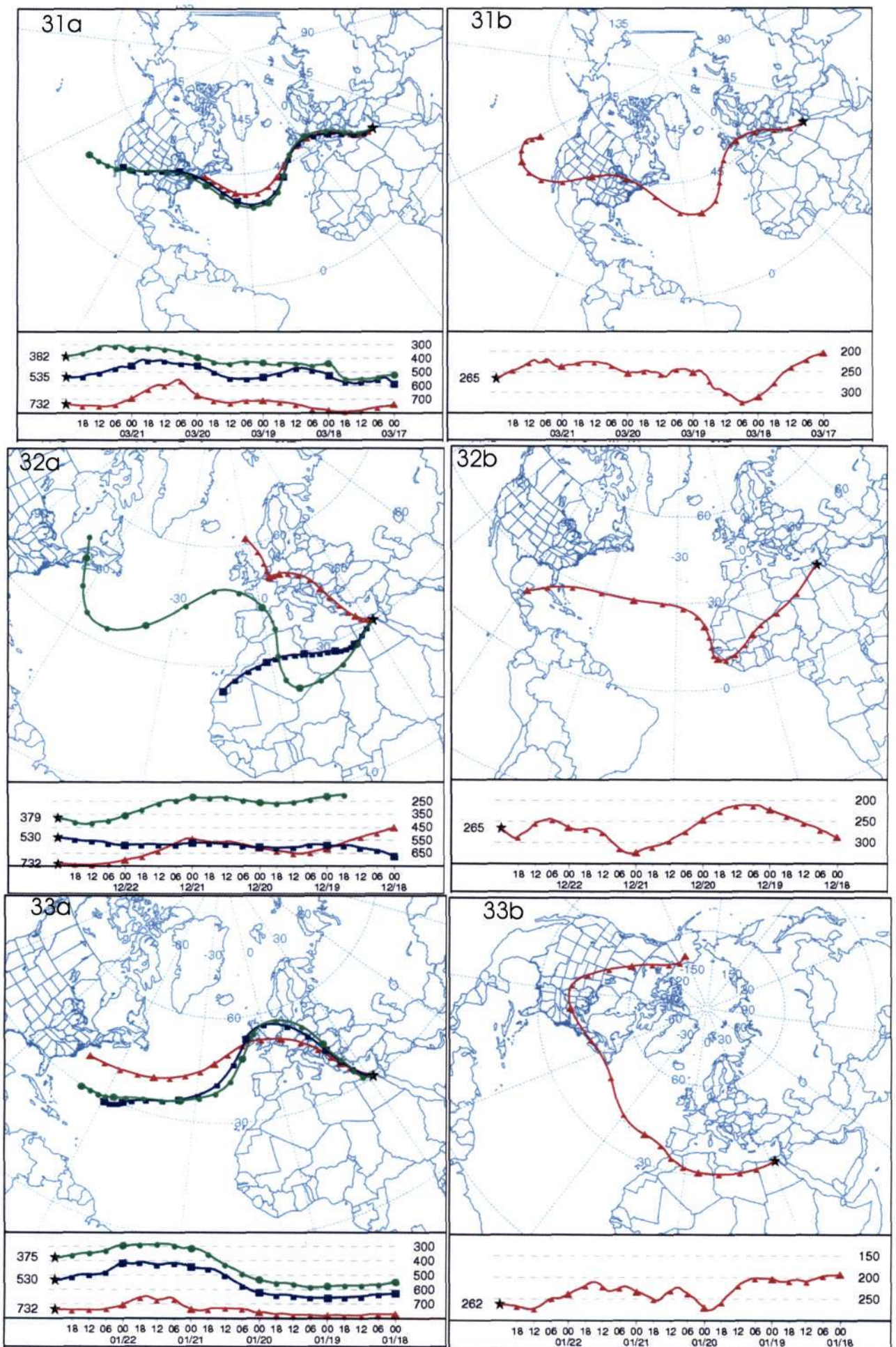


Figure D3: continued (31) 22 March 2002 (32) 23 December 2002 and (33) 23 January 2002  
a) Horizontal and vertical plots of back trajectories originating at 2.5, 5 and 7.5 km  
b) Horizontal and vertical plots of back trajectories originating at 10 km







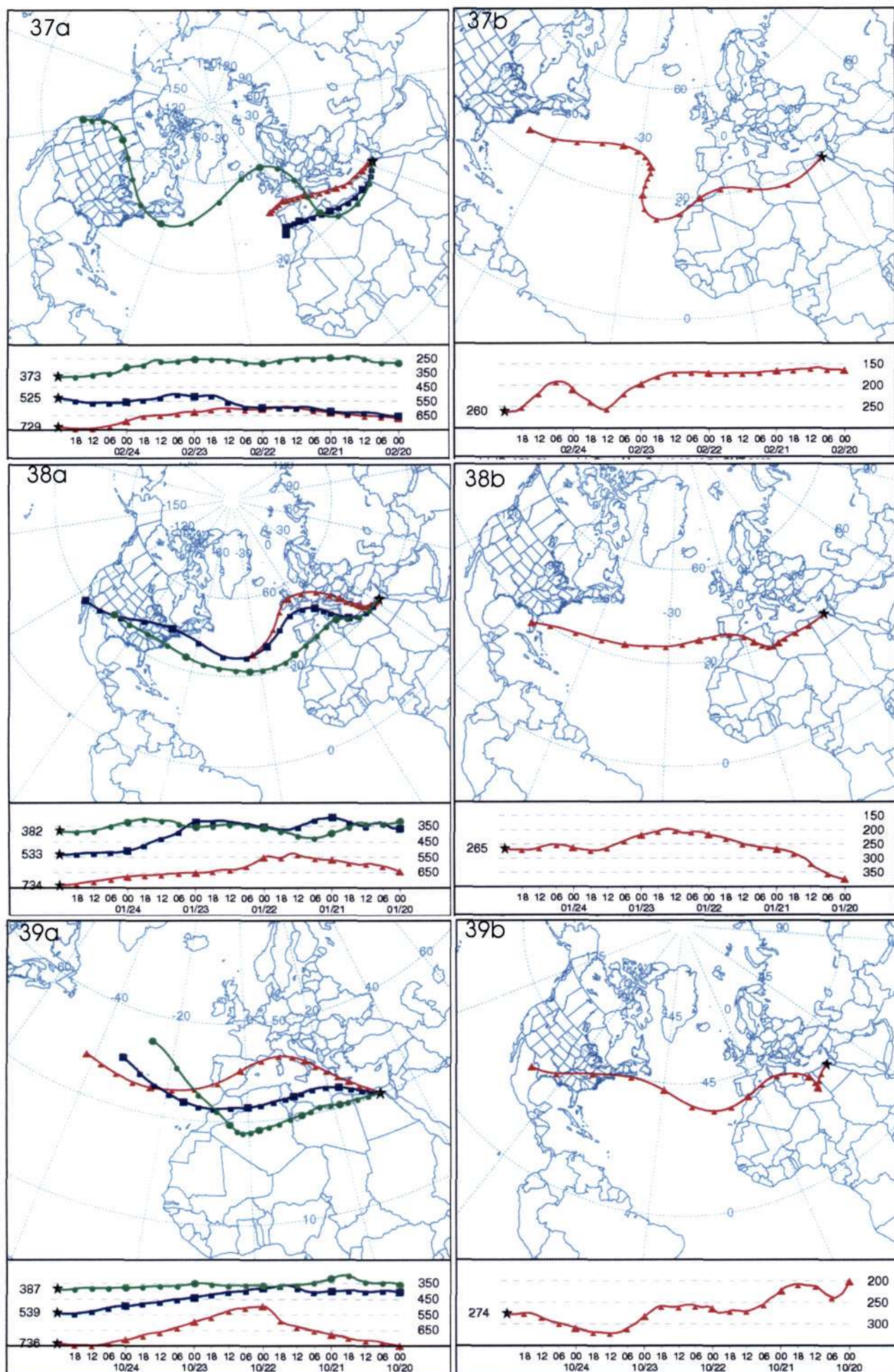


Figure D3: continued (37) 25 February 2000 (38) 25 January 2002 and (39) 25 October 1999  
a) Horizontal and vertical plots of back trajectories originating at 2.5, 5 and 7.5 km  
b) Horizontal and vertical plots of back trajectories originating at 10 km



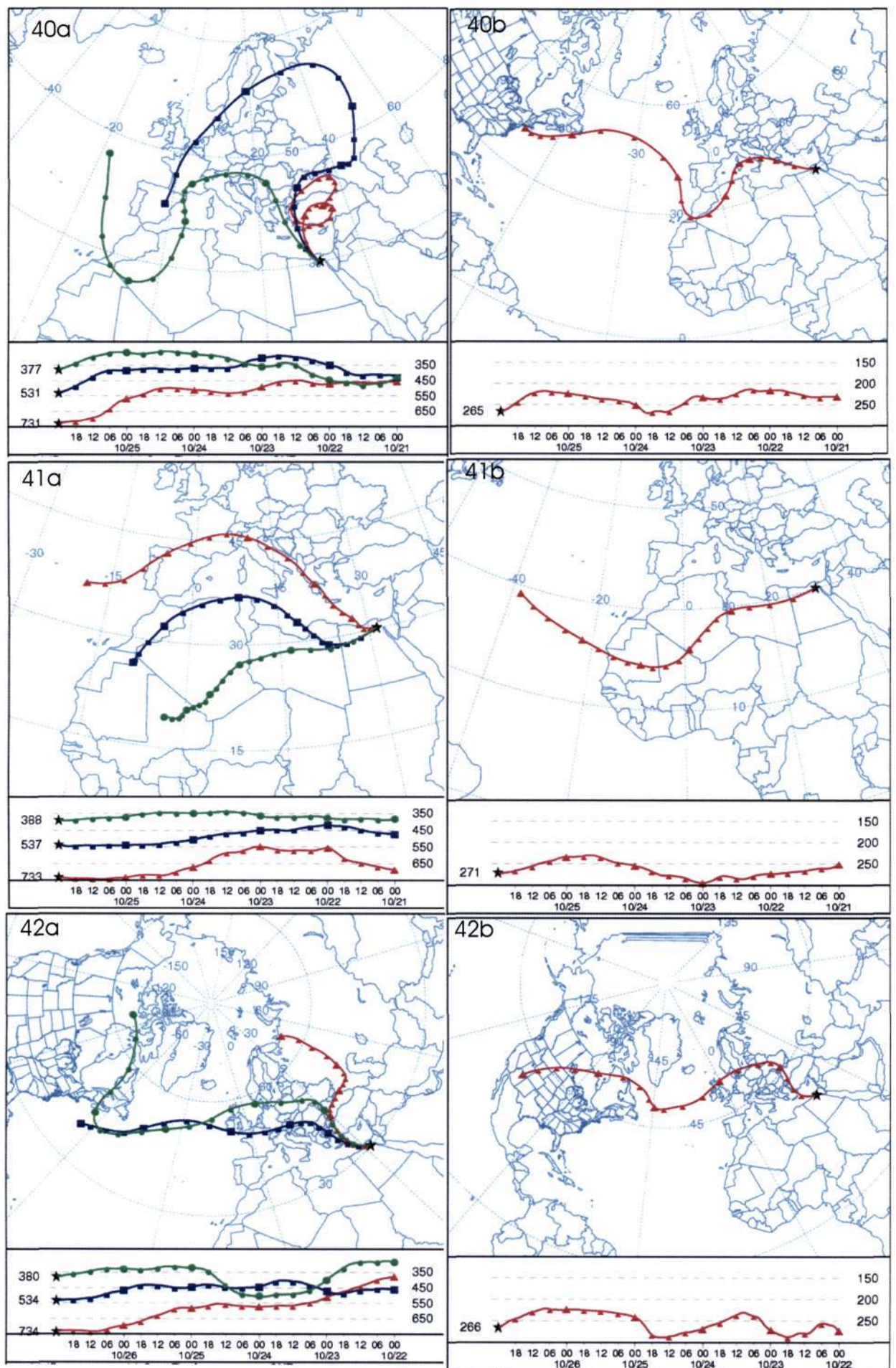


Figure D3: continued (40) 26 October 2000 (41) 26 October 2001 and (42) 27 October 2000  
a) Horizontal and vertical plots of back trajectories originating at 2.5, 5 and 7.5 km  
b) Horizontal and vertical plots of back trajectories originating at 10 km



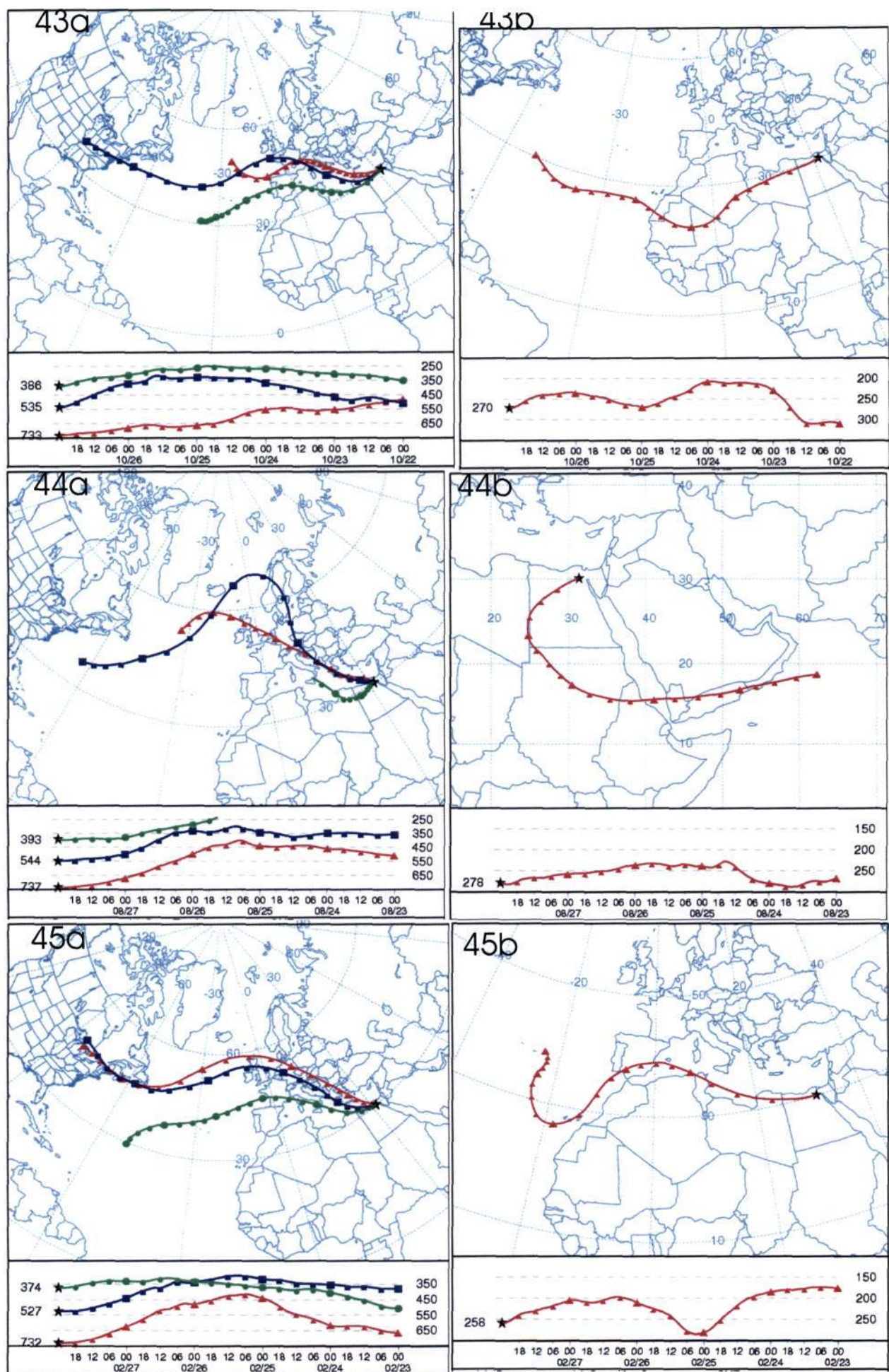


Figure D3: continued (43) 27 October 2001 (44) 28 August 2000 and (45) 28 February 2000  
a) Horizontal and vertical plots of back trajectories originating at 2.5, 5 and 7.5 km  
b) Horizontal and vertical plots of back trajectories originating at 10 km



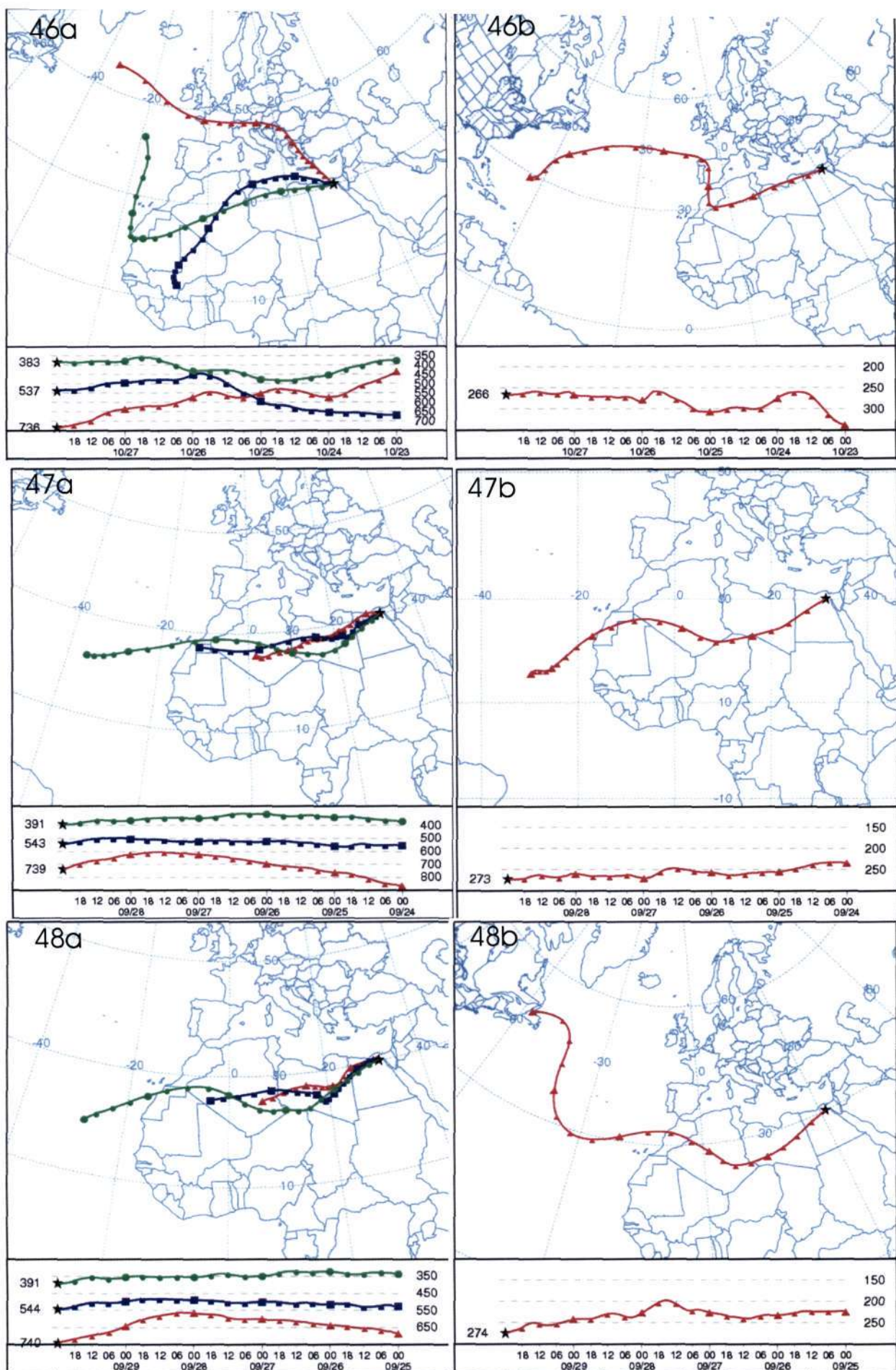


Figure D3: continued (46) 28 October 2000(47) 29 September 2002 and (48) 30 September 2002

- a) Horizontal and vertical plots of back trajectories originating at 2.5, 5 and 7.5 km  
 b) Horizontal and vertical plots of back trajectories originating at 10 km



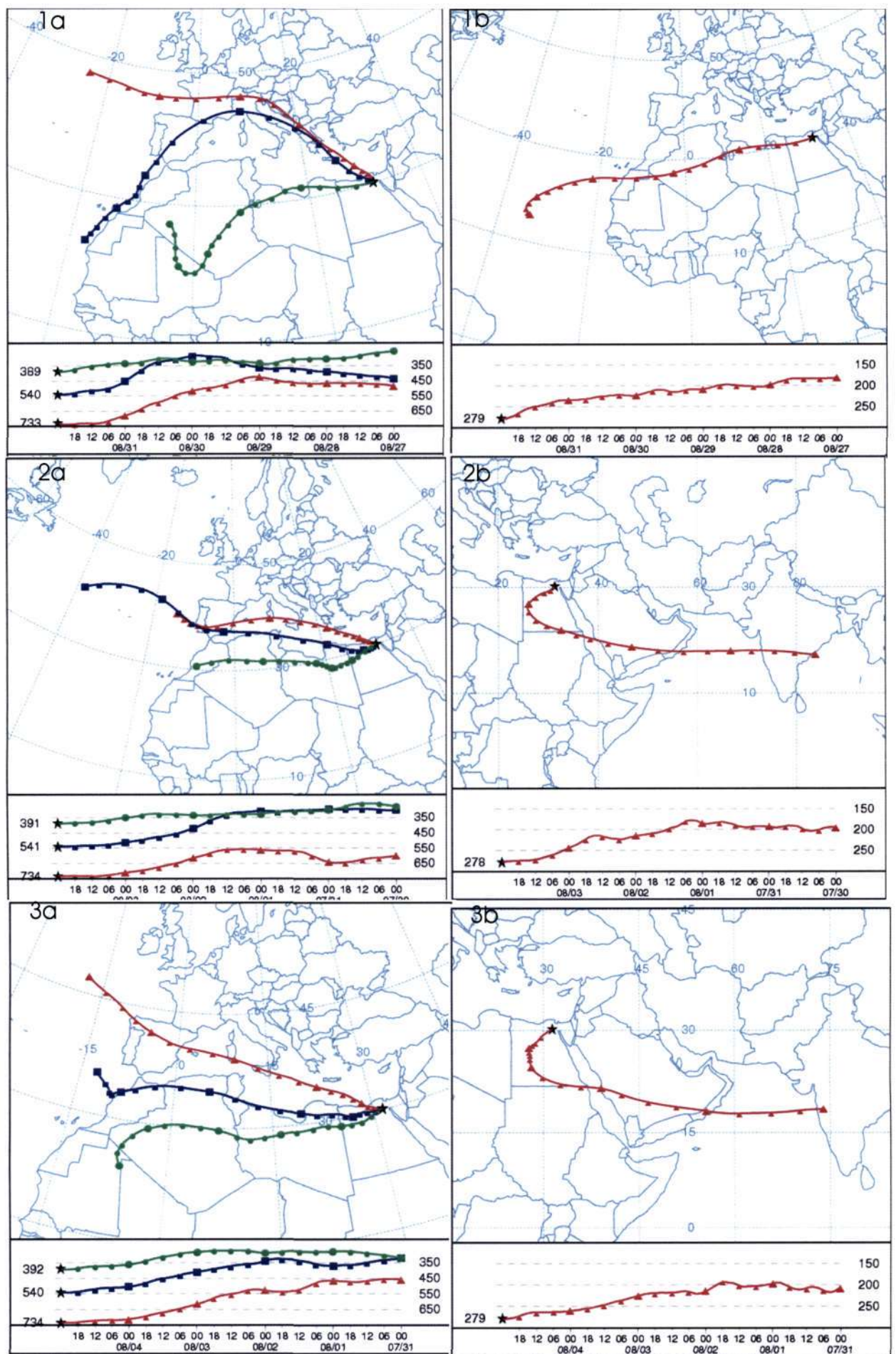


Figure D4: 5-day back trajectory HYSPLIT model results for Group 4. (1) 1 September 2000 (2) 4 August 1999 and (3) 5 August 1999  
a) Horizontal and vertical plots of back trajectories originating at 2.5, 5 and 7.5 km  
b) Horizontal and vertical plots of back trajectories originating at 10 km



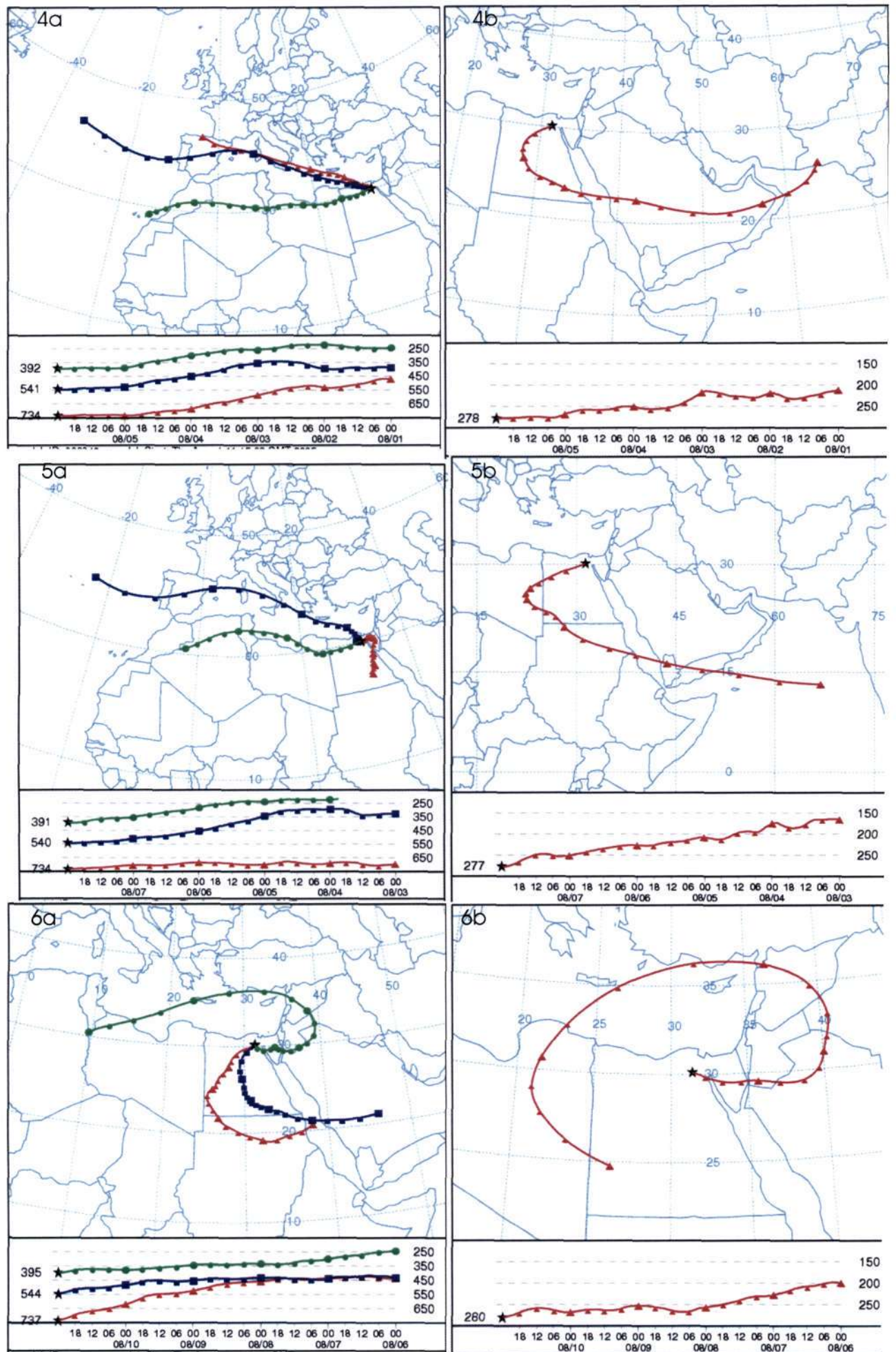


Figure D4: continued (4) 6 August 1999 (5) 8 August 1999 and (6) 11 August 2001  
a) Horizontal and vertical plots of back trajectories originating at 2.5, 5 and 7.5 km  
b) Horizontal and vertical plots of back trajectories originating at 10 km



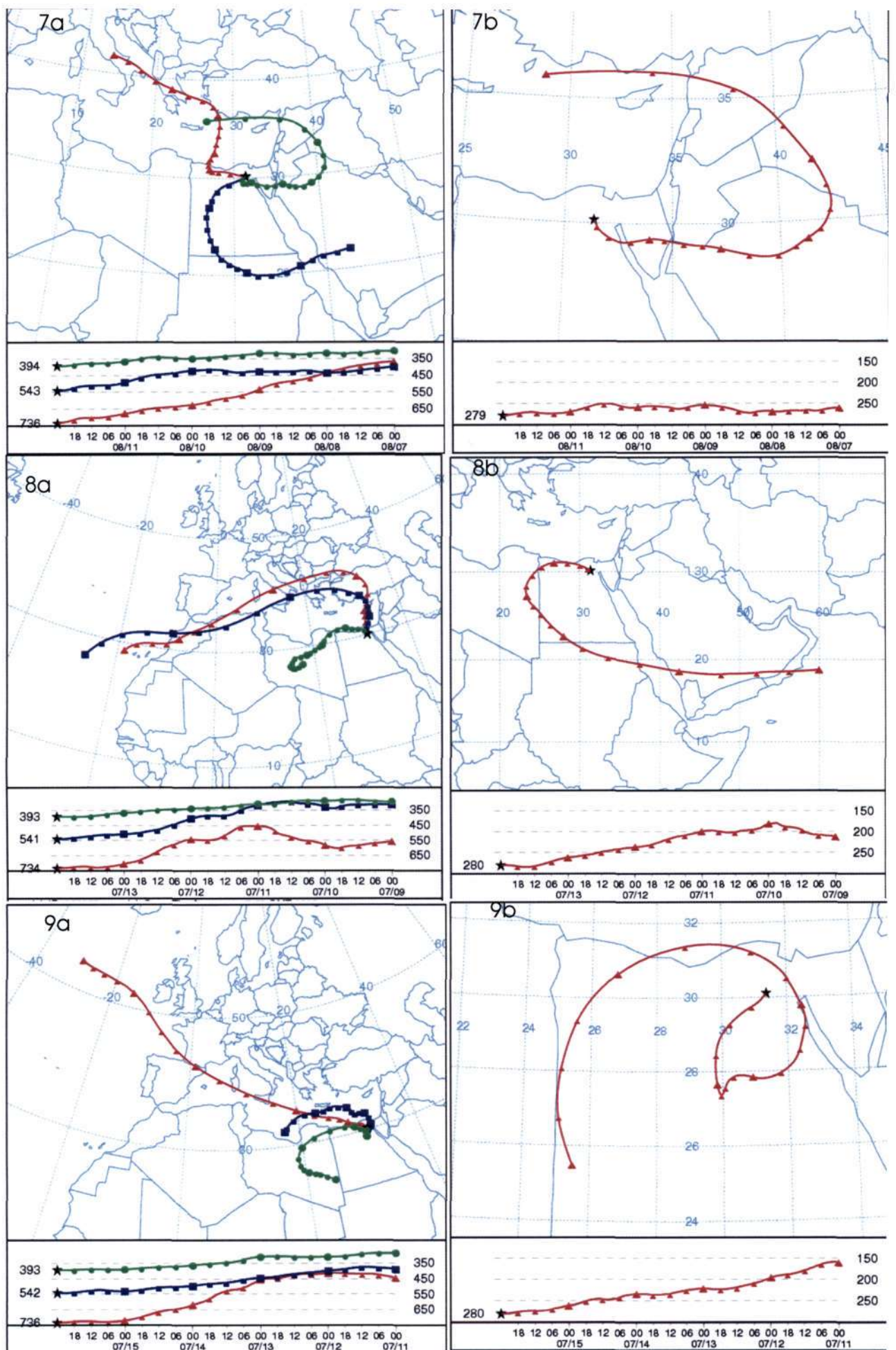


Figure D4: continued (7) 12 August 2001 (8) 14 July 2000 and (9) 16 July 2000  
a) Horizontal and vertical plots of back trajectories originating at 2.5, 5 and 7.5 km  
b) Horizontal and vertical plots of back trajectories originating at 10 km



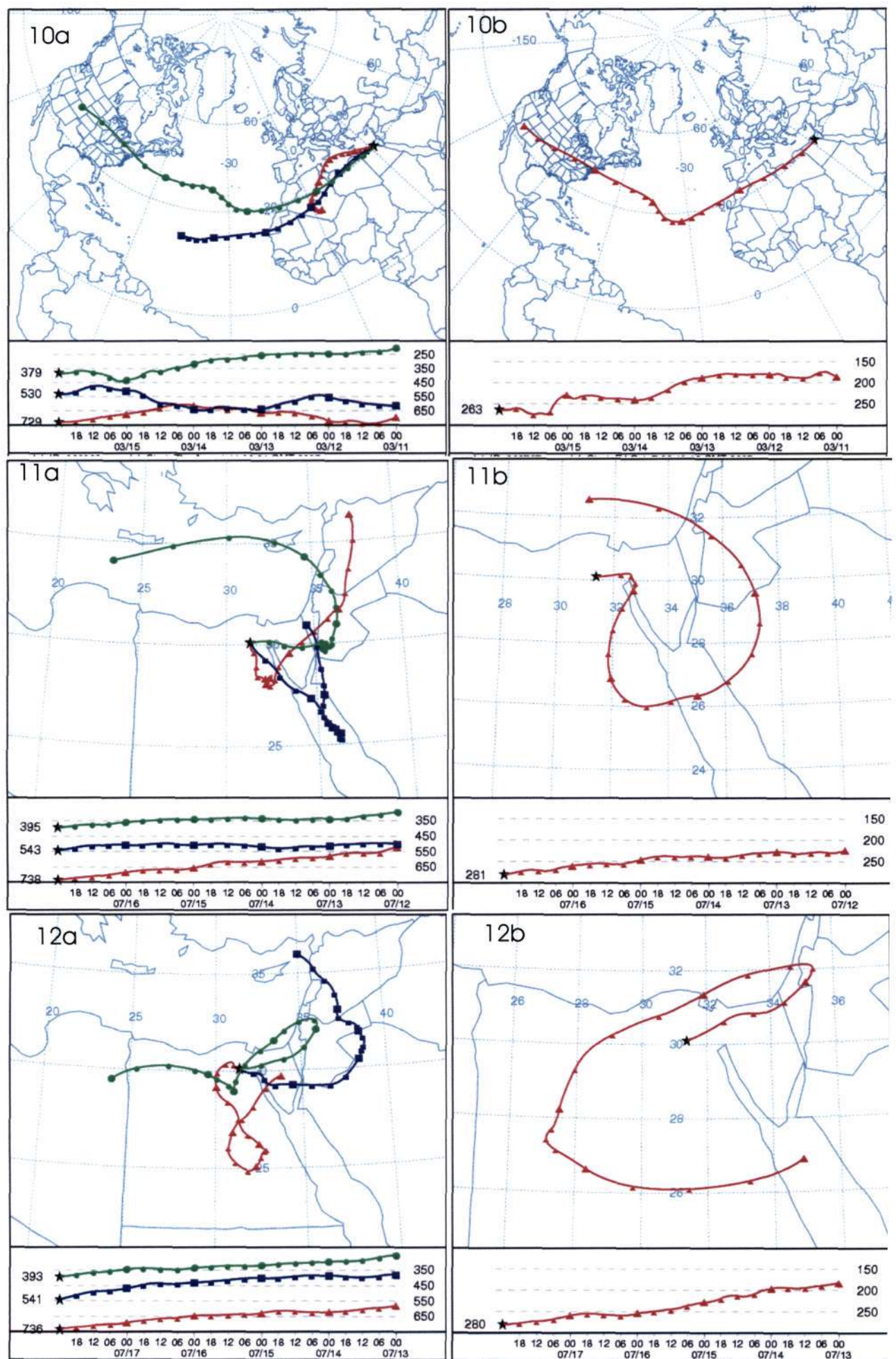


Figure D4: continued (10) 16 March 2002 (11) 17 July 2000 and (12) 18 July 2000  
a) Horizontal and vertical plots of back trajectories originating at 2.5, 5 and 7.5 km  
b) Horizontal and vertical plots of back trajectories originating at 10 km



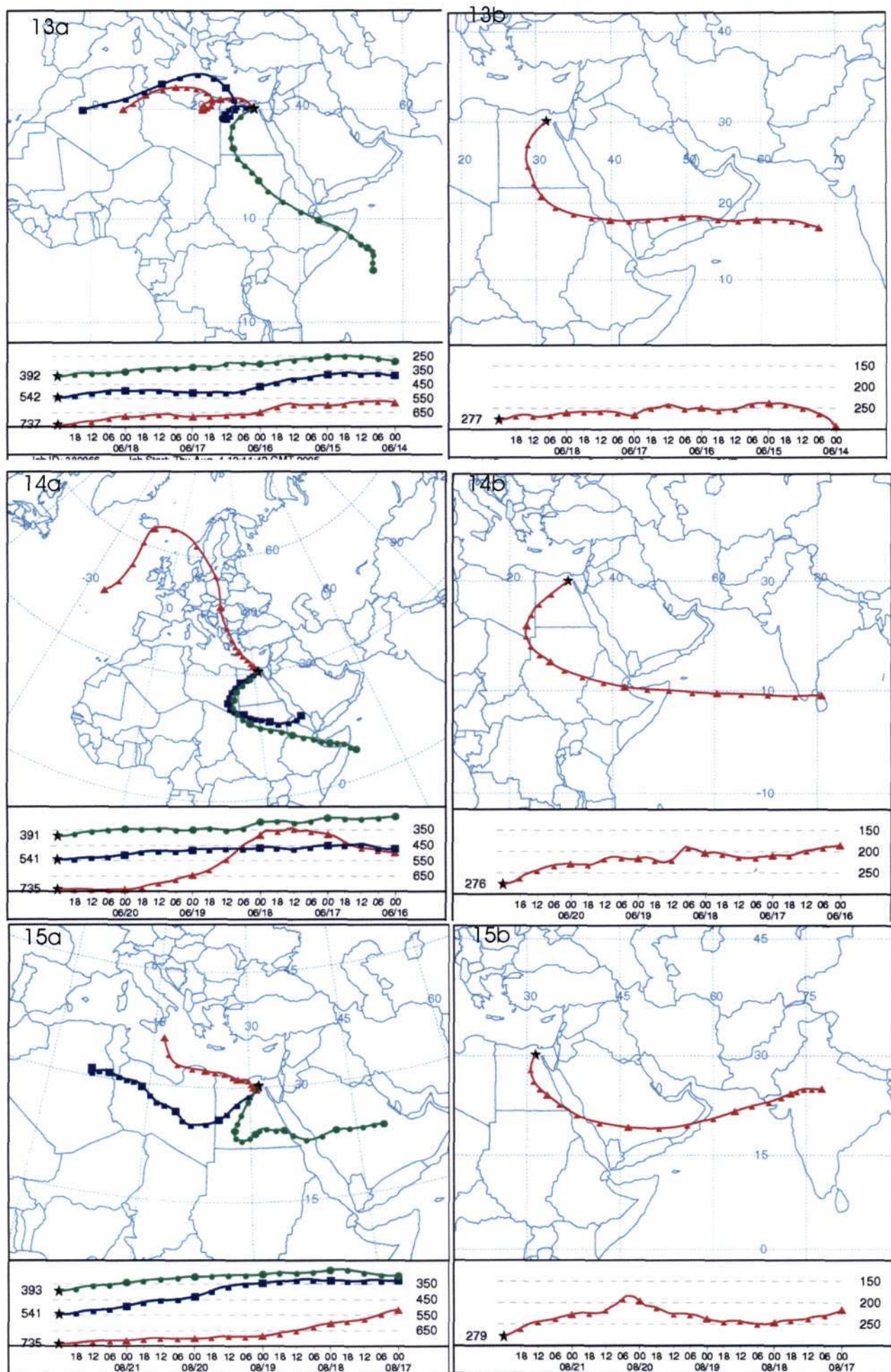
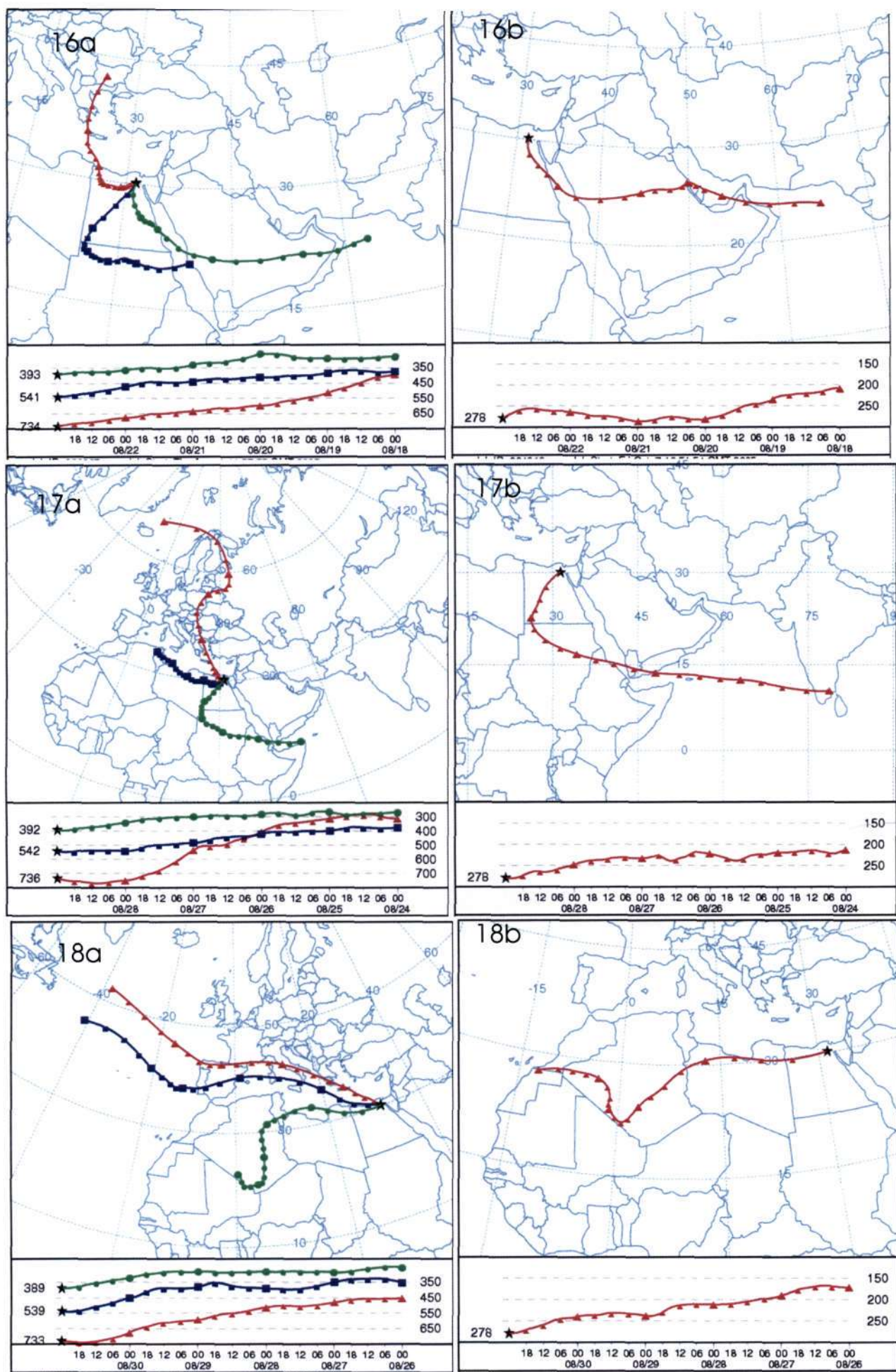
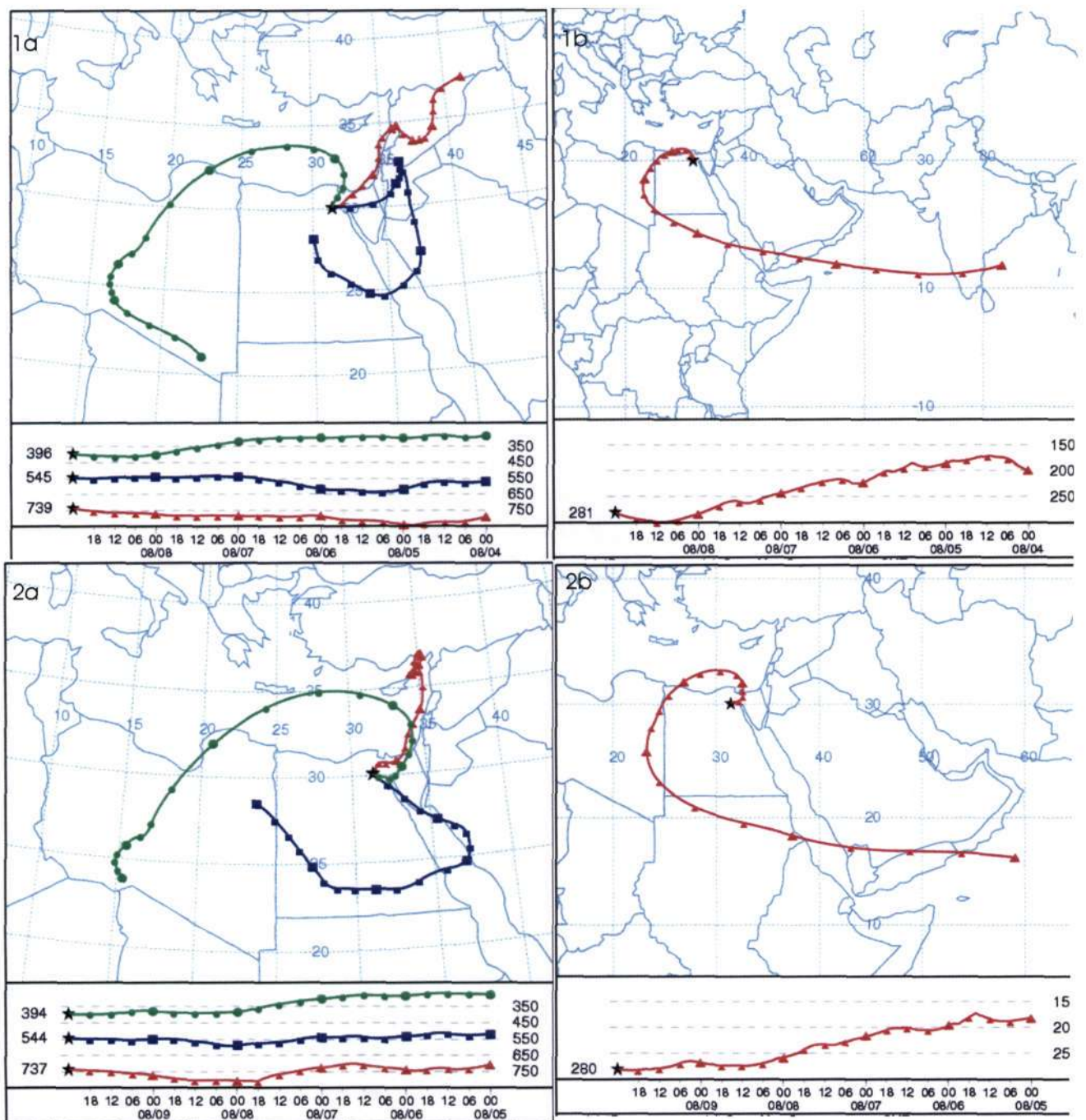


Figure D4: continued (13) 19 June 1999 (14) 21 June 2000 and (15) 22 August 2000  
a) Horizontal and vertical plots of back trajectories originating at 2.5, 5 and 7.5 km  
b) Horizontal and vertical plots of back trajectories originating at 10 km









**Figure D5: 5-day back trajectory HYSPLIT model results for Group 5. 1) 10 August 1999 and 2) 9 August 1999**  
**a) Horizontal and vertical plots of back trajectories originating at 2.5, 5 and 7.5 km**  
**b) Horizontal and vertical plots of back trajectories originating at 10 km**